Defining the role of the transcription factor T-bet in the immune system

Lo, Jonathan Wai Pang

Awarding institution:
King's College London

Defining the role of the transcription factor T-bet in the immune system

A thesis submitted to the School of Medicine at King's College London

for the degree of Doctor of Philosophy

By

Jonathan Wai Pang Lo

Department of Experimental Immunobiology

Division of Transplantation Immunology and Mucosal Biology

LORD Lab, 5th Floor Tower Wing

Guy's Hospital, King's College London

London, SE1 9RT

ABSTRACT

T-bet (Tbx21) was first discovered to have a role in the adaptive immune system almost 20 years ago. It was found to be a key regulator in the function of $CD4^+$ T helper 1 (T_H1) cells. T-bet has been shown to be expressed and have a function in the other subsets of T helper cells. Understanding the role of T-bet and the role it plays in T cell differentiation and plasticity has become vital, as well as, the function of T-bet in other immune cells.

Within the lab, a new mouse line has been developed that is able to fluorescently trace the lineage of T-bet expressed cells. Experiments have involved phenotyping this mouse line and determining the base-line level of T-bet expressing cells within each cell compartment. Further experiments will investigate the expression level of fate mapped T-bet cells, mainly the $CD4^+$ T cells, in disease models in this mouse line.

Further analysis of these T-bet traced cells have been performed to see whether these cells are more plastic and able to illicit a switch to a T_H1 response and if there is a developmental aspect to expressing T-bet in development of $CD4^+$ T cells. This thesis looks into these cells in more depth.

I also have had the use of another mouse line which is able to delete T-bet in cells using tamoxifen treatment. This mouse line has given me the chance to delete T-bet from $CD4^+$ T cells after they have developed and see if there is any change in plasticity and, also compare them with the deletion of T-bet in innate lymphoid cells.

Finally, I have also used another mouse line which deletes T-bet in specifically regulatory T cells. This mouse line was used in a heart transplant model to see whether the deletion of T-bet would have any effect in the ability of T_{regs} to aid in tolerance of the heart transplant and prevent rejection of the graft.

This thesis aims to learn more about the role of T-bet within the immune response and especially in the $CD4^+$ T cell compartment, as despite the on-going research there is still a big unknown area of how the master regulators of $CD4^+$ T cells regulate the plasticity and differentiation of these cells. Using these mouse models, I have discovered more about the insight into this and provide suitable and hopefully more understanding towards this subject.

This thesis is dedicated to

Agnes Lo, Patrick Lo and Benjamin Lo

for all their continued support throughout my PhD and my life.

CONTENTS

Abstract…….....2

Contents 4

List of Tables 10

List of Figures..... 11

List of Abbreviations 14

Acknowledgements 18

Chapter 1 19

Introduction..... 19

1.1 The many cellular mechanisms of the immune system aid in protecting and maintaining health 19

1.1.1 The innate immune system…….19

1.1.2 The adaptive immune system…….21

1.2 T-bet 24

1.3 T-bet expression in the immune system 26

1.4 The role of T-bet in $CD4^+$ T cells..... 27

1.4.1 $CD4^+$ T helper cell differentiation..... 27

1.4.2 The role of T-bet in T_H1 cells..... 30

1.4.3 The role of T-bet in T_H2 cells..... 32

1.4.4 The role of T-bet in T_H17 cells..... 33

1.4.5 The role of T-bet in T_{regs} cells..... 34

1.4.6 The role of T-bet in formation of $CD4^+$ memory cells 35

1.5 The role of T-bet in $CD8^+$ T cell function and memory $CD8^+$ formation 35

1.6 The role of T-bet in B cells 36

1.7 The role of T-bet in γδ T cells 36

1.8 The role of T-bet in NKT cells 37

1.9 The role of T-bet in NK cells 37

1.10 The role of T-bet in dendritic cells 38

1.11 The role of T-bet in innate lymphoid cells 39

1.11.1 ILC differentiation and the differences between subsets 39

1.11.2 The role of T-bet in ILCs during mucosal immune responses 41

1.12 Experimental mouse models of IBD 43

1.12.1 The T cell transfer model 44

1.12.2 The DSS model 44

1.12.3 Parasite models: using *Nippo* and *H.Poly* 45

1.12.4 The anti-CD40 model 46

1.13 Hypothesis and Aims 49

Chapter 2 50

Materials and Methods 50

2.1 Animal husbandry 50

2.2 Genotyping 50

2.3 Cell Isolation and preparation 51

2.4 Cell separation technique 52

2.4.1 $CD4^+$ magnetic bead separation 52

2.4.2 Cell sorting 52

2.5 Naïve T cell transfer model of colitis 53

2.6 Anti-CD40 model of severe inflammation of the liver 54

2.7 DSS-induced colitis mouse model 54

2.8 Parasite infections of mice 54

2.9 Cell culture 55

2.10 *Ex vivo* colon organ culture 56

2.11 ELISA **56**

2.12 Flow cytometry **56**

2.13 Cytokine secretion assay **59**

2.14 Heterotopic Heart Transplant **60**

2.15 Donor Specific Antibody (DSA) Assay **60**

2.16 RNA extraction **61**

2.17 cDNA synthesis and quantitative PCR **61**

2.18 Liver histology **62**

2.19 ALT measurements of mouse serum **62**

2.20 *In vitro* Tamoxifen treatment **62**

2.21 *In vivo* Tamoxifen treatment **63**

2.22 Statistical analysis **63**

Chapter 3 ..... **64**

3.1 Initial phenotyping of CD45^{+} lymphocytes in blood, and lymphoid organs and mucosal sites of the T-bet^{cre} x ROSA26YFP$^{fl/fl}$ mice **68**

3.2 Phenotyping YFP expression in lymphoid and myeloid cells of the T-bet^{cre} x ROSA26YFP$^{fl/fl}$ mice **70**

3.3 Extensive phenotyping of immune T cells within the thymus **72**Error! Bookmark not defined.

3.3.1 Phenotyping CD4^{+} and CD8^{+} T cell development in the thymus **72**

3.3.2 Phenotyping YFP^{+} DN1s and DN2 in the thymus **75**

3.3.3 Phenotyping γδT cell development in the thymus **78**

3.3.4 Phenotyping NKT cell development in the thymus **81**

3.4 Phenotyping of progenitor cells in the bone marrow **83**

3.5 Phenotyping of immune cells in the peripheral organs **84**

3.5.1 Phenotyping T cells in the spleen and colon……..**84**

3.5.2 Phenotyping ILCs in the spleen and colon……**87**

3.6 Discussion 89

Chapter 4 93

4.1 Phenotyping the naïve YFP^{+} CD4^{+} T cells in the T-bet^{cre} x ROSA26YFP$^{fl/fl}$ mice 97

4.2 Identifying the naïve YFP^{+} CD4^{+} T cells 99

4.2.1 Are these YFP^{+} naïve T cells stem cell-like memory T cells? 99

4.2.2 Are these YFP^{+} naïve T cells virtual memory or memory-naïve T cells? 102

4.2.3 Are these YFP^{+} naïve CD4^{+} T cells precursors to CD5^{high} pathogen-independent memory-phenotype (MP) cells? 105

4.3 Investigating whether the YFP^{+} naïve CD4 T cell subset differs with age 106

4.3.1 The YFP^{+} naïve CD4^{+} T cells could not be found in the foetus of these mice ... 107

4.3.2 Naïve YFP^{+} CD4^{+} T cells are present within in the periphery in neonates 109

4.3.3 During weaning, the YFP^{+} naïve CD4^{+} T cells develop a phenotype more similar to those in adult mice 111

4.3.4 Are there any phenotypic difference between younger and older YFP^{+} naïve CD4^{+} T cells in these mice? 113

4.4 Are the YFP^{+} naïve CD4 T cells functionally different to YFP^{-} naïve CD4 T cells? 115

4.4.1 *In vitro* analysis of the YFP^{+} naïve CD4 T cells shows a dominant IFNγ production and possible predetermined T$_H$1 phenotype 115

4.4.2 *In vivo* analysis of the YFP^{+} naïve CD4 T cells 118

4.5 Do YFP^{+} naïve CD4^{+} T cells require bystander activation for IFNγ production or provide bystander activation to YFP^{-} naïve CD4^{+} T cells? 123

4.5.1 Transferred naïve YFP^{-} CD45.2 CD4^{+} T cells do not become YFP^{+} without the presence of a disease phenotype 124

4.5.2 IFNγ production from CD45.2 YFP^{+} cells are observed when there are limited cell numbers in co-culture with CD45.1 CD4^{+} T cell 126

4.5.3 *In vivo* co-transfer of CD45.1 and CD45.2 YFP$^+$ naïve CD4$^+$ T cells shows bystander activation of CD45.2 YFP$^+$ naïve CD4$^+$ T cells to produce a sufficient disease phenotype 128

4.6 Discussion 129

Chapter 5 132

5.1 Use of the T-bet fate mapping mouse line shows that previous T-bet expression allows for T$_H$17 cell plasticity 133

5.1.1 Previously naïve YFP$^-$ CD4$^+$ T cells become effector YFP$^+$ IL-17A-producing CD4$^+$ T cells with the induction of colitis 133

5.1.2 *In vitro* culture of YFP$^+$ IL17A$^+$ IFNγ$^-$ CD4$^+$ T cells show a predominance to switching to IFNγ production 135

5.1.3 Transfers of YFP$^+$ IL17A$^+$ IFNγ$^-$ CD4$^+$ T cells into Rag2$^{-/-}$ mice reveals a possible predominance to switching to IFNγ production 138

5.1.4 Summary of the plasticity of YFP$^+$ T$_H$17 cells 141

5.2 Using the inducible deletion model of T-bet in fully developed CD4$^+$ T cell populations to test for plasticity under healthy conditions 142

5.2.1 *In vitro* tamoxifen induced deletion of T-bet in cultures of CD4$^+$ cells from CreER^{T2}-Tbet$^{fl/fl}$ mice 142

5.2.2 *In vitro* skewing experiments in CD4$^+$ T cells after tamoxifen-induced T-bet deletion 144

5.2.3 *In vivo* tamoxifen induced deletion of T-bet in CD4$^+$ cell of CreER^{T2}-Tbet$^{fl/fl}$ mice 146

5.3 Using the inducible deletion model of T-bet to test for plasticity in pathological environments 148

5.3.1 Testing the plasticity of T$_H$2-driven parasite models after inducing T-bet deletion 148

5.3.2 Summary of plasticity of T$_H$2-driven parasite models after inducing T-bet deletion 154

5.3.3 Testing the plasticity of T_H17-driven DSS-induced colitis after inducing T-bet deletion 154

5.3.4 Summary of the plasticity of T_H17 driven disease using DSS-induced colitis after inducing T-bet deletion 157

5.4 Discussion 158

Chapter 6 160

6.1 The role of T-bet in $CD4^+$ T_{reg} 161

6.2 The role of T-bet in NK cells and ILC1s in liver disease 164

6.2.1 Activation of CD40 causes severe inflammation of the colon, but also causes severe inflammatory hepatocellular injury in the liver 164

6.2.2 Hepatic $CD90^+$ $NKp46^+$ cells are more prolific activated producers of IFNγ ... 167

6.2.3 Conventional NK cells and not ILC1s are the main population of IFNγ producing cell in anti-CD40 mediated hepatitis 169

6.2.4 Anti-CD40 mediated hepatitis is not dependent on T-bet to drive the disease phenotype 171

6.3 Discussion 173

Chapter 7 176

7.1 The use of the lineage T-bet expressing mouse model provided insights into immune cells that have previously expressed T-bet 176

7.2 The expression of T-bet is not necessary to maintain $CD4^+$ T cell survival or plasticity 179

7.3 A novel model of hepatitis involving the activation of CD40L on NK cells causes severe inflammation of the liver 181

Bibliography 182

List of Tables

Table 1. Summary of the mouse models used in this project and the current known research on IBD ……..…….. 47

Table 2. List of T cell skewing conditions …….. 54

Table 3. List of flow cytometry antibodies used for the various panels and experiments…… 56

Table 4. Summary table showing the surface markers used to define stem cell-like memory cells, virtual memory T cells, naïve-like memory T cells (TMNP) and memory-phenotype cells.…….. 94

List of Figures

Figure 1. T-bet expression in immune cell populations……..26

Figure 2. Schematic diagram showing the differentiation pathway of naïve $CD4^+$ T cells into helper T cells……...29

Figure 3. Schematic diagram showing the differentiation pathway of innate lymphoid cells……...41

Figure 4. Schematic diagram showing the activation pathway of APCs with NK cells or ILCs via the costimulatory molecules CD40 and its ligand CD154 in the anti-CD40 model of colitis……47

Figure 5. Gating strategy for sorting naïve T cells using the Aria machine…….53

Figure 6. Schematic showing the strategy of generating the T-bet^{cre} line…….67

Figure 7. Phenotyping the blood of the T-bet^{cre} x $ROSA26YFP^{fl/fl}$ showed all subtypes of cell to only express YFP in double homozygous mice…….68

Figure 8. Phenotyping YFP expression in the $CD45^+$ lymphocytes in the colon, mLN and spleen……...69

Figure 9. Phenotyping YFP expression in subsets of innate and adaptive immune cells in the spleen…….71

Figure 10. Gating strategy used to identify the different CD4 and CD8 T cells in the thymus…….73

Figure 11. Phenotyping the YFP expression within the CD4 T cell compartment in the thymus…….74

Figure 12. Flow cytometry analysis of the $CD44^+$ $CD25^-$ YFP^+ and $CD44^+$ $CD25^+$ YFP^+ cells thymus…….76

Figure 13: Phenotyping the YFP expression in developing γδT cell in the thymus of T-bet^{cre} x $ROSA26YFP^{fl/fl}$ mice……. 79

Figure 14. Phenotyping the YFP expression in developing NKT cells in the thymus of T-bet^{cre} x $ROSA26YFP^{fl/fl}$ mice……. 81

Figure 15. Phenotyping of YFP expression in the lymphoid precursors in the bone marrow of T-bet^{cre} x $ROSA26YFP^{fl/fl}$ mice…….. 83

Figure 16. Phenotyping of the spleen and colon showing YFP^+ expression in naïve $CD4^+$ T cells in the T-bet^{cre} x $ROSA26YFP^{fl/fl}$ mice……...85

Figure 17. Phenotyping of YFP expression in NK cells and ILCs in the spleen and colon of T-bet^{cre} x $ROSA26YFP^{fl/fl}$ mice…….87

Figure 18. Extensive phenotyping of the T-bet^{cre} x ROSA26YFP$^{fl/fl}$ shows consistent levels of YFP^{+} CD4^{+} T cells in the major organs and lymphoid tissue…….98

Figure 19. Gating strategy for identifying stem cell-like memory T cells in the T-bet^{cre} x ROSA26YFP$^{fl/fl}$ mice…….. 100

Figure 20. Phenotyping of the stem cell-like memory T cells in the T-bet^{cre} x ROSA26YFP$^{fl/fl}$ mice……101

Figure 21. Gating strategy of the T_{MNP} and virtual memory cells in the T-bet^{cre} x ROSA26YFP$^{fl/fl}$ mice…….103

Figure 22. Phenotyping of the T_{MNP} and virtual memory cells in the T-bet^{cre} x ROSA26YFP$^{fl/fl}$ mice…….104

Figure 23. Phenotyping the CD5^{+} YFP naïve T cells in the T-bet^{cre} x ROSA26YFP$^{fl/fl}$ mice……106

Figure 24. Phenotyping the cells in the E15.5-E16 foetus of T-bet^{cre} x ROSA26YFP$^{fl/fl}$ mice……107

Figure 25. Phenotyping of the 1-week-old T-bet^{cre} x ROSA26YFP$^{fl/fl}$ mice……109

Figure 26. Phenotyping of the 3-week-old T-bet^{cre} x ROSA26YFP$^{fl/fl}$ mice……111

Figure 27. Phenotyping of 25 and 50-week-old T-bet^{cre} x ROSA26YFP$^{fl/fl}$ mice……112

Figure 28. *In vitro* culture of YFP^{+} CD4^{+} T cells shows that even without skewing YFP^{+} CD4^{+} T cells can produce a large amount of IFNγ upon activation and stimulation…114

Figure 29. *In vitro* T cell skewing of YFP^{+} CD4^{+} T cells shows that even under T_H2, T_H17 and T_{reg} skewing conditions YFP^{+} CD4^{+} T cells can produce IFNγ upon activation and stimulation…….116

Figure 30. T cell transfer of 500,000 naïve CD4^{+} T cells generates a predominately IFNγ response and only a small IL-17A response……..…….118

Figure 31. T cell transfer of 100,00 naïve YFP^{+} CD4^{+} T cells have a reduced disease phenotype despite still generating a predominately IFNγ response and lacks an IL-17A response…….119

Figure 32. T cell transfer of 25,000 naïve YFP^{-} and naïve YFP^{+} CD4^{+} T cells do not get a disease phenotype but YFP^{+} CD4^{+} T cell transferred still have an increased production of IFNγ and reduced IL-17A when compared to YFP^{-} CD4^{+} T cell transferred……121

Figure 33. T cell transfer of 10,000,000 naïve CD45.2^{+} CD4^{+} YFP^{-} T cells into CD45.1 mice do not develop a disease phenotype and remain YFP^{-}…….124

Figure 34. *In vitro* culture of CD45.1, CD45.2 YFP^{+} and CD45.2 YFP^{-} with IL-2 and anti-CD3/CD28 shows spontaneous production of IFNγ by CD45.2 YFP^{+} to still occur ……126

Figure 35. *Rag2*$^{-/-}$ mice co-transferred with 25,000 cells at a 90:10 ratio of CD45.1:CD45.2 YFP^{+} naïve CD4^{+} T cells……..128

Figure 36. A subset of IL-17A^{+} IFNγ^{-} producing CD4^{+} T cells express YFP during disease……133

Figure 37. IL-17A^{+} IFNγ^{-} YFP^{+} CD4^{+} T cells produce more IFNγ and less IL-17A than IL-17A^{+} IFNγ^{-} YFP^{-} CD4^{+} T cells upon reactivation and re-stimulation *ex vivo* of T cell transfer colitis induced mice……135

Figure 38. IL-17A^{+} IFNγ^{-} YFP^{+} CD4^{+} T cells produce more IFNγ and less IL-17A upon retransfer into *Rag2*$^{-/-}$ mice……..138

Figure 39. *In vitro* testing of dose response and optimal time for exposure of cultured CD4^{+} T cells from CreER^{T2}-Tbet$^{fl/fl}$ with tamoxifen……...142

Figure 40. *In vitro* testing of naïve CD4^{+} T cell skewing after tamoxifen induced deletion of T-bet in CD4^{+} T cells from CreER^{T2}-Tbet$^{fl/fl}$ mice……...144

Figure 41. *In vivo* testing of tamoxifen induced deletion of T-bet in CD4^{+} T cells from CreER^{T2}-Tbet$^{fl/fl}$……..146

Figure 42. Infection with *Nippostrongylus brasiliensis* after tamoxifen-induced deletion of T-bet in CD4^{+} T cells from CreER^{T2}-Tbet$^{fl/fl}$ mice……...148

Figure 43. Parasite infection with *Heligmosomoides polygyrus* after tamoxifen induced deletion of T-bet in CD4^{+} T cells from CreER^{T2}-Tbet$^{fl/fl}$…….151

Figure 44. DSS-induced colitis in tamoxifen treated WT/Hom and Het/Hom CreER^{T2} T-bet$^{fl/fl}$ mice……154

Figure 45. Phenotyping of the Foxp3^{cre} x T-bet$^{fl/fl}$ mouse line at steady state…….161

Figure 46. Cardiac allograft survival between Foxp3^{cre} mice and Foxp3^{cre} x T-bet$^{fl/fl}$ ..162

Figure 47. Typical colitis clinical aspects of the anti-CD40 colitis model in *Rag2*$^{-/-}$ mice……164

Figure 48. Clinical aspects in the liver of the anti-CD40 colitis model in *Rag2*$^{-/-}$ mice..165

Figure 49. IFNγ production in the liver is produced predominately from CD90^{+} NKp46^{+} cells…….167

Figure 50. Phenotyping the CD90^{+} NKp46^{+} NK and ILC1 population in the liver…...169

Figure 51. Comparing liver disease in *Rag2*$^{-/-}$ vs TRnUC mice with anti-CD40……170

List of Abbreviations

APC	Antigen presenting cell
BSA	Bovine serum albumin
CD	Cluster of differentiation or Crohn's Disease
ChIP	Chromatin immunoprecipitation
cLP	Colonic lamina propria
DC	Dendritic cell
DSS	Dextran sodium sulphate
EDTA	Ethylene-diamine-tetraacetic acid
ELISA	Enzyme-linked immunosorbent assay
EOMES	Eomesodermin
FACS	Fluorescence-activated cell sorting
FCS	Foetal calf serum
Foxp3	Forkhead Box P3
γδ T cells	Gamma Delta T cells
GATA3	GATA-binding protein 3
GFP	Green fluorescent protein
GI	Gastrointestinal
GWA	Genome wide association (study)
H&E	Haematoxylin and eosin
Hh	*Helicobacter hepaticus*
HT	*Helicobacter typhlonius*
H. poly	*Heligmosomoides polygyrus*
HLA	Human leucocyte antigen
IBD	Inflammatory bowel disease
IFN	Interferon

IL	Interleukin
ILC	Innate lymphoid cell
i.p.	Intraperitoneally
i.v.	Intravenuous
Lin^-	$Lineage^-$ (negative)
LP	Lamina propria
LPL	Lamina propria leukocytes
LTi	Lymphoid tissue inducer (cell)
MFI	Mean (median) fluorescence intensity
MHC	Major histocompatibility complex
mLN	Mesenteric lymph nodes
Nippo	*Nippostrongylus brasiliensis*
NK	Natural killer
NKT	Natural killer T cell
PBS	Phosphate-buffered saline
PCR	Polymerase chain reaction
PFA	Paraformaldehyde
PMA	Phorbol 12-myristate 13-acetate
PP	Peyer's patches
Rag1	Recombination activating gene 1
Rag2	Recombination activating gene 2
mRNA	Messenger ribonucleic acid
RORγt	Retinoic acid related-orphan receptor γt
RPMI	Roswell Park Memorial Institute medium
RT-qPCR	Real-time quantitative polymerase chain reaction
STAT	Signal transducer and activator of transcription
TAE	Tris-acetate-EDTA

T-bet	T-box expressed in T cells
Tbx21	T-box transcription factor 21 (gene encoding T-bet)
TBR1	T-box brain protein 1
TCR	T cell receptor
TCT	T cell transfer
T_H	T helper
TNFα	Tumour necrosis factor-α
T_{reg}	Regulatory T-cell
TRUC	*Tbx21*$^{-/-}$ x *Rag2*$^{-/-}$ Ulcerative Colitis
TRnUC	*Tbx21*$^{-/-}$ x *Rag2*$^{-/-}$ non-Ulcerative Colitis
UC	Ulcerative colitis
WT	Wild type

ACKNOWLEDGEMENTS

Firstly, I would like to gratefully acknowledge the support and guidance given by both of my supervisors and mentors Professor Graham Lord and Dr Richard Jenner. I am grateful to the MRC Centre for Transplantation for the funding over the past 3 years for this studentship at King's College London.

Secondly, I would like to acknowledge lab members: fellow PhD students and post-doctoral scientists, in the Lord Lab for their technical assistance, supervision, constructive feedback, critical appraisals, and for assisting in any large-scale experiments. Particular thanks to Ian Jackson, Joana Pereira das Neves, Nelomi Anandagoda, Luke Roberts, Jan-Hendrik Schroeder, Arnulf Hertweck, Nicholas Powell, Emilie Stolarczyk and Natividad Garrido Mesa. I would also like to thank Professor Lord's PA Julie Reason, who has been incredibly helpful in administrative matters.

I would also like to thank Professor Robert Goldin, Hiromi Kudo and other support staff at the Department of Cellular Pathology at Imperial College London for cutting, preparing and staining liver histology segments. Also, thanks must go to Roger Bishop, Sue Rodway, Medina Gowers and other staff at the Pathology and Diagnostic Laboratories at the Royal Veterinary College for their work on processing and analysing the ALT blood serum samples. I would like to thank Dr Helena Helmby for her assistance and for setting up the parasite infection models with either *Nippostrongylus brasiliensis* (Nippo) *or Heligmosomoides polygyrus* (H. poly) in mice at The London School of Hygiene and Tropical Medicine. Also, I am thankfully to Professor Laurie Glimcher of Cornell University for the kind gift of TRUC mice. I also have to thank Wilson Wong's group, and in particular Lucy Meader for her services and assistance in performing the cardiac allografts in the Foxp3^{cre} x T-bet$^{fl/fl}$ mice. I also gratefully thank Susanne Heck and her team at the BRC Flow Core at Guy's and St Thomas' Trust for all the assistance and service they provided.

Lastly, I would like to thank my family and my partner Katy Scott. Their continued patience and support have been valuable in making this thesis be completed.

Chapter 1

Introduction

1.1 The many cellular mechanisms of the immune system aid in protecting and maintaining health

Humans have evolved to form a complex and multifaceted immune system in order to maintain homeostasis and health against various pathogens (Chaplin, 2010). The immune system of a human comprises of two main arms: the innate immune system and the adaptive immune system (Medina, 2016, Parkin and Cohen, 2001).

1.1.1 The innate immune system

In brief, the innate immune system involves a large variety of immune cells and molecules that are able to recognise a broad range of molecule patterns, which are shared by microbes and toxins that are not found in the host (Chaplin, 2010). There are numerous cell types involved in the innate immune system, including dendritic cells, macrophages, neutrophils, eosinophils, basophils, mast cells, megakaryocyte, natural killer (NK) cells, γδT cells, and epithelial cells (Chaplin, 2010, Medina, 2016, Parkin and Cohen, 2001, Gandhi et al., 2010). One of the first defence mechanisms of the innate immune system is the response from epithelial cells to pathogens. Pathogens have conserved regions on their surface called pathogen-associated molecular patterns (PAMPs), which are recognised through various genes encoded pattern recognition receptors (PRRs), of which Toll-like receptors have been the most heavily studied, on the surface of these cells (Tosi, 2005, Akira et al., 2006, Medzhitov and Janeway, 2000). Once PRRs recognise PAMPs, a proinflammatory and anti-microbial response occurs by activating the cells to produce, signal or activate various adaptor molecules, signalling kinase pathways and transcription factors (Mogensen, 2009). PRR-induced signal transduction results in the activation of a variety of molecules, including cytokines, chemokines, cell adhesion molecules, and immunoreceptors (Akira et al., 2006), which are the cause of the early host response to infection, and, simultaneously these different molecular responses link the innate

immune response to the adaptive immune response (Iwasaki and Medzhitov, 2015, Turvey and Broide, 2010).

Two of the more important innate host response cytokines are IL-1 and TNFα. Both IL-1 and TNFα have been shown to be produced after activation of LPS from TLRs (Lu et al., 2008). In an example of gram-negative bacteria induced sepsis, both these cytokines, subsequently, can activate other cytokine production, chemokines and reactive oxygen species. They both also cause the expression of adhesion molecules from both epithelial cells and other leukocytes (Beutler and Cerami, 1989, Cohen, 2002). Both IL-1 and TNF-α can also promote the production of IL-6 (Oppenheim, 2001, Tosi, 2005).

The activation of chemokines has also been shown to be important in acute innate immune activation. Chemokines are a specialized group of cytokine-like polypeptides. All chemokines are ligands to G protein-coupled, 7-transmembrane segment receptors, which have an important role in activating other immune cells and promoting their cell migration to areas of inflammation (Baggiolini, 2001, Kim, 2004, Rossi and Zlotnik, 2000, Tosi, 2005). Chemokines and their receptors are classified into 4 different families, which are determined by the first two cysteine residues of the respective chemokine peptide sequence. Each of at least 16 CXC-chemokines binds to 1 or more of the CXC-receptors (CXCR), of which there are 6 CXCRs. Correspondingly, there are 10 CC- chemokine receptors (CCRs), which bind to at least 28 CC chemokines. The chemokine receptors tend to be expressed on all immune cells and the chemokines secreted by activated innate immune cells aid in recruiting further immune cells to the site of infection and help to link the innate and adaptive immune system by recruiting cells of the adaptive immune system. For example, Epstein-Barr Virus has been shown to induce chemokine production causing recruitment of NK cells, B cells and both $CD4^+$ T helper cells and $CD8^+$ cytotoxic T cells (Kim, 2004, Glass et al., 2003). The type of chemokine and chemokine receptors have been found to be associated with different inflammatory conditions, for example between a T_H1 (IL-12 and IFNγ) versus T_H2 (IL-4 and IL-13) immune response (Bisset and Schmid-Grendelmeier, 2005). The specificity of these immune responses has been strongly influenced by the chemokines released from specific cells, the vascular adhesion molecules expressed in those tissues, the chemokine receptors expressed by various populations of lymphocytes (Bisset and Schmid-Grendelmeier, 2005, Glass et al., 2003, Kim, 2004).

As well as recruiting other immune cells to the area of foreign microbes, upon recognition of foreign pathogen molecules, the link between the innate and adaptive immune response has also been highlighted with antigen presentation. Antigen-presenting cells (APCs) are a heterogeneous group of immune cells that mediate the cellular immune response by processing and presenting antigens for recognition by both $CD4^+$ T helper cells and $CD8^+$ cytotoxic T cells (Thomson and Knolle, 2010). This occurs in APCs, which classically consists of dendritic cells, which are the most potent APC, macrophages and B cells (Knight and Stagg, 1993, Chaplin, 2010). APCs initially phagocytose pathogens, degrade the pathogens into peptides and then load and present these foreign peptides onto either class I or class II major histocompatibility complex (MHC). MHC class I bind to $CD8^+$ cytotoxic T cells and MHC class II are specific for $CD4^+$ T helper cells. The high avidity interaction between either of the MHC and co-stimulatory molecule of CD80 on the APC and the respective T cell receptor (TCR) and CD28 on the surface of either $CD4^+$ T cells and $CD8^+$ T cells causes strong interactions of the TCR and leads to T cell stimulation and the production of IL-2 and the receptor for IL-2 (Sprent, 1995). The specificity of the antigen peptide being presented to the specifically rearranged T cell receptor is also what provides the adaptive immune response to have specificity. Activated and stimulated T cells then proliferate and differentiate into effector T cells and an effective immune response against further infection from this specific pathogen occurs (Chaplin, 2010, Iwasaki and Medzhitov, 2015, Sprent, 1995).

1.1.2 The adaptive immune system

The two main arms of the adaptive immune system comprise of both T cells and B cells. T cells develop in the thymus, whereas B cells develop in the bone marrow. T cells can be separated into αβT cells and γδT cells. αβT cells $CD4^+$ T helper cells and $CD8^+$ cytotoxic T cells, which as explained above recognise either MHCII or MHCI respectively. Upon activation via their respective MHC interaction and costimulation, $CD4^+$ T cells main role is to regulate cellular and humoral immune responses by their own secretion of anti- or pro-inflammatory cytokines. Whereas, $CD8^+$ T cells main purpose, after activation, is to kill infected cells with intracellular microbes (Chaplin, 2010, Parkin and Cohen, 2001). $CD4^+$ and $CD8^+$ T cells differentiate into different subsets depending on what type of antigen they are exposed to. The differentiation of T cells occurs upon the activation of either one of the naïve $CD4^+$ or $CD8^+$ T cells into an effector T cell (Mosmann et al., 1986, Zhu and Paul, 2008). After

stimulation, stimulated naïve $CD4^+$ T_H cells produce IL-2 and are termed as T_H0. T_H0 cells differentiate into T_H1, T_H2, and T_H17 depending on the milieu of the cytokines present. T_H1 cells express the transcription factor T-bet and by the production of IFNγ (Szabo et al., 2000). T_H2 cells express the transcription factor GATA-3 and produce IL-4, IL-5, IL-13, and GM-CSF (Zhang et al., 1997, Zheng and Flavell, 1997). Finally, T_H17 cells express the transcription factor RORC2 (or RORγt) and produce the cytokines IL-6 and IL-17A (Ivanov et al., 2006, Unutmaz, 2009). T_H17 cells have been shown to be early responders to extracellular bacteria and fungi and help to further recruit neutrophils in order to eliminate the invading pathogen (Bettelli et al., 2006, Harrington et al., 2005, Park et al., 2005). In general, T_H1 cells predominantly support cell mediated immune responses to bacteria and viruses, whilst T_H2 cells support humoral and allergic responses (Hsieh et al., 1993, Le Gros et al., 1990, Swain et al., 1990, Zheng and Flavell, 1997).

Similarly to $CD4^+$ T cells, $CD8^+$ T cells also have the ability to produce T_H1, T_H2 and T_H17 like cytokine responses, and are termed T cytotoxic cell type 1 (T_C1), T cytotoxic cell type 2 (T_C2), T cytotoxic cell type 17 (T_C17) (Thomas et al., 2001, Mittrücker et al., 2014). T_C1 cells, like T_H1 cells, produce IFNγ and are regulated by the expression of T-bet. However, T_C1 cells also require Blimp-1, Id2 and IRF4 expression and they also produce TNFα, granzymes and perforin (Kaech and Cui, 2012b, Kim et al., 2011, Man et al., 2013). T_C2 cells also produce granzymes and perforin, as well as the similar cytokines and requirement of GATA3 like T_H2 cells. (Tang et al., 2012, Omori et al., 2003, Cho et al., 2012). T_C17 cells, like T_H17 cells, also express RORγt and produce IL-17A (Huber et al., 2013, Hinrichs et al., 2009, Hamada et al., 2009).

A small subset of αβT cells express NK1.1 and are termed NKT cells. NKT cells also develop in the thymus from the T cell lineage committed $CD3^+$ cell, but NKT cells are $CD4^-$ and $CD8^-$ and recognise glycolipid antigens presented by the CD1d molecule. They are predominantly immunoregulatory and are based on their production of large quantities of cytokines such as, IFNγ, IL-4, granulocyte-macrophage colony stimulating factor (GM-CSF) and TNFα (Godfrey et al., 2004, Godfrey et al., 2005, Godfrey et al., 2010). The development of the NKT cells in the thymus will be further discussed in Chapter 3; and since T-bet plays a vital role in the maturity of NKT cells (Simonetta et al., 2016, Townsend et al., 2004), analysed in more depth too.

γδT cells are another small subset of T cells, typically accounting for 0.5-5% of all T cell populations (Zhao et al., 2018, Kobayashi and Tanaka, 2015). They were initially discovered in the late 1980s, after the discovery of the γ chain of the TCR (Born et al., 1987, Hayday et al., 1985), and since then a large amount of research has been undertaken in order to discover more about the function and development of these cells. γδT cells also $CD4^-$ and $CD8^-$ and develop in the thymus from the T cell lineage committed $CD3^+$ cell. Different subsets of γδ T cells develop in the thymus of either murine or human species. In mice the different peripheral subsets exist as: $CD44^+$ $CD122^+$ dendritic epidermal T cells (DETCs), which are found in the epidermis and produce IFNγ, $CD44^+$ $CD25^+$ $CCR6^+$ IL-17-producing γδ T cells and $CD27^+$ IFNγ-producing γδ T cells (Turchinovich and Pennington, 2011, Ribot et al., 2009). γδ T cells have been shown to be a vital source of IL-17A in lymphoid organs and peripheral tissue (Jensen et al., 2008, Sutton et al., 2009, Martin et al., 2009). In humans, γδ T cells are also a minority population and are identified in the periphery, especially in the epithelial layer of mucosal surfaces. Identification of human γδ T cells can be done using the variable regions of TCR-δ: Vδ1 or Vδ2 (Hayday, 2000). $V\delta1^+$ cells have been shown to be largely found in the mucosal sites and share similar phenotypes to mouse γδ intraepithelial cells (Pang et al., 2012, Ribot et al., 2009). These $V\delta1^+$ cells have a function in wound healing and tissue homeostasis and also produce IFNγ. Whereas, $V\delta2^+$ cells are mainly $V\gamma9^+$ and are predominately found in the peripheral blood. These $V\gamma9V\delta2^+$ cells are only found in humans and not in murine subsets of γδ T cells

Lastly, the final arm of the adaptive immune system are B cells. B cells comprise of around 15% of the peripheral lymphocyte population in the blood. The main function of B cells is their ability to produce immunoglobulins (Ig) in response to invading pathogens. There are five subclasses of Igs: IgG, IgM, IgD, IgE and IgA, which all have differing immune function and responses (Schroeder and Cavacini, 2010). IgG and IgA are subdivided again into four and two classes respectively: IgG1, IgG2, IgG3, IgG4, IgA1 and IgA2 (Schroeder and Cavacini, 2010). The immunoglobulin is made up of a light and heavy chain and within these chains are variable regions the antigen binding site of the immunoglobulin are created. The different antibodies become incredibly variable in their ability to recognise many different antigens due to each of the heavy and light chains containing 3 highly variable subregions(Medina, 2016, Schroeder and Cavacini, 2010, Thomas et al., 2009). Each Ig, therefore, consists of two antigen-binding sites, which are the same. The terminal carboxyl region of the heavy and light chains is constant

in the five subclasses of antibodies. The heavy chain constant domains pair to form Fc regions, which is responsible for the majority of the effector functions of the Ig molecule, including binding to Fc receptors and activating the complement system. B cells develop in the bone marrow and differentiate from haematopoietic stem cells. The RAG1 and RAG2 genes rearrange the antigen receptors of B cells, similar to the reassembly of the TCR (Jankovic et al., 2004, Thomas et al., 2009). The amino terminal region of both heavy chains is made by the combination of encoded genes for a variable (V_H), diversity (D_H) and joining (J_H) region. This VDJ formation makes up one of the hypervariable regions and contributes to the antigen-binding site of a B cell. This process occurs during the pre-B cell development stage and when B cells reach an immature stage, they begin to express IgM on their surface (LeBien and Tedder, 2008). Upon reaching maturity, naïve mature B cells express both IgM and IgD on their surface (LeBien and Tedder, 2008). As explained above, different $CD4^+$ T helper cells become activated and produce cytokine responses depending on the pathogenic environment they are found. These cytokines influence mature B cells into class or isotype switching of the immunoglobulin. Class switching involves the process whereby the established surface immunoglobulin on the mature B cell are able to rearrange their VDJ regions into an alternative heavy chain). It has been shown that IL-10 production from T cells causes class switching from IgG1 to IgG3 (Malisan et al., 1996). T_H2 cytokines of IL-4 and IL-13 cause the switching to IgE. Whilst, production of TGF-β switches to IgA. IFNγ production from T_H1 cells causes the switching to IgG2. B cells simultaneously undergo somatic hypermutation, whilst the process of class switching is occurring. Somatic hypermutation causes increased affinity of the B cell to the antigen. The resulting process of somatic hypermutation, class switching and clonal expansion results in the formation of plasma cells and the secretion of the surface immunoglobulin into antibodies and provides an effective response against that specific pathogen. The process of somatic mutation and clonal expansion usually occurs in the germinal centre of the spleen and other secondary lymphoid tissues (Schmidlin et al., 2009).

1.2 T-bet

T-bet, or T-box expressed in T-cells, is coded in the genome by *Tbx21* gene on chromosome 11 in mice and chromosome 17 in humans, is a member of the T-box family of transcription factors and comprises of a 62kDa 530 amino acid protein. The identification of the recombination-activating gene (RAG) from jawed fish (Flajnik and Kasahara, 2009) helped to

determine a possible link between the evolution of the adaptive immune system from primitive innate-like B and T cell subset of cells, which has been recognised in jaw-less organisms, for example lampreys and amphioxus (Horton Amy and Gibson-Brown Jeremy, 2002). The research in the 1970's in the genetic composition of the adaptive immune system was hugely influential in discovering the process of somatic hypermutation (Weigert et al., 1970) and variable-diversity-junction rearrangement (VDJ rearrangement) of both the T cell receptor (TCR) and B cell receptor (BCR) (Tonegawa, 1976) at their antigen recognition sites; and it was discovered that these regions were shared within the RAG gene. The recombination of antigen recognition sites at the TCR and BCR contributes to the adaptive immune system having specificity and memory. Therefore, this understanding of how the two antigen recognition receptor sites were involved in the adaptive immune system of T and B cells helped to analyse the role of other genes in the adaptive immune system. Studying the early pre-evolutionary organisms such as lampreys and amphioxus, made startling new understandings into these innate-like B and T cells. They required genes such as eomesodermin (EOMES), T-box brain protein 1 (TBR1) and T-bet subfamily of T-box genes. T-bet being first described as the master regulator of differentiation for naïve $CD4^+$ T cells into T helper 1 (T_H1) cells (Szabo et al., 2000). Furthermore, better understanding of T cell transcriptional pathways have allowed for more defined knowledge into the regulation of T cell polarity. In understanding how the evolution of organisms and their immune systems developed has been able to shed new knowledge into T-bet being expressed in innate cells as well (Lazarevic et al., 2013).

Since then, using new and more developed genome analysis techniques has allowed further expansion of knowledge about how transcription factors behave within the genome. As T-bet plays an important role in many cells, not just $CD4^+$ T cells, their molecular mechanisms have been further understood using these techniques. Transcription factors, like T-bet, bind to their target genes at accessible promotor and enhancer regions, thus either activating or repressing them. Chromatin immunoprecipitation (ChIP) analysis is one of these new techniques and has allowed identification of the role T-bet plays in immune cells. ChIP-sequencing, or ChIP-seq has allowed for even further understanding of the promoter and enhancer regions which T-bet controls. Extensive understanding can be gained by investigating the parallel roles of T-bet in both the innate and adaptive immune system.

As already stated, T-bet was first cloned in 2000 by Szabo et al. and it was found to be the master regulator of T_H1 cells. It was found to bind to the promotor regions of both *Il2* and *Ifng* gene loci. In T cell skewing experiments, it was found that T-bet was quickly induced in naïve $CD4^+$ T cells in T_H1 conditions, but not in other T helper cell polarising conditions (Szabo et al., 2000). Also, further understanding was found that the *Ifng* gene was regulated and activated by T-bet and $CD4^+$ T cells highly produced IFNγ when T-bet was retrovirally transduced into $CD4^+$ T cells. (Szabo et al., 2000). Szabo et al., lastly discovered that T-bet was able to drive the plasticity of already committed T_H2 cells back to a T_H1 lineage. IFNγ production and inhibition of IL-4 and IL-5 in *in vitro* differentiated T_H2 cells was observed with retroviral transduction of T-bet was performed within these cells.

1.3 T-bet expression in the immune system

T-bet has been shown to be expressed solely in the immune system. As well as in $CD4^+$ T cells, T-bet has also been found to be expressed in $CD8^+$ T cells (Intlekofer et al., 2005), natural killer (NK) cells (Townsend et al., 2004), ILCs (Powell et al., 2012), dendritic cells (DCs) (Lugo-Villarino et al., 2003), monocytes (Lighvani et al., 2001), B cells (Liu et al., 2003), NKT cells (Matsuda et al., 2006), γδ T cells (Yin et al., 2002) and is summarised in Figure 1. T-bet being expressed in so many different cell types demonstrates that it has a vital role in the immune system, at both healthy steady state and during immune responses.

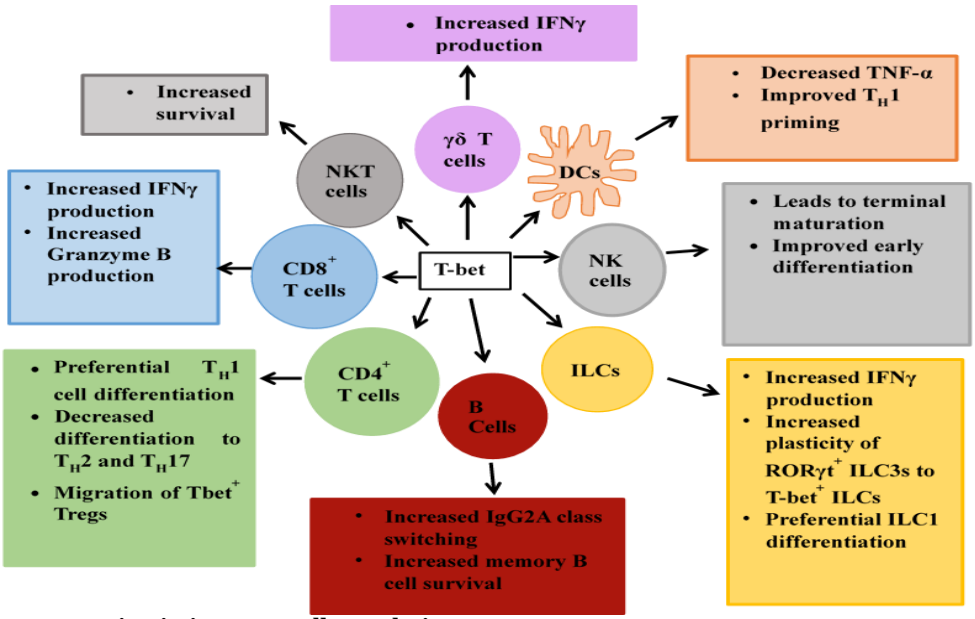

Figure 1: T-bet expression in immune cell populations

Schematic showing the different cell types currently known to express T-bet, and the function of T-bet within these cells, adapted from (Lazarevic et al., 2013)

1.4 The role of T-bet in CD4$^+$ T cells

1.4.1 CD4$^+$ T helper cell differentiation

A vast amount of knowledge about the different subsets of CD4$^+$ T helper cells has been discovered over the past 30 odd years. A brief history of CD4$^+$ T cell discovery is first described to understand the importance of T-bet in this population of cells. Initially CD4$^+$ T cells were thought to have two important immune responses: one being antibody-mediated and the second as cell-mediated (Zhu and Paul, 2008). The first important discovery, by Mosmman and Coffman, showed that there were two subtypes of CD4$^+$ T cells giving them different functions. They discovered that T_H1 cells were producers of IL-2, IFNγ, GM-CSF and IL-3 as a response to antigen presenting cells (Mosmann et al., 1986). During this time, IL-4 producing CD4$^+$ T helper cells were also discovered by Kim Bottomly (Killar et al., 1987). *In vitro* differentiation of helper CD4$^+$ T cells were first reported by two groups, William Paul and Susan Swain. They both found that naïve CD4$^+$ T cells were unable to make any of the effector cytokines and instead required T cell receptor (TCR) activation to produce any cytokines. They also found that IL-4 stimulation drove the CD4$^+$ T cells to produce even more IL-4 (Le Gros et al., 1990, Swain et al., 1990). It was within these first studies that also identified the DNA-binding factor GATA-3 and the signal transducer and activator of transcription (STAT) 6 (Zhang et al., 1997, Zheng and Flavell, 1997). *In vitro* studies were also carried out on CD4$^+$ T cells and subsequently found that naïve CD4$^+$ T cells could be differentiated into producing IFNγ after TCR stimulation and response to antigen presenting cells (APCs) with Listeria antigens presented. The APCs produced IL-12, which has since been found to be crucial for T_H1 differentiation and to cause IFNγ to be produced (Hsieh et al., 1993). Originally, it was thought that CD4$^+$ T cells were controlled by the interaction between the cytokines that were within their environment, with IL-4 working as a positive feedback loop for T_H2 and IL-12 for T_H1 differentiation. However, it was later discovered that T-bet was the main transcription factor that caused the increase positive feedback loop on T_H1 CD4$^+$ T cell differentiation and IFNγ production (Szabo et al., 2000).

After discovering the key transcription factors for T_H1 and T_H2 cells were T-bet and GATA3 respectively, the next subset of CD4$^+$ T helper cells to be discovered were T helper 17 (T_H17). These were cells that produced IL-17 in response to IL-23 and did not produce the normal T_H1

or T_H2 cytokines, despite lowly expressing T-bet and GATA3. Furthermore, it was found that conventional T_H1 and T_H2 cytokines, IFNγ and IL-4, suppressed T_H17 differentiation (Harrington et al., 2005, Park et al., 2005). Similar to the *in vitro* studies performed on T_H1 and T_H2 cells, *in vitro* experiments showed that naïve $CD4^+$ T cells would differentiate into T_H17 cells upon stimulation of the TCR when provided with IL-6 and TGFβ (Bettelli et al., 2006, Mangan et al., 2006, Veldhoen et al., 2006). Despite T_H17 cells expressing T-bet and GATA3 at low level, it was found that the main transcription factor to control the differentiation of naïve $CD4^+$ T cells into T_H17 cells was the orphan nuclear receptor RORγt (Ivanov et al., 2006).

Finally, the final major subset of T helper cell to be discovered were regulatory T cells (T_{regs}). T_{regs} are known to express CD25, whereas other differentiated T cell subsets do not express CD25 (Sakaguchi et al., 1995). However, it was not until years later when the transcription factor Foxp3 would be discovered to be the master transcription factor to regulated the differentiation into natural T_{regs} (nT_{regs}) (Hori et al., 2003, Fontenot et al., 2003). This was further proved in mice suffering from the autoimmune disease scurfy and from human IPEX patients, both of which have mutations in their *Foxp3* gene and therefore lack the presence of any $CD4^+$ $CD25^+$ T_{regs}. Again, *in vitro* studies were carried out to how that TGFβ was essential for the differentiation of naïve $CD4^+$ T cells into $Foxp3^+$ $CD4^+$ T cells. These TGFβ driven T_{regs} develop without the presence of proinflammatory cytokines and the TGFβ has been shown to work in a positive feedback mechanism to drive T_{regs} to differentiate. These T_{regs} were coined as induced T_{regs} (iT_{regs}) (Chen et al., 2003).

The differentiation pathway of the main four subsets of $CD4^+$ T helper cell from a naïve $CD4^+$ T cell is summarised in the Figure 2:

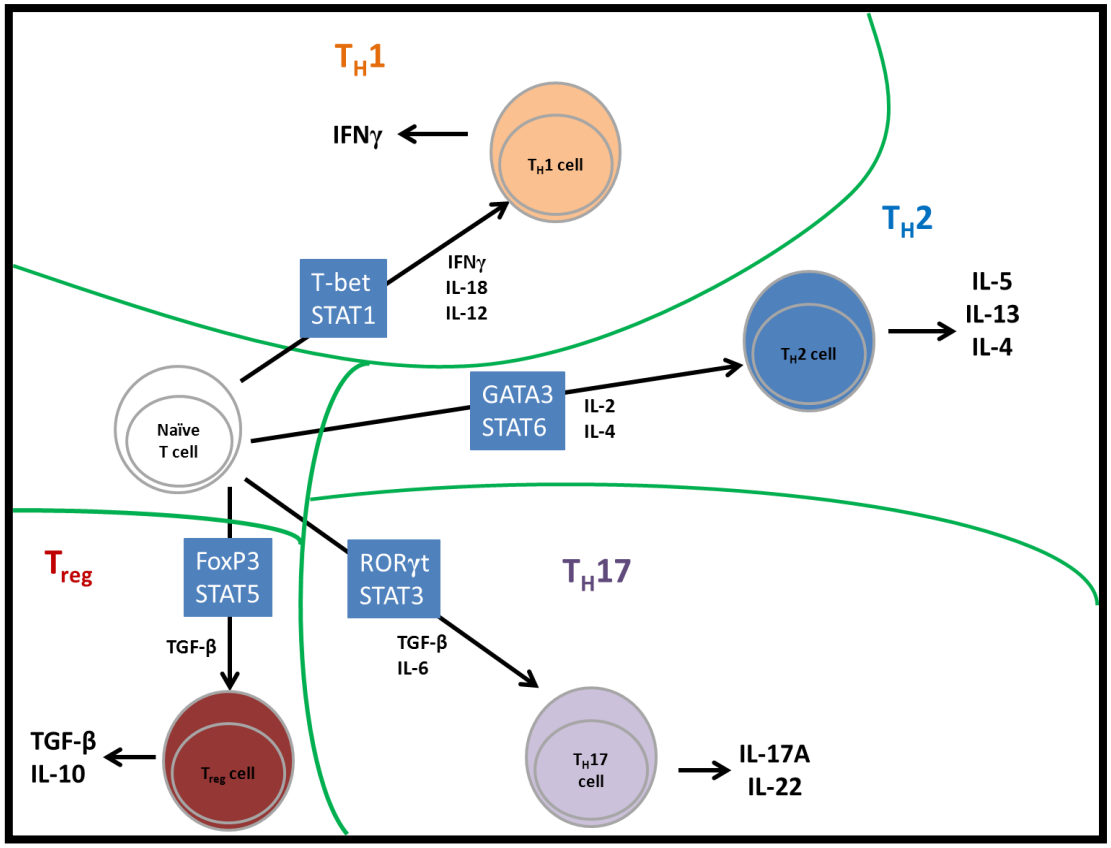

Figure 2: Schematic diagram showing the differentiation pathway of naïve CD4$^+$ T cells into helper T cells
Schematic showing the requirements for naïve CD4$^+$ T cells to differentiated into the four different subsets of T helper cell, adapted from (Lazarevic et al., 2013).

As can be seen on the schematic, T helper cells, not only require transcription from the master transcription factors that control each subset, but also rely on the activation and repression of STATs in order to activate these transcription factors to begin with. The JAK-STAT pathway involves both a canonical and non-canonical pathway. In the canonical pathway of JAK-STAT activation, when the receptor recognises its respective ligand, for example a cytokine, the receptor becomes dimerized (Li, 2008). This dimerization leads to activation of receptor-associated JAK kinases (Seif et al., 2017, Villarino et al., 2015, Bright and Sriram, 1998, O'Shea and Murray, 2008, Li, 2008). The activation of JAK kinases phosphorylates tyrosine residues in the tail of the receptors. The phosphor-tyrosine residues work as a docking region for STAT proteins, which become phosphorylated by JAKs. Phosphorylated STAT proteins also then dimerize via Src-homology 2 (SH2)-domain–phospho-tyrosine interactions and these dimerized phosphorylated STATs then translocate to the nucleus, where they activate transcriptional activators, inducing expression of target genes, for example T-bet or GATA3 (Levy and Darnell, 2002, Li, 2008, O'Shea and Murray, 2008).

In T_H1 cells, IFNγ receptor (IFNγR) and IL-12 receptor (IL-12R) are both dependent on the expression of T-bet after TCR signalling via STAT1 and STAT4 respectively in naïve $CD4^+$ T cells (Mullen et al., 2001, Schulz et al., 2009, Szabo et al., 2000, Thieu et al., 2008). As said already, T_H2 cells require STAT6 and is highly upregulated after the induction of IL-4 on the IL-4R (Takeda et al., 1996, Zhu et al., 2001). T_H17 cells need STAT3 activation and are activated by IL-6, IL-21 and IL-23, and increased STAT3 activation has shown to have an increase in the number of T_H17 cells present (O'Shea et al., 2011). Lastly, STAT5 expression is highly necessary for T_{reg} differentiation. Mice that were deficient for STAT5, were unable to survive and it was found that STAT5 was important in regulating Foxp3 (Burchill et al., 2007, Yao et al., 2007).

With this background knowledge of T cell differentiation, it was initially believed that each subset was terminally differentiated. However, it has since been found that the T helper cell subsets are able to switch on and off the different master transcription factors that control them, even after initial differentiation. Therefore, it has since been found that T-bet has a role in the other T helper subsets as well as just controlling T_H1 differentiation.

1.4.2 The role of T-bet in T_H1 cells

As explained previously, T-bet is induced when naïve $CD4^+$ T cells are activated by their TCR, IFNγ and IL-12. IL-12 activates STAT4 signalling which further induces more T-bet expression. The IFNγ production from T_H1 functions as a positive feedback to also enhance T-bet expression within these T_H1 cells via STAT1 signalling.

Zhu et al., used a T-bet reporter mouse line, whereby a ZsGreen (an improved variant of the fluorescent green protein) coding region was inserted in the start of the T-bet translational site of the bacterial artificial chromosome (BAC) clone (Zhu et al., 2012). They found using this mouse line that ZsG protein would be expressed but not the complete T-bet protein from the BAC meaning that T-bet can continue to be expressed from the endogenous *Tbx21* gene. They found a few different fundamental properties regarding T-bet expression using this green reporter mouse. Firstly, the induction of T-bet was not actually required for its own autoregulation, if IL-12 or IFNγ were present (Zhu et al., 2012). They also found that self T-

bet expression was found to induce itself in IL-12 and IFNγ independent pathways (Zhu et al., 2012).

As well as T-bet inducing T_H1 cells to produce IFNγ, T-bet was found to have a major role in the creation of transcriptionally able T_H1 cell-specific genes in $CD4^+$ T cells (Lazarevic et al., 2013). T-bet has been shown to modify the chromatin in the genome. T-bet recruits enzymes that creates chromatin histone modifications by either activating genes, with H3 or H4 acetylation and H3 lysine demethylation, or repressing genes with H3K27 trimethylation (Miller Sara and Weinmann Amy, 2010). T_H1 polarised cells have been shown to increase expression at gene loci, which are known to be positively regulated by T-bet. Whereas, T-bet repression of genes in T_H1 cells were observed by H3K27 trimethylation repression (Hatton et al., 2006). T-bet has been shown to bind to the promotor region of the *Ifng* gene causing remodelling of the *Ifng* locus by epigenetic chromatin modifications as described above. Additionally, it was observed that T-bet binds to enhancer regions downstream of the *Ifng* gene (Hatton et al., 2006). The *Ifng* gene has been shown to be more enhanced by H2.0-like homeobox protein (HLX) and the run-related transcription factor 3 (RUNX3) (Djuretic et al., 2006). Both of these proteins are mediated by transactivation of T-bet in T_H1 cells (Djuretic et al., 2006).

CCCTC-binding factor (CTCF) is a highly conserved zinc finger protein and is involved in the transcriptional regulation, insulator activity and regulations of the chromatin architecture (Phillips and Corces, 2009). In T_H1 cells, T-bet also organises the three-dimensional architecture of *Ifng* locus promoting definite *Ifng* expression. It achieves this by enhancing the binding of CTCF (Phillips and Corces, 2009) to the *Ifng* locus (Sekimata et al., 2009). The binding of T-bet to this location causes looping of the CTCF-dependent chromatin and in turn brings T-bet-binding enhances and the CTCF-binding region closer together at the promotor region of *Ifng* (Sekimata et al., 2009). This change in configuration by T-bet promotes *Ifng* expression in T_H1 cells.

However, T-bet not only drives the *Ifng* gene expression but also directing activates half of T_H1 cell-specific genes. These range from cytokines, such as IFNγ and TNFα, chemokines, like CC-chemokine ligand 3 (Ccl3) and Ccl4, and chemokine receptors, for example CXCR3 and CCR5. These are essential for effective immune function and migration of T_H1 cells (Thieu et

al., 2008, Jenner et al., 2009, Lord et al., 2005). However, T-bet expression can also indirectly drive the differentiation of other $CD4^+$ T helper cells. In T-bet knockout mice, an increase in T_H2 and T_H17 cytokines and transcription factors have been witnessed (Lazarevic et al., 2010, Szabo et al., 2000). This suggested that T-bet has a role in inhibiting the other $CD4^+$ T helper cells.

1.4.3 The role of T-bet in T_H2 cells

In comparison with T-bet for T_H1 cells, GATA3 has been found to be the master transcription factor for T_H2 cells. However, GATA3 is expressed in naïve $CD4^+$ T cells, unlike with T-bet expression. When naïve $CD4^+$ T cells are activated, the genomic transcripts cause non-selective histone acetylation of T_H1 and T_H2 genes (Avni et al., 2002). Therefore, during the initial activation of the naïve $CD4^+$ T cell, T-bet and GATA3 gene expression compete to become their respective subtype. Hwang et al., showed that T-bet was able to inhibit GATA3 expression in T_H2 cells. T-bet and GATA3 interact when TCR activation coupled with IL-2-inducible T cell kinase (ITK)-mediated phosphorylation of T-bet occurs (Hwang et al., 2005). Furthermore, they showed that T-bet binding to RUNX3 causes T_H2 inhibition (Kanhere et al., 2012, Djuretic et al., 2006, Hwang et al., 2005). Zhu et al., further showed that in T_H1 cells T-bet binds to the GATA3 gene locus and causes the promotion of repressive chromatin modifications, resulting in less GATA3 expression.

As well as T-bet being able to control the initial differentiation of T_H2 cells, there have also been studies showing that $CD4^+$ T cells can be redirected into other helper T cell lineages with the expression of the master transcription factors. T_H1 and T_H2 cells have been shown to counter each other during differentiation, where IFNγ production inhibits T_H2 cytokines and the reverse has also been shown that IL-4 stops the IFNγ and IL-12 production (Fiorentino et al., 1989). However, differentiated T_H1 and T_H2 cells have also been shown to be plastic (Hegazy et al., 2010). Hegazy et al. showed that in infections of *Lymphocytic choriomeningitis* virus (LCMV) differentiated T_H2 cells were able to become more T_H1-like when cultured *in vitro* with IL-12 and IFNγ. The *in vitro* cells expressed both GATA3 and T-bet (Hegazy et al., 2010). *In vitro* studies, performed by Sundrud et al, have shown that when $CD4^+$ T cells are cultured in T_H1 skewing conditions to form polarised T_H1 cells are placed into T_H2 polarising media, this causes a promotion of T_H2 cell phenotypes in these initially skewed T_H1 cells.

Furthermore, proof of T_H1-T_H2 plasticity has been shown by the conversion of T_H1 polarised cells into a more T_H2 polarised subtype when GATA3 was overexpressed. The opposite happened in T-bet overexpressed T_H2 skewed cells, with them becoming T_H1-like (Sundrud et al., 2003). *In vivo* studies by Murphy et al., showed that T_H1 $CD4^+$ T cells were able to produce both T_H1 and T_H2 cytokines in infections of *Leishmania major*. These T_H1 differentiated $CD4^+$ T cells produced IFNγ *in vivo*, however when they were presented with IL-2 and IL-4 *ex vivo* the T_H1 $CD4^+$ T cells appeared to have a T_H2 phenotype (Murphy et al., 1996).

1.4.4 The role of T-bet in T_H17 cells

The master transcription for T_H17 cells is RORγt, which controls the differentiation of the naïve $CD4^+$ T cell to commit to the T_H17 lineage (Ivanov et al., 2006). However, it has been found that T_H17 cells also express both T-bet and GATA3 at low levels (Wilson et al., 2009). T_H17 cells, especially under inflammatory conditions, have shown to be able to produce IFNγ (Harbour et al., 2015). Therefore, T-bet has a role in both directing the differentiation of T_H17 in conjunction with RORγt and is able to plastically convert T_H17 cells into T_H1-like cells. In naïve $CD4^+$ T cells, T-bet has been shown to block RUNX1 induced commitment to T_H17 cells and in T-bet knockout mice, a larger proportion of T_H17 cells producing IL-17A, IL-17F and IL-21 was observed when $CD4^+$ T cells were skewed towards T_H17. Further studies have shown that Runx expression drove the development of IFNγ production in T_H17 cells and T-bet and STAT4 were also induced in these cells. However, it was shown that the STAT4 was not vital, and the T-bet expression was more important, to produce maximum IFNγ from these cells (Wang et al., 2014).

T_H17 have also been shown to behave plastically with the ability to convert into T_H1- and T_H2-like phenotypes. *In vitro* experiments have shown that TGF-β and IL-6 derived T_H17 cells can become IL-12-producing T_H1 or IL-4-producing T_H2 cells due to the ability of T_H17 cells to express both T-bet and GATA3 (Wilson et al., 2009). Furthermore, Wilson et al. found that T-bet and RORγt have been shown to be co-expressed in T_H17 cells, which produce both IFNγ and IL-17A. During disease response and autoimmunity, T_H17 cells have shown plasticity. The conversion of T_H17 into a T_H1-like phenotype has been shown to cause diabetes, arthritis and IBD and blocking IFNγ can reduce the disease phenotype in animal models (Bending et al., 2009, Globig et al., 2014, Nistala et al., 2010, Reinert-Hartwall et al., 2015, Garrido-Mesa et

al., 2013). A model of experimental autoimmune encephalomyelitis (EAE), using a lineage fate mapped IL-17A mouse, was able to identify subsets of "ex-T_H17" cells which were responsible for IL-17A production in the spinal cord producing the EAE (Hirota et al., 2011).

1.4.5 The role of T-bet in T_{regs} cells

Despite the main function of T_{regs} being to control the proinflammatory cytokines produced by the other T helper subsets, T-bet has been shown to have a role in T_{regs}. Foxp3 is the main transcription factor responsible for naïve $CD4^+$ T cell differentiation into T_{regs} (Fontenot et al., 2003). This was mainly observed in induced T_{regs} (iT_{regs}) in the periphery. Koch et al. found that the T-bet was expressed in iT_{regs} during T_H1 driven inflammation and the gene locus itself was open (Koch et al., 2012, Koch et al., 2009a, Koch et al., 2009b). They also found that when T-$bet^{-/-}$ T_{regs} were transferred into recipient scurfy mice, which lack their own functional T_{regs} due to scurfy mice having a mutation in Foxp3, they were unable to overcome a T_H1 mediated disease phenotype. However, it is still poorly known how T-bet is able to control the function of iT_{regs} and how T-bet and Foxp3 are regulated in the genome when both are expressed in iT_{regs}. But, Koch et al. have shown that the expression of T-bet in iT_{regs} is expressed a lot lower compared to the expression of T-bet in T_H1 cells (Koch et al., 2009b). Therefore, full T_H1 cell differentiation does not occur in iT_{regs}, and low levels of T-bet expression is maintained by silencing the *Il12rb2* locus. But, iT_{regs} have shown to require T-bet expression to induce CXCR3 expression and aid their migration, thus migrating and suppressing T_H1 mediated inflammatory responses (Koch et al., 2009a, Pandiyan and Zhu, 2015, Tan et al., 2016a).

Lastly, as well as expressing T-bet, T_{regs} also have plasticity with T_H17 cells. T_H17 and T_{regs} are both activated by TGFβ and therefore during differentiation, and even afterwards, are both able to co-express Foxp3 and RORγt (Lee et al., 2009). During differentiation, the determining factor that causes intermediate $Foxp3^+ROR\gamma t^+$ cells to either differentiate into T_H17 or T_{regs} are the cytokine environment in which they are present. Much research has been performed to show that proinflammatory cytokines from T_H17 impedes T_{regs} and IL-10 from T_{regs} prevents conversion to T_H1 and T_H17 (Chen et al., 2007b, Josefowicz and Rudensky, 2009). When taken *ex vivo* into IL-6 media, T_{regs} have been shown to convert to T_H17 and produce IL-17A. Furthermore, a proportion of T_H17 cells have been shown to be from Foxp3 iT_{regs} within the intestinal mucosa (Weaver et al., 2006).

1.4.6 The role of T-bet in formation of $CD4^+$ memory cells

Although much is known about the differentiation and plasticity of effector $CD4^+$ T cells, not much has been reported on $CD4^+$ memory T cells. Therefore, a defined role of T-bet in $CD4^+$ memory cell formation is even less well documented. However, T_H1 effector $CD4^+$ T cell have been shown to require T-bet to develop into memory $CD4^+$ T cells. In T_H1 cells two subsets have been identified using the expression of Ly6C, with either $Ly6C^{hi}$ or $Ly6C^{low}$ cells. Both of these subsets of T_H1 effector cells also express P-selectin glycoprotein ligand 1 (PSGL1) (Lazarevic et al., 2013). T_H1 $PSGL1^+$ $Ly6C^{hi}$ cells were the fully differentiated effector cell and $PSGL^+$ $Ly6C^{low}$ cells were found to be T_H1 memory cells (Marshall et al., 2011). Marshall et al. also found that $PSGL1^+Ly6C^{hi}$ cells had higher expression of T-bet, IFNγ, granzyme B and CXCR3 whereas $PSGL1^+Ly6C^{low}$ had lower levels of T-bet expression. They also showed that T-bet expression was graded, whereby increased T-bet expression was essential for the $PSGL1^+$ $Ly6C^{hi}$ to proliferate and fully differentiate and lower T-bet expression was necessary to form $PSGL^+$ $Ly6C^{low}$ memory cells (Marshall et al., 2011).

1.5 The role of T-bet in $CD8^+$ T cell function and memory $CD8^+$ formation

The main function of $CD8^+$ T cells, or cytotoxic T cells, are to remove intracellular pathogens and viruses by producing IFNγ in response. $CD8^+$ T cells are also able to lyse cells during an infection by secreting cytotoxic granules containing granzyme B and perforin. However, it was originally found that despite T-bet being expressed in $CD8^+$ T cells, it is not necessary to drive their IFNγ production (Szabo et al., 2000). It has been found that $CD8^+$ T cells require both T-bet and Eomes. When $CD8^+$ T cells have both T-bet and EOMES knocked out, they are unable to function properly. $T\text{-}bet^{-/-}$ $Eomes^{-/-}$ $CD8^+$ T cells were found to produce minimal IFNγ and also were unable to clear lymphocytic choriomeningitis virus (LCMV) infection (Intlekofer et al., 2005).

Furthermore, T-bet and EOMES together have been found to have a role in generating memory $CD8^+$ T cells (Joshi et al., 2011, Intlekofer et al., 2005). Like $CD4^+$ T cells, when the TCR is stimulated in $CD8^+$ T cells, T-bet expression is quickly upregulated. Afterwards, short-lived effector cells, or SLECs, become fully differentiated due to the enhancement and preservation of STAT4-mediated mTOR kinase activity from strong IL-12 receptor signals (Rao et al.,

2010). This results in the induction of T-bet expression and EOMES repression by inhibiting FOXO1 (Takemoto et al., 2006). After an infection is cleared from the system, many of the effector $CD8^+$ T cells die. Memory precursor effector cells (MPECs) have been described as the small proportion of effector $CD8^+$ T cells that survive apoptosis. They require both IL-7 and IL-15 in order to survive. T-bet was shown to suppress IL-7R and has been found to cause a switch from effector memory cell to central memory cell in $CD8^+$ T cells (Intlekofer et al., 2007). Joshi et al. also reported that in $CD8^+$ T cells the expression of T-bet decreases and Eomes expression increases to form MPECs. However, T-bet expression is still required at low levels in MPECs to maintain induction of CD122, thus allowing for the survival and future proliferation of memory $CD8^+$ T cells (Intlekofer et al., 2005, Joshi et al., 2011).

1.6 The role of T-bet in B cells

Since certain subsets of B cells are able to produce IFNγ in response to viral infection, T-bet expression was highly likely in B cells. Peng et al. found that T-bet had a role in B cells to generate IgG2A antibodies during class switching (Peng et al., 2002). IgG2A is the most abundant immunoglobulin isotype produced during bacterial and viral infections. During class switching, T-bet in B cells induces the expression of Iγ2a transcripts, thus aiding in the switching to an IgG2A class (Peng et al., 2002, Barnett et al., 2016, Myles et al., 2017).

As well as class switching, T-bet has also had a role in promoting IgG2A B cell memory survival. It achieves this by regulating STAT1 transcription in IgG2A B cells (Wang et al., 2012).

1.7 The role of T-bet in γδ T cells

γδ T cells are a type of T cell that develops from the thymus during the same double negative stages as CD4 and CD8 T cell development, as described before in Chapter 1.1.2. γδ T cells are a small population of immune cell and in humans, at healthy steady state there are typically around 3-5% found in the peripheral blood (Kobayashi and Tanaka, 2015). Naïve γδ T cells have been shown to not require T-bet expression to mature, but only express T-bet upon γδ TCR activation (Yin et al., 2002). This IFNγ production has been found to the regulated by inducible T-bet and constitutive EOMES expression (Chen et al., 2007a). T-bet expression is

important for the IFNγ production function of $CD27^+$ IFNγ-producing γδ T cells and in T-$bet^{-/-}$ mice only half the normal proportion of $CD27^+$ IFNγ-producing γδ T cells were found (Chen et al., 2007a). Other work by Sumaria et al. showed that there are T-bet^+ expressing $CD24^-$ γδ thymocytes located in the thymus of mice. These IFNγ-committed $CD45RB^+$ cells gradually express T-bet but not RORγt, compared to the IL-17A-committed $CD44^{hi}CD45RB^-$ γδ thymocytes that express RORγt but not T-bet (Sumaria et al., 2017).

1.8 The role of T-bet in NKT cells

NKT cells, like γδ T cells, are another small population of immune cell. They express both a CD3 associated TCR and a few of the typical NK cell markers, like NK1.1, CD122 and some of the Ly49 markers (Matsuda et al., 2006). The TCR in NKT cells is a semi-invariant TCR which comprises of a Vα14-Jα18 rearrangement, which usually associates with either Vβ8, Vβ7, or Vβ2. NKT cells recognise glycolipids by MHC class I-like CD1d (Godfrey et al., 2005, Lantz and Bendelac, 1994). T-bet expression is required for iNKT development and maturation in the thymus (Townsend et al., 2004). In T-bet-deficient mice, the number of iNKT cells are markedly decreased. As CD122 is a target gene of T-bet and aids in the survival of cells, the T-$bet^{-/-}$ iNKT cells are unable to survive (Matsuda et al., 2006, Townsend et al., 2004). However, the remaining iNKT cells that were present in the T-$bet^{-/-}$ mice were still fully functioning and able to produce IL-4 and IL-13 to cause airway hyperreactivity.

1.9 The role of T-bet in NK cells

Szabo et al. not only discovered that T-bet was the master transcription factor in $CD4^+$ T cells, but T-bet was also highly expressed in NK cells (Szabo et al., 2000). Since then, the role of T-bet has been found to be important in regulating the development and terminal maturation of NK cells (Gordon et al., 2012, Townsend et al., 2004). However, both groups found that T-bet was not solely responsible for NK cell development. In T-$bet^{-/-}$ mice, there is a marked reduction in the number of NK cells, but they are not completely removed. Therefore, they found that NK cells also relied on Eomes expression, and when T-bet was deleted, Eomes expression was able to compensate (Gordon et al., 2012, Townsend et al., 2004). Furthermore, TNF-related apoptosis inducing ligand (TRAIL) expression in developing immature NK cells was reliant on T-bet expression. However, upon maturation and subsequent loss of TRAIL,

Eomes was shown to be more essential in NK cells (Gordon et al., 2012, Townsend et al., 2004). Soderquest et al. further found that in T-bet$^{-/-}$ mice, NK cell were unable to progress from the CD27^{hi} CD11b^{hi} stage (Soderquest et al., 2011).

1.10 The role of T-bet in dendritic cells

Dendritic cells (DCs) are antigen presenting cells (APCs), which function to present antigen to naïve CD4^{+} T cells via MHCII or naïve CD8^{+} T cells via MHCI. However, DCs have also been shown recently to be able to produce IFNγ themselves and also express T-bet. T-bet expression in DCs was also found to be essential in efficiently priming T_H1 cells, and Lugo-Villarino et al. showed that during *Listeria* infection experiments, T-bet$^{-/-}$ DCs were unable to mount an effective immune response with adjuvant activity of CpG DNA compared with normal wildtype DC cells treated with the same (Lugo-Villarino et al., 2005).

T-bet expression in DCs play an important role in gut inflammation. In mice that have had both T-bet and the RAG2 gene knocked out, spontaneous colitis was observed and have since been named TRUC (*Tbx21*$^{-/-}$*Rag2*$^{-/-}$ulcerative colitis) mice, due to the colitis resembling human ulcerative colitis (Garrett et al., 2007). This model of colitis was driven by the microbiota of the mice, namely *Helicobacter typhlonius* and mice that lacked this pathogen were protected from colitis. This colony of mice that did not generate colitis were named TRnUC (*Tbx21*$^{-/-}$*Rag2*$^{-/-}$ no ulcerative colitis) (Powell et al., 2012). T-bet has been shown to regulate TNFα production in colonic DCs. In TRUC mice, there is an increase in TNFα production from CD103^{-} CD11b^{+} colonic DCs. The production of TNFα results promotes apoptosis and epithelial cell permeability, this allowing the microbiota to infiltrate and cause an inflammatory response (Garrett et al., 2007). Anti-TNFα antibodies have shown to be able to prevent and reverse the disease pathology (Lazarevic and Glimcher, 2011, Mohamed and Lord Graham, 2016). However, in TRUC mice, TNFα blockade only alleviates the disease up to twelve weeks. Therefore, in the TRUC mice, another innate cell drives the disease after this period. ILC3s have since been found to be cell which mediates the disease in TRUC mice after TNFα-mediated inflammation and will be discussed in more detail below (Powell et al., 2012).

1.11 The role of T-bet in innate lymphoid cells

Recently a novel cell type was discovered named innate lymphoid cells (ILCs). It has been reported by many groups that ILCs share many functional, differential pathways and genomic characteristics with $CD4^+$ helper T cells. The main difference between ILCs and $CD4^+$ T cells are that ILCs do not respond to antigens as ILCs lack a somatically rearrangeable receptor like in T and B cells. ILCs also lack typical cell lineage markers used to identify other immune cell types. They have been found to express CD25 and IL7-R (Artis and Spits, 2015, Diefenbach et al., 2014, Spits et al., 2013). The ILCs consist of ILC1s, which also includes NK cells, ILC2 and ILC3s, which also includes LTi cells. ILCs are mainly tissue resident immune cells and have been found mainly in mucosal barrier sites, as well as in immune surveillance organs, like the liver and spleen.

1.11.1 ILC differentiation and the differences between subsets

ILC1s have been shown to be like T_H1 cells, where both express T-bet and produce IFNγ and TNFα. ILC1s, like T_H1, also respond to intracellular pathogens (Fuchs et al., 2013, Bernink et al., 2017, Klose et al., 2014). ILC1s also require IL-12 cytokine stimulation, like T_H1 cells, and upon activation are potent producers of IFNγ. Since the discovery of ILCs, NK cells have also been grouped into ILC1s and are often described as "cytotoxic ILC1s". ILC1s have been shown to be phenotypically different depending on which tissue they reside in. The three main tissue-specific ILC1s are: liver ILC1s, thymic ILC1s and intestinal ILC1s. Liver ILC1s are distinct from liver NK cells by their differing expressions of CD49b and TRAIL, whereby ILC1s are $TRAIL^+$ $CD49b^-$ and NK cells are $TRAIL^-$ $CD49b^+$ (Takeda et al., 2005, Tang et al., 2016). Liver ILC1s do not circulate through the body and instead only reside within the liver (Peng et al., 2013).Thymic ILC1s were generated both *in vitro* and *in vivo* from the double negative 1 subset of cells (Vargas et al., 2011). Thymic ILC1s again differ to normal NK cells, as they require GATA3 to develop and express IL-7R. (Vosshenrich et al., 2006). Thymic ILC1s mimic liver ILC1s though, in that they both express Ly49 at low levels and are $CD69^{high}$ and $CD11b^{high}$ (Seillet et al., 2016). Lastly, ILC1s found in the intestine do not require IL-15R activation for development or survival (Fuchs et al., 2013). Fuchs et al. identified intraepithelial ILC1s as $CD56^+$ within the non-T cell gate in the tonsils. They found that intraepithelial ILC1s also expressed CD160, CD49a, CXCR6, CD69 and CD39 (Fuchs et al., 2013).

ILC2s have similarities to T_H2, whereby both express GATA3 and produce IL-4, IL-5 and IL-13. Both cell types also require the stimulation from IL-25, IL-33 and thymic stromal lymphopoeitin (TSLP) to become activated. They also require the expression of amphiregulin, which is an epidermal growth factor receptor ligand. Comparatively with T_H2 cell, ILCs respond to helminth infection, allergens and are involved in tissue repair (Mjösberg et al., 2011, Monticelli et al., 2011, Price et al., 2010). The production of IL-4, IL-5 and IL-13 from ILC2s promotes the recruitment of neutrophils and eosinophils to sites of inflammation. Similar to ILC1s, different subsets of ILC2s exist depending on where the ILC resides. There are four subtypes of ILC2s: natural helper ILC2s, nuocytes, innate helper ILC2s and multipotent progenitor (MPP) ILC2s. Natural helper ILC2s typically express c-Kit, Sca-1, IL-33R and IL-25R and are predominantly found in adipose tissue in fat-associated lymphoid structures (Moro et al., 2009). Nuocytes, like natural helper ILCs, express c-kit, Sca-1, IL-33R and IL-25R, but they also express ICOS. Nuocytes are classically found residing in the mesenteric lymph nodes, intestines and lungs (Licona-Limón et al., 2013). Nuocytes have been shown to be highly activated producers of IL-13 in response to helminth infections (Neill et al., 2010). Innate helper ILC2s are found in the spleen, liver and mesentries and express similar surface markers to nuocytes and natural helper ILCs, except they lack the IL-25R marker. Lastly, MPP ILC2s are found in the gut only and appear to be a separate subtype of ILC2 compared with natural helper ILC2s, nuocytes and innate helper ILC2s. The expression of surface markers on MPP ILC2s are different from the other ILC2 subsets too. They do not express ICOS or CD25 and have been found to have intermediate expression of c-kit and IL-33R. They are still Sca-1^+ and IL-$25R^+$ though, and it is the presence of IL-25, which has been observed to drive the proliferation of the MPP ILC2 population in the gut (Saenz et al., 2010).

ILC3s resemble T_H17 cells, as they both express RORγt and produce IL-17A and IL-22 in response to microbiota pathogens in the mucosa. ILC3s are generally found in mucosal tissue, mainly in the intestines and lungs. In comparison to T_H17 cells, a subset of ILC3s also express T-bet and produce IFNγ. Before ILCs were discovered, lymphoid tissue inducer (LTi) cells were thought to be a separate subset of cell, but since the discovery of ILCs, LTis have been grouped into the ILC3 category. LTis express CCR6 (Cella et al., 2008) and are found in the intestinal lamina propria forming clusters in the crypts of the intestine, which formed the peyers patches. The T-bet expressing ILC3s also express NK cell p46-related protein (NKp46) (Artis

and Spits, 2015, Bernink et al., 2017, Diefenbach et al., 2014, Spits and Cupedo, 2012). ILC3s respond to IL-1β, IL-23 (Melo-Gonzalez and Hepworth, 2017) and more recently IL-6 (Powell et al., 2015). Nkp46^{+} ILC3s do not express CCR6 though. Despite this T-bet expression in ILC3s, the expression of RORγt is the most crucial for driving the development and differentiation of ILC3s (Luci et al., 2008, Sanos et al., 2008). The different types of ILC3s: LTi, NKp46^{-} ILC3s and NKp46^{+} ILC3s have different functions and role in the immune system.

The differentiation pathway of ILCs is summarised in Figure 3:

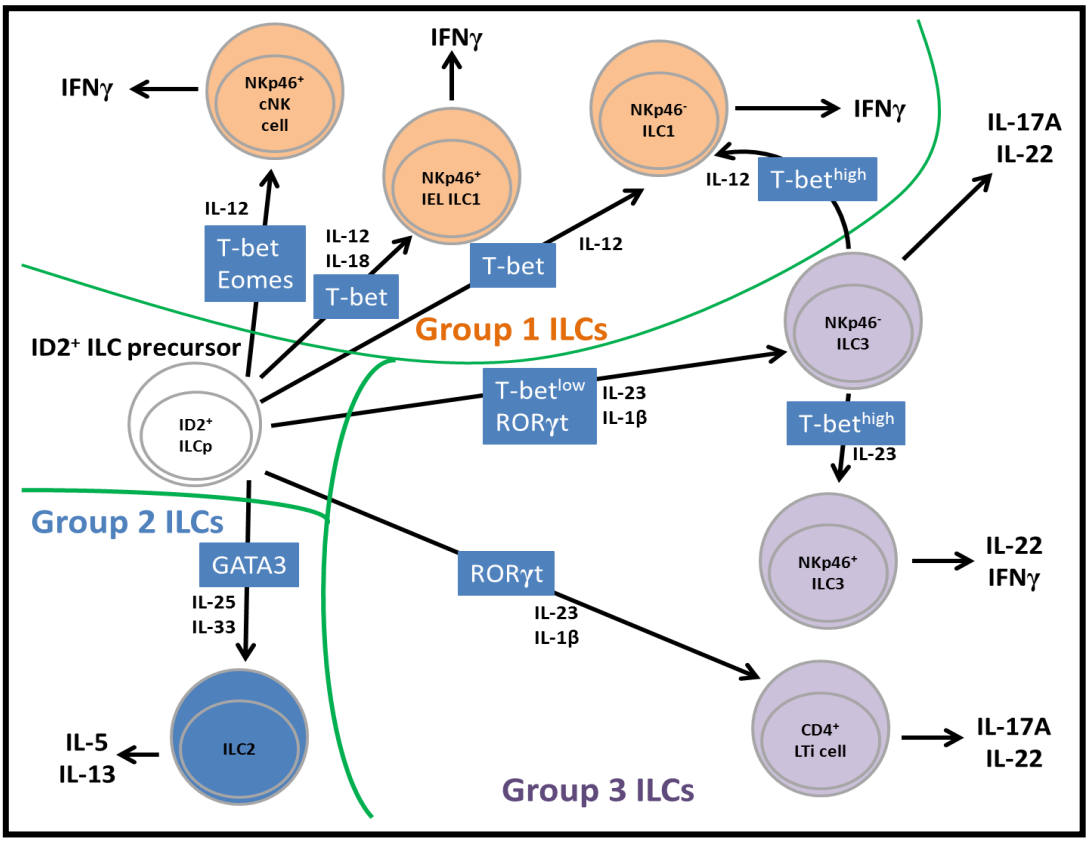

Figure 3: Schematic diagram showing the differentiation pathway of innate lymphoid cells

Schematic showing the requirements for ID2^{+} ILCp to differentiated into the different subsets of ILCs, adapted from (Lazarevic et al., 2013)

1.11.2 The role of T-bet in ILCs during mucosal immune responses

As well as being responsible for ILC1 differentiation and maintenance, T-bet has been shown to be expressed in ILC2s and ILC3s, like T-bet being expressed in T_H2 and T_H17 cells, to aid

plasticity of ILCs. ILCs have mainly been found to be necessary in mucosal immunity and are predominately found to be present in sites of mucosal immune barrier sites, for example the intestinal lamina propria. In TRUC mice, after twelve weeks of the disease, NKp46^{-} ILC3s produced increased amounts of IL-17A and IL-22 (Powell et al., 2012). Use of TRUC mice have allowed further understanding of the role T-bet has in ILCs. As explained above, after 12 weeks ILC3s drives the disease in TRUC mice. TRUC disease phenotypes were improved in mice either administered with an anti-CD90 antibody or when IL-23 blocking antibody was administered. The deletion of T-bet also prolongs the survival of ILC3s via increased expression of IL-7R (Mohamed and Lord Graham, 2016). The TRUC model has been a useful model for studying the role T-bet the regulation of mucosal inflammation in response to the microbiota in DCs and T-bet$^{-/-}$ ILC3s.

However, there is also an important role of T-bet in ILC1s and NKp46^{+} ILC3s in pathological immune responses in the mucosal tissue. ILC1s have been found to be highly involved in the immune response to *Clostridium difficile* (Abt et al., 2015) with their high production of IFNγ in response to the pathogen. ILC1s are also incredibly important in regulating the disease in Crohn's disease (Bernink et al., 2013). In coeliac disease, there also has been shown to be an increase in IFNγ producing ILC1s. Interestingly IFNγ therapy in IBD trials were unable to treat the disease (Kortekaas Krohn et al., 2017). ILCs have been observed to be incredibly plastic, especially with Nkp46^{+} ILC3s being able to express T-bet to become ILC1-like and produce IFNγ during mucosal inflammation (Rankin et al., 2013). Nkp46^{+} ILC3s switch due to the presence of IL-12, which causes the increased expression of T-bet via STAT4 expression, similar to the T_H17 switch to T_H1-like phenotype. ILC1s have been shown to be highly activated in the inflamed colonic lamina propria (cLP) in anti-CD40 induced colitis. The anti-CD40 colitis model in RAG$^{-/-}$ mice causes myeloid cells to become activated in the cLP and produce prolific amounts of IL-12, which in turn drives the ILC1s in the cLP to produce vast amounts of IFNγ and cause inflammation of the tissue (Buonocore et al., 2010, Powell et al., 2012, Uhlig et al., 2006).

As well as NKp46^{+} ILC3s being able to plastically switch to a T-bet expressing ILC1-like phenotype, ILC2s have been reported to be able to switch to ILC1-like properties too (Belz, 2016). As explained, IL-1 cytokines are heavily involved in the activation and stimulation of ILCs. IL-18, IL-33 and IL-1β for ILC1s, ILC2s and ILC3s respectively (Ohne et al., 2016).

Ohne et al. showed that ILC2 also express the IL-1R and can also be primed and stimulated by IL-1β. However, they also showed that IL-1β activation of the ILC2s is unable to cause the *Ifng* promotor to be upregulated and expressed. The ILC2s also required stimulation from IL-12 in order to express T-bet and produce IFNγ, whilst still expressing GATA3 (Ohne et al., 2016). Both Silver et al. and Bal et al. also showed that during airway inflammation ILC2s were able to switch to an ILC1-like phenotype under IL-1β and IL-12 conditions. These ILC1-like T-bet$^+$ ILC2s drove pathogenesis of the airway inflammation in their experiments (Bal et al., 2016, Silver et al., 2016)

These observations show that T-bet has a crucial role in ILCs, in not only the differentiation of ILC1s, but also in the plasticity of ILC subtypes to express T-bet in ILC2s and ILC3s to form ILC1-like cells. Furthermore, with the comparisons between ILCs and CD4$^+$ T cells, the role of T-bet in ILCs has shown even greater importance, especially during inflammatory responses.

1.12 Experimental mouse models of IBD

In humans, IBD is an inflammatory condition that affects the gastrointestinal (GI) tract. There are two main types of IBD: Crohn's Disease (CD) and ulcerative colitis (UC). UC typically only affects the colon but CD causes disease in any of the GI tract (Baumgart and Sandborn, 2007). Both CD and UC can relapse and remiss and have similar symptoms consisting and ranging from: diarrhoea, abdominal pain and rectal bleeding. Currently, there are only treatments for IBD but no cure. These treatments have emerged from studies with either animal models and then patient studies, resulting in clinical trials for specific immunomodulatory drugs and immunosuppression (Baumgart and Sandborn, 2007). With this lack of cure in mind, more mouse models have become vital in order to understand more about specific cell responses in mouse IBD-induced models. There are already around fifty well established and widely used mouse models of IBD (Uhlig Holm and Powrie, 2009, Mizoguchi, 2012). As quite a few different colitis models were used in this thesis, a brief overview of each of the IBD mouse models used will be given below.

As mentioned above, the TRUC model has been extensively used by this group already to study the role T-bet has in IBD, with respect to both DCs and ILCs. In this thesis, the non-spontaneous colitis model of TRnUC was used. However, there are other IBD models available

to study IBD. The other models used within this thesis were: The T cell transfer model, the DSS model, *Nippo* and *H. Poly* parasite infection models and lastly the anti-CD40 model.

1.12.1 The T cell transfer model

The T cell transfer (TCT) model is a very important model, which allows studying the naïve $CD4^+$ T cell response to foreign microbiota in the recipient mice. The TCT model also allows studies into the effect of T_{regs} on regulating the immune response from these transferred $CD4^+$ T cell (Eri et al., 2012). In 1993, Fiona Powrie first discovered the T cell transfer model as a viable model of IBD and further developed the model to be able to investigate the effectiveness of T_{regs} against $CD4^+$ T helper cell responses to IBD (Mottet et al., 2003, Powrie et al., 1993, Powrie et al., 1994). In this model, naïve ($CD4^+$ $CD25^-$ $CD62L^+$ $CD44^-$) CD4 T cells from wildtype mice are sorted and adoptively transferred into adaptive immune deficient $Rag^{-/-}$ mice. Care must also be taken to match gender and mouse genetic background in this model. The donor naïve T cells cause colitis in the $Rag^{-/-}$ mice by identifying the foreign intestinal microbiota antigens and cause severe gut inflammation in both the small intestine and colon. The activated CD4 T cells secrete high amounts of IFNγ and a smaller amount of IL-17A, both of which are proinflammatory and cause the gut inflammation observed in this model. The model normally takes about six to eight weeks to develop post injection. Histology from the colon typically shows excessive neutrophil and eosinophil infiltration, crypt destruction and transmural inflammation (Eri et al., 2012, Ostanin et al., 2009).

As mentioned above, co-transfer of the naïve $CD4^+$ T cells with $CD4^+$ $CD25^+$ T_{regs} into the *Rag*$^{-/-}$ mice allowed investigations into the interaction between the regulation of the inflammation of IBD by T_{regs}. It was found that the onset of colitis is prevented in this model when both naïve CD4 T cells and T_{regs} were transferred. However, it was also shown that the transfer of natural T_{regs} can overturn an established TCT colitis via an IL-10 dependent method (Izcue et al., 2006, Izcue and Powrie, 2008).

1.12.2 The DSS model

The dextran sodium sulphate (DSS) model is an acute model of colitis that has been used for around thirty years now. In 1985, Ohkusa et al. first published observations of DSS-induced

colitis that they have been able to induce in hamsters (Ohkusa, 1985). This led to more studies being established and induced in mice (Okayasu et al., 1990). The DSS model involves typically giving concentrations of 2-5% DSS in the drinking water for around 4-9 days. The variations in concentration, duration and even molecular weight of DSS have different effects (acute, chronic or relapsing colitis) on the mice. Different mouse strains, backgrounds and gut microbiota have also been found to have different susceptibility and disease outcomes (Perše and Cerar, 2012). The DSS model has shown to provide great insights into the clinical aspects of UC and the impact and outcome from the use of many therapeutic drugs used in human IBD treatments. DSS causes colitis in mice due its toxicity to the epithelial cells in the colon. This causes destruction and damage to the epithelial cells and the integrity of the epithelial layer itself becomes compromised. This ultimately causes the permeability of the mucosal layer to be increased and allows bigger molecules like DSS through the epithelial layer. The loss of the tight junctions in the colon occurs after the first day of DSS treatment and there is a marked increase in production of proinflammatory cytokines, like IFNγ, IL-17A, IL-6, IL-12, IL-13, TGFβ and TNFα, produced from $CD4^+$ T helper cells, B cells, macrophages and neutrophils (Ito et al., 2008, Ito et al., 2006, Kiesler et al., 2015). On day three, there is the first visible signs by histology of basal crypt damage and loss and an increase in infiltration by inflammatory cells like neutrophils and eosinophils. This immune response to the destruction of the epithelial layer during DSS treatment mimics human IBD in the physical cell damage of the colon and causing a dysregulation of the microbiota and the intestinal mucosa (Chassaing et al., 2014b, Eichele and Kharbanda, 2017, Kiesler et al., 2015, Perše and Cerar, 2012).

1.12.3 Parasite models: using *Nippo* and *H.Poly*

Parasitic infections can result in IBD in humans and therefore, there are many animal models that have been developed and used to investigate the effect of each parasite in causing colitis, and also during colitis. For this thesis, *Nippostrongylus brasiliensis and Heligomosomoides polygyrus* were used to test potential inflammatory T_H2 and ILC2 responses in the intestines. Experiments using the *Nippo* parasite infection were used to induce an IL-13 T_H2 response in these mice. IL-13 is induced more strongly than IL-4 and IL-5 in response to *Nippo* (Harvie et al., 2010, Urban et al., 1998). In *H. Poly* infections, by day three larvae have developed and positioned themselves in the wall of the small intestine. When the larvae become full adult parasites, their antigens are recognised and eventually expelled due to large production of IgG1

from B cells and IL-4 from $CD4^+$ T_H2 cells and ILC2s (Donskow-Łysoniewska et al., 2013, Mohammadi et al., 2015, Wahid and Behnke, 1992). These parasite models are important for being able to study the interactions between the immune system, and in particular T_H2 and ILC2 responses, to parasite infections.

1.12.4 The anti-CD40 model

The anti-CD40 model of colitis has been widely used by groups for around the last twenty years. This model of colitis was defined and established in 2006 by Holm Uhlig et al. (Uhlig et al., 2006). Although it had been previously shown by other groups that CD40-CD40L activation of myeloid cells caused T cells to become activated and produce proinflammatory cytokines like IFNγ, IL-12 and IL-23p40 in IBD. (Radtke et al., Watanabe et al., 2004, Luckett-Chastain et al., 2015, Liu et al., 1999, Liu et al., 2000, Uhlig et al., 2006). This had not been shown to influence the innate lymphocytes. However, when anti-CD40 is given to immune competent and complete mice, the anti-CD40 activated the B cells and the disease readouts were generally B cell driven (Blair et al., 2009). Therefore, in this model, an agonistic monoclonal antibody for anti-CD40 is injected via intraperitoneal injections into mice lacking an adaptive immune system, $Rag^{-/-}$ mice. In this system, there is a very acute onset of inflammation in the mouse (Uhlig et al., 2006). The mice develop both systemic inflammation, observed by splenomegaly and severe wasting disease, and local inflammation, observed by both colitis and hepatitis (Uhlig et al., 2006). In the $Rag^{-/-}$ mice, the main inflammatory cytokines responsible for this colitis model were IL-12 and IFNγ (Uhlig et al., 2006). The difference in background of the $Rag^{-/-}$, either Balb/c or C57BL/6, have different severities of disease and therefore different doses are required upon providing the anti-CD40. Since C57BL/6 background mice generally illicit a more T_H1 response and produce more IFNγ than IL-4, and Balb/c background respond more with T_H2 cytokines like IL-4 than IFNγ (Luckett-Chastain et al., 2015). These cytokine differences have also been seen to occur with the innate immune responses from the ILCs in these differing background mice (Watanabe et al., 2004). Therefore, the typical dose of the anti-CD40 drug for Balb/c $Rag^{-/-}$ mice is 125-150μg and for C57BL/6 $Rag^{-/-}$ mice is 25-50μg. The mice take around seven days to develop acute colitis, despite regaining weight from the wasting disease suffered during this time. The colitis remains and if further dosing is provided then the mice suffer further acute trauma and severe wasting disease. Figure 4 below shows the schematic of the CD40-CD40L interaction with an APC and

either T cells, NK cells or ILCs to cause the APC to produce IL-12, which in turn cause a positive feedback to produce more IFNγ (Uhlig et al., 2006). This anti-CD40 proves to be incredibly useful at defining the role played by APCs, T cells, ILCs and NK cells in developing and causing acute colitis.

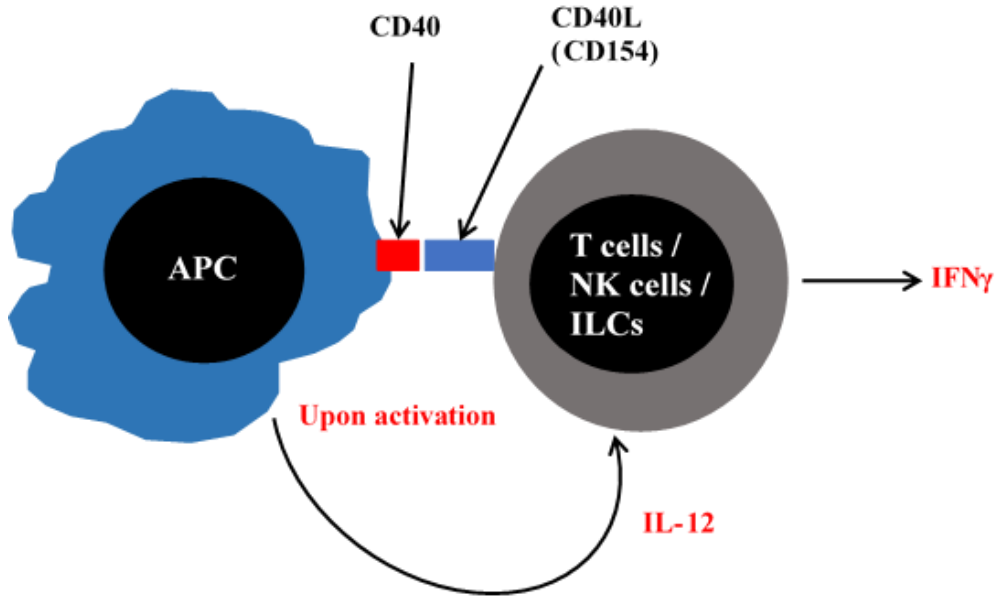

Figure 4: Schematic diagram showing the activation pathway of APCs with NK cells or ILCs via the costimulatory molecules CD40 and its ligand CD154 in the anti-CD40 model of colitis

Below is a summary table of the mouse models of IBD used throughout this project:

Summary table of the mouse models of IBD used		
Mouse Model	**Main result**	**References**
Knockout of T-bet and T and B cells (*Tbx21*$^{-/-}$ *x Rag2*$^{-/-}$ mice)	Mice develop spontaneous colitis within 4 weeks in a TNFα via DCs and IL-17 via ILC3s causing manner. Disease has been found to also be dependent on microbiota within the intestine and was mainly driven by *Helicobacter typhlonius*.	(Garrett et al., 2007, Powell et al., 2012)
Adoptive transfer of CD4^{+} T cells into Rag$^{-/-}$ mice	Mice develop colitis after 6-8 weeks of transfer of naïve CD4^{+} T cells. Main response comes from pathogenic	(Powrie et al., 1993, Powrie et al., 1994)

	effector T_H1 responses to pathogens in the intestine of the recipient mice.	
DSS chemical induced colitis	Like most chemically induced colitis, DSS disrupts the epithelial barrier of the intestinal mucosa causing inflammation, diarrhoea and bleeding and neutrophil infiltration. Both acute and chronic models can be induced depending on cycle of treatment. DSS can be performed on both immunocompetent and immunodeficient mice.	(Chassaing et al., 2014a, Ohkusa, 1985, Okayasu et al., 1990, Perše and Cerar, 2012)
Parasitic helminth models of IBD	Helminths, for example *Nippostrongylus brasiliensis* and *Heligomosomoides polygyrus* were used in this project. Immune responses to helminth have shown a switch to T_H2 or ILC2 immune responses, like IL-4, IL-5, IL-13, in both adaptive and innate immune system	(Elliott et al., 2007, Filbey et al., 2014, Harvie et al., 2010, Mohammadi et al., 2015, Reynolds et al., 2012)
Agonistic anti-CD40 activated induced colitis	Showed severe acute colitis develops after 7 days of intraperitoneal injections of the agonist anti-CD40 in immunodeficient (*Rag*$^{-/-}$ mice). Data showed colitis was caused from IFNγ NK cells and IL-17A from ILC3s driven by dendritic cells producing IL-12 and IL-23.	(Hue et al., 2006, Uhlig Holm and Powrie, 2009, Uhlig et al., 2006)

Table 1: Summary of the mouse models used in this project and the current known research on IBD

1.13 Hypothesis and aims

The hypotheses to be tested in this thesis are:

1. The expression of T-bet has been shown in many cell types, as described already, however the ontogeny of these T-bet expressing cells is still not fully known. Learning about where and when T-bet becomes expressed in developing cells will provide further insight into known T-bet expressing cells. Using a new T-bet fate mapping mouse line that can trace any cell, which previously has expressed T-bet. This thesis hypothesises that utilising this mouse line will be able to predict and identify the ontogeny of T-bet expressing cells within the immune system and will be able to classify any novel and previously unobserved T-bet expressing cells.
2. T-bet has already been shown to play a role in the plasticity of $CD4^+$ T cells in disease, as explained already above. This thesis will aim to test the hypothesis that certain subsets of plastic T_H17 cells are already pre-determined to become T_H1-like, by using the fate mapping mouse line. Furthermore, that temporal deletion of T-bet in $CD4^+$ T cells will cause a switch to more T_H2 and T_H17 settings.
3. T-bet has been shown to regulate CXCR3 expression in T_{regs}. Using a model of cardiac transplantation with $Foxp3^{cre}$ x $T\text{-}bet^{fl/fl}$ mice, the hypothesis that knocking T-bet from T_{regs} will not prevent cardiac transplant rejection.
4. T-bet expression has been shown to be important in anti-CD40 mediated ILC1 IFNγ driven colitis. Using the same colitis model, the hypothesis that administering anti-CD40 would drive acute hepatitis by IFNγ production from ILC1s and be dependent on T-bet.

The aims of this thesis, in order to address these hypotheses, are:

1. Characterise T-bet in immune cells, using a newly bred $T\text{-}bet^{cre}$ x $ROSA26^{fl/fl}$ mouse line that can identify and trace previously expressed T-bet expression in cells
2. Characterise the role T-bet has in differentiation of naïve $CD4^+$ T cells, using the newly bred mouse line
3. Characterise the role T-bet has in regulating the plasticity of $CD4^+$ T cells, using the newly bred mouse line
4. Characterise the role T-bet has in regulating other immune cell types during inflammation

Chapter 2

Materials and Methods

2.1 Animal husbandry

C56BL/6 wildtype (WT) (Charles River), BALB/c *Rag2*$^{-/-}$ (Jackson labs), C56BL/6 *Rag1*$^{-/-}$ (Jackson labs), *Rosa26*$^{YFP/+}$ (Jackson labs), Cre-*ER*^{T2} (Jackson labs) and CD45.1 (Jackson labs) were sourced commercially. *T-bet*$^{fl/fl}$ and *T-bet*$^{cre/+}$ mice were previously generated by our group (Gökmen et al., 2013, Garrido-Mesa et al., 2019) and made using Genoway. *T-bet*$^{cre/+}$ mice were then bred with *Rosa26*$^{YFP/+}$ to generate the *T-bet*$^{cre/+}$ *Rosa26*$^{YFP/+}$ line and subsequent genotyping was performed to check for usability. Foxp3^{gfpcre} mice were generously given to us by A. Rudensky, which were then bred with the *T-bet*$^{fl/fl}$ line and subsequent genotyping was performed to check for usability. Cre-*ERT2* were bred with the *T-bet*$^{fl/fl}$ line and subsequent genotyping was performed to check for usability. *Tbx21*$^{-/-}$ *x Rag2*$^{-/-}$ (TRnUC) mice were generated from the original described TRUC colony (Garrett et al., 2007, Powell et al., 2012). Mice were housed and bred at Charles River, apart from the experiments for embryo and 1-week old T-bet^{cre} Rosa26YFP$^{fl/fl}$ mice. They were maintained by staff at King's College London in facilities that are Home Office approved and regulated. All mice used were aged between 6-12 weeks, unless stated otherwise. All animal experiments were performed in accredited facilities in accordance with the UK Animals (Scientific Procedures) Act 1986 (Home Office Licence Numbers PPL: 70/6792 and 70/8127)

2.2 Genotyping

DNA was isolated by digestion at 56°C of ear or tail samples in 200µl of lysis buffer (5 mM EDTA, 100 mM Tris-HCl pH 8.5, 0.2% SDS, 200 mM NaCl, 1mg/ml Proteinase K). Digested samples were then diluted 1:4 in nuclease-free water. PCR reaction comprises 12.5µl of 2x Mango Mix (Bioline Ltd., London, UK), 1 µl of each of PCR primers, which were diluted in nuclease-free water to 25µM (primers from Sigma-Aldrich), 1µl genomic DNA and then nuclease free water was added to make up to 25µl. This was then run on 1% agarose gel mixed

with (Tris-acetate-EDTA) TAE and run on a electrophoresis and then bands were viewed on a UV spectrometer.

2.3 Cell Isolation and preparation

Adult mice were euthanized using approved Schedule 1 methods by inhalation of a rising concentration of carbon dioxide gas and then followed by cervical dislocation. Embryo and neonatal mice were euthanised by using approved Schedule 1 methods of decapitation. Organs were dissected in a laminar flow cabinet using aseptic technique. Spleen, thymus, liver, mesenteric lymph nodes (mLN), peripheral (axillary, inguinal and cervical) lymph nodes (pLN), colon and small intestines were excised and placed in cold Phosphate Buffered Saline (PBS) solution.

Colon and small intestine lamina propria cells were isolated using the protocol developed by Sanos and Diefenbach (Sanos and Diefenbach, 2010). Small intestine and colon were cleaned, and faeces were removed. Afterwards, they were cut into 1-2cm pieces using surgical scissors and put into 10mls of Hank's Balanced Salt Solution (HBSS) without Mg^{2+}/Ca^{2+} (Invitrogen) mixed with 5mM of EDTA and 10mM HEPES (Fisher Scientific) and incubated at 37.5^{o}C with agitation for 20 minutes. Next, intestinal pieces were filtered, and the subsequent intestinal pieces were sliced into fine pieces using scalpels and were collected in complete animal medium consisting of: *Roswell Park Memorial Institute Medium (RPMI)* (Gibco, Grand Island, NY) with 10% heat-inactivated fetal calf serum (FCS) (Gibco, Grand Island, NY), 2mm glutamine, 100U/ml penicillin and 100µg/ml streptomycin, HEPES (Fisher Scientific), non-essential amino acids, sodium pyruvate and 2-mercaptoethanol (Sigma). Digestion enzymes were then added at a concentration of 0.5mg/ml collagenase (Roche), 10µg/ml DNase (Roche) and 1.5mg/ml dispase II (Roche), and the intestinal pieces were incubated for a further 20 minutes at 37^{o}C with agitation. After incubation, the digestion mix was filtered once more and centrifuged at 860g for 10 minutes at 4^{o}C. The pellet was then resuspended in 10mls of 40% Percol (Sigma) (made up with complete RPMI, as listed above) and layered on top of 5mls of 80% Percol and spun at 900g for 20 minutes at 20^{o}C without brakes. After the centrifugation, the cloudy interface layer of intestinal lamina propria cells was retrieved and washed in PBS and centrifuged again at 860g for 5 minutes at 4^{o}C. Cells were then ready to be used.

Splenic, thymus, liver, mLN and pLN cells were isolated into a single cell suspension in complete animal RPMI with the use of mesh filter and general mechanical destruction. The suspension was spun down at 860g for 5 minutes at 4ºC and mLN and pLN were resuspended and kept on ice until ready to be used. Spleen, thymus and liver cell pellets were resuspended, and red blood cells were lysed using a standard red blood lysis buffer (ACK) consisting of: 155mM NH4Cl, 10mM KHCO3, 0.1mM EDTA with a pH of 7.3. This was then spun down at 860g for 5 minutes at 4ºC and afterwards the spleen and thymus cells were resuspended in cold PBS and were ready to be use. The liver pellet was then resuspended in 4mls of 40% Percol (Sigma) (made up with complete RPMI, as listed above) and layered on top of 2mls of 60% Percol and spun at 900g for 20 minutes at 20ºC without brakes. All cells were counted using trypan-blue staining in a haemocytometer to assess cell viability and count live cells.

2.4 Cell separation technique

2.4.1 $CD4^+$ magnetic bead separation

Mouse spleens, mLNs, pLNs, livers, thymuses, colons and small intestines were processed into single cell suspensions as described above. $CD4^+$ cells were purified using LS positive selection magnetic-activated columns (MACs) and anti-CD4 (L3T4) beads (MACS; Miltenyi Biotec, Bergisch Gladbach, Germany).

2.4.2 Cell sorting

$CD4^+$ MACs sorted cells described above were further sorted for higher purification. Cells were stained using surface marker antibodies for fluorescence activated cell sorting. Cell sorting was performed after $CD4^+$ MACs bead separation using a FACS Aria machine (BD Biosciences). $CD4^+$ MACs sorted cells were pooled into 100 x 10^6 total in 600µl of PBS and stained for 20 minutes at 4°C in the dark. The following antibodies were used: anti-CD4-PerCPCy5.5, anti-CD25-PE, anti-CD62L-PECy7 (MEL-14; Thermo Fisher) and anti-CD44-Pacific Blue (IM1.8.1; Thermo Fisher). Single positive compensation controls and unstained controls were used to set up instrument settings and for gating strategies. Sort gating strategies for the various sorts are shown in the corresponding results section. The FACS Aria had a 70µm nozzle insert and used FACS Diva software to run the machine (both BD Biosciences).

The Aria sorting machine was operated by a member of the BRC flow cytometry core and used the manufacturer's recommended settings for the drop delay and sort stream amplitude and frequency. Sheath fluid used in the Aria was sterile PBS, which sorted cells were collected into tubes and kept at 4°C to maintain viability of sorted cells. Purity of cells are performed post-sort with at least a purity of 95% and viability of the cells were accessed using tryphan-blue staining in a haemocytometer.

2.5 Naïve T cell transfer model of colitis

Spleens and mLNs were harvested from either WT donor C56/BL6 mice or T-bet^{cre} x ROSA26YFP$^{fl/fl}$ mice and mechanically disrupted, as described before. Erythrocytes were lysed using in ACK buffer, similar to before. CD4^{+} cells were extracted using MACs separation as explained before. Naïve CD4^{+} T cells (CD4^{+} CD25^{-} CD44^{low} CD62L^{high}) were sorted using the FACS Aria to a purity of <95%, washed and resuspended in sterile PBS. *Rag2*$^{-/-}$ mice were injected via intraperitoneally with 0.5 x 10^{6} naïve CD4^{+} cells per mouse, and humanely culled after 6-8 weeks following adoptive transfer of cells. Mice were monitored for their health every week for signs of illness. Gating for the T-bet^{cre} x ROSA26YFP$^{fl/fl}$ sorting is shown in Figure 4. Wildtype gating for naïve T cells were the same but without the final YFP gate.

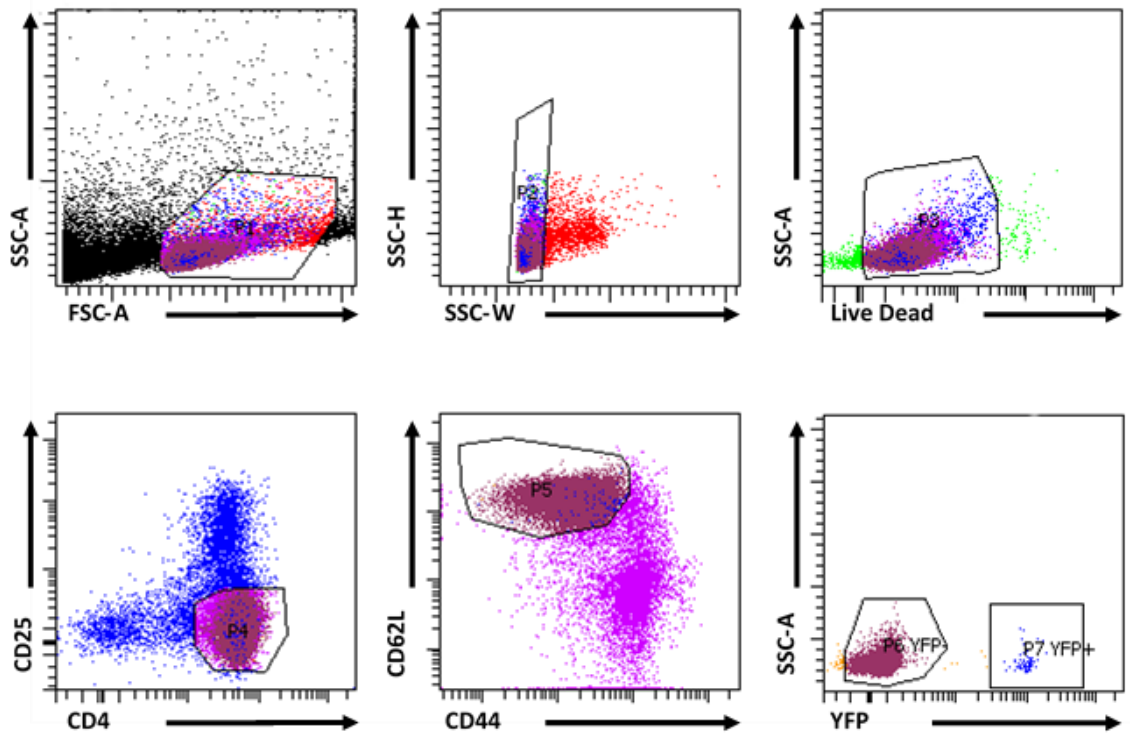

Figure 4: Gating strategy for sorting naïve T cells using the Aria machine

2.6 Anti-CD40 model of severe inflammation of the liver

125µg of agonistic anti-CD40 mAb (clone FGK4.5) or rat IgG2a isotype control mAb (clone 2A3) (both from BioXCell, West Lebanon, US) was used for BALB/c *Rag2*$^{-/-}$ mice, or, 50µg was used for C56BL/6 *Rag1*$^{-/-}$ and were administered via intraperitoneal injection in sterile PBS. Mice were observed and weighed on a daily basis for signs of disease including: diarrhoea, rectal bleeding, clinical features of peritonism, hunched appearance and piloerection. Mice were sacrificed on day 7 post injection of anti-CD40. Following culling, organs were harvested and weighed, including colon, mLN, spleen and liver.

2.7 DSS-induced colitis mouse model

Colitis was induced in Cre-ER^{T2} x T-bet$^{fl/fl}$ Het/Hom mice and littermate WT/Hom control mice by adding dextran sulphate sodium (DSS) (36-50 KDa, MP Biomedicals, Ontario, USA) to the drinking water at the concentration of 3% for a period of 5 days, after which DSS was removed and put back onto sterile drinking water. Mice from the non-colitic group were administered sterile drinking water throughout. Mice were sacrificed 5 days after the DSS was removed. Body weight, rectal bleeding and stool consistency were assessed daily for each mouse and these parameters were each assigned a score according to the criteria proposed (Cooper et al., 1993) and these data were used to analyse an average daily disease activity index (DAI) score.

2.8 Parasite infections of mice

Cre-ER^{T2} x T-bet$^{fl/fl}$ Het/Hom mice and littermate WT/Hom control mice were infected with either *Nippostrongylus brasiliensis (Nippo) or Heligmosomoides polygyrus* (H. poly) via oral gavage. The mice were sacrificed after either 7 or 9 days depending on the experiment and intestinal egg and worm counts were performed. Upon sacrifice, organs were excised and taken to King's College London, where the cells were extracted using the above methods and flow cytometry analysis could be performed. These parasite infections were set up and analysed in collaboration with a group at the London School of Hygiene and Tropical Medicine.

2.9 Cell culture

Unfractionated single cell suspensions of splenocytes ($2x10^6$/mL), mLN ($1x10^6$/ml) and cLP cells ($1x10^6$/mL) were cultured in complete animal medium (as described before) for 48 hours in a CO_2 controlled incubator at 37°C and 5% CO_2. Sorted $CD4^+$ T cells were also cultured on pre-incubated anti-CD3/anti-CD28 bound plates and given IL-2 (Sigma-Aldrich).

For $CD4^+$ T cell skewing experiments, sorted $CD4^+$ T cells were also cultured on pre-incubated anti-CD3/anti-CD28 bound plates and then specific cytokines were added for either T_H0, T_H1, T_H2, T_H17 and T_{reg} skewed conditions. These cultures were kept in sterile conditions and in a CO_2 controlled incubator at 37°C and 5% CO_2 for 7 days. Cells were split and monitored under a microscope during the entire culture period. These conditions are listed in Table 1 below. Supernatants were harvested, and cytokines concentrations measured by ELISA (R&D systems or eBiosceince).

T_H0	**T_H1**	**T_H2**	**T_H17**	**T_{reg}**
hIL-2 (20ng/ml) **1µl/0.5ml medium**	Anti-IL-4 (5µg/ml) **5µl/0.5ml medium**	mIL-4 (20ng/ml) **1µl/0.5ml medium**	Anti-CD28 (5 µg/ml) **2.5µl/0.5ml medium**	hIL-2 (20ng/ml) **1µl/0.5ml medium**
	mIL-12 (20ng/ml) **1µl/0.5ml medium**	Anti-IFNγ (20ng/ml) **10µl/0.5ml medium**	mIL-1β (10ng/ml) **0.5µl/0.5ml medium**	hTGFβ (2ng/ml) **1.5µl/0.5ml medium**
	hIL-2 (20ng/ml) **1µl/0.5ml medium**	hIL-2 (20ng/ml) **1µl/0.5ml medium**	mIL-6 (20ng/ml) **1µl/0.5ml medium**	
			hTGFβ (2ng/ml) **1µl/0.5ml medium**	
			Anti-IFNγ (20ng/ml) **10µl/0.5ml medium**	
			Anti-IL-4 (5µg/ml) **5µl/0.5ml medium**	

Table 2: List of T cell skewing conditions

All skewing conditions for $CD4^+$ T cell skewing cultures used and cultured for seven days, with the first two days on pre-incubated anti-CD3/anti-CD28 plate.

2.10 *Ex vivo* colon organ culture

3mm punch biopsies (Miltex) were used to acquire colon biopsies from murine colons at full thickness. 3 biopsies were cultured in 500μL of complete animal RPMI for 48 hours in a CO_2 controlled incubator at 37°C and 5% CO_2. Culture supernatants were harvested, and cytokine concentrations were measured by ELISA (R&D systems or eBiosceince).

2.11 ELISA

Cytokine concentrations from the supernatants of cultured cells and ex vivo colon organ cultures were measured by ELISA. Samples and standards were measured in duplicate. Standard curves were created with the standards provided in the kits, in accordance to the manufacturer's protocols. ELISA kits were purchased from Thermo Fisher for the following cytokines; IL-17A, IFNγ, IL-22 and TNFα.

2.12 Flow cytometry

Single suspension extracted cells from the various tissues used were plated out into flow cytometry tubes (Sarstedt) at a concentration of 1 x 10^6 per ml. Cells were stimulated with 50ng/ml phorbol 12-myristate 13-acetate (PMA) (Sigma Aldrich) and 1μg/ml ionomycin (Sigma Aldrich) for 4 hours. For any intracellular staining, 2μM monensin (Sigma Aldrich) was added for the final 2 hours to inhibit intracellular protein exportation. FcR receptor blocking antibodies were added at a concentration of 1:100 for 15minutes at 4°C. Next, surface staining antibodies were added together with live/dead stain (Invitrogen) and incubated for 20 minutes at room temperature in the dark. After incubation, cells were washed and spun down in sterile PBS. Cells were ready to be analysed by the BD LSRFortessa machine (BD Biosciences). For intracellular staining, cells were fixed and permeabilised using the Foxp3 fixation/permeabilization buffer kit (Thermo Fisher). The Foxp3 fix/perm buffer was used following the manufacturer's instructions. Following staining, cells were washed and resuspended in sterile PBS and stored in the dark at 4°C awaiting acquisition. Cells were acquired within 24 hours of staining. Fluorochromes used are listed in Table 2. Samples were acquired using a BD LSRFortessa (BD Biosciences) flow cytometer. Sample data was recorded

in FCS 3.0 data format using BD FACSDiva 6.0 software (BD Biosciences). Analysis of the data was performed using FlowJo software (Treestar Inc., Ashland, OR, USA).

Compensation of the experiments were carried out using compensation beads, OneComp Beads and UltraComp Beads (BD Biosciences). Compensation beads were stained with a single fluorochromes conjugated with monoclonal antibody, which are the same as used to label the cells in the same experiment. Compensation beads were labelled and stained for 20 minutes at room temperature and in the dark. Unstained cells were also used for negative staining. Unstimulated and monensin only administered cells were also used for negative stimulation staining of cytokines. Isotype and Fluorescence-Minus One (FMO) samples were also used to set up negative control staining of either surface markers or intracellular staining of transcription factors. BD FACSDiva software automatically calculate the compensation for the spectral overlap values. These were inspected manually, and any necessary manual corrections or fine tuning of the compensation values were adjusted.

Antigen	**Clone**	**Company**
Live Dead	Fixable blue or aqua	Thermo Fisher
CD45.1	A20	Biolegend
CD45.2	104	Biolegend
CD3	17A2	Thermo Fisher
CD4	RM4-5	Biolegend
CD8	53-6.7	Biolegend
CD5	53-7.3	Thermo Fisher
CD44	IM7	Biolegend / Thermo Fisher
CD62L	MEL-14	Biolegend
CD25	PC61	Biolegend
CD127 (IL-7R)	A7R34	Biolegend
CD27	LG.7F9	Thermo Fisher
CD28	37.51	Biolegend
CD49d	R1-2	Thermo Fisher
CD95	15A7	Thermo Fisher
CD11a	M17/4	Thermo Fisher

CD122 (IL-2R)	TM-b1	Thermo Fisher
CCR7	4B12	Biolegend
CXCR3	CXCR3-173	Biolegend
T-bet	4B10	Biolegend
RORγt	B2D	Thermo Fisher
Foxp3	FJK-16S	Thermo Fisher
GATA3	LS0-823	BD Biosciences
IL-10	JES5-16E3	Thermo Fisher
IL-5	TRFK5	Biolegend
IL-13	eBio13A	Thermo Fisher
IFNγ	XMG1.2	Biolegend / Thermo Fisher
γδTCR	GL3	Thermo Fisher
CD1d tetramer	PBS57-loaded or -unloaded CD1d tetramers	NIH Tetramer Core Facility
F4/80	BM8	Thermo Fisher
B220	RA3-6B2	Thermo Fisher
TRAIL	N2B2	Thermo Fisher
DX5	DX5	BD Biosciences / Thermo Fisher
CD11c	N418	Thermo Fisher
CD11b	M1/70	BD Biosciences
Ly49D	eBio4E5	Thermo Fisher
Ly49H	3D10	Thermo Fisher
Ly49E/F	CM4	Thermo Fisher
Ly49G2	eBio4D11	Thermo Fisher
Granzyme B	NGZB	Thermo Fisher
Perforin	eBioOMAK-D	Thermo Fisher
Nkp46	29A1.4	Thermo Fisher
NK1.1	PK136	Thermo Fisher
NKG2D	CX5	Thermo Fisher
EOMES	DAN11MAG	Thermo Fisher

c-kit	ACK2	Thermo Fisher
Sca-1	D7	Thermo Fisher
Hematopoietic Lineage Cocktail	consisting of: CD3 (17A2), B220 (RA3-6B2), CD11b (M1/70), TER-119 (TER-119), Gr-1 (RB6-8C5)	Thermo Fisher
ICOS	C398.4A	Thermo Fisher
Ter119	Ter119	Thermo Fisher
Gr-1	RB6-8C5	Thermo Fisher
MHCII	M5/114.15.2	Thermo Fisher
CCR6	29-21.17	Biolegend
Flt3	A2F10	Thermo Fisher
α4β7	DATK-32	Thermo Fisher

Table 3: List of flow cytometry antibodies used for the various panels and experiments.

All antibodies are anti-mouse antibodies used for flow and have the clone used and the company from where the antibody was purchased.

2.13 Cytokine secretion assay

As can be seen from the above, flow cytometry can be used to identify production of cytokines from specific cells. However, this also requires fixation and permeabilising the cells beforehand and makes the cells unusable. Therefore, a cytokine secretion capture kit was used in order to identify, sort and obtain specific cytokine secreting cells. The mouse IFN-γ secretion assay (PE) and mouse IL-17A secretion assay (APC) kit were purchased from Miltenyi Biotec and an adapted protocol from a previous PhD student was used. In brief, after cells were isolated from colon and mLN, in the previously described protocol, they were resuspended in complete media at 1 x 10^7/ml and stimulated using 1μg/ml ionomycin and 10ng/ml PMA for 4 hours. After stimulation, cells were then washed and centrifuged twice in 2mls of cold PBS. The cells were then resuspended into 90μl/10^6 of total cells of cold complete media and 10μl/10^6 of total cells of mouse IFNγ capture reagent and mouse IL-17A capture reagent were added. These cells were then vortexed and incubated on ice for 5 minutes. Next, 1ml/10^6 of total cells of warm (37°C) media was added to the suspension and the cells were incubated for 45 minutes at 37°C. The cells were gently inverted every 5 minutes during this 45-minute incubation in order to resuspend settled cells. Once cells had been incubated for 45 minutes, they were removed and placed on ice and a further 2mls of ice-cold PBS was added. The cells

were then washed and centrifuged twice, and cells were once again resuspended into 90µl/10^6 of total cells. FcR receptor blocking antibodies were added at a concentration of 1:100 and incubated at 4°C for 15 minutes. After this, 10µl per 10^6 total cells of mouse IFN-γ Detection antibody (PE) and mouse IL-17A Detection antibody (Biotin) were added and vortexed and incubated on ice for 10 minutes. Cells were then washed with 2mls of cold PBS and resuspended again resuspended into 90µl/10^6 of total cells. Whereby, 10µl per 10^6 total cells of mouse Anti-Biotin-APC and antibodies for CD4 and a Live/Dead stain were added. Cells were then vortexed and incubated for 10 minutes on ice. After this, cells were once again washed and centrifuged and resuspended in PBS and were ready to be sorted on the BD Aria like before with gating on Live $CD4^+$ cells and the different $IFN\gamma^+$ and $IL\text{-}17A^+$ cells. These cytokine-producing cells were then further gated by their positive or negative expression of YFP.

2.14 Heterotopic Heart Transplant

Heart allotransplantation was performed between whole MHC mismatched BALB/c ($H2^d$ donors) and C57BL/6 ($H2^b$ recipients) mice as described in the protocol by Corry et al. [48]. The allograft was kindly performed by a very competent and trained person from Wilson Wong's group. After surgery, mice were monitored daily in particular with close attention of the graft viability via direct palpitation of the abdomen where the transplanted heart was in position. Graft rejection was defined when a cardiac pulse from the graft had stopped.

2.15 Donor Specific Antibody (DSA) Assay

Anti-donor-specific IgG were determined by flow cytometry. This was to determine the level of rejection in the cardiac transplant in the $Foxp3^{cre}$ control vs $Foxp3^{cre}$ $T\text{-}bet^{fl/fl}$ mice. Donor splenocytes were used as target cells and single cell suspensions of the splenocytes were extracted using the method as previously described. Splenocytes were first incubated with 2% BSA, 5% normal goat serum and FcR receptor blocking antibodies for 20 minutes at 4°C. After this, a surface stain for CD3 was added and incubated for a further 20 minutes at 4°C. Cells were then washed and centrifuged at 1800RPM and the supernatant was resuspended. Afterwards, 5µl of serum was added and incubated again at 4°C for 20 minutes. Cells were then washed and centrifuged again, after which cells were resuspended and IgG-FITC was

added and incubated at 4°C for 20 minutes. After this last incubation, cells were washed and centrifuged and resuspended at a suitable volume and ready to be acquired using a BD LSRFortessa (BD Biosciences) flow cytometer.

2.16 RNA extraction

RNA extraction was performed using Trizol (Invitrogen) according to the manufacturer's instructions, in an allotted RNA workspace. Equipment and surfaces were cleaned with RNase Zap (Ambion Inc., Austin, TX, USA) to decrease nuclease contamination. Cells were resuspended in 1ml of Trizol. Samples were either processed immediately or stored at -80°C. After culling animals, whole liver segments (3cm) were harvested and snap frozen in liquid nitrogen and then stored at -80^{o}C pending RNA extraction. Frozen liver segments were then homogenised using a Tissue Lyzer II (Qiagen) with a Stainless-Steel Bead (5mm) (Qiagen) set to 25Hz/s for 5 minutes in 1mL Trizol reagent (Invitrogen). 200µl of chloroform (Sigma Aldrich) was then added to cells or tissue homogenates, with the sample then mixed and incubated at room temperature for 2 minutes. Next, this was centrifuged at 12000 RPM for 15 minutes at 4°C prior to allow phase separation. The upper aqueous layer was carefully transferred to a fresh eppendorf without interrupting the interphase layer, with 500µl of cold isopropanol was then added. After mixing the suspension with a vortex, the sample was centrifuged for 15 minutes at 4°C. The supernatant was cautiously pipetted out, and 1 ml of 75% ethanol was added to the pellet to ash it and the suspension was centrifuged for another 5 minutes at 7500RPM at 4°C. The supernatant was, again, then removed, and the pellet was air dried before it was resuspended in an appropriate volume of nuclease-free water. RNA samples were then checked for the quality, contamination and concentration using a NanoDrop spectrophotometer. RNA was then stored at -80°C awaiting further analysis.

2.17 cDNA synthesis and quantitative PCR

cDNA was generated with the cDNA synthesis kit (Bioline) according to the manufacturer's protocol. Quantitative PCR was used in order to quantify mRNA transcripts, with the use of TaqMan gene expression assays (Applied Biosystems, Warrington, UK). Gene expression was normalized to the expression of β-actin, as the control housekeeping gene, to generate ΔCT values and relative abundance quantified using the $2^{-\Delta CT}$ method (Schmittgen and Livak, 2008).

The following Taqman qPCR primers were used: IL-17A (Mn00439619), IFN-γ (Mn01168134), IL-4 (Mn99999154), IL23p19 (Mn00518984), IL12p40 (Mn00434165) and β-actin (4352341E).

2.18 Liver histology

2-3cm segments of liver were fixed in 10% paraformaldehyde. 5µm sections were stained with either haematoxylin and eosin, NKp46 or F4/80 depending on the sample and slides. Liver histology preparation and staining was performed by Professor Robert Goldin at the Department of Cellular Pathology at Imperial College London.

2.19 ALT measurements of mouse serum

After an approved Schedule 1 method of CO_2 killing, around a maximum of 1ml of blood was drawn up via a cardiac puncture. The blood was then spun down in a centrifuge at 1000g for 20 minutes and carefully pipette out the aqueous serum layer. The serum was then analysed for ALT levels by staff at the Pathology and Diagnostic Laboratories at the Royal Veterinary College

2.20 *In vitro* Tamoxifen treatment

For the *in vitro* tamoxifen experiments, specific *in vitro* 4-OHT tamoxifen was purchased from Sigma (Cat no: H7904). After the spleens and mLNs of ERTH2^{cre} x T-bet$^{fl/fl}$ mice were harvested via approved Schedule 1 method and cells were extracted as previous described. CD4 T cells were sorted and plated out on a pre-incubated CD3/CD28. *In vitro* tamoxifen was given to the cells at a concentration of either 0, 0.25, 0.5, 1 or 2µM and for either 0, 4, 6, 12 or 24 hours. In other experiments, cells were plated out at $0.5x10^6$ per well and T_H1 skewing cytokines, as shown in Table 1, were given. After day 2, the cells were removed from the anti-CD3/anti-CD28 and split with the addition of 1µM *in vitro* tamoxifen for the remaining 5 days.

2.21 *In vivo* Tamoxifen treatment

For *in vivo* tamoxifen treatment of the ERTH2^{cre} x T-bet$^{fl/fl}$ mice, the specific *in vivo* 4-OHT tamoxifen was purchased from MP Biomedicals (Cat no: 02156738). The stock was initially dissolved in ethanol, before then being diluted in sunflower oil at a concentration of 10mg/1000µl and then stored at -80°C. Before injecting the diluted tamoxifen, this tamoxifen was heated to 37°C prior to administration. 100µl (1mg) of warmed tamoxifen was given per mouse by intraperitoneal injection on 3 days either consecutively or over a 5 day period (Geiser et al., 2012), after which were left for two weeks before analysis. Mice were monitored for their weight for the duration of the period. Mice were checked for T-bet deletion two weeks after administering tamoxifen.

2.22 Statistical analysis

Statistical analyses were carried using GraphPad Prism 7 (GraphPad Software Inc., La Jolla, CA, USA). Non-parametric data were analysed using the Mann-Whitney test and normally distributed data were analysed using the Student's T-test. For grouped data, a non-parametric 1-way ANOVA test (Kruskal-Wallis test) with Dunn's corrections were performed. Statistical significance was found if a p value was less than 0.05. Non-parametric data was expressed as medians.

Chapter 3

Results: Characterisation of immune cells in T-bet^{cre} x ROSA26YFP$^{fl/fl}$ mice

As described in Chapter 1, T-bet is expressed in many subsets of cells within the innate and adaptive immune system, including $CD4^+$ T cells, $CD8^+$ T cells, NK cells, ILCs, DCs, macrophages, B cells, NKT cells and γδT cells (Intlekofer et al., 2005, Lighvani et al., 2001, Liu et al., 2003, Lugo-Villarino et al., 2003, Powell et al., 2012, Szabo et al., 2000, Townsend et al., 2004, Yin et al., 2002).

Since T cells (CD4, CD8, NKT and γδT cells) develop in the thymus, phenotyping of the thymus was performed in these cells. Upon entering the thymus, these lymphoid progenitors become committed to becoming T cells (Germain, 2002). At this stage, the cells are called "Double-Negative" (DN) as they do not yet express CD4 or CD8, but double negative thymocytes have been shown to express differing levels of CD44 and CD25 depending on what stage of the double negative development they are in (Godfrey et al., 1993). DN1s are identified as $CD3^-$ $CD25^-$ $CD44^+$ and are able to give rise to αβ T cells, γδ T cells, NK cells, dendritic cells, macrophages, and B cells. DN1s actually consist of 5 DN1 stages (DN1a-e), which are characterised by their expression of CD117 and CD24. The expression of CD117 at the DN1a-b stage has been shown to be the most important for the DN1 to give rise to the T cell lineage (Porritt et al., 2004). Upon establishing the T cell specific lineage DN1s progress onto DN2s by expressing CD25 as well, thus are identified as $CD3^-$ $CD25^+$ $CD44^+$. After progressing into DN2, where they migrate to the cortex of the thymus, the T cells begin rearrangement of their T cell receptors using the recombinant-activating genes 1 and 2 (RAG1 and RAG2) to rearrange the V(D)J rearrangement of the variable (V), diversity (D) to the joining (J) region (Mombaerts et al., 1992). DN2s that have successfully formed an invariant pre-TCRα stop expressing CD44 and express CD25 only and become DN3s. DN3s which have been able to successfully rearrange their TCRβ associates with the invariant pre-TCRα chain. At this point, it also associates with CD3 to form the pre-TCR complex(van Oers et al., 1995) This β selection causes the developing T lymphocyte to downregulate CD25 leading to the

progression to the DN4 stage. Upon becoming DN4s, the thymocytes quickly express CD8 first, followed by CD4; becoming double positive cells (DP) (C A Janeway, 1992). DP cells then begin TCRα rearrangement to produce the αβ T cell receptor. DP cells in the thymus make up around 90% of the lymphoid cells in a young individual's thymus. Positive selection occurs at the DP stage, where the cells are exposed to either MHCI or MHCII on cortical epithelial cells, to define if they are CD4s or CD8s. Positive selection supposedly takes a few days to occur and interaction between the TCRαβ and either MHCI or MHCII needs to be continual in order for that DP to be positively selected. Most DPs do not interact and have enough signal from the MHC and/or costimulatory molecules and are left to die by neglect. Depending on their interaction with MHCI or MHCII and costimulatory molecule interaction, the DP becomes a "single-positive" (SP) $CD4^+$ or $CD8^+$ T cell. MHCI defines the DP into $CD8^+$ and MHCII defines it into a $CD4^+$ T cell. These $CD4^+$ and $CD8^+$ SP cells enter the medulla of the thymus and undergo negative selection. This is where the SP cells interact with medullary epithelial cells and thymic dendritic cells, some of which have self-antigen presented on their MHC. A small proportion of these SP cells that interact with these self-antigens are negatively selected and receive apoptosis signals and the cells that respond to self-antigen are killed (E Robey and Fowlkes, 1994, Starr et al., 2003, von Boehmer et al., 1989, Radtke et al., 1999). The resulting SP $CD4^+$ and $CD8^+$ T cells are the mature naïve T cells that leave the thymus and enter the periphery. As T-bet expression has been reported in these cells after they have developed, the expression of any YFP cells in these cell populations during development would be interesting and novel.

NKT cells express T-bet during their development process in order to gain their effector functions and be able to produce IFNγ (Townsend et al., 2004). NKT cells also develop from within the thymus, during the DP stage of lymphocyte T cell development (Godfrey and Berzins, 2007). NKT cell selection requires their ligation to glycolipid antigens presented by CD1d on DP T cells, and then go through a 4 stage developing stage of maturity in order to become mature (Godfrey and Berzins, 2007). These are identified by different surface markers and are: Immature stage 1 ($NK1.1^-$ $CD24^+$ $CD44^{low}$ $DX5^-$), immature stage 2 ($NK1.1^-$ $CD24^-$ $CD44^{low}$ $DX5^-$), immature stage 3 ($NK1.1^-$ $CD24^-$ $CD44^+$ $DX5^-$), immature stage 4 ($NK1.1^-$ $CD24^-$ $CD44^+$ $DX5^+$) and finally mature NKT cells ($NK1.1^+$), which then exit the thymus and are found in the periphery (Godfrey and Berzins, 2007). Therefore, T-bet^{cre} x $ROSA26YFP^{fl/fl}$

mice would be able to identify any T-bet expressed NKT cells within the thymus as they develop further to maturity.

γδT cells also develop within the thymus during the DN2-DN3 stage where T cell receptor rearrangement occurs. It has also been shown that γδT cells in the periphery can induce the expression of T-bet, after signalling through its T cell receptor has been activated. These have been shown mainly in the IFNγ-producing γδT cells as opposed to the IL-17A-producing γδT cells (Turchinovich and Pennington, 2011). Progenitor γδT cells are the γδT cells that have first come from the DN2 phase of T cell development with γδTCRs and express CD24, CD27 and CD25 (Pang et al., 2012, Ribot et al., 2009). This population then very quickly downregulates CD25 and the expression of the γδ receptor rises to form the immature γδT cells, which is therefore $CD24^+$ $CD27^+$. From this immature γδT cells, the three mature populations arise in the thymus, which all lack CD24 expression. The IL-17A-producing γδT cells is $CD24^-$ $CD27^-$ $CD25^-$ $CD44^+$ and the IFNγ-producing γδT cells is $CD24^-$ $CD27^+$ $CD25^-$. $T\text{-}bet^{cre}$ x $ROSA26YFP^{fl/fl}$ mice will be capable of identifying any T-bet fate expressed γδT cells, and not just in the expected IFNγ γδT cell.

The lymphoid progenitor, which enters the thymus for the T cell development described above, develops and originates from the bone marrow. Thus, the bone marrow was phenotyped with respect to the expression of YFP. The common lymphoid progenitor (cLP), which can differentiate into T, B and NK cells, the common helper-like ILC progenitor (ChILP), which is the progenitor for ILC1s and ILC3s, and lastly the ILC2 progenitor (ILC2p), which only give rise to $GATA3^+$ ILC2s all originate from the bone marrow. cLPs are identified as being $lineage^-$ $IL\text{-}7R^+$ $\alpha4\beta7^-$ $Flt3^+$ $c\text{-}kit^+$, ChILPs are identified by $lineage^-$ $IL\text{-}7R^+$ $\alpha4\beta7^+$ $Flt3^-$ $CD25^-$ and ILC2ps are identified as $lineage^-$ $IL\text{-}7R^+$ $\alpha4\beta7^+$ $Flt3^-$ $CD25^+$ (Klose et al., 2014, Kondo et al., 1997, Parigi et al., 2018, Xu et al., 2015).

For the periphery, the spleen is the main organ that helps to polarise the immune cells during an infection. It is the largest lymphoid organ and its main function is to drain the blood (Morris and Bullock, 1919). Therefore, the spleen was the first site in the periphery to be extensively phenotyped in these mice. The colon was also phenotyped at steady state, as it is one of the

main mucosal sites of inflammation during inflammatory bowel disease. Colitis models will be used in Chapter 4 to phenotype the YFP^{+} cells in a disease setting.

The use of mouse models has allowed research into subsets of cells during development at both a steady healthy state and also during an inflammatory response. For the purposes of this thesis, in order to study the role of T-bet in these immune cells, a newly developed mouse line has been crossed using two genetic manipulated mouse breeds. The T-bet^{cre} line was generated within the lab by a previous colleague (Gökmen et al., 2013). In brief, a knock-in by introducing an IRES-Cre cassette downstream of the Stop codon in the T-bet gene, as shown in Figure 6.

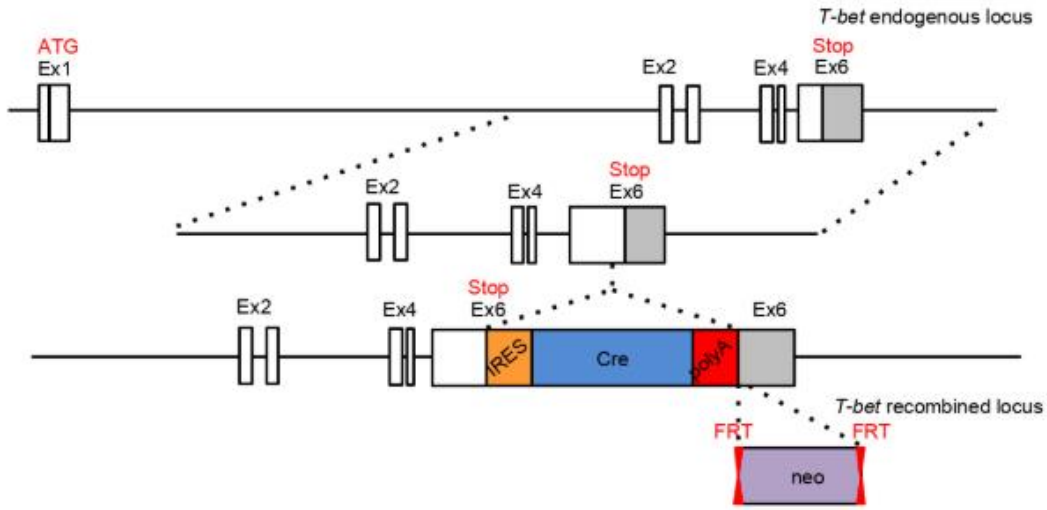

Figure 6: Schematic showing the strategy of generating the T-bet^{cre} line

The ROSA26YFP flox line was bought from Jackson and they were bred as heterozygous genotype (Rosa-YFPfl/$fl^{+/-}$) with the homozygous genotype of the T-bet^{cre} (T-$betcre^{+/+}$) in order to use the litters from this line. The litters should all be T-$betcre^{+/-}$(Het) x Rosa-YFPfl/$fl^{+/-}$(Het).

Use of the T-bet fate mapping mouse line allows the tracking of cells which have previously expressed T-bet. This is a novel mouse line which has not been previously documented. The initial aim was to characterise the different immune cell compartments: this would give more insight into the expression of T-bet in immune cells and aid the understanding of the ontogeny of various immune cell subsets.

3.1 Initial phenotyping of CD45^{+} lymphocytes in blood, and lymphoid organs and mucosal sites of the T-bet^{cre} x ROSA26YFP$^{fl/fl}$ mice

Initial phenotyping of the blood of the mouse was performed to ensure that the use of the T-bet^{cre} model was not going to cause excess expression of YFP. The use of cre-lox model can cause leakiness especially when cre expressing mice are crossed using homozygous mice (Song and Palmiter, 2018). The double homozygous mice (T-betcre$^{+/+}$(Hom) x Rosa-YFPfl/fl$^{+/+}$(Hom)) only had YFP expression in CD4, CD8 and B cells, in comparison with the wild type control, which expressed no YFP (Figure 1). This observation made it clear that under double homozygous (T-betcre$^{+/+}$(Hom) x Rosa-YFPfl/fl$^{+/+}$(Hom)) breeding, the mice expressed too much Cre, resulting in all cells expressing YFP. The double heterozygous mice (T-betcre$^{+/-}$(Het) x Rosa-YFPfl/fl$^{+/-}$(Het)) showed YFP^{+} cells in the CD4^{+}, CD8^{+} and B cell compartments that were more likely to be observed within these cell subsets in the blood.

7A **Phenotyping of the blood of T-betcre$^{+/-}$ x Rosa-YFPfl/fl$^{+/-}$ vs T-betcre$^{+/+}$ x Rosa-YFPfl/fl$^{+/+}$**

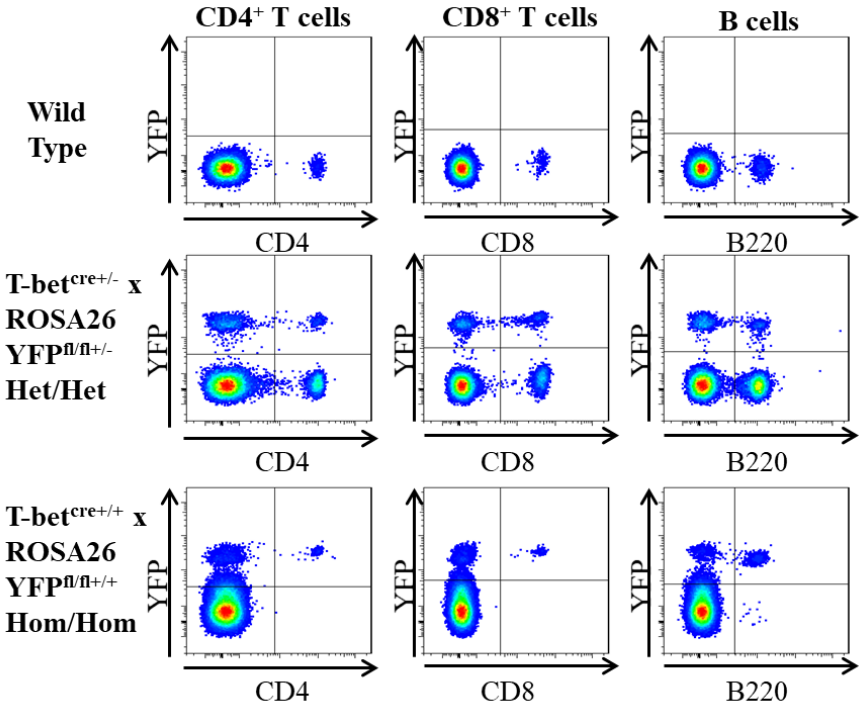

Figure 7. Phenotyping the blood of the T-bet^{cre} x ROSA26YFP$^{fl/fl}$ showed all subtypes of cell to only express YFP in double homozygous mice

A. Representative flow cytometry plots showing CD4, CD8 and B220 cells in stained samples in blood of either wildtype, T-betcre$^{+/-}$ x Rosa-YFPfl/fl$^{+/-}$ Het/Het or T-betcre$^{+/+}$ x Rosa-YFPfl/fl$^{+/+}$ Hom/Hom mice. Cells were gated on live cells using flow cytometry, (n=3 of each genotype)

Once the use of T-betcre$^{+/-}$ x Rosa-YFPfl/fl$^{+/-}$ Het/Het mice was established, further initial phenotyping was performed on CD45^{+} lymphocytes in the colon, mLN and spleen of healthy T-bet^{cre} x ROSA26YFP$^{fl/fl}$ mice. This was to estimate the percentage of YFP expected within the lymphocyte population in this mouse. The percentage of YFP expressing CD45^{+} cells was small but significantly different within each organ: 15% in the spleen and around 5-10% in the colon and mLN (Figure 8).

8A

Phenotyping of the colon, mLN and spleen of T-betcre$^{+/-}$ x Rosa-YFPfl/fl$^{+/-}$

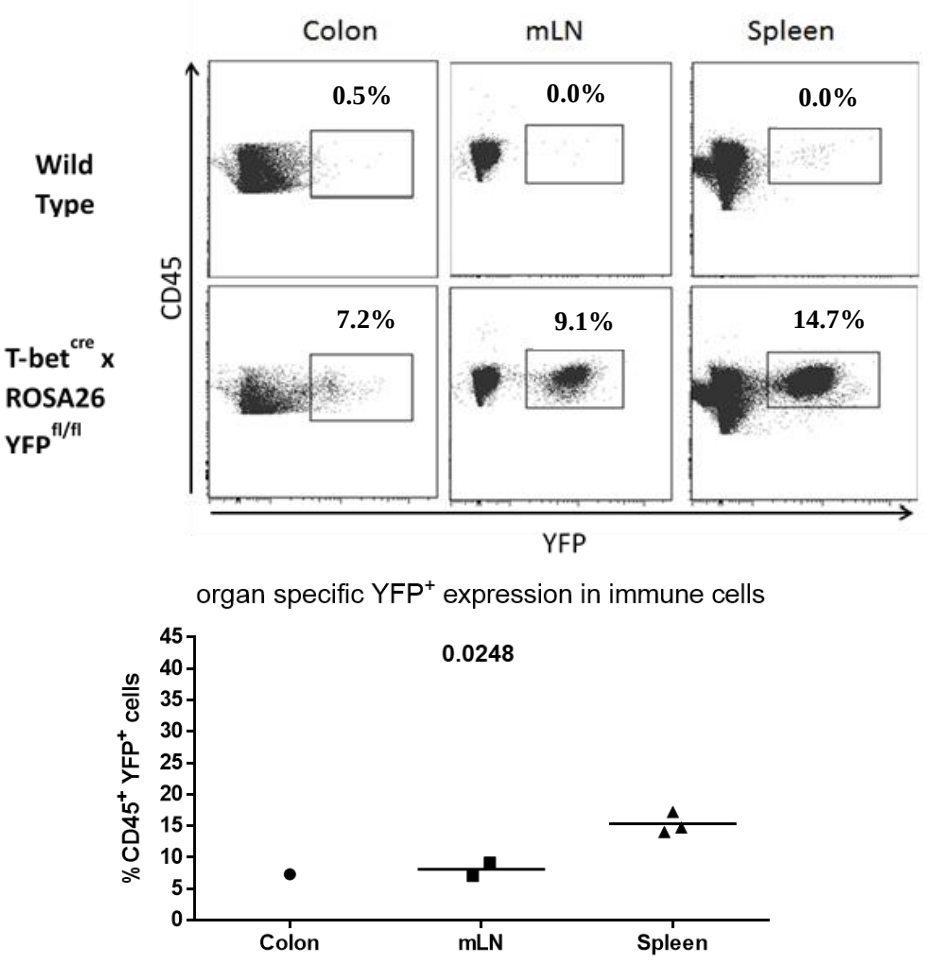

Figure 8. Phenotyping YFP expression in the CD45^{+} lymphocytes in the colon, mLN and spleen

A. Representative flow cytometry plots and dot plot showing CD45^{+} cells in stained samples in either normal C56BL/6 wildtype or T-bet^{cre} x ROSA26YFP$^{fl/fl}$ Het/Het mice. Cells were gated on live cells using flow cytometry (n = 3, colon pooled into 1). Kruskal-Wallis test performed with Dunn's corrections showing overall analysis for all groups.

3.2 Phenotyping YFP expression in lymphoid and myeloid cells of the T-bet^{cre} x ROSA26YFP$^{fl/fl}$ mice

After initial phenotyping of the blood and CD45$^+$ population, a basic investigation into specific cell types was performed to determine YFP expression within the lymphocyte and myeloid compartments. Three simple panels to look at NK cells, ILCs, T cells, B cells and myeloid cells in adult mice were used. Figure 9A, 9B and 9C show the gating strategy for each of the panels using the spleen of these mice. The spleen, being the main secondary lymphoid organ, would be ideal to identify these cell populations as it is where most immune regulation occurs.

For these panels, NK cells were identified as lineage$^-$ (consisting of CD3, CD5, Gr-1, CD11c, F4/80, CD19, Ter119) CD45$^+$ NKp46$^+$ NK1.1$^+$; and NKT cells as lineage$^+$ CD45$^+$ NKp46$^+$ NK1.1$^+$. Although this very loosely identified the NK cells, the gate also included NKp46$^+$ ILC1s and ILC3s. As NKT cells were gated on lineage, and, as CD3$^+$ staining and gating for the NKp46$^+$ population within this, was used to identify the NKT cells. NKT cells recognise glycolipids via presentation by MHC-like CD1d molecules and this marker will be used later in NKT cell development in the thymus.

The lymphoid panel gave an initial, but useful, phenotyping of YFP$^+$ expression in CD4$^+$ T cells, CD8$^+$ T cells and CD19$^+$ B cell as shown by the gating strategy below.

Finally, the myeloid panel used gave an early insight into the YFP expression in these mice for the populations identified as dendritic cells (CD45$^+$, CD11c$^+$, MHCII$^+$ and F4/80$^-$) and F4/80$^+$ monocytes (CD45$^+$, F4/80$^+$, CD11c$^-$).

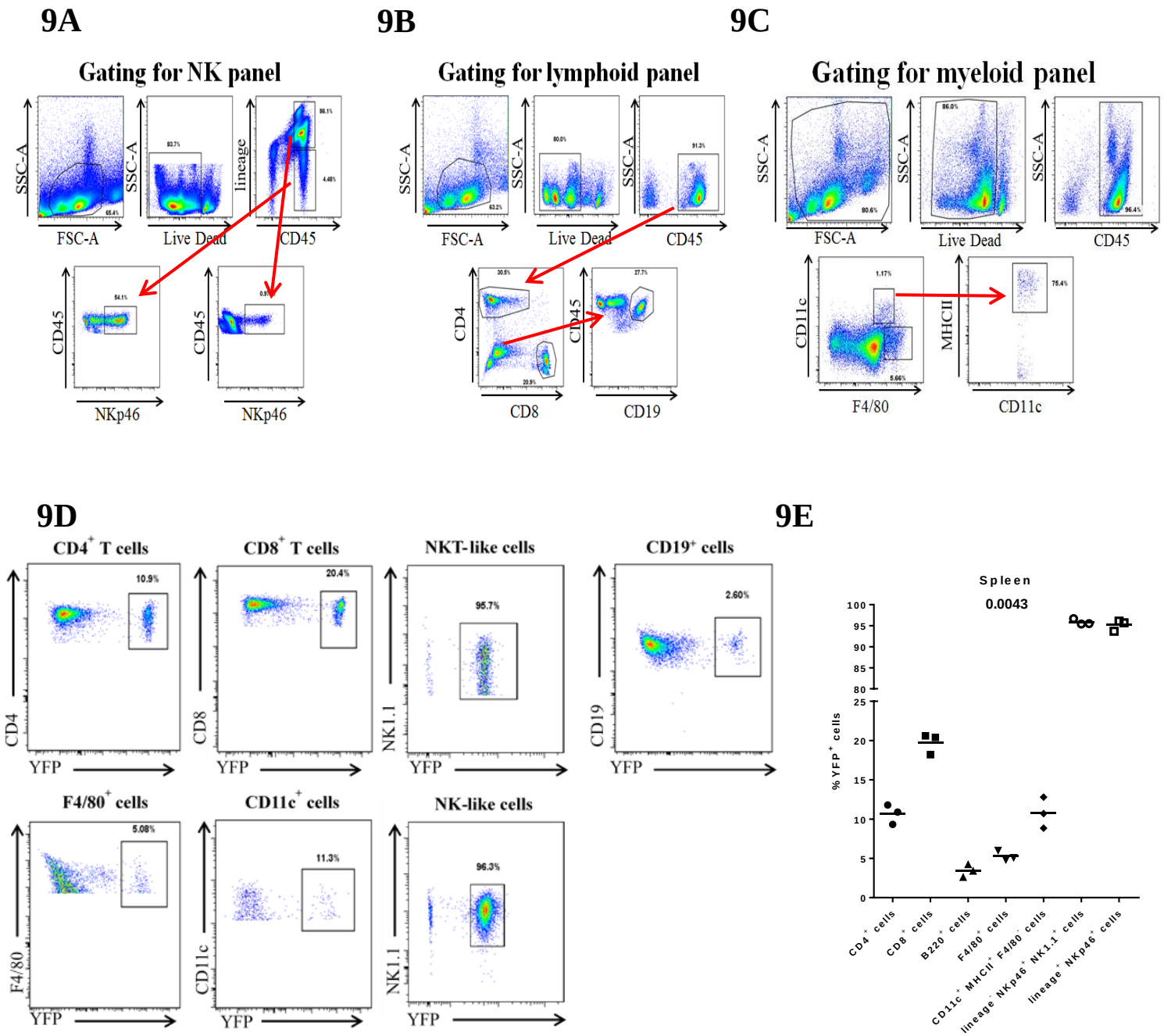

Figure 9. Phenotyping YFP expression in subsets of innate and adaptive immune cells in the spleen

A. Flow cytometry gating strategy showing the strategy for gating of NK and NKT cells in the T-bet^{cre} x ROSA26YFP$^{fl/fl}$. B. Flow cytometry gating strategy showing the strategy for gating of lymphoid cells in the T-bet^{cre} x ROSA26YFP$^{fl/fl}$. C. Flow cytometry gating strategy showing the strategy for gating of myeloid cells in the T-bet^{cre} x ROSA26YFP$^{fl/fl}$. D. Flow plots of the different populations highlighted from the gating strategies showing the amount of YFP^{+} expression in each population. E. Dot plot of the different populations highlighted from the gating strategies showing the amount of YFP^{+} expression in each population (n = 3). Kruskal-Wallis test performed with Dunn's corrections showing overall analysis for all groups.

The flow plot and the dot plot for the results of the phenotyping panels displayed significantly differing percentage of YFP^+ cells in the different identified populations (P=0.0043). From the initial phenotyping, there was around 10% of YFP^+ $CD4^+$ T cell and 20% of $CD8^+$ YFP^+ T cells. NKT and NK cells were almost all YFP^+ and this was consistent as T-bet expression is required for both NKT and NK cells to become fully mature during development, but once they have reached terminal maturation they no longer require T-bet in order for their survival (Godfrey et al., 2010, Matsuda et al., 2006, Townsend et al., 2004). The 3% of splenic B cells were shown to be YFP^+. B cells have been shown to express T-bet in a pathological response disease during class switching to IgG2A and promote the survival of these subsequent IgG2A memory B cells (Liu et al., 2003). These mice were healthy and therefore, as expected, only a small proportion of B cells were YFP^+. The $F4/80^+$ and $CD11c^+$ cell populations were identified to be monocytes and dendritic cells respectively and both require the expression of T-bet to produce IFNγ in response to disease (Lighvani et al., 2001, Lugo-Villarino et al., 2005, Lugo-Villarino et al., 2003). Again, since these mice were phenotyped during a steady healthy state, the percentages of YFP^+ $F4/80^+$ and $CD11c^+$ shown are relatively low.

3.3 Extensive phenotyping of immune T cells within the thymus

The initial phenotyping of most cell types in the spleen showed that the mouse itself was a beneficial and reliable model. Since the key role of T-bet is the master regulator of T_H1 cell differentiation from naïve T cells in the periphery, phenotyping of the thymus was performed next, as this is the site of $CD4^+$ T cell development. However, as already stated, T-bet has been shown to be expressed in developing NKT cells and γδT cells. Both these populations also develop in the thymus before entering the periphery, therefore these developing cell types were also extensively phenotyped.

3.3.1 Phenotyping $CD4^+$ and $CD8^+$ T cell development in the thymus

Gating strategy (Figure 10) of the YFP expression in the developing T cells in the thymus of the T-bet^{cre} x $ROSA26YFP^{fl/fl}$ were based on the background knowledge on T cell development already published.

10A **Gating Strategy for T cells in the thymus**

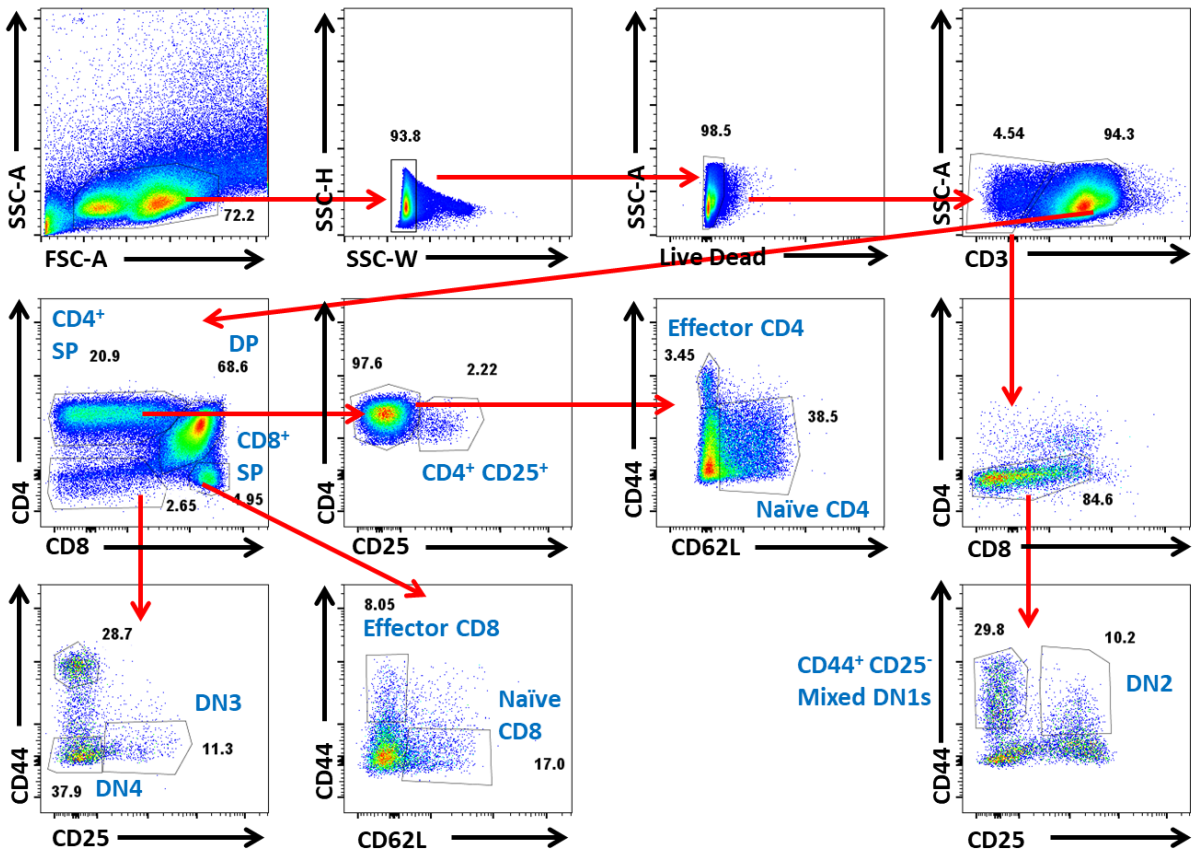

Figure 10: Gating strategy used to identify the different CD4 and CD8 T cells in the thymus

A. Representative flow plots showing the gating strategy used for each T-bet^{cre} x ROSA26YFP$^{fl/fl}$ thymus. Each important subtype is outlined in blue.

T-bet is not required for the development of CD4^{+} or CD8^{+} T cells as the cells should still be naïve and not have been exposed to any antigen. Therefore, no YFP expression should be seen in the thymus. Using the gating strategy from Figure 10, Figure 11 shows the results of YFP expression within each of these different population.

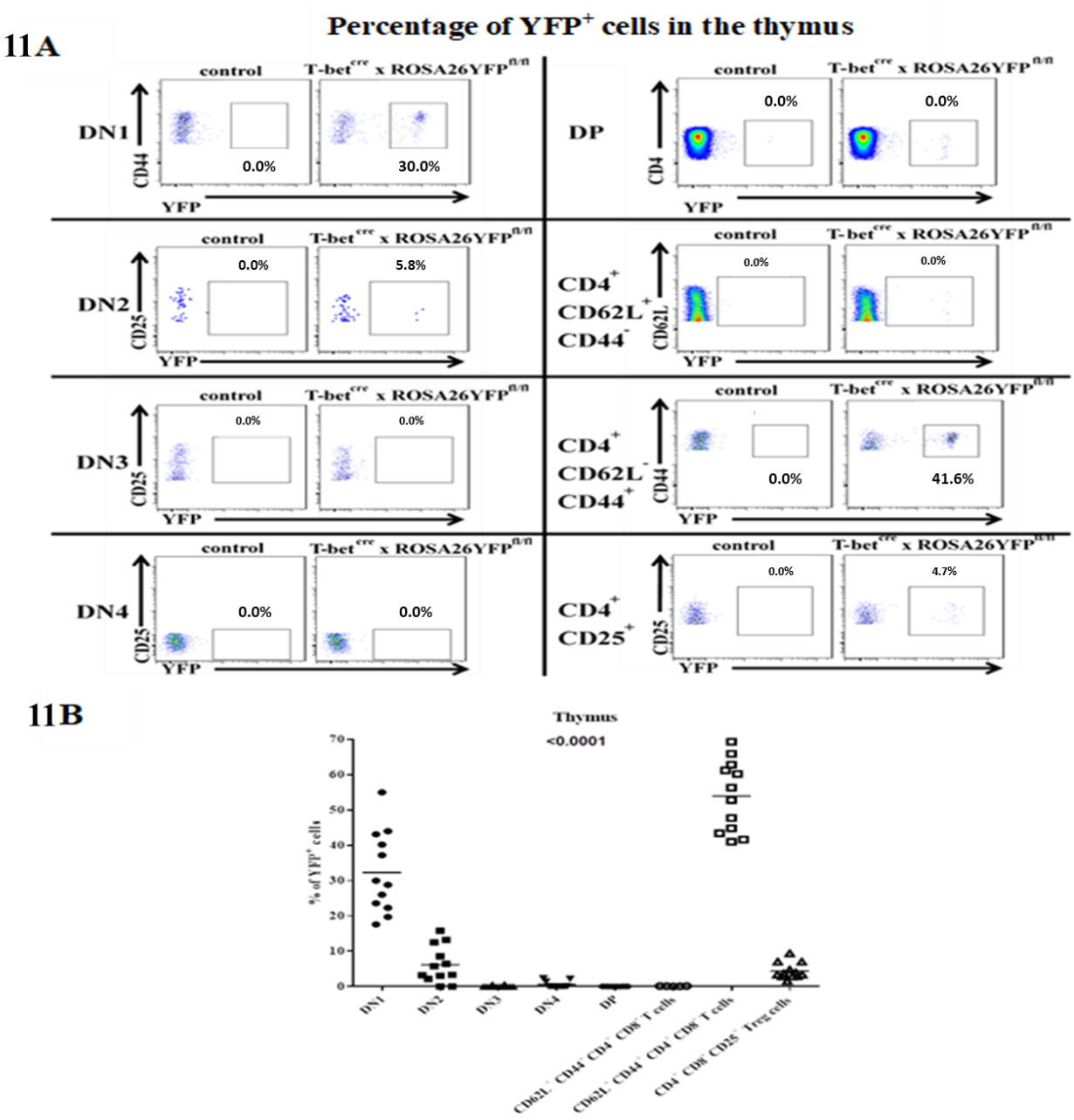

Figure 11: Phenotyping the YFP expression within the CD4 T cell compartment in the thymus

A. Representative flow plots (all gated as shown previously) showing expression of YFP in the T-bet^{cre} x ROSA26YFP$^{fl/fl}$ compared with a litter mate wild-type control for DN1 (CD3$^-$ CD44$^+$ CD25$^-$), DN2 (CD3$^-$ CD44$^+$ CD25$^+$), DN3 (CD3$^+$ CD44$^-$ CD25$^+$), DN4 (CD3$^+$ CD44$^-$ CD25$^-$), DP (CD3$^+$ CD4$^+$ CD25$^+$), naïve CD4$^+$ T cells (CD3$^+$ CD4$^+$ CD8$^-$ CD62L$^+$ CD44$^-$), memory CD4$^+$ T cells (CD3$^+$ CD4$^+$ CD8$^-$ CD62L$^-$ CD44$^+$) and regulatory CD4$^+$ T cells (CD3$^+$ CD4$^+$ CD8$^-$ CD25$^+$). B. The dot plot showing the compiled results of the phenotyping results of the T-bet^{cre} x ROSA26YFP$^{fl/fl}$ mice (n = 12). Kruskal-Wallis test performed with Dunn's corrections showing overall analysis of P<0.0001 for all groups. Individual comparisons are shown also using the same Kruskal-Wallis test.

T cell development in the thymus in the T-bet^{cre} x ROSA26YFP$^{fl/fl}$ showed significantly interesting results when comparing the amount of YFP$^+$ cells in some of different developing cell types ($P<0.0001$). DN1s and DN2s seemed to have a high percentage of YFP$^+$ cells (around 30% and 5% respectively), which should not have been the case in terms of developing T cells. The initial hypothesis was that these YFP$^+$ T cells were being negatively selected due to their expression of T-bet. However, due to this limited panel and gating these experiments do not rule out these cells as either thymic resident NK cells or developing NKT cells and as CD117 and CD24 were not included in this panel they could not be defined as solely T cell specific lineage DN1s and DN2s. Further analysis using extensive panels for thymic NK and developing NKT cells will be shown in the next section. As expected, in the other developing T cells, the DN3s, DN4s and DP cell populations were completely negative (0%) for YFP expression. Single positive naïve CD4s were also fully negative (0%) for expression of YFP, which is expected as the naïve CD4s had yet to leave the periphery, encounter antigens and become activated. There was a small population (around 2-3%) of effector (CD62L$^-$ CD44$^+$) CD4$^+$ T cells found within the thymus that expressed high levels (around 50%) of YFP. These effector memory CD4$^+$ T cells are the effector memory CD4$^+$ T cells that are found within the thymus to help protect it during disease (Mueller and Mackay, 2015) and explains the high level of YFP. Lastly, CD4$^+$ CD8$^-$ CD25$^+$ T regulatory cells showed around 5% of YFP expression. A small proportion of T_{regs} have been shown to express T-bet as T_H1-like T_{regs} that are able to produce IFNγ and rely on the expression of CXCR3 to migrate to areas of inflammation and disease (Pandiyan and Zhu, 2015, Stock et al., 2004).

3.3.2 Phenotyping YFP$^+$ thymic resident NK and NKT cells in the thymus

The CD25$^-$ CD44$^+$ and CD25$^+$ CD44$^+$ identified cells shown previously had unexpectedly high levels of YFP expression. These could not be solely defined as specifically T cell specific lineages of DN1s or DN2s; due to the lack of CD117 and CD24 markers within the gating strategy. Moreover, surface markers used previously did not encompass thymus resident cells, for example thymic NK cells. Further experiments were performed to identify these cells. Figure 12 shows analysis of the YFP$^+$ CD25$^-$ CD44$^+$ and CD25$^+$ CD44$^+$ in comparison with the YFP$^-$ CD25$^-$ CD44$^+$ and CD25$^+$ CD44$^+$ cells. This experiment looked at expression of NK and NKT markers (DX5, CD122, NK1.1 and CD127) on the CD25$^-$ CD44$^+$ and CD25$^+$ CD44$^+$.

12A

Analysis of the YFP^{+} vs YFP^{-} CD25^{-} CD44^{+} cells in the thymus

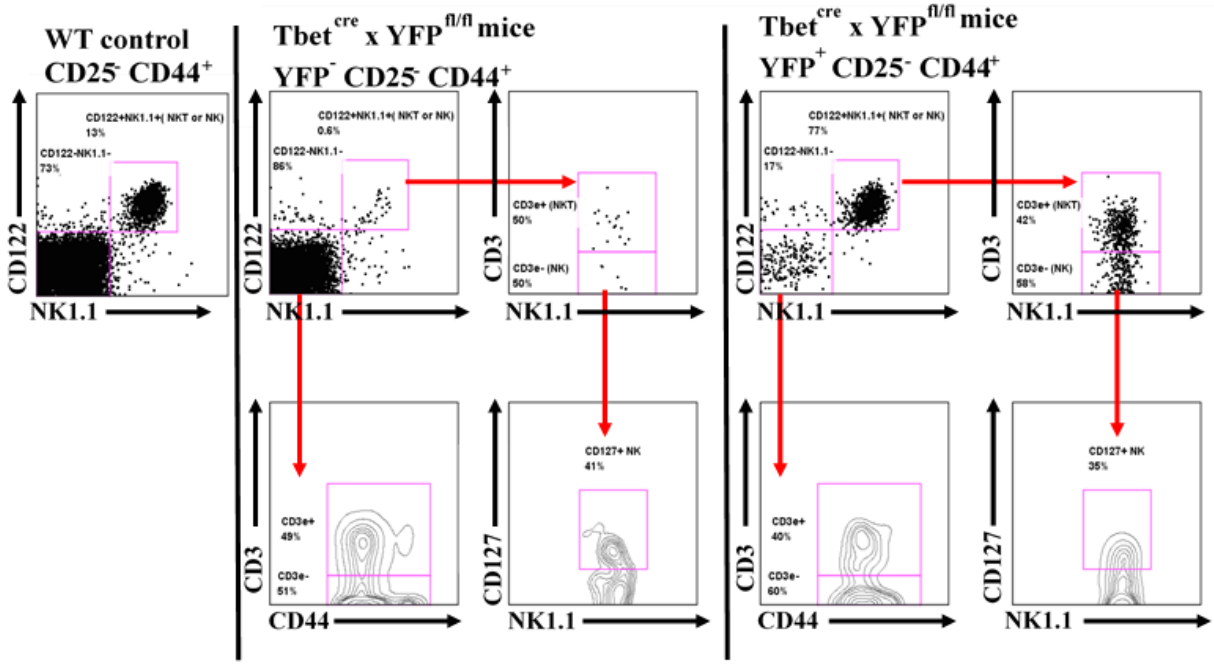

12B

Analysis of the YFP^{+} vs YFP^{-} CD25^{+} CD44^{+} cells in the thymus

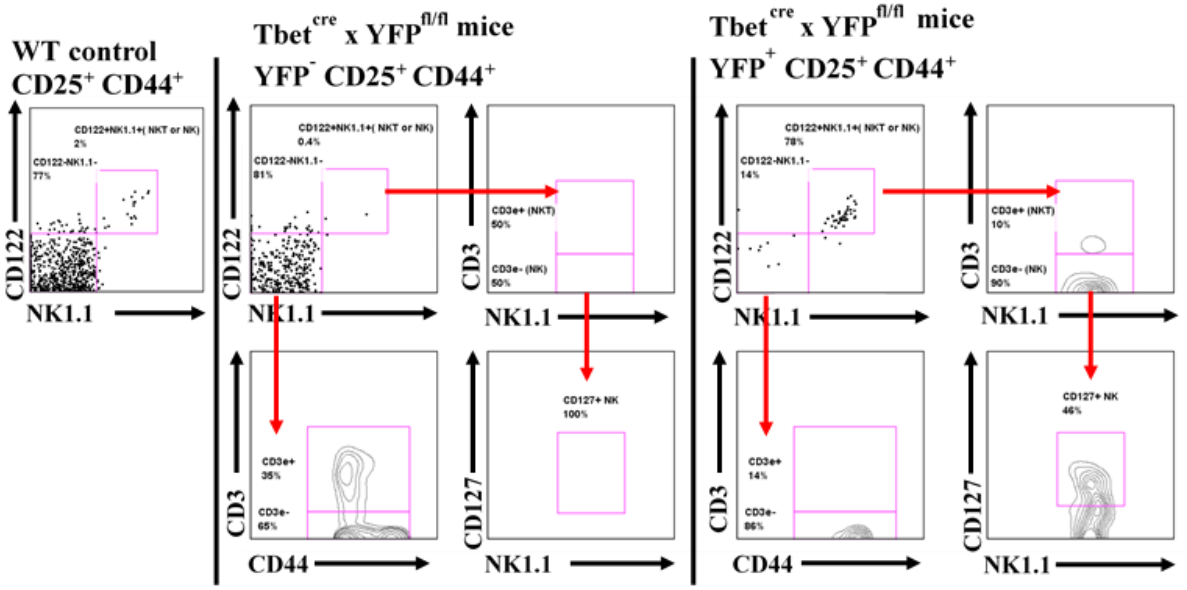

12C

Analysis of the individual NK and NKT markers on both YFP$^-$ and YFP$^+$ CD25$^-$ CD44$^+$ and YFP$^-$ and YFP$^+$ CD25$^+$ CD44$^+$ cells in the thymus

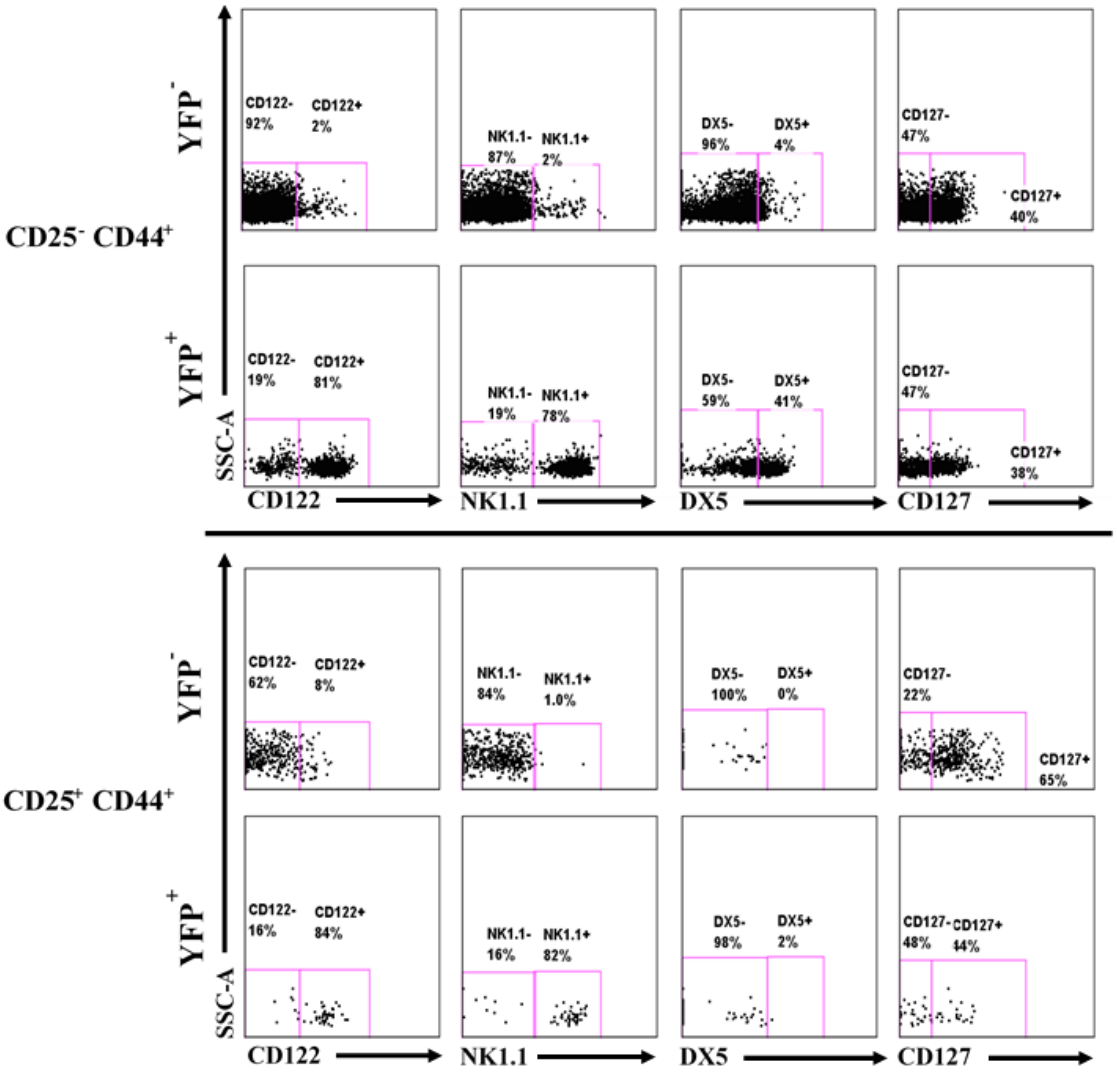

Figure 12: Flow cytometry analysis of the CD44$^+$ CD25$^-$ YFP$^+$ and CD44$^+$ CD25$^+$ YFP$^+$ cells in the thymus

A. Representative flow plots of live CD4$^-$ CD8$^-$ CD44$^+$ CD25$^-$ from the thymus of T-bet^{cre} x ROSA26YFP$^{fl/fl}$ mice. B. Representative flow plots of analysis of live CD4$^-$ CD8$^-$ CD44$^+$ CD25$^+$ from the thymus of T-bet^{cre} x ROSA26YFP$^{fl/fl}$ mice. C. Representative flow plots showing analysis of individual NK and NKT markers on YFP$^-$ and YFP$^+$ cells in both CD44$^+$ CD25$^-$ and CD44$^+$ CD25$^+$. (n = 6)

Analysis of the CD44$^+$ CD25$^-$ (Figure 12A) showed that the majority (77%) of YFP$^+$ CD44$^+$ CD25$^-$ cells expressed either NK (35% for CD127$^+$ NK1.1$^+$ CD122$^+$) or NKT (42% for CD122$^+$ NK1.1$^+$ CD3e$^+$) markers. These YFP$^+$ cells could be either thymic resident NK cells that develop from the CD44$^+$ CD25$^-$ population or developing NKT cells. Figure 12B shows the analysis of the CD44$^+$ CD25$^+$. This population of cells are present in a smaller number and are

therefore more difficult to analyse, but they follow the same general pattern as the $CD44^+$ $CD25^-$ population. 90% of the YFP^+ cells expressed $CD127^+$ and $NK1.1^+$ identifying them as thymic resident NK cells. As there is no YFP expression after the DN2 stage (in the DN3 and DN4 shown in Figure 11) and with cells entering the DN3 stage believed to have fully committed to the T cell lineage, this is also evidence to support the notion that the YFP^+ DN cells are not cells, which are committed to the T cell lineage: T-bet is not expressed by DN T cell precursors. Both $CD44^+$ $CD25^-$ YFP^+ and $CD44^+$ $CD25^+$ YFP^+ cell populations expressed high levels of either NK markers in comparison with their YFP^- counterparts (Figure 12C).

3.3.3 Phenotyping γδT cell development in the thymus

As previously described, γδT cells develop within the thymus too. Since IFNγ production is dependent on T-bet expression to be able to produce IFNγ, use of this mouse line will be able to trace the lineage of these IFNγ-producing γδT cells from their developmental stages. As stated before, γδT cells also develop within the thymus (Turchinovich and Pennington, 2011). Using the below gating and flow cytometry panel, I have potentially identified some of the developing γδT cells for the purpose of analysing T-bet fate mapped γδT cells. In this case, progenitor γδT cells were identified as $CD3^+$ $TCR\gamma\delta^+$ $CD25^+$ $CD24^+$ $CD27^+$, immature γδT cells were identified as $CD3^+$ $TCR\gamma\delta^+$ $CD25^-$ $CD24^+$ $CD27^+$, IFNγ-producing γδT cells that eventually leave the thymus were identified as $CD3^+$ $TCR\gamma\delta^+$ $CD25^-$ $CD24^-$ $CD27^+$, which typically encompasses the γδT cells found in the lymph nodes, gut, spleen and liver. Finally there were possibly two IL-17A producing γδT cells that could potentially exist within this gating strategy from the thymus, $CD3^+$ $TCR\gamma\delta^+$ $CD25^-$ $CD24^-$ $CD27^-$ which are usually found in the lymph nodes, and $CD3^+$ $TCR\gamma\delta^+$ $CD25^+$ $CD24^-$ $CD27^-$, which are typically found in the dermis, peritoneal cavity and reproductive tract.

13A

Gating Strategy for γδ T cells in the thymus

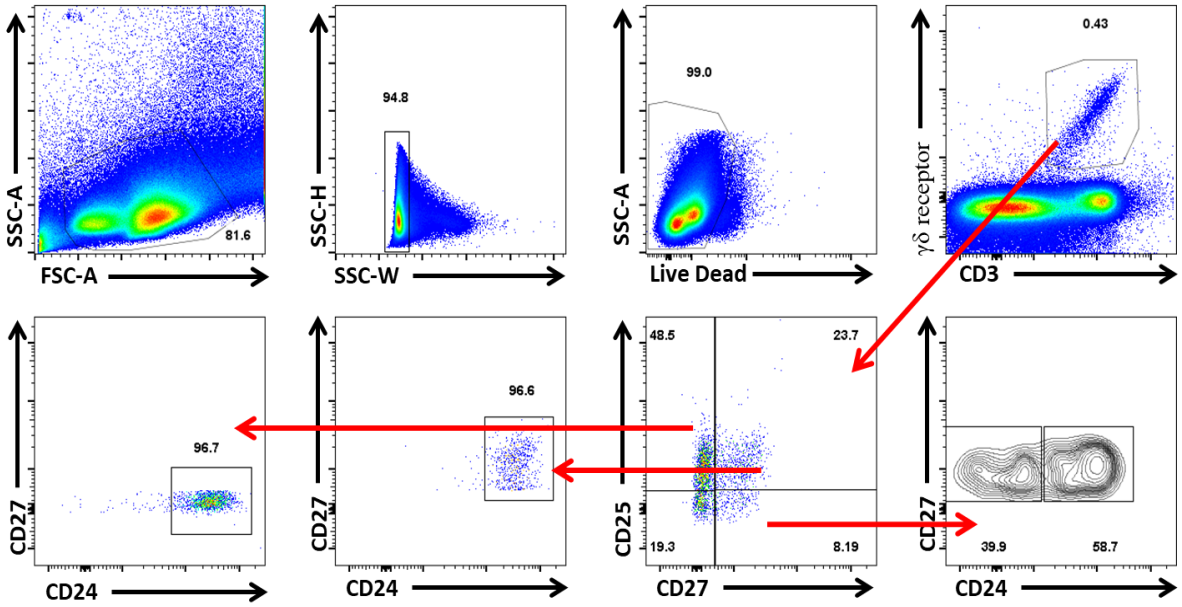

13B

Analysis of the percentage of YFP⁺ γδ T cells in the thymus

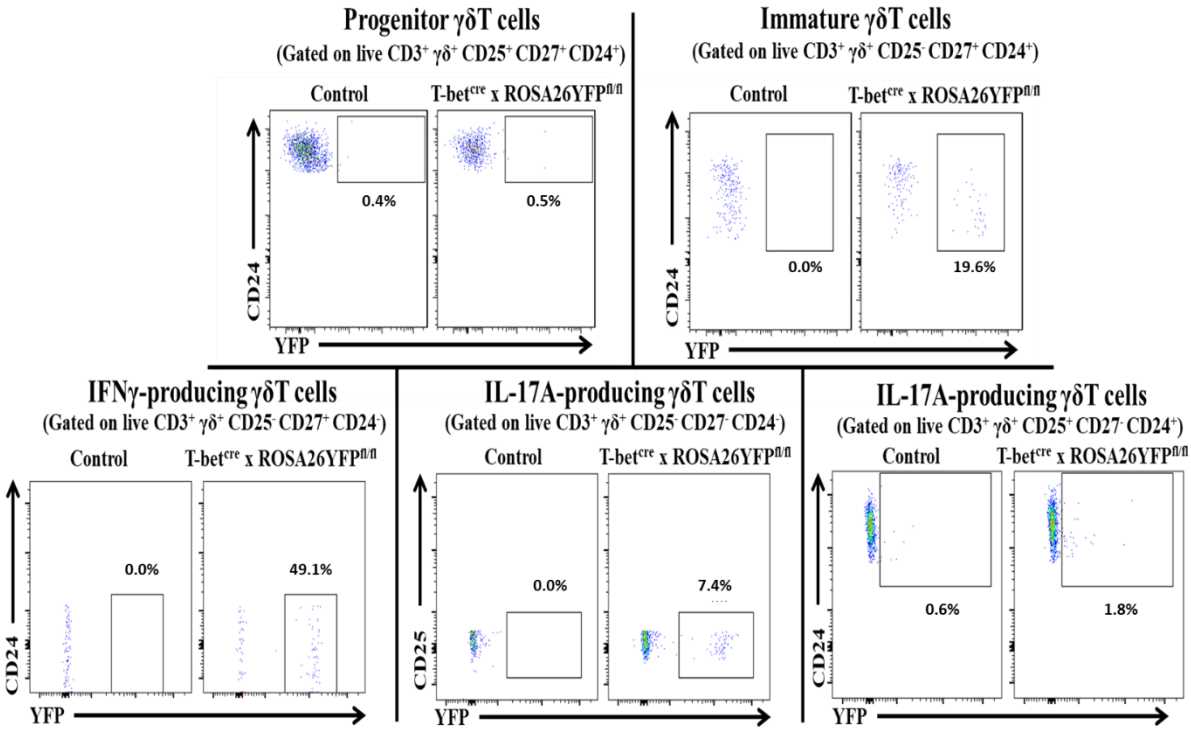

13C **Percentage of YFP$^+$ γδ T cells in the thymus**

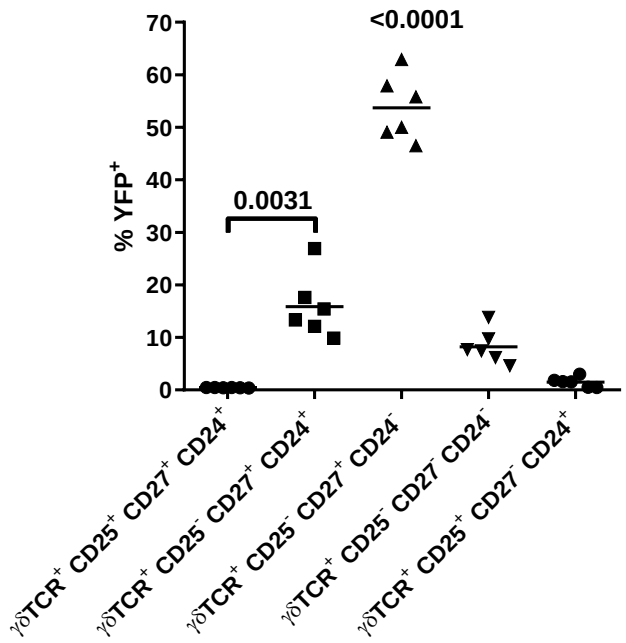

Figure 13: Phenotyping the YFP expression in developing γδT cell in the thymus of T-bet^{cre} x ROSA26YFP$^{fl/fl}$ mice.

A. Representative flow plots showing the gating strategy used to identify γδT cell in the thymus of T-bet^{cre} x ROSA26YFP$^{fl/fl}$ mice. B. Representative flow plots showing YFP$^+$ expressing cells of the four populations of developing γδT cells: progenitor γδT cells (CD25$^+$ CD27$^+$ CD24$^+$), immature γδT cells (CD25$^-$ CD27$^+$ CD24$^+$), IFNγ-producing γδT cells (CD25$^-$ CD24$^-$ CD27$^+$) and the two IL-17A-producing γδT cells (CD25$^-$ CD27$^-$ CD24$^-$ and CD25$^+$ CD27$^-$ CD24$^+$), from the thymus of T-bet^{cre} x ROSA26YFP$^{fl/fl}$ mice. C. Dot plot showing the mean percentage of YFP$^+$ expressing cells from the different stages of γδT cells development (n = 6). Kruskal-Wallis test performed with Dunn's corrections showing overall analysis of P<0.0001 for all groups. Individual comparisons are shown also using the same Kruskal-Wallis test.

Figure 13B and 13C show significant differences in the percentage of YFP$^+$ cells from the phenotyping results of the γδT cells in the thymus during development. As expected, in the progenitor (CD3$^+$ TCRγδ$^+$ CD25$^+$ CD24$^+$ CD27$^+$) γδT cells there was no YFP$^+$ expression in any of the cells. Surprisingly, there is a significant increase when the progenitor γδT cells downregulate CD25 expression and become immature (CD3$^+$ TCRγδ$^+$ CD25$^-$ CD24$^+$ CD27$^+$) γδT cells and this was shown by around 20% of them being YFP$^+$, meaning that some of the cells have expressed T-bet despite not being fully mature. These YFP$^+$ immature γδT cells could be predisposed to becoming IFNγ-producing γδT cells. As expected, the biggest population of YFP$^+$ γδT cells were the IFNγ-producing (CD3$^+$ TCRγδ$^+$ CD25$^-$ CD24$^-$ CD27$^+$) γδT cells with almost 60% of the cells being YFP$^+$. Interestingly, there was a small population (around 8%)

of CD25$^-$ CD24$^-$ CD27$^-$ IL-17A-producing γδT cells that are YFP$^+$, but there was no YFP$^+$ cells in the CD25$^+$ CD24$^+$ CD27$^-$ IL-17A-producing cells.

3.3.4 Phenotyping NKT cell development in the thymus

Similar to the γδT cell and CD4 and CD8 T cell populations, mature NKT cells also develop in the thymus from an immature state. NKT cells were gated as shown below in Figure 14A. Developing NKT cells were identified as immature stage 1 (NK1.1$^-$ CD24$^+$ CD44^{low} DX5$^-$), immature stage 2 (NK1.1$^-$ CD24$^-$ CD44^{low} DX5$^-$), immature stage 3 (NK1.1$^-$ CD24$^-$ CD44$^+$ DX5$^-$) and finally mature NKT cells (NK1.1$^+$ CD44$^+$). Interestingly, immature stage 4 NKT cells were unable to be identified in this gating strategy.

14A **Gating Strategy for NKT cells in the thymus**

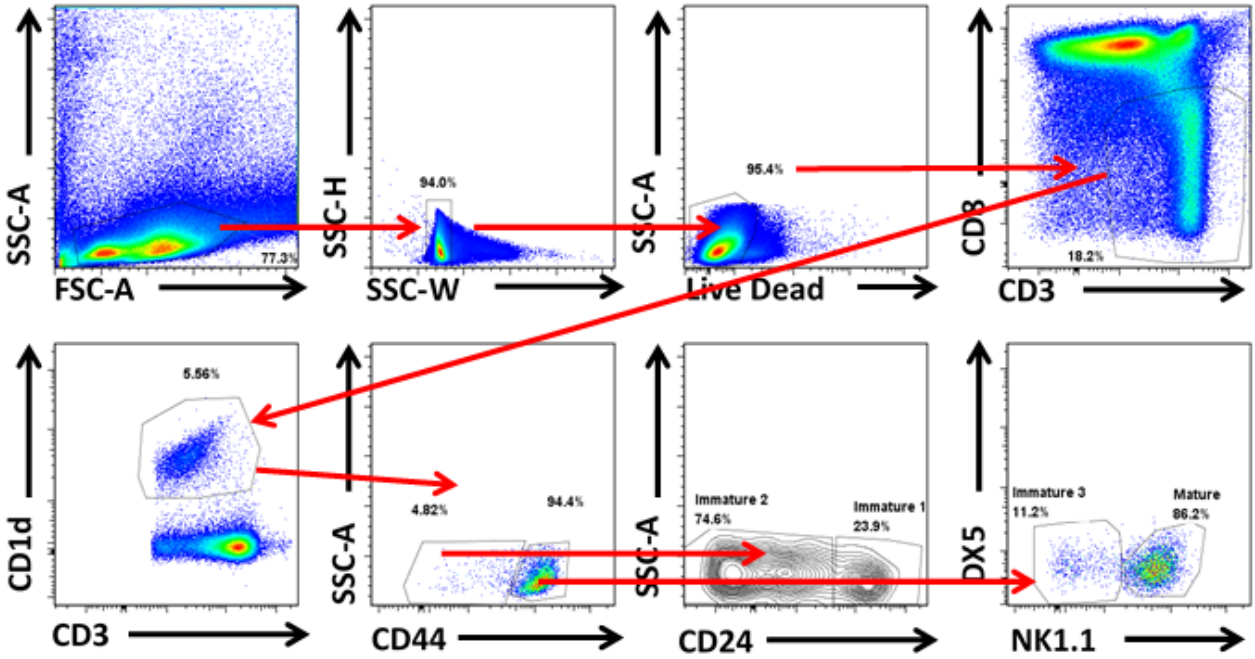

14B

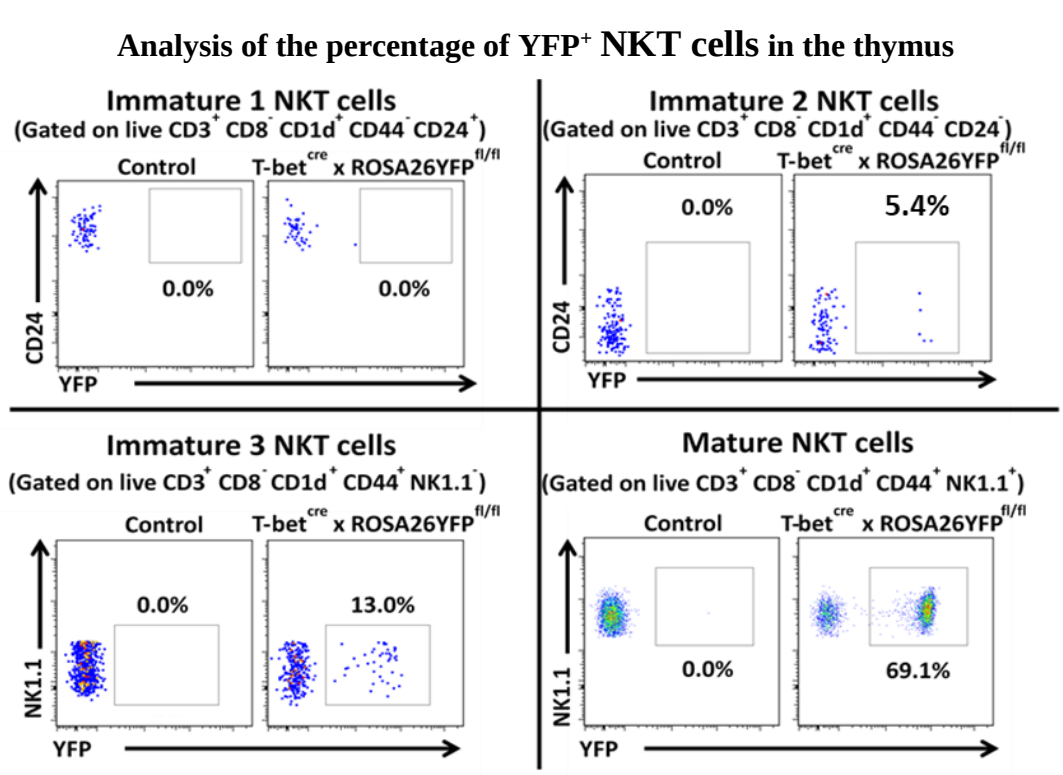

14C

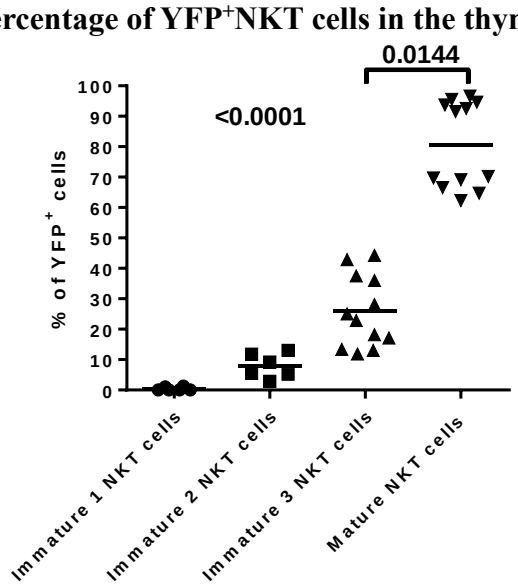

Figure 14: Phenotyping the YFP expression in developing NKT cells in the thymus of T-bet^{cre} x ROSA26YFP$^{fl/fl}$ mice

A. Representative flow plots showing the gating strategy used to identify NKT cell in the thymus of T-bet^{cre} x ROSA26YFP$^{fl/fl}$ mice. B. Representative flow plots showing YFP^{+} expressing cells of the four populations of developing NKT cells: Immature 1 NKT cells (CD44^{-} CD24^{+}), immature 2 NKT cells (CD44^{-} CD24^{-}), immature 3 (CD44^{+} CD24^{-} NK1.1^{-}) and mature NKT cells (CD44^{+} NK1.1^{+}), from the thymus of T-bet^{cre} x ROSA26YFP$^{fl/fl}$ mice. C. Dot plot showing the mean percentage of YFP^{+} expressing cells from the different stages of NKT cells development. (n = 12) Kruskal-Wallis test performed with Dunn's corrections showing overall analysis of P<0.0001.

Figure 14C show that there is a significant difference in the percentage of YFP^+ cells in the developing NKT cell stages. Both Figures 11B and 11C show that the immature stage 1 NKT cell begin demonstrating no YFP expression, but as the NKT cell develops further along its developmental stages the percentage of YFP^+ expressing cells increases substantially per stage of development. The immature stage 2 NKT cells showed around 5-10% cells expressing YFP, the immature 3 NKT cells varied from around 15% up to 40% of cells expressing YFP and lastly a majority of the mature NKT cells were YFP^+ (around 60-90%).

3.4 Phenotyping of progenitor cells in the bone marrow

Upon phenotyping the T lymphocyte populations in the thymus, it was important to research the cells in the bone marrow; since the common lymphoid (cLP) enters the thymus after developing from within the bone marrow. Phenotyping of the bone marrow was performed to investigate the YFP expression of progenitor cells. The cells phenotyped were the cLP, ChILP and ILC2p, with a gating strategy established and shown in Figure 15A.

15A

Gating Strategy for progenitor cells in the bone marrow

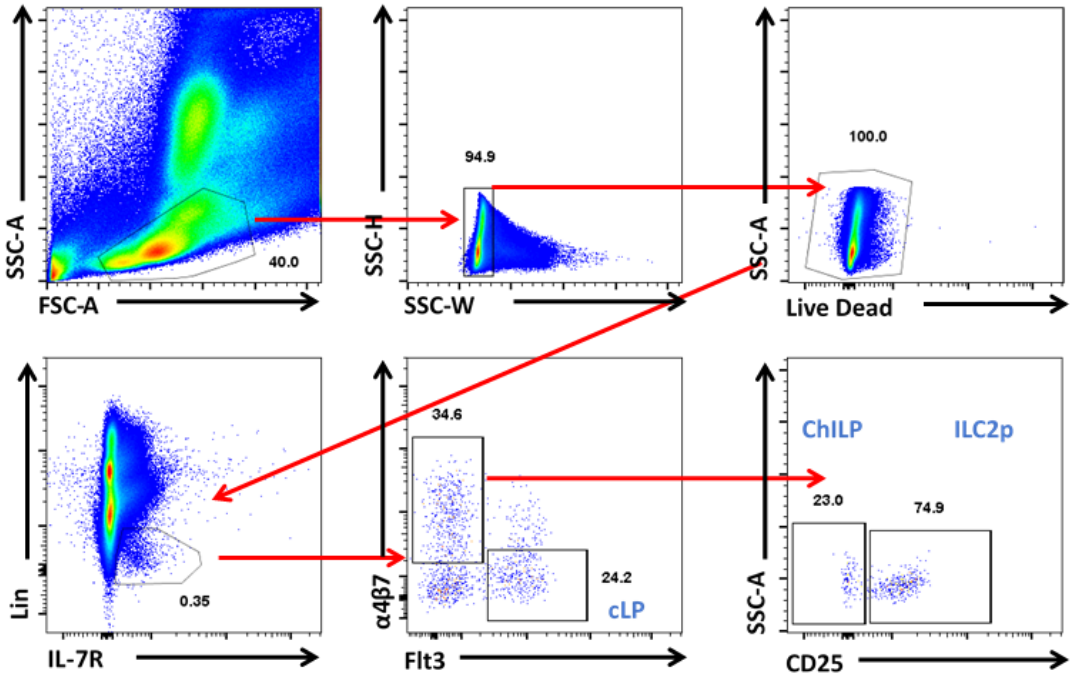

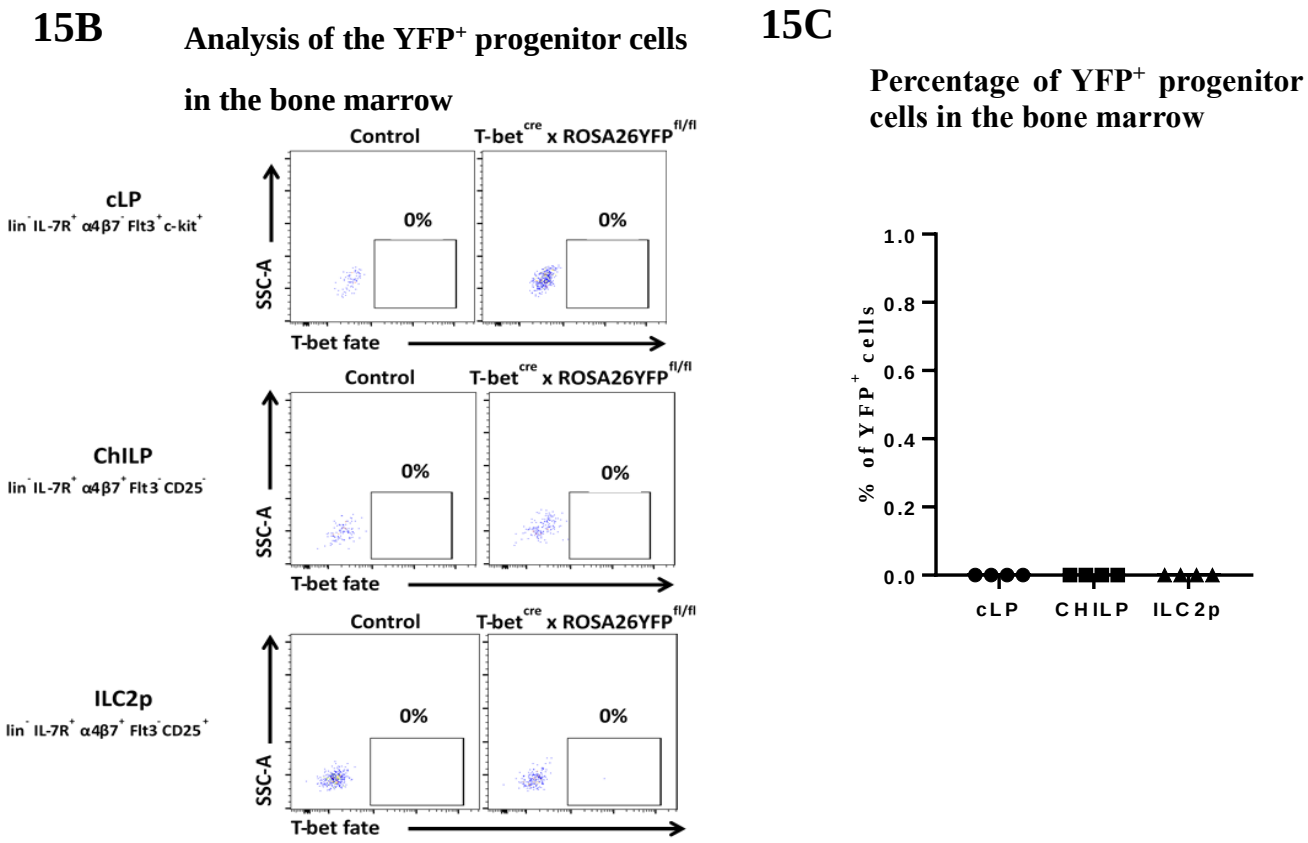

Figure 15: Phenotyping of YFP expression in the lymphoid precursors in the bone marrow of T-bet^{cre} x ROSA26YFP$^{fl/fl}$ mice

A. Representative flow plots showing the gating strategy used to identify the different precursor cells (labelled in blue) in the bone marrow of T-bet^{cre} x ROSA26YFP$^{fl/fl}$ mice. B. Representative flow plots showing YFP^{+} expressing cells of the three populations of progenitor cells: common lymphoid progenitor (lineage^{-} (CD3^{-} CD5^{-} B220^{-} CD19^{-} CD11b^{-} Ter-119^{-} Gr-1^{-} NK1.1^{-}) IL-7R^{+} α4β7^{-} Flt3^{+} c-kit^{+}), common helper-like ILC progenitor cells (lineage^{-} IL-7R^{+} α4β7^{+} Flt3^{-} CD25^{-}) and the ILC2p (lineage^{-} IL-7R^{+} α4β7^{+} Flt3^{-} CD25^{+}), from the bone marrow of T-bet^{cre} x ROSA26YFP$^{fl/fl}$ mice. C. Dot plot showing the mean percentage of YFP^{+} expressing cells from the progenitor population in the bone marrow (n = 4).

From these results, there was a trend to see that potentially there was no YFP^{+} expression in either the cLP, ChILP, ILC2p, in the bone marrow as expected. However, this was only tested on a small number of mice and should be checked on a few more mice just to absolutely confirm the lack of YFP^{+} cells in the bone marrow of these mice.

3.5 Phenotyping of immune cells in the peripheral organs

3.5.1 Phenotyping T cells in the spleen and colon

Following on from the developing T cells in the thymus, the focus was to phenotype the CD4^{+} and CD8^{+} T cells in the periphery. Figures 16A show the gating strategy used to identify the different subpopulations CD4^{+} and CD8^{+} T cells in the spleen and colon.

16A

Gating Strategy of CD4 and CD8 T cells in both spleen and colon

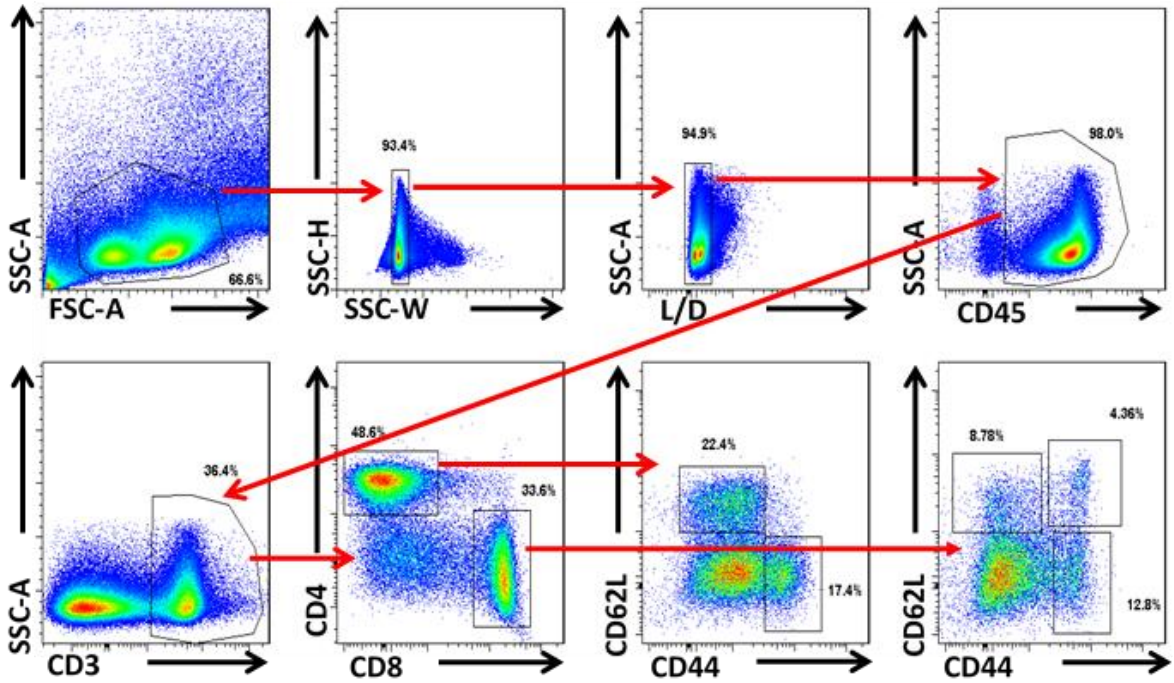

16B

YFP expression in T cell populations in the spleen

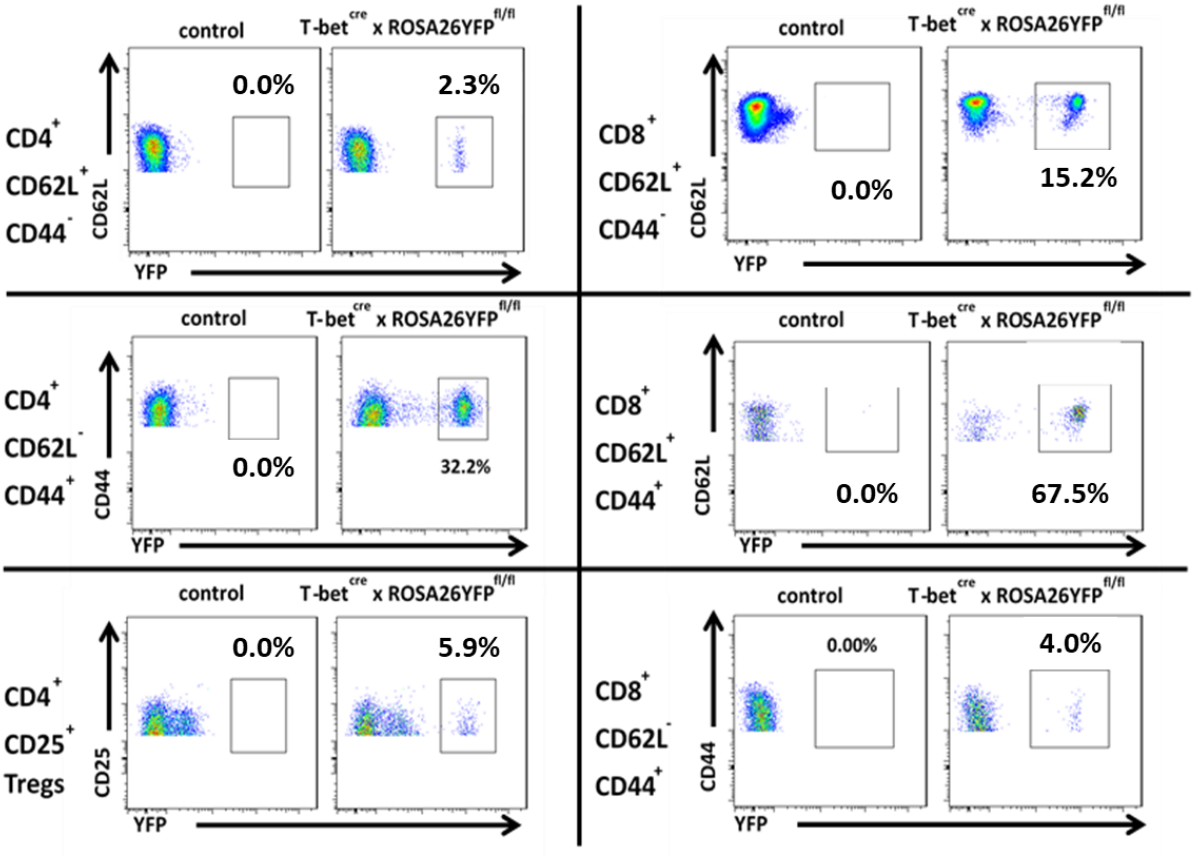

16C **YFP expression in T cell populations in the colon**

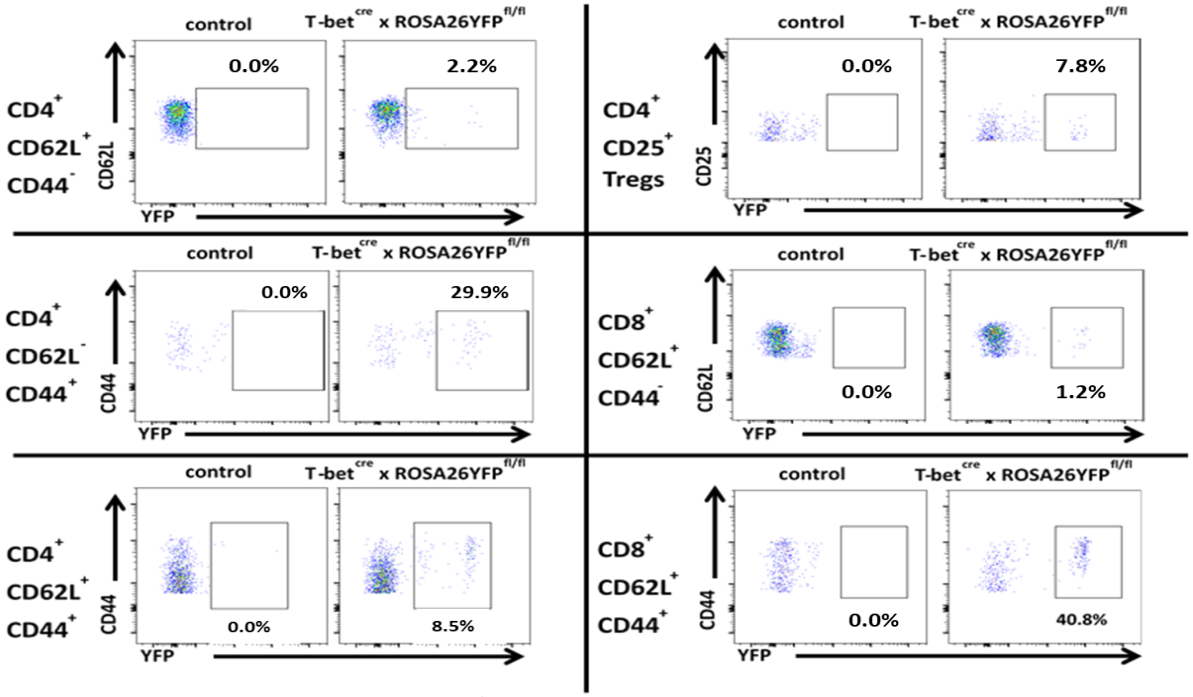

16D **Percentage of YFP+ in T cell populations in the colon and spleen**

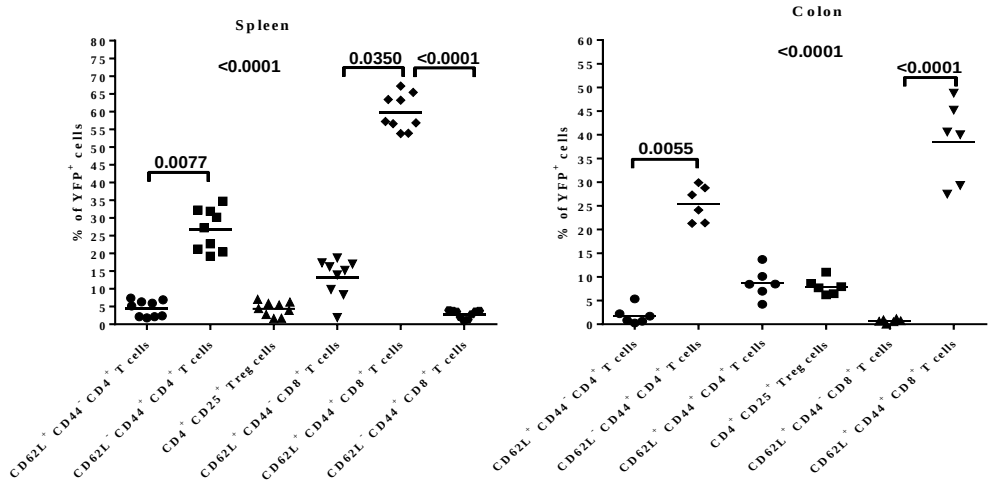

Figure 16: Phenotyping of the spleen and colon showing YFP+ expression in naïve CD4+ T cells in the T-bet^{cre} x ROSA26YFP$^{fl/fl}$ mice

A. Representative flow plots showing the gating strategy used to identify the different CD4+ and CD8+ cells in the spleen and colon of T-bet^{cre} x ROSA26YFP$^{fl/fl}$ mice. B. Representative flow plots showing YFP+ expressing cells of the six populations gated for: naïve CD4+ T cells (CD3+ CD4+ CD8- CD25- CD62L+ CD44-), effector CD4+ T cells (CD3+ CD4+ CD8- CD25- CD62L- CD44+), regulatory T cells (CD3+ CD4+ CD8- CD25+), naïve CD8+ T cells (CD3+ CD4- CD8+ CD62L+ CD44-), effector CD8+ T cells (CD3+ CD4- CD8+ CD62L- CD44+) and central memory CD8+ T cells (CD3+ CD4- CD8+ CD62L+ CD44+) from the spleen of T-bet^{cre} x ROSA26YFP$^{fl/fl}$ mice. C. Representative flow plots showing YFP+ expressing cells of the six populations gated for: naïve CD4+ T cells, effector CD4+ T cells, central memory CD4+ T cells (CD45+ CD4+ CD8- CD62L+ CD44+), regulatory T cells, naïve CD8+ T cells and central memory CD8+ T cells from the colon of T-bet^{cre} x ROSA26YFP$^{fl/fl}$ mice. D. Dot plot showing the mean percentage of YFP+ expressing cells from the different subtypes of T cells in the spleen (n = 9) and colon (n = 6). Kruskal-Wallis test performed with Dunn's corrections showing overall analysis of P<0.0001 for all groups. Individual comparisons are shown also using the same Kruskal-Wallis test.

Both $CD4^+$ and $CD8^+$ of naive T cells had not yet encountered foreign antigen on their respective TCR to undergo differentiation and activation. However, both naïve cell types left the thymus completely YFP^-, and yet in the spleen and colon, the two naïve subsets of $CD4^+$ and $CD8^+$ T cells both showed cells that were YFP^+. Around 2-3% of naïve CD4s and around 16% of naïve CD8s in the spleen, and around 2-3% of naïve CD4s and 1% of naïve CD8s in the colon were YFP^+. The effector CD4s showed around 25% of YFP^+ cells in both the spleen and the colon. Some T_{regs} express T-bet, and the same percentage as seen in the thymus, around 5% of YFP^+ cells, were also identified in the spleen and colon of the mice. The effector $CD8^+$ cells were only present in the spleen of the mice at a healthy state and they had a small proportion (around 5%) of YFP^+ expressing cells. The central memory $CD8^+$ T cell population had a high percentage (around 60% in the spleen and 40% in the colon) of cells that were YFP^+.

3.5.2 Phenotyping ILCs in the spleen and colon

ILCs share many features with T cells, as explained previously. The role of T-bet in their plasticity and function was investigated using this mouse line, since T-bet plays a role in the function and differentiation of ILCs. As the ILC precursor in the bone marrow showed no YFP^+ cell expression, the ILC populations were loosely phenotyped in the spleen and colon. Figure 17A shows the gating strategy used for both organs. Data from this initial phenotyping laid foundations for understanding plasticity in ILCs and was followed up by another project.

17A

Gating Strategy of ILCs in both spleen and colon

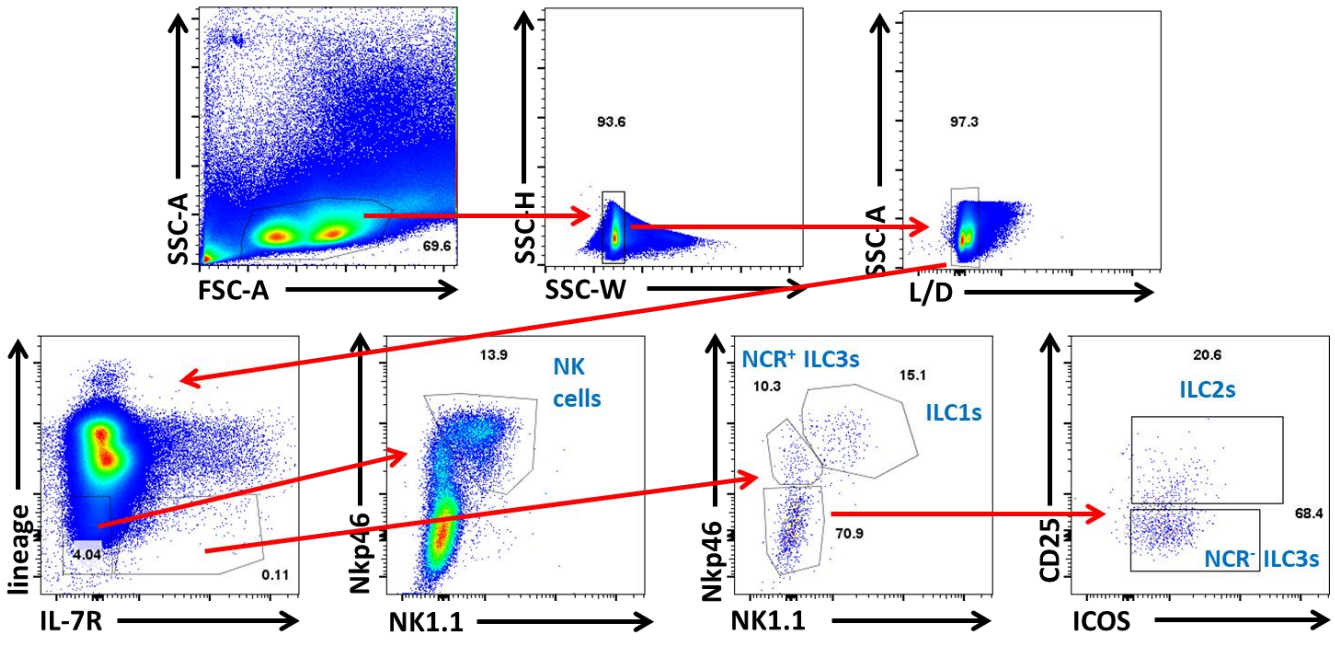

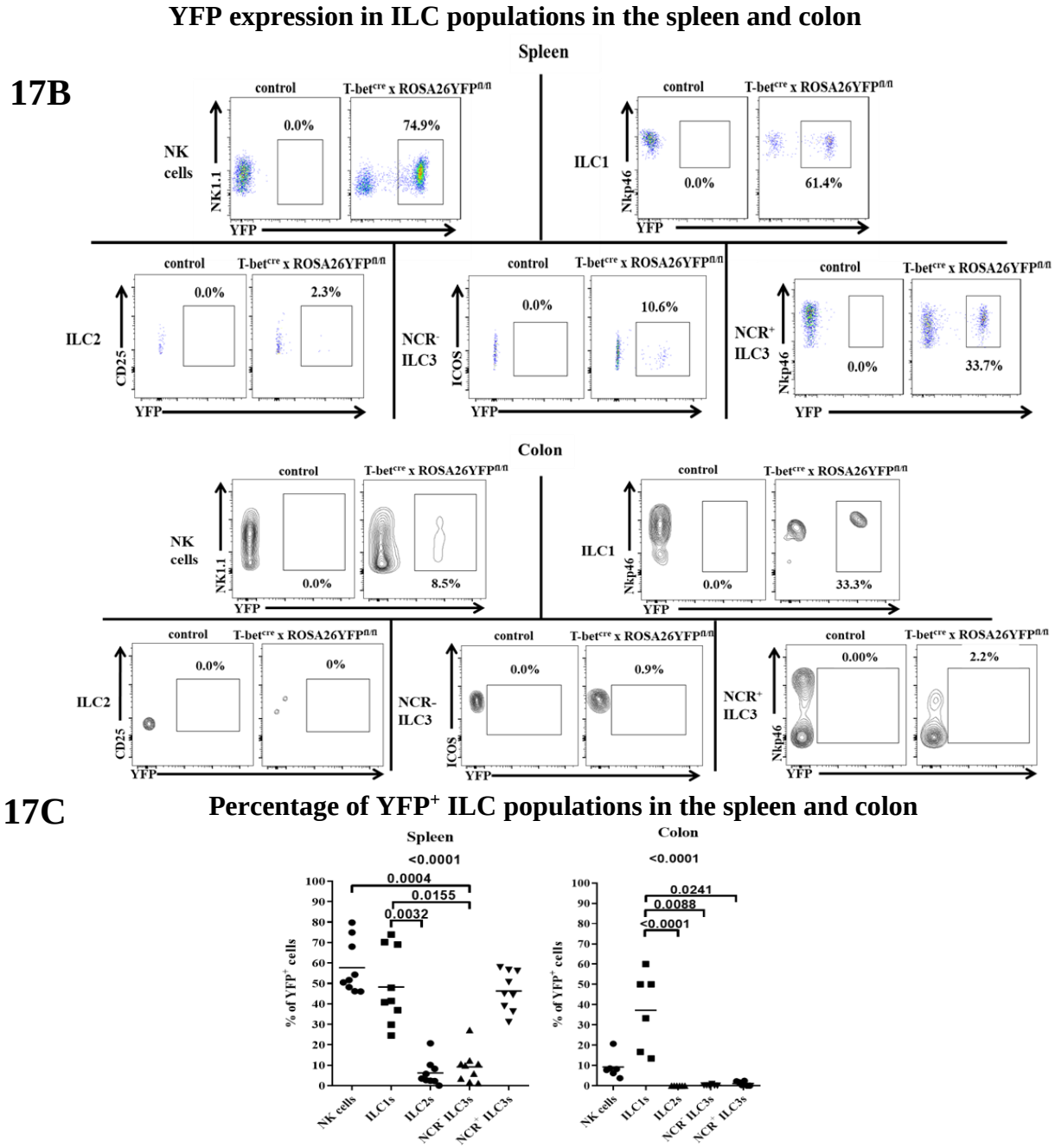

Figure 17: Phenotyping of YFP expression in NK cells and ILCs in the spleen and colon of T-bet^{cre} x ROSA26YFP$^{fl/fl}$ mice

A. Representative flow plots showing the gating strategy used to identify the different ILC subsets (labelled in blue) in the spleen of T-bet^{cre} x ROSA26YFP$^{fl/fl}$ mice. B. Representative flow plots showing YFP^{+} expressing cells of the 4 populations gated for: NK cells (lin^{-} (same lineage cocktail as before) IL-7R^{-} Nkp46^{+} NK1.1^{+}), ILC1s (lin^{-} IL-7R^{+} Nkp46^{+} NK1.1^{+}), ILC2s (lin^{-} IL-7R^{+} Nkp46^{-} NK1.1^{-} CD25^{+} ICOS^{+}), NCR^{-} ILC3s (lin^{-} IL-7R^{+} Nkp46^{-} NK1.1^{-} CD25^{-} ICOS^{+}) and ILC3s (lin^{-} IL-7R^{+} Nkp46^{+} NK1.1^{-}), from the spleen and colon of T-bet^{cre} x ROSA26YFP$^{fl/fl}$ mice. C. Dot plot showing the mean percentage of YFP^{+} expressing cells from the different subtypes of ILCs in the spleen (n=9) and colon (n=6). Kruskal-Wallis test performed with Dunn's corrections showing overall analysis of P<0.0001 for all groups in both spleen and colon. Individual comparisons are shown also using the same Kruskal-Wallis test.

Figures 17B and 17C show that in the spleen and colon of this mouse there are significant differences ($P<0.0001$) with YFP expressing ILCs in the periphery, despite the precursor cells leaving the bone marrow as YFP^-. Furthermore, in a healthy state there are not many (around 0.5-1% in the spleen and colon) lin^- IL-$7R^+$ cells present in the periphery. The percentage of NK cells in the spleen that expressed YFP^+ was high (around 60%) but low (around 10%) in the colon. ILC1s require T-bet to develop and differentiate into ILC1s, and around 50% of the ILC1s in the spleen and colon were YFP^+. There were very few YFP^+ ILC2s and NCR^- ILC3s in both the spleen and colon. Although in the spleen there was still around 10% of YFP^+ ILC2s and NCR^- ILC3s. Whereas in the colon there were hardly any ILC2s to gate on, but there were no YFP^+ NCR^- ILC3s. Finally, ILCs are known to express T-bet when differentiating into NCR^+ ILC3s upon activation and stimulation. In these mice, there was interestingly around 33% of the NCR^+ ILC3s which were YFP^+. Again, the lack of ILCs in the colon made it difficult to see the true percentage of YFP^+ cells in this organ.

3.6 Discussion

The results presented in this chapter show the YFP expression of T-bet in the lineage of different cell types in the mouse at a stable phenotypic manner. This novel mouse line has been innovative in being able to trace the lineage of cells that have expressed T-bet despite not necessarily being T-bet^+ at the time. This chapter focussed on the phenotyping of developing cells in both the thymus and the bone marrow and subsequent peripheral mature cells.

As expected, the developing thymic SP $CD4^+$ and $CD8^+$ T cells were all YFP^-. Double negative T cells in the thymus were also YFP^-. The results showing the DN1 and DN2 population would need further surface markers of CD24, CD117 and CD127; in order to fully determine the lineage of the double negative T cell lineage and determine if those DN1 T cells and DN2 T cells are truly YFP^- or not (Ceredig and Rolink, 2002, Allman et al., 2003, Porritt et al., 2004). However, the data shown in these mice showed that the DN3, DN4 and DP cells were all YFP^-. Therefore, since in this mouse model if a cell starts to express the YFP then it stays YFP forever due to the excision of the STOP codon. Therefore, since the subsequent phenotyping data showed that the T cells further down the development pathway were not yellow, this most likely means that the DN1 and DN2 T cell lineage will also be YFP^-. Furthermore, the phenotyping data showed that of the cells which were $CD3^-CD44^+$ $CD25^-$ and $CD3^-$

$CD44^+CD25^+$ they were mainly either thymic resident NK and/or thymic NKT cells with their expression of CD122, NK1.1, DX5 and/or CD3e. It has also been shown by others that $CD127^+$ thymic NK cells develop from the DN1 ($CD44^+CD25^-$) (Vargas et al., 2011).

This model has also demonstrated YFP expression in γδT cell development in the thymus. There were interesting findings in the results for the γδT cell development in the thymus. 20% of the $CD25^-$ $CD27^+$ $CD24^+$ immature γδT cells being YFP^+, meaning that some of the cells expressed T-bet despite not being fully mature. These YFP^+ immature γδT cells could be predisposed to becoming IFNγ-producing γδT cells. As expected, a majority of the $CD25^-$ $CD27^+$ $CD24^-$ IFNγ-producing γδT cells showed to be YFP^+. A small population of $CD25^-$ $CD24^-$ $CD27^-$ IL-17A-producing γδT cells were shown to be YFP^+, but there was no YFP^+ cells in the $CD25^+$ $CD24^+$ $CD27^-$ IL-17A-producing cells. It has been shown that γδT cells are able to produce both IL-17A and IFNγ spontaneously and do not need to undergo clonal expansion (Paul et al., 2014, Ribot et al., 2009). Under inflammatory conditions, it has been shown that $CD27^-$ γδT cells are also able to produce both IL-17A and IFNγ, which explains why some of the $CD27^-$ conventional IL-17A-producing γδT cells are YFP^+ (Sheridan et al., 2013). The limitations of the flow cytometry panel in these experiments meant that it was unable to fully characterise the γδT cells in the thymus. Unfortunately, further surface markers are necessary for identifying some of the $CD25^-$ $CD24^-$ $CD27^+$ IFNγ-producing γδT cells, which are $CD122^+$ and $CD44^+$, and $CD25^-$ $CD24^-$ $CD27^-$ IL-17A-producing γδT cells have also been shown to be $CD44^+$ (Hayday and Pao, 1998, Pang et al., 2012, Ribot et al., 2009, Sheridan et al., 2013). Further analysis of γδT could also be achieved using this mouse model since T-bet is required for IFNγ in $CD27^+$ γδT cells (Yin et al., 2002), as well as T-bet has also been shown to be important in IFNγ production in $CCR6^+$ $CD27^-$ IL-17A-producing γδT cells (Barros-Martins et al., 2016). Therefore, the lineage of mature γδT cells could be traced back to their development in the thymus with further experiments.

Regarding the NKT cell development phenotyping in the thymus, the amount of YFP^+ cells increased throughout the maturity stages of the NKT cell. As has been shown previously by many groups, T-bet is progressivly upregulated and, when absent NKT cells do not mature beyond the immature stage 2 (Godfrey et al., 2010, Matsuda et al., 2006, Simonetta et al., 2016).

The cLP, ChILP and ILC2 progenitor cells in the bone marrow cells also were shown to be YFP^-. The cell types in the periphery that were expected to be YFP^+ (NK cells, memory CD4, memory CD8s, ILC1s and NCR^+ ILC3s) were observed. Both naïve cell types left the thymus completely YFP^-, but there was a small subset of both $CD4^+$ and $CD8^+$ T cells that were YFP^+. The effector CD4s showed around 25% of YFP^+ cells in both the spleen and the colon. Some activated $CD4^+$ helper T cells, which have previously seen antigen and become memory cells, will have been T_H1 T-bet^+ cells and therefore YFP^+. Within the thymus, regulatory T cells can express T-bet, and the same percentage, around 5% of YFP^+ cells that were found in the thymus, were also identified in the spleen and colon of the mice. The effector $CD8^+$ cells were only present in the spleen of the mice at a healthy state and they had a small proportion (around 5%) of YFP^+ expressing cells. In healthy steady state mice, there will not be as many effector CD8s without the activation of the TCR receptor. Upon activation via their TCR by viral antigens, CD8s strongly upregulate T-bet (and also EOMES) in order to produce a high amount of IFNγ, granzyme B and perforin (Intlekofer et al., 2005). It has been shown that T-bet itself becomes downregulated after effector CD8s have cleared a pathogen (Joshi et al., 2011). The central memory $CD8^+$ T cell population had a high percentage (around 60% in the spleen and 40% in the colon) of cells that were YFP^+. After an infection has been cleared, 95% of effector CD8s die by apoptosis (Kaech and Cui, 2012a), but the remaining cells become central memory CD8 T cells. Therefore, of the remaining central memory CD8s, these YFP^+ $CD8^+$ T cells may be the ones that came from the effector CD8 T cells and allow for early IFNγ response when the same virus antigen infection is presented again.

NK cells have been shown to require T-bet in order to mature and also aid in their function to produce IFNγ, but they do not require T-bet for NK cell development (Simonetta et al., 2016). The high proportion of YFP^+ expressing NK cells identified in the spleen was therefore expected. In the colon only 10% of the NK cells were shown to be YFP^+, but the mucosal sites contained fewer cells within the tissue at healthy state. It may be only during inflammation that these cells proliferate and migrate into the colon.

ILC1s and NCR^+ ILC3s require T-bet to differentiate from the ChILP (Artis and Spits, 2015). Around 50% and 30% of the ILC1s and NCR^+ ILC3s respectively expressed YFP in the spleen, and a mean of 30% of the ILC1s expressed YFP in the colon. Lastly, in the bone marrow the ILC2p did not express YFP. However, upon exiting the bone marrow, around 10% of ILC2s in

the spleen were found to be YFP^+. Subsequent data in another project looking at the T-bet^+ ILC2s has been carried out in this model to identify the plasticity of ILC2s. However, the staining for ILCs in this panel were not sufficient to fully identify the different subsets of ILC1, ILC2 and ILC3s. Therefore the addition of T-bet itself, GATA3 and RORγt to identify ILC1s, ILC2s and ILC3s respectively would have been more decisive (Dutton et al., 2018, Diefenbach et al., 2014).

However, the data from this chapter showed that the T-bet^{cre} x $ROSA26YFP^{fl/fl}$ mice line was a valuable and working mouse line to trace the lineage of T-bet expressing cells and would possibly be useful in identifying any previously T-bet expressed cells that no longer are T-bet^+ nor been discovered by previous groups.

Chapter 4

Results: Characterising the naïve YFP$^+$ CD4 T cells

T-bet is the master transcription factor of T_H1 differentiation from naïve T cells (Szabo et al., 2000). A small percentage (around 5%) of T-bet fate mapped YFP$^+$ naïve (CD4$^+$ CD25$^-$ CD44$^-$ CD62L$^+$) CD4 T cells have been identified in the spleen of heathy T-bet^{cre} x ROSA26$^{fl/fl}$ mice. "Naïve" implies that the CD4 T cell has not yet experienced any antigen and thus not become activated. Naïve T cells are identified by the difference in their surface markers compared to their memory CD4 T cell counterparts. Traditional phenotyping methods simply define naïve CD4$^+$ T cells to be only CD62L$^+$ and CD44$^-$, central memory CD4$^+$ T cells to be both CD62L$^+$ and CD44$^+$, whilst effector CD4$^+$ T cells are only CD44$^+$ and CD62L$^-$ as shown in the previous chapter. However, to fully phenotype these mice and their CD4$^+$ T cell compartment, more extensive surface markers were necessary. Additional phenotyping of other organs and secondary lymphoid organs were also performed to widen the scope of the phenotyping data. Additional surface markers used to differentiate between naïve, central memory and effector CD4$^+$ T cells are CCR7, CD28 and CD27, whereby naïve CD4$^+$ T cells are CD62L$^+$ CD44$^-$ CCR7$^+$ CD28$^+$ CD27$^+$, central memory CD4$^+$ T cells are CD62L$^+$ CD44$^+$ CCR7$^+$ CD28$^+$ CD27$^-$ and effector CD4$^+$ T cells defined as CD62L$^-$ CD44$^+$ CCR7$^-$ CD28$^+$ CD27$^-$ (Hu and August, 2008, Sallusto et al., 1999, Williams et al., 2011, Zhu et al., 2010, Berard and Tough, 2002). CCR7 is a chemokine receptor and is known to be expressed on naïve T cells, central memory T cells, dendritic cells and B cells. The ligands for CCR7 are two chemokines CCL19 and CCL21. Unlike most chemokines, which are induced by inflammation and infections, CCL19 and CCL21 are always expressed. Chemokines are vital in controlling immune cell movement in homeostasis. This is especially important for naïve T cells, which are required to migrate to secondary lymphoid. CD28 and CD27 are costimulatory molecules found on the surface of CD4$^+$ T cells and require sufficient binding and activation. Along with the stimulation of the T cell receptor, they are essential for the CD4$^+$ T cell to become activated. All three of these molecules are highly expressed in the naïve CD4$^+$ T cell population as they circulate through the periphery and organs. Upon activation of naïve T cells into effector cells, they stop expressing these markers, and CD62L, and express CD44. Central memory cells have been shown to express CCR7, CD62L and CD27, because they are recirculating memory cells that will be able to illicit an immunological response to previously encountered antigen. Use of

these more extensive surfaces markers to identify naïve and memory T cell have enabled others to report on small $CD4^+$ and $CD8^+$ T cell populations and have identified these as: stem cell-like naïve T cells, memory naïve-like T cells and virtual memory T cells.

In 2011, Gattinoni et al. described a subset of CD4 and CD8 T cells that were stem cell-like memory cells (Gattinoni et al., 2011). These cells appear naïve and express many similar surface markers. Much of the previous research on these cells focused on human stem cell-like memory cells and other groups have mainly focussed on CD8s (Ahmed et al., 2016, Gattinoni et al., 2009). However, as there are many similarities between CD4 and CD8 naïve and memory T cells, the $CD4^+$ T cells were phenotyped for the possibility that they were stem cell-like memory. Stem cell-like memory cells are also $CD62L^+$ $CD44^-$ $CCR7^+$ $CD28^+$ and $CD27^+$ like naïve T cells. Stem cell-like memory cells have also been shown to express higher levels of CD95, CD122 (IL-2R), CXCR3, LFA-1 and Sca-1 (Gattinoni et al., 2011, Gattinoni et al., 2009). Many of these additional markers share common expression on the $CD44^+$ memory cell populations.

Haluszczak et al, in 2009, reported on another possible small cell population derived from the standard $CD8^+$ $CD44^+$ memory cells (Haluszczak et al., 2009). They showed that there was a population of memory cells which they termed "virtual memory" T cells which are different to the homeostatic proliferating memory T cells. Since then more research by multiple groups has investigated these virtual memory cells, although always in CD8 T cells (Lee et al., 2013, White et al., 2016). Virtual memory CD8 T cells have been shown to be $CD62L^-$ $CD44^+$ $CD122^+$ $CD49d^-$ $CXCR3^+$.

Another study, by Pulko et al in 2016, also identified another memory T cell with naïve-like phenotype, which they named "T_{MNP} cells". These T_{MNP} cells again were only identified in human samples and in the CD8 population and they have not been reported in the CD4 population. They identified T_{MNP} cells as $CD62L^+$ $CD44^-$ $CD49d^+$ $CXCR3^+$ (Pulko et al., 2016).

In 2017, Kawabe et al. reported on a new $CD4^+$ $CD44^+$ $CD62L^-$ memory cell type that can develop independently from pathogen activation. They are named memory-phenotype (MP)

cells (Kawabe et al., 2017, Sprent and Surh, 2011). These MP cells have been identified in both germ-free and antigen free (defined by having offspring of GF mice that were weaned onto and subsequently raised on the elemental Ag-free diet being specifically dietary commensal antigen free) mice (Kim et al., 2016). Furthermore, these MP cells appear to develop from naïve $CD62L^+$ $CD44^-$ cells, which are still present in mice that have had a thymectomy during development. Kawabe et al. showed that these cells require MHCII and CD28 for their development. They also found that MP cells arise from $CD5^{hi}$ naïve cells, but that naïve $CD5^+$ CD4s have a lower level of T-bet expression compared to MP cells, which they showed have $T\text{-}bet^{lo}$, $T\text{-}bet^{int}$ and $T\text{-}bet^{hi}$ states. Lastly, they also showed that $T\text{-}bet^{hi}$ MP cells are crucial in host defences against pathogens and were responsible for IFNγ production (Kawabe et al., 2017).

Summary table on the small $CD4^+$ and $CD8^+$ T cell populations			
Cell type	**Group**	**Surface markers that define them**	**Reference**
Stem cell-like memory cells	Gattinoni et al.	$CD8^+$ $CD62L^+$ $CD44^-$ $CCR7^+$ $CD28^+$ $CD27^+$ $CD95^+$ $CD122^+$ $CXCR3^+$ LFA-1^+ Sca-1^+	(Gattinoni et al., 2011)
Virtual memory T cells	Haluszczak et al.	$CD8^+$ $CD62L^-$ $CD44^+$ $CD122^+$ $CD49d^-$ $CXCR3^+$	(Haluszczak et al., 2009)
Memory T cell with naïve-like phenotype – "T_{MNP} cells"	Pulko et al	$CD8^+$ $CD62L^+$ $CD44^-$ $CD49d^+$ $CXCR3^+$	(Pulko et al., 2016)
Memory-phenotype (MP) cells	Kawabe et al.	$CD4^+$ $CD44^+$ $CD62L^-$ $CD5^{hi}$ $T\text{-}bet^{hi}$	(Kawabe et al., 2017)

Table 4: Summary table showing the surface markers used to define stem cell-like memory cells, virtual memory T cells, naïve-like memory T cells (T_{MNP}) and memory-phenotype cells.

From Table 4, all three small T cell populations express CXCR3. CXCR3 is another chemokine receptor involved in migration of activated T cells. CXCR3 has three chemokine that bind to

it, these are: CXCL9, CXCL10 and CXCL11. Furthermore, T-bet has been shown to have an important role in regulating the expression of CXCR3, and in T-bet$^{-/-}$ mice, the ability of effector cells to infiltrate and home to sites of inflammation was greatlt defected due to the loss of CXCR3, since T-bet was shown to directly transactivate CXCR3 (Groom and Luster, 2011, Oghumu et al., 2013, Tan et al., 2016b). CXCR3 has been shown to not be expressed on naïve T cells, but effector and memory T cells do highly express CXCR3. The upregulation of CXCR3 is followed after DC-induced T cell activation, prior to T cell proliferation in an antigen-specific manner (Groom and Luster, 2011, Oghumu et al., 2013, Tan et al., 2016b).

It was also important to understand whether the expression of YFP in these mice were a developmental or environmental effect. As the immune phenotype of mammals is vastly different at differing ages of their life, it was important to determine whether there were any visible changes to the YFP expression from embryonic mice to old age. Embryos aged E15.5 - E16 were used, as at this age the thymus and foetal liver have almost fully developed (Gordon and Manley, 2011, Zorn, 2008). During foetal organogenesis the foetal liver is also the main site of stem cells and progenitor cells, as opposed to the adult liver, which mainly has metabolic functions (Ito et al., 2013). As mice and human age, the CD4$^+$ T cell population changes. As mammals get older, the proportion of naïve CD4$^+$ T cells declines, but the percentage of the memory CD4$^+$ compartments rises (Nikolich-Žugich, 2005). Aged naïve CD4$^+$ T cells show a reduction in CD28 (Lefebvre and Haynes, 2012, Moro-García et al., 2013). CD28 is required for the activation of naïve CD4$^+$ T cells, and as this becomes downregulated with age, it was important to investigate whether this also occurred in the YFP$^+$ naïve CD4$^+$ T cell population or whether this population shows any other phenotypic differences.

Further phenotyping and analysis of these YFP$^+$ naïve CD4$^+$ T cells were carried out to identify the surface markers of these cells, to investigate potential importance for T cell differentiation, and investigations were carried out to find if these YFP$^+$ naïve CD4$^+$ T cells play a defining role during pathogenic response in the mucosa. The ideal way to view how these YFP$^+$ naïve CD4$^+$ T cells functioned *in vivo* was to transfer them into a *Rag2*$^{-/-}$ mice. Typically, in the T cell transfer colitis model, which is a wasting disease, it has been shown to be predominately an IFNγ driven disease model, with IL-17A also being produced to certain lower levels (Aranda et al., 1997, Coombes Janine et al., 2005, Powrie et al., 1993, Powrie et al., 1997). Interestingly,

transfer of naïve $CD4^+$ T cells from T-$bet^{-/-}$ mice results in an IL-17A driven disease (Gökmen et al., 2013).

Bystander activation of both CD4 and CD8 T cells has been shown to occur where unrelated T cells become stimulated and activated from cytokines produced from other antigen-specific T cell stimulation (Boyman, 2010). Furthermore, bystander activation of T cells has been shown by previous groups to be essential for the proliferation and expansion of other T cells (Boyman, 2010, Tough et al., 1996). Relevant to the memory-phenotype (MP) T cell phenotyping for the YFP^+ naïve $CD4^+$ T cells, it has been shown that bystander activation occurred in MP $CD8^+$ T cells by IFNγ, IL-12 and IL-18 (Tough et al., 2001). Unfortunately, not as much is known about bystander activation in bulk $CD4^+$ T cells, let alone MP $CD4^+$ T cells. However, some bystander activation of $CD4^+$ has been observed which relies on an IL-2 dependent manner. This may have different effects to the MP $CD8^+$ bystander activation that has been observed by other groups due to IL-2 being required for cell survival of $CD4^+$ T cells (Boyman, 2010). It has also been shown that the $CD4^+$ T cell bystander activation might require an antigen response to be able to activate other cells (Eberl et al., 2000, van Aalst et al., 2017, Di Genova et al., 2010). Upon identifying this subset of naïve YFP^+ $CD4^+$ T cell, it would be important to determine whether they have any effect via bystander activation on the other non-YFP expressing $CD4^+$ T cells.

4.1 Phenotyping the naïve YFP^+ $CD4^+$ T cells in the T-bet^{cre} x ROSA26$YFP^{fl/fl}$ mice

Figure 18 showed more extensive phenotyping data of these cell types, including CD28, CD27 and CCR7, and within more peripheral organs than previously shown, to further distinguish between the naïve and memory populations in this mouse line.

18A **Representative flow plots showing YFP expression in naïve, effector and central memory CD4⁺ T cells in different organs in the T-bet^{cre} x ROSA26YFP$^{fl/fl}$ mice**

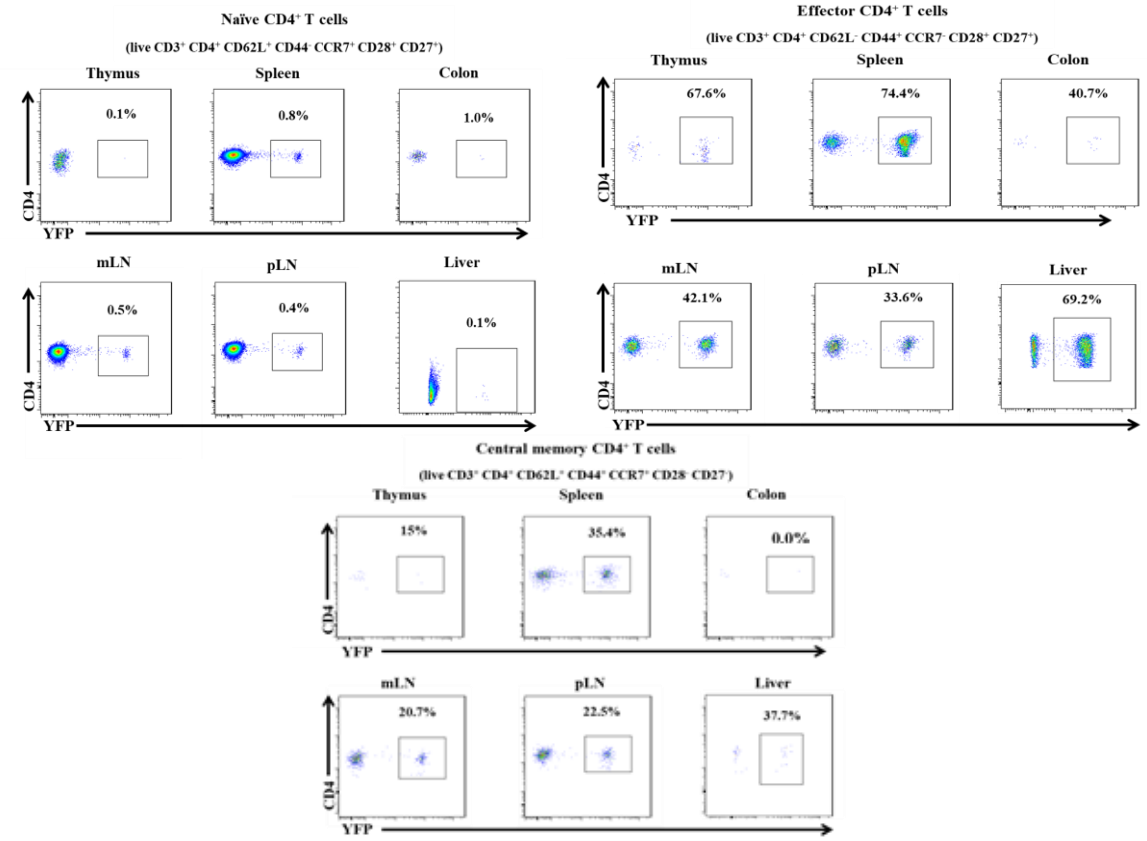

18B **Dot plots showing YFP expression in naïve, effector and central memory CD4⁺ T cells in different organs in the T-bet^{cre} x ROSA26YFP$^{fl/fl}$ mice**

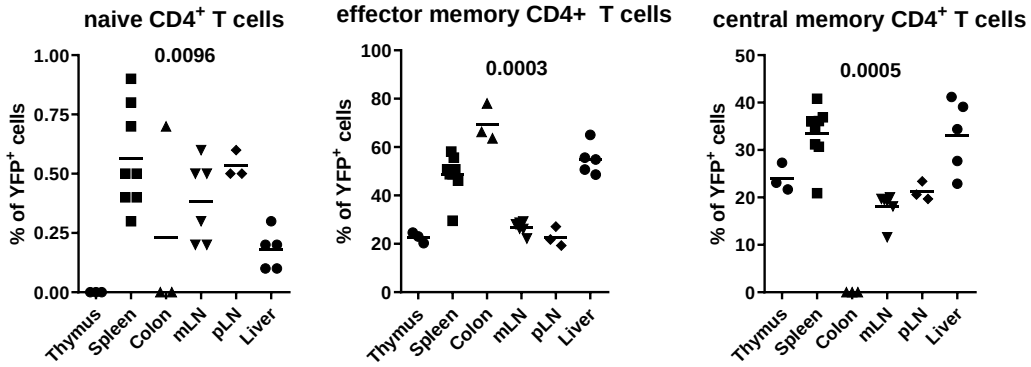

Figure 18: Extensive phenotyping of the T-bet^{cre} x ROSA26YFP$^{fl/fl}$ shows consistent levels of YFP⁺ CD4⁺ T cells in the major organs and lymphoid tissue

A. Representative flow cytometry plots showing naïve CD4⁺ T cells (live CD3⁺ CD4⁺ CD62L⁺ CD44⁻ CCR7⁺ CD28⁺ CD27⁺), effector CD4⁺ T cells (live CD3⁺ CD4⁺ CD62L⁻ CD44⁺ CCR7⁻ CD28⁺ CD27⁻) and central memory CD4⁺ T cells (live CD3⁺ CD4⁺ CD62L⁻ CD44⁺ CCR7⁻ CD28⁻ CD27⁻) in the thymus, spleen, colon, mesenteric lymph nodes, peripheral lymph nodes and the liver of the T-bet^{cre} x ROSA26YFP$^{fl/fl}$. B. Dot plot showing the overall percentage of cells expressing YFP from the same gated naïve, effector memory and central memory CD4⁺ T cells in each of the organs. (n = 3 for thymus, colon, pLN, n = 5 for liver, n = 6 for mLN and n = 8 for spleen). Kruskal-Wallis test performed with Dunn's corrections showing overall statistical analysis for all groups.

Around 0.5-1% of definitive naïve $CD4^+$ T cells were YFP^+ (Figure 18B) and showed that between these different organs there was a significant difference in the amount of YFP expression. As stated previously, YFP expression in effector memory and central memory cells was expected to be high because a subset of both memory populations will have upregulated T-bet upon T_H1 differentiation. This is shown again in the thymus, spleen, colon, mLN, pLN and liver of these mice, with a range of 30-70% YFP^+ cells in the effector memory population and 20-40% in the central memory population. The lack of cells in the flow plots showed that there are not many central memory cells, especially in the thymus, colon and liver in these healthy mice.

4.2 Identifying the naïve YFP^+ $CD4^+$ T cells

After finding these novel YFP^+ T-bet fate mapped naïve $CD4^+$ T cells, the next step was to identify this cell and further test its function. The T-bet fate mapping mouse is a novel mouse line and therefore any cell populations that do not fully fit with assumptions made from previous research are of interest. Potential identities of these YFP^+ naïve CD4s, based on existing research, are explored below.

4.2.1 Are these YFP^+ naïve T cells stem cell-like memory T cells?

Figure 19 below shows the gating strategy used to identify these stem cell-like memory cells and the subsequent phenotyping from it is shown in Figure 20. The spleen, mLN and liver were phenotyped as there were not enough cells in the colon in a healthy state to obtain significant data.

19A **Gating strategy used for identifying stem cell-like memory T cells in the T-bet^{cre} x ROSA26YFP$^{fl/fl}$ mice**

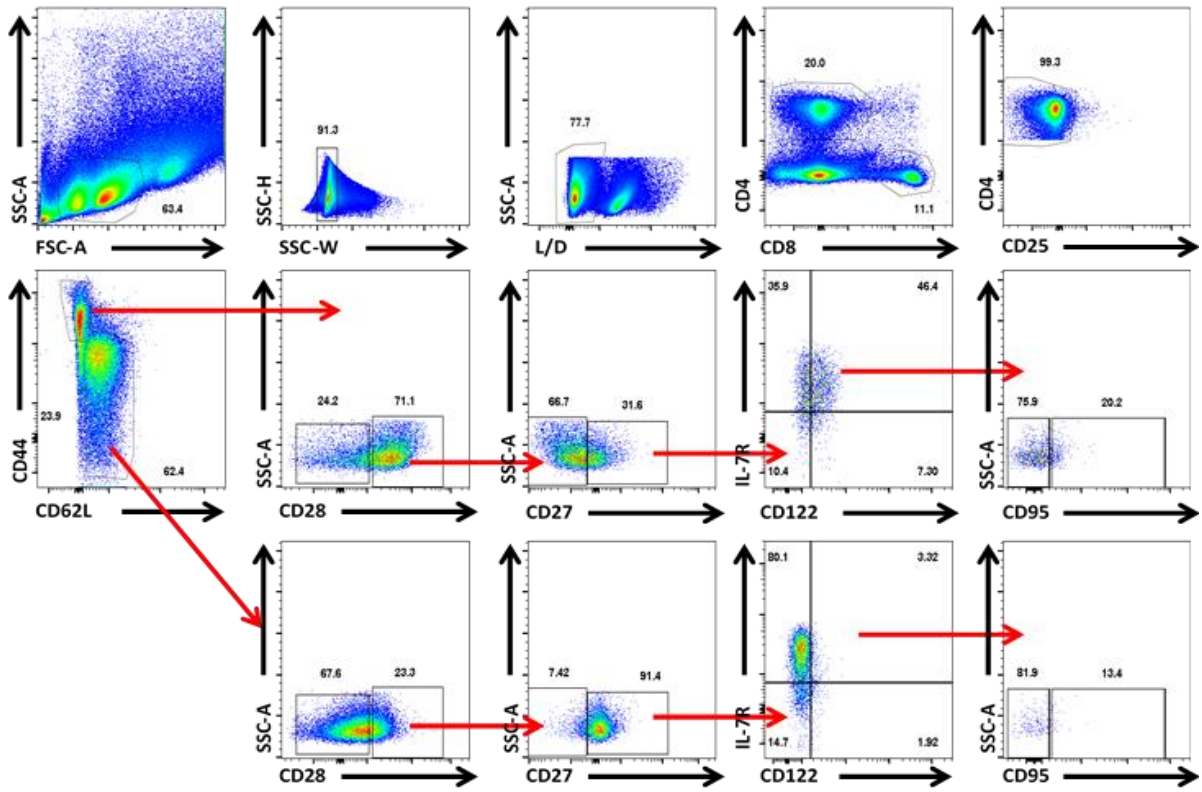

Figure 19: Gating strategy for identifying stem cell-like memory T cells in the T-bet^{cre} x ROSA26YFP$^{fl/fl}$ mice

A. Gating strategy shown for identifying stem cell-like memory T cells in the naïve ($CD62L^+$ $CD44^-$) compartment in the spleen.

20A **YFP expression in naïve CD4$^+$ T cells and in stem cell-like memory CD4$^+$ T cells in the T-bet^{cre} x ROSA26YFP$^{fl/fl}$ mice**

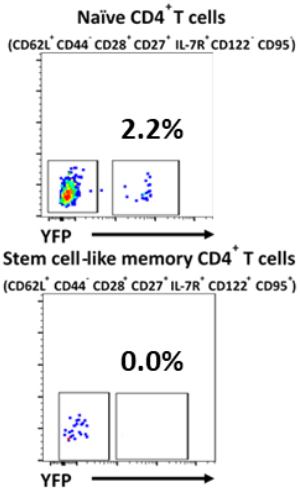

20B **Phenotyping stem cell-like memory CD4$^+$ T cell surface markers between naïve YFP$^+$ and naïve YFP$^-$ in the T-bet^{cre} x ROSA26YFP$^{fl/fl}$ mice**

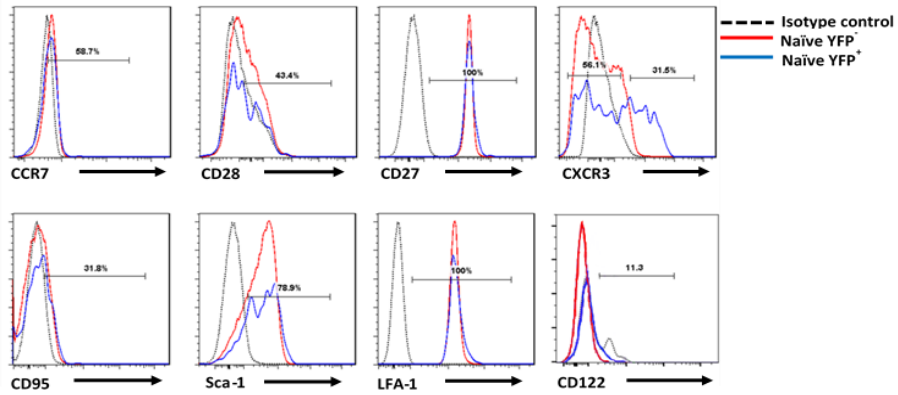

20C **Phenotyping stem cell-like memory CD4$^+$ T cell surface markers between naïve YFP$^+$, naïve YFP$^-$, effector YFP$^+$ and effector YFP$^-$ in the T-bet^{cre} x ROSA26YFP$^{fl/fl}$ mice**

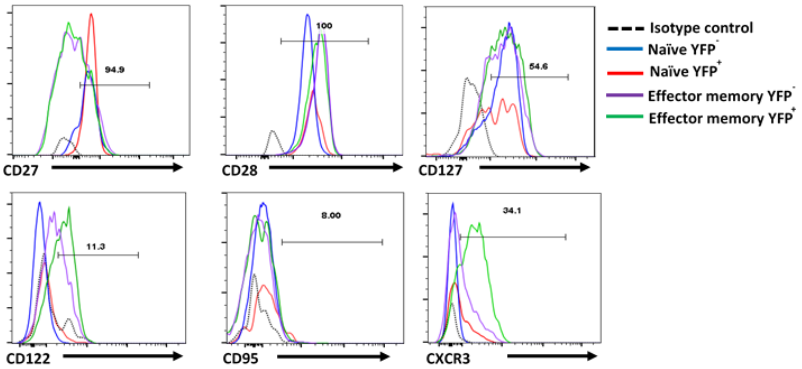

Figure 20: Phenotyping of the stem cell-like memory T cells in the T-bet^{cre} x ROSA26YFP$^{fl/fl}$ mice

A. Representative flow plots showing YFP$^+$ expression in the naïve and stem cell-like memory cell populations in the spleen. B. Representative flow histograms comparing typical stem cell-like memory cell surface markers in YFP$^-$ vs YFP$^+$ naïve CD4 T cells in the spleen. C. Representative flow histograms comparing typical stem cell-like memory cell surface markers in YFP$^-$ vs YFP$^+$ naïve and effector memory CD4 T cells. These cells were gated using FMOs and isotype controls for CXCR3, IL-7R, CD122, CD95, CD27 and CD28. (n = 12)

Figures 19A and 20A show that not only are there very few $CD122^+$ and $CD95^+$ $CD4^+$ stem cell-like memory cells found in the spleen, but also very few of these do not express YFP in comparison with the naïve $CD4^+$ population, which still have around 2% YFP expression, as previously seen. This supports the hypothesis that these naïve YFP^+ CD4 T cells are not stem cell-like memory T cells. This was further demonstrated by gating on the naïve ($CD62L^+$ $CD44^-$) YFP^- and YFP^+ $CD4^+$ T cell populations, and then analysing the different cell surface markers separately in Figure 20B and further comparing them to the memory population ($CD44^+$ $CD62L^-$) YFP^- and YFP^+ population in Figure 20C. Compared to the naïve YFP^- and YFP^+ CD4 T cell population, both had equal expression of CCR7, CD28 and CD27 in comparison with the isotype control. Sca-1 and LFA-1 were both high in comparison with the control and positive, but there was no difference between the naïve YFP^- and naïve YFP^+ cells.

Figure 20C shows the comparison between the naïve YFP^-, naïve YFP^+, effector memory YFP^- and effector memory YFP^+ cells. This comparison highlighted that the standard memory markers, like CD95 and CD122, were higher in the two effector memory populations in comparison with both naïve populations, as expected since these markers are upregulated when they become effector memory cells. Contrasting this are the naïve markers, CD27 and CD127, which are downregulated in the two memory populations. The flow plots and surface marker expression were the same for mLN and liver, but these are not shown here.

4.2.2 Are these YFP^+ naïve T cells virtual memory or memory-naïve T cells?

To test whether the YFP^+ naïve CD4 T cells here are virtual memory T cells or memory naïve-like T_{MNP} cells, similar flow cytometry phenotyping experiments to those with the stem cell-like naïve cells was undertaken. Figure 21A shows the gating used for identifying these populations.

21A

Gating strategy used for identifying both memory-naïve T (T_{MNP}) cells and virtual memory T cells in the T-bet^{cre} x ROSA26YFP$^{fl/fl}$ mice

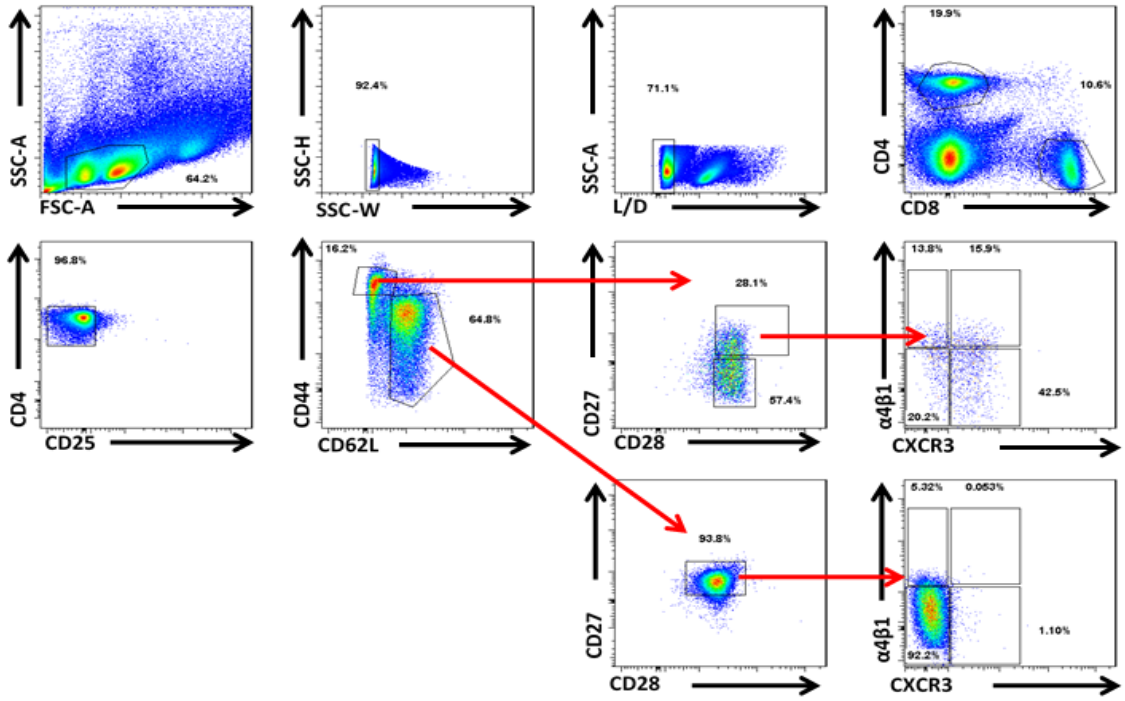

Figure 21: Gating strategy of the T_{MNP} and virtual memory cells in the T-bet^{cre} x ROSA26YFP$^{fl/fl}$ mice

A. Gating strategy shown for identifying memory naïve-like and virtual memory T cells in the naïve ($CD62L^+$ $CD44^-$) compartment in the spleen.

22A **YFP expression in naïve CD4$^+$ T cells and in T_{MNP} CD4$^+$ T cells in the T-bet^{cre} x ROSA26YFP$^{fl/fl}$ mice**

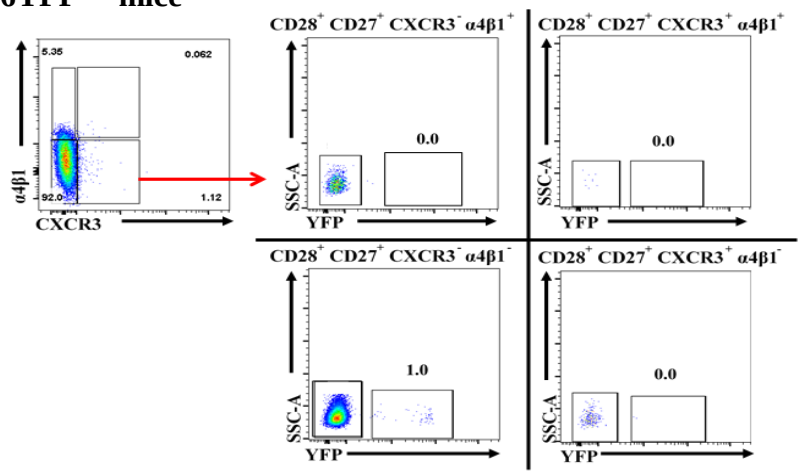

22B **YFP expression in naïve CD4$^+$ T cells and in virtual memory CD4$^+$ T cells in the T-bet^{cre} x ROSA26YFP$^{fl/fl}$ mice**

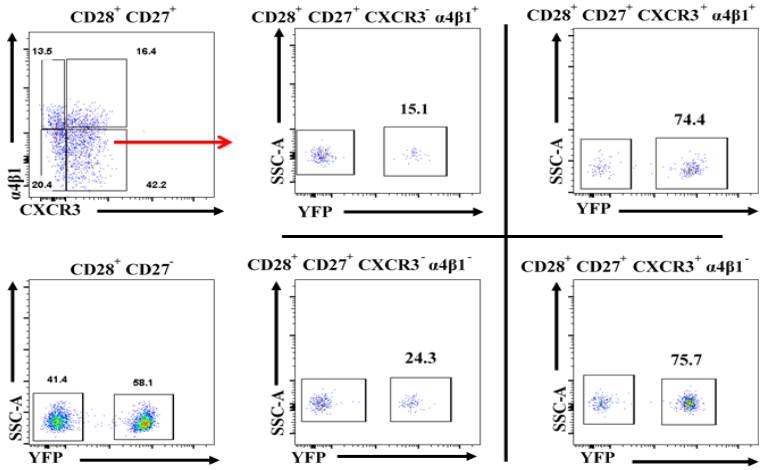

22C **Phenotyping T_{MNP} and virtual memory CD4$^+$ T cell surface markers between naïve YFP$^+$, naïve YFP$^-$, effector YFP$^+$ and effector YFP$^-$ in the T-bet^{cre} x ROSA26YFP$^{fl/fl}$ mice**

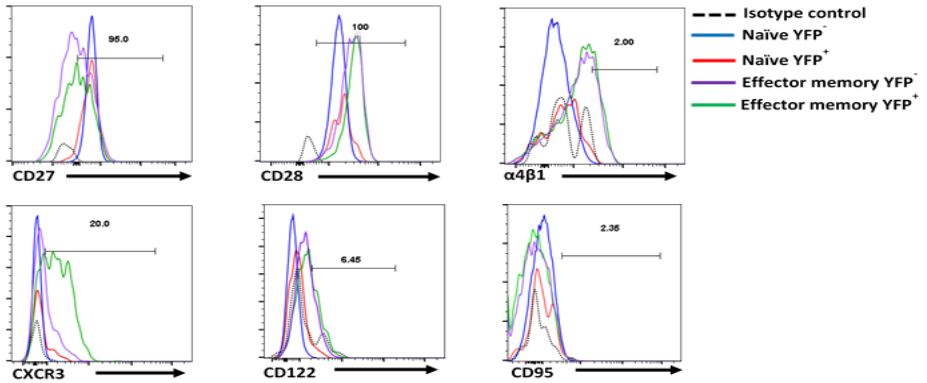

Figure 22: Phenotyping of the T_{MNP} and virtual memory cells in the T-bet^{cre} x ROSA26YFP$^{fl/fl}$ mice

A. Representative flow plots showing YFP$^+$ expression shown in the naïve (CD62L$^+$ CD44$^-$ CD28$^+$ CD27$^+$ CXCR3$^-$ α4β1$^-$) and the T_{MNP} cells (CD62L$^+$ CD44$^-$ CD28$^+$ CD27$^+$ CXCR3$^+$ α4β1$^+$) in the spleen. C. Representative flow plots showing the YFP$^+$ expression in the virtual memory T cells (CD62L$^-$ CD44$^+$ CD122$^+$ CD49d$^-$ CXCR3$^+$) in the spleen. D. Representative flow histograms showing the surface marker expression from YFP$^-$ vs YFP$^+$ naïve and effector memory CD4 T cells from the spleen. These cells were gated using FMOs and isotype controls for CXCR3, α4β1, CD122, CD95, CD27 and CD28. (n = 12)

Figures 21A and 22A show that within the $CD62L^+$ $CD44^-$ $CD27^+$ $CD28^+$ population there are very few single $CXCR3^+$ and single $\alpha4\beta1^+$ cells, and even fewer double positive ones (the T_{MNP} cells). These markers are also present within the $CD44^+$ $CD62L^-$ memory population and therefore it was a useful biological control for the $CD62L^+$ $CD44^-$ population. The only YFP^+ population that existed was found in the double negative ($CXCR3^-$ $\alpha4\beta1^-$) population, which should be the truly naïve $CD4^+$ T cells. Therefore, these YFP^+ naïve $CD4^+$ T cells are not the same T_{MNP} that have been identified by other groups.

Figure 22B shows the YFP^+ expression for the $CD44^+$ $CD62L^-$. Since virtual memory cells are identified by this, as well as CD49d and CXCR3. In the $CD44^+$ $CD62L^-$ $CD49d^-$ $CXCR3^+$ population, which are the virtual memory cells, there was a high level of YFP^+ (around 75% of cells) but as these cells cannot be found in the $CD62L^+$ $CD44^-$ $CD49d^-$ $CXCR3^+$ population, the naïve $CD49d^-$ $CXCR3^+$ cells might not be related to virtual memory cells.

Lastly, Figure 22C shows the surface markers of YFP^+ vs YFP^- naïve and effector memory cells. This again shows that the naïve $CD4^+$ T cells have similar expressions of the markers previously shown in figure 20C, including the 20-30% YFP^+ $CXCR3^+$. Both the YFP^- and YFP^+ naïve $CD4^+$ T cells were negative for $\alpha4\beta1^+$, especially in comparison with the effector memory $CD4^+$ T cells.

Figures 20C and 22C highlighted that these naïve YFP^+ $CD4^+$ T cells are phenotypically different to both YFP^- and YFP^+ memory cells.

4.2.3 Are these YFP^+ naïve $CD4^+$ T cells precursors to $CD5^{high}$ pathogen-independent memory-phenotype (MP) cells?

Since Kawabe et al. lacked a T-bet fate mapping mouse, they could not determine if MP cells were derived from a population of naïve $CD4^+$ T cells that have previously expressed T-bet. They showed that all MP cells highly expressed CD5 and were able to develop from peripheral naïve $CD4^+$ T cells even after their mice had been given a thymectomy. However, using the T-bet^{cre} x $ROSA26YFP^{fl/fl}$ mice, the expression of CD5 can be analysed in these YFP^+ naïve T cell populations in the mice.

23A **Representative flow plots showing CD5$^+$ expression in YFP$^+$ naïve CD4$^+$ T cells in the T-bet^{cre} x ROSA26YFP$^{fl/fl}$ mice**

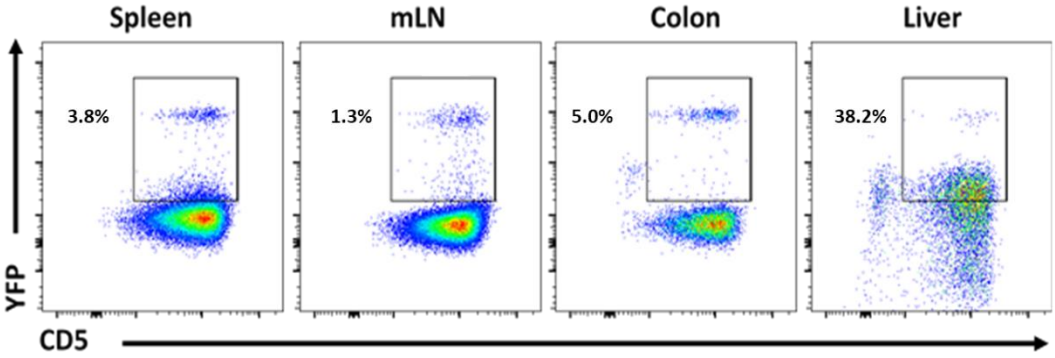

23B

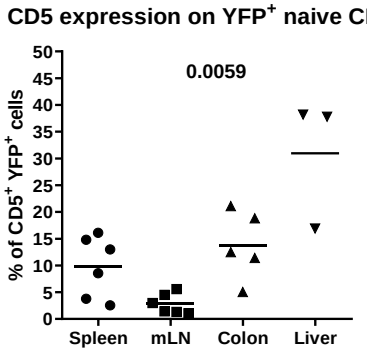

Figure 23: Phenotyping the CD5$^+$ YFP naïve T cells in the T-bet^{cre} x ROSA26YFP$^{fl/fl}$ mice

A. Representative flow plots showing CD5$^+$ YFP$^+$ expression in naïve gated (live CD3$^+$ CD4$^+$ CD62L$^+$ CD44$^-$) CD4$^+$ T cells in the spleen, mLN, colon and liver. B Dot plot showing the number of CD5$^+$ YFP$^+$ cells in the spleen, mLN, colon and liver. (n=6 for spleen and mLN, n=5 for colon and n=3 for liver). Kruskal-Wallis test performed with Dunn's corrections showing overall statistical analysis for all groups.

Figures 23A and 23B show that all the YFP$^+$ cells are CD5^{high} but not all the CD5$^+$ cells are YFP$^+$. The gate was gated using a CD5 isotype control and FMO to judge where the expression of CD5 started. Only around 10% in the spleen, 3% in the mLN, 15% in the colon and a range of 15-30% in the liver are YFP$^+$ CD5$^+$. The naïve YFP$^+$ cells could be precursors to MP cells that Kawabe et al. identified. Further analysis of these cells would be necessary to identify them more precisely.

4.3 Investigating whether the YFP$^+$ naïve CD4 T cell subset differs with age

Although the identity of this population has not yet been clarified, understanding whether the frequency of these YFP$^+$ naïve CD4$^+$ T cells vary with age was essential. Although these mice were not housed in germ-free or pathogen-free isolators, the foetal and even 1-week old

neonates should not have fully established immune systems and thus their naïve CD4 T cells should be naïve. Therefore, this would give an idea of whether the YFP^+ CD4 T cells are already present from the developing foetus and/or if the presence of a microbiota and an immunological environment are necessary for them to be present.

4.3.1 The YFP^+ naïve $CD4^+$ T cells could not be found in the foetus of these mice

For these experiments, the T-bet^{cre} mother was used as a YFP^- control, since the parents are breed as separate lines and the offspring are only used at the F1 generation, and we had other suitable genotyped T-bet^{cre} x $ROSAYFP^{fl/fl}$ adult (6-8 weeks old) mice that we used to compare the foetal YFP expression against. Unfortunately, there were no CD4 or CD8 T cells found in thymus and therefore these data are not shown. Figure 24 shows the data gathered from this.

24A **Representative flow plots showing YFP expression in naïve, effector and central memory CD4$^+$ T cells from foetal and adult T-bet^{cre} x ROSA26YFP$^{fl/fl}$ mice**

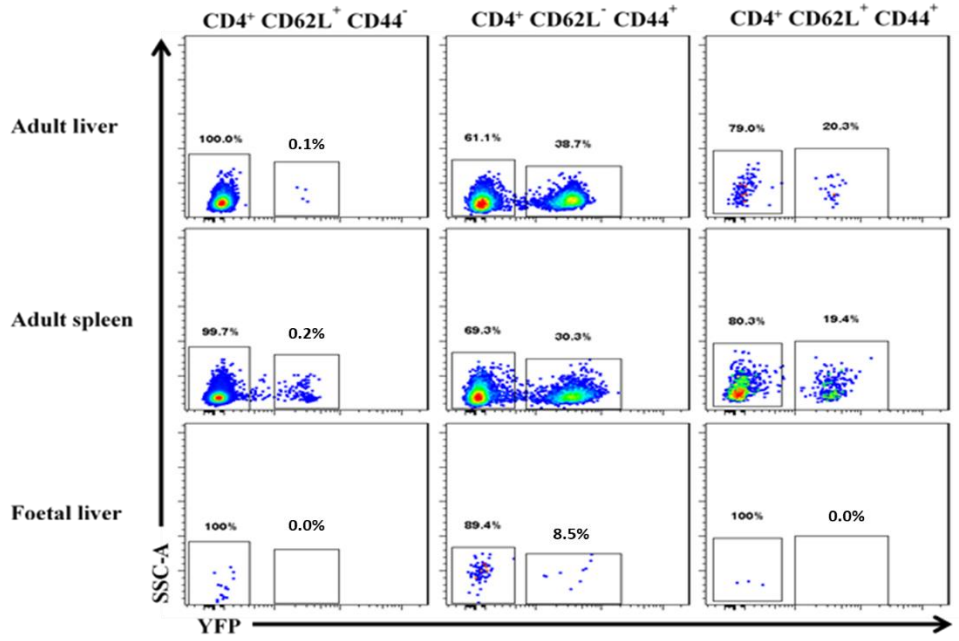

24B **Representative flow plots showing YFP expression in naïve, effector and central memory CD8$^+$ T cells from foetal and adult T-bet^{cre} x ROSA26YFP$^{fl/fl}$ mice**

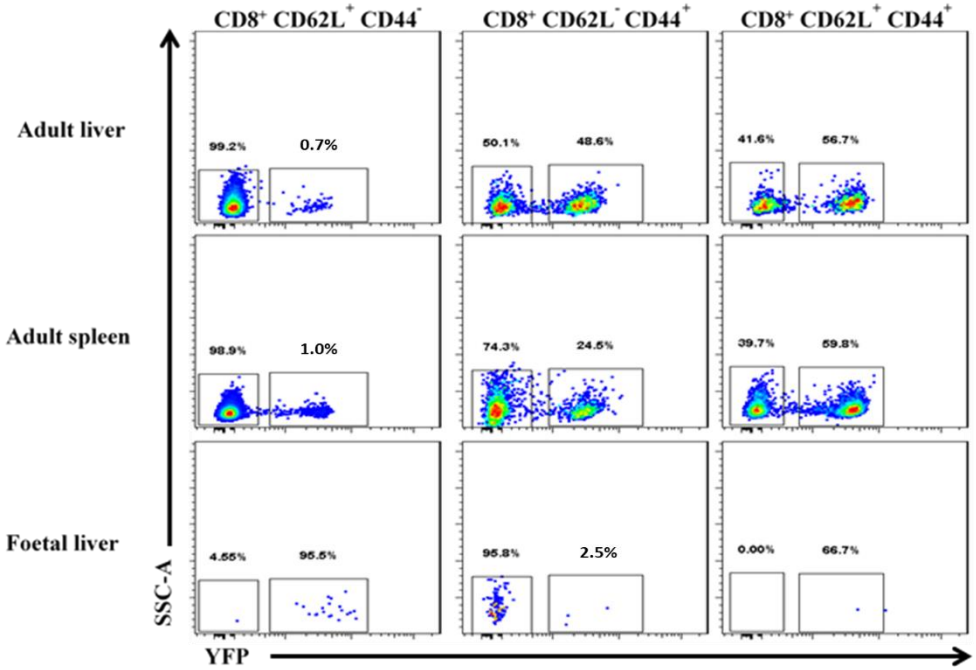

Figure 24: Phenotyping the cells in the E15.5-E16 foetus of T-bet^{cre} x ROSA26YFP$^{fl/fl}$ mice

A. Representative flow plots showing naïve (CD62L$^+$ CD44$^-$), effector (CD62L$^-$ CD44$^+$) and central memory (CD62L$^+$ CD44$^+$) CD4$^+$ T cells in the adult liver, adult spleen and foetal liver of T-bet^{cre} x ROSA26YFP$^{fl/fl}$ mice. B. Representative flow plots showing naïve (CD62L$^+$ CD44$^-$), effector (CD62L$^-$ CD44$^+$) and central memory

($CD62L^+$ $CD44^+$) $CD8^+$ T cells in the adult liver, adult spleen and foetal liver of T-bet^{cre} x $ROSA26YFP^{fl/fl}$ mice. (n=3 for the adult liver and spleen, n=1 for foetal liver but pooled from 10 foetuses)

Analysis of the $CD4^+$ and $CD8^+$ T cells in the foetal liver provided interesting preliminary results since the ten foetal liver samples had to be pooled into one sample and therefore this experiment needs repeating in order to observe if this potential finding is conclusive. However, firstly, from Figure 24A, it can be observed from this one sample that there were no YFP^+ naïve or central memory $CD4^+$ T cells found in the foetal liver, but there were some (around 9%) YFP^+ effector memory $CD4^+$ T cells. From this one sample, there was a high percentage (over 90%) of YFP^+ naïve $CD8^+$ T cells and only around 2-3% YFP^+ effector memory $CD8^+$ T cells (Figure 24B). These cells were still in utero, and therefore would only have been exposed to any maternal antigens from the mother. This could make the observation of the high percentage of YFP^+ naïve $CD8^+$ T cells interesting especially considering that in adult mice only around 0.5-1% of naïve CD8s were YFP^+. Therefore, there could be the possibility that these YFP^+ naïve CD8s either die or the remaining YFP^- $CD8^+$ T cells expand massively upon birth. From this one sample analysis no YFP^+ naïve $CD4^+$ could be found in the foetal liver, hypothesising that the expression of T-bet^+ fate mapped naïve T cells only occurs after birth during neonatal development. Formation of these cells could be driven more by the microbiota and other environmental factors post-birth. Another potential observation made here was the low percentage of both CD4 and CD8 T cells in the foetal liver. This could have been due to a lack of proliferation due to a lack of antigen activation as foetuses.

4.3.2 Naïve YFP^+ $CD4^+$ T cells are present within in the periphery in neonates

After observing a possible lack of YFP^+ naïve $CD4^+$ T cells in the foetal liver, 1-week-old mice were phenotyped next. Surface markers typically found on memory and naïve $CD4^+$ T cells were also phenotyped like that previously shown in the 6-8-week-old mice (Figures 20 and 22).

25A

Percentage of YFP$^+$ naïve CD4$^+$ T cells in organs of 1-week-old T-bet^{cre} x ROSA26YFP$^{fl/fl}$ mice

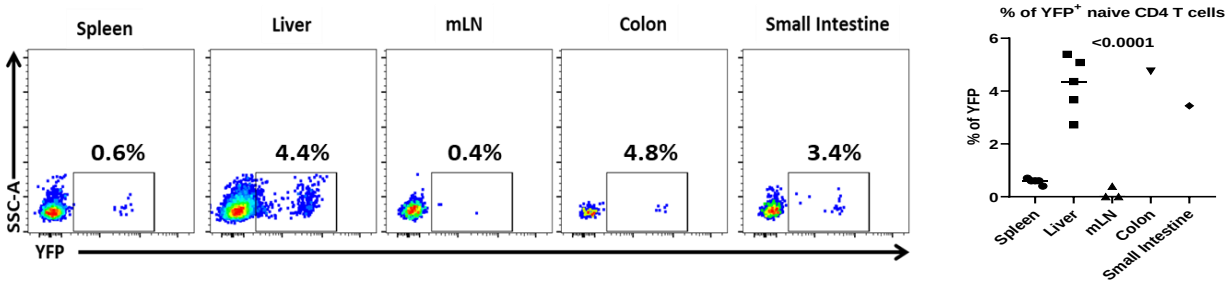

25B

Representative flow plots showing naïve and memory surface markers of YFP$^-$ and YFP$^+$ naïve CD4$^+$ T cells from T-bet^{cre} x ROSA26YFP$^{fl/fl}$ mice

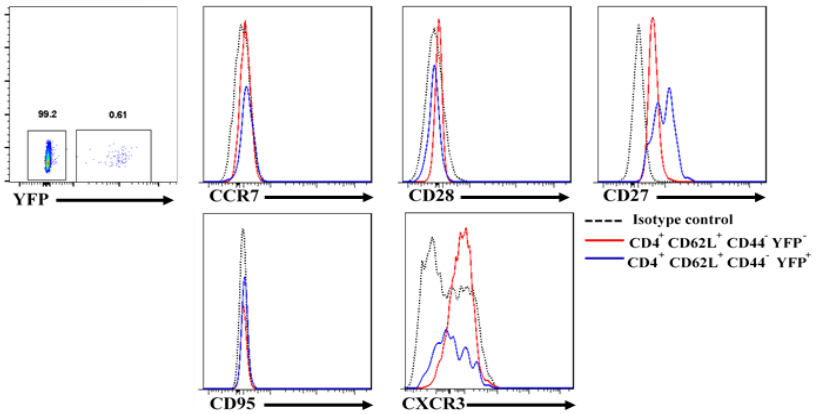

Figure 25: Phenotyping of the 1-week-old T-bet^{cre} x ROSA26YFP$^{fl/fl}$ mice

A. Representative flow plots and overall dot plot showing the percentage of YFP$^+$ naïve (CD62L$^+$ CD44$^-$) CD4$^+$ T cells in the spleen, liver, mLN, colon and small intestine of 1-week old T-bet^{cre} x ROSA26YFP$^{fl/fl}$ mice. B. Representative flow histograms showing CCR7, CD28, CD27, CD95 and CXCR3 expression on either YFP$^-$ or YFP$^+$ naïve (CD62L$^+$ CD44$^-$) CD4$^+$ T cells in the spleen of 1-week old T-bet^{cre} x ROSA26YFP$^{fl/fl}$ mice. (n=5 for spleen, liver, n = 3 and n=1 for colon and small intestine). Kruskal-Wallis test performed with Dunn's corrections showing overall statistical analysis for all groups.

Figure 25A shows that there is significant difference in the percentage of YFP$^+$ CD4 naïve T cells in the different organs of 1-week old litters. Around 5% and 0.5% of naïve CD4$^+$ T cells expressed YFP in the liver and spleen respectively. This percentage of naïve CD4$^+$ T cells matched the proportion seen in the 6-8-week-old mice. At 1 week old, there were still very few cells in the mLN, pLN and colon due to the size of the mice. The peripheral organs of these mice have yet to require much cell infiltration at mucosal sites of inflammation. This made it more difficult to analyse the cells within these organs and mice had to be pooled together to get sufficient numbers for flow analysis. Interestingly, of the naïve CD4$^+$ T cells that were present in the mLN, pLN and colon there were no YFP$^+$ cells that could be identified. Figure

25B showed differences to the previous data shown in the 6-8-week-old mice. These YFP^+ naïve $CD4^+$ T cells in the spleen were shown not to express the migratory chemokines receptors CCR7 and CXCR3 and the costimulatory molecule CD28, but they were $CD27^+$. This indicates that the naïve YFP^+ $CD4^+$ require more of an environmental microbiota immune response to migrate from the spleen into the peripheral sites of the mucosa.

4.3.3 During weaning, the YFP^+ naïve $CD4^+$ T cells develop a phenotype more similar to those in adult mice

During their first 3 weeks, the mice are fed milk from their mother and are also adapting to the environmental microbiota within the cages that they are housed. These environmental responses prime the immune system of the mice with external pathogenic antigens, which naïve $CD4^+$ T helper cells will specifically recognise and become activated and proliferate, and which are no longer only from maternally found antigens from when the foetus was developing or from the milk during weaning. Therefore, examination of YFP expression at this stage of development will provide insights into T-bet expression during early immune priming.

26A

Percentage of YFP^{+} naïve CD4^{+} T cells in organs of 3-week-old T-bet^{cre} x ROSA26YFP$^{fl/fl}$ mice

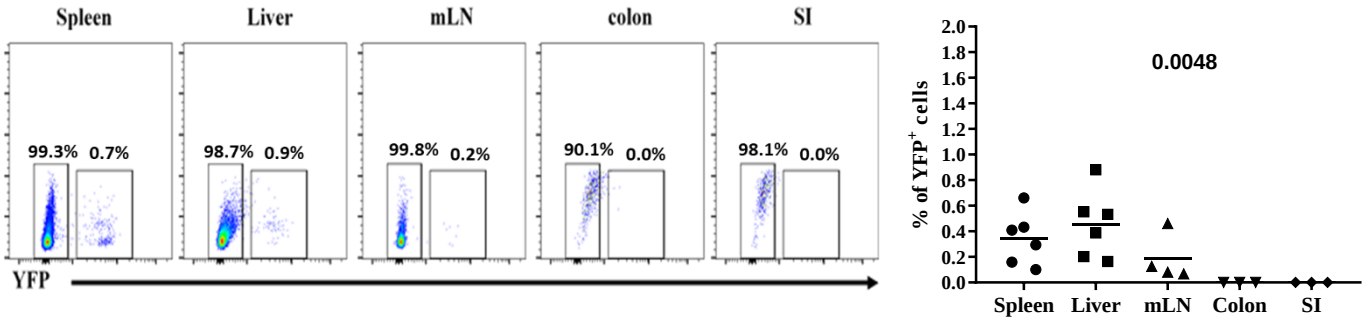

26B

Representative flow plots showing naïve and memory surface markers of YFP^{-} and YFP^{+} naïve CD4^{+} T cells from 3-week-old T-bet^{cre} x ROSA26YFP$^{fl/fl}$ mice

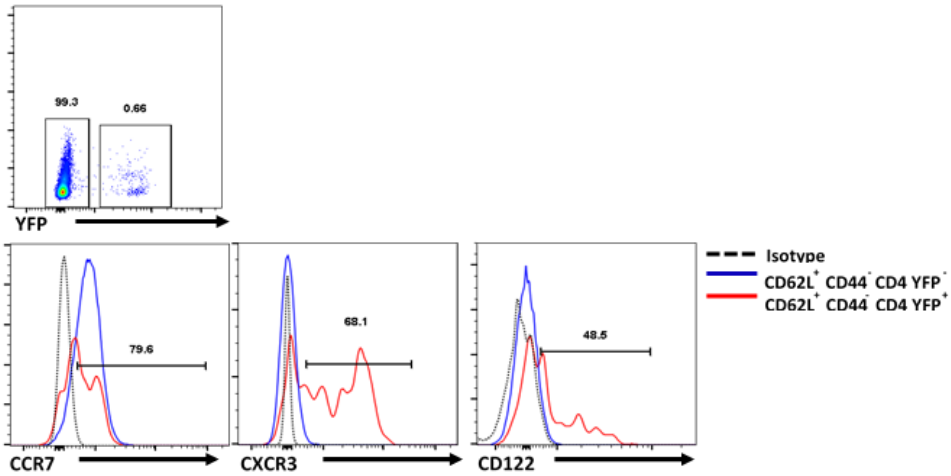

Figure 26: Phenotyping of the 3-week-old T-bet^{cre} x ROSA26YFP$^{fl/fl}$ mice

A. Representative flow plots and overall dot plot showing the percentage of YFP^{+} naïve (CD62L^{+} CD44^{-}) CD4^{+} T cells in the spleen, liver, mLN, colon and small intestine of 3-week-old T-bet^{cre} x ROSA26YFP$^{fl/fl}$ mice. Kruskal-Wallis test performed with Dunn's corrections showing overall statistical analysis for all groups. B. Representative flow histograms showing CCR7, CXCR3 and CD122 expression on either YFP^{-} or YFP^{+} naïve (CD62L^{+} CD44^{-}) CD4^{+} T cells (shown on the top left) in the spleen of 3-week old T-bet^{cre} x ROSA26YFP$^{fl/fl}$ mice. (n=6 for spleen and liver n = 4 for mLN, n=3 for colon and SI). Kruskal-Wallis test performed with Dunn's corrections showing overall statistical analysis for all groups.

The 3-week-old mice showed that despite the number of naïve CD4^{+} T cells increasing in each of the organs as the mice get older, the percentage of YFP^{+} naïve CD4^{+} T cells do not increase in the spleen and liver and stay at the same level as the 6-8-week-old mice. The YFP^{+} naïve CD4^{+} cells are still not visible in the mLN, colon and small intestine though and this may still

be due to the lack of environmental microbiota antigens present in the gut of the mice. Figure 26B shows the difference in splenic YFP$^+$ naïve CD4$^+$ cells to the 1-week old YFP$^+$ naïve CD4$^+$ T cells. From the histograms, unlike in the 1-week old naïve CD4s, these naïve CD4s have now expressing migratory chemokine receptors, CCR7 and CXCR3, the latter of which expressed on more cells (around 60%) in these 3-week-old mice in comparison to the adult 6-8-week-old ones previously phenotyped (around 30%). Also, it was surprising to find that these YFP$^+$ naïve CD4s highly expressed CD122, as later in adulthood they stop expressing CD122 (Figure 20 and 22).

4.3.4 Are there any phenotypic difference between younger and older YFP$^+$ naïve CD4$^+$ T cells in these mice?

Figure 27 shows mice aged 25 and 50 weeks old. These ages were used due to availability of mice at the time, but mice are considered old for breeding around the age of 25 weeks and therefore this seemed like a reasonable age to phenotype.

27A

Percentage of YFP$^+$ naïve CD4$^+$ T cells in organs of 25-week-old and 50-week-old T-bet^{cre} x ROSA26YFP$^{fl/fl}$ mice

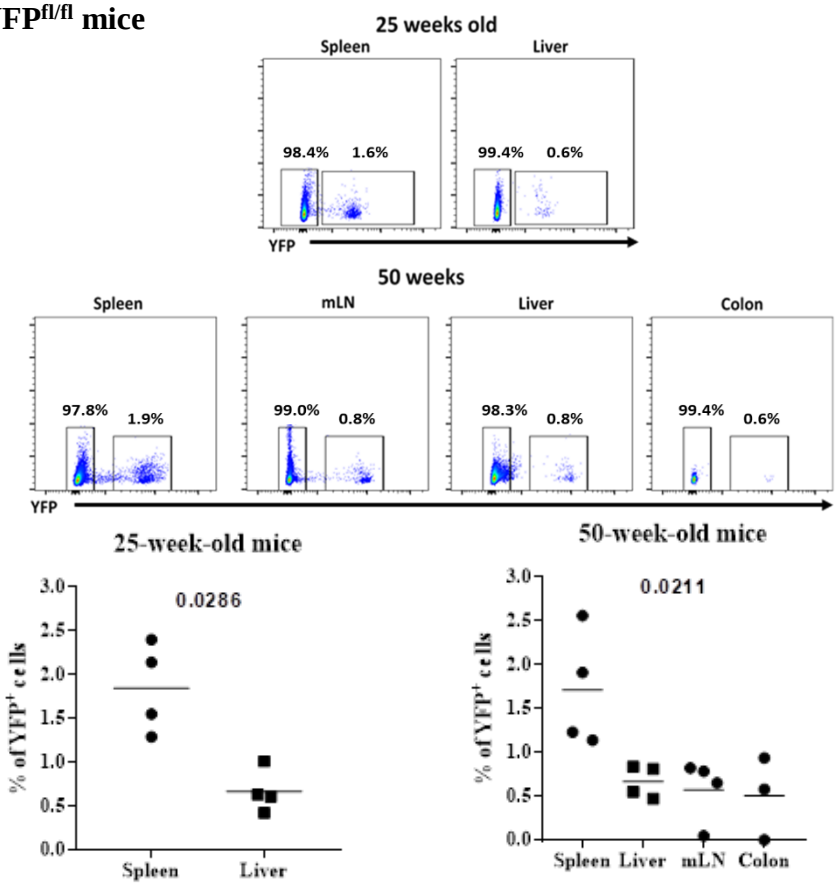

27B

Representative flow plots showing naïve and memory surface markers of YFP$^-$ and YFP$^+$ naïve and effector CD4$^+$ T cells from 50-week-old T-bet^{cre} x ROSA26YFP$^{fl/fl}$ mice

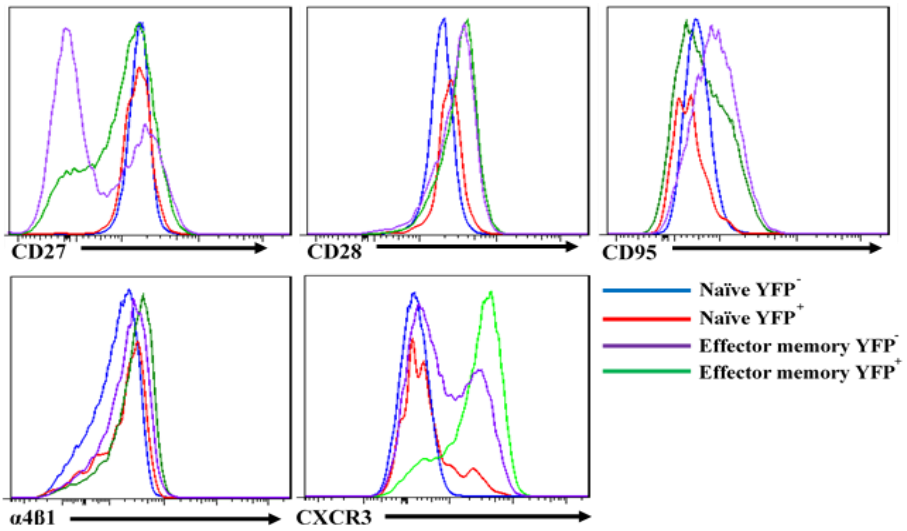

Figure 27: Phenotyping of 25 and 50-week-old T-bet^{cre} x ROSA26YFP$^{fl/fl}$ mice

A. Representative flow plots and overall dot plot showing the percentage of YFP$^+$ naïve (CD62L$^+$ CD44$^-$) CD4$^+$ T cells in the spleen and liver for 25-week-old mice and the spleen, liver, mLN and colon of 50-week-old T-bet^{cre} x ROSA26YFP$^{fl/fl}$ mice. B. Representative flow histograms showing CD27, CD28, CD95, CXCR3 and α4β1 expression on either YFP$^-$ or YFP$^+$ naïve (CD62L$^+$ CD44$^-$) and memory (CD62L$^-$ CD44$^+$) CD4$^+$ T cells in the spleen of 50-week old T-bet^{cre} x ROSA26YFP$^{fl/fl}$ mice. (n=4 for spleen, liver, mLN and colon). Mann-Whitney test used for 25 week old mice and Kruskal-Wallis test performed with Dunn's corrections showing overall statistical analysis for all groups used for 50 week old mice.

The most interesting observation from the aged mice was that the percentage of YFP$^+$ naïve increases with age in the spleen, from 0.5-1% in 6-8-week-old mice to around 1.5% in the 25-week-old mice and finally around 2% in the 50-week-old mice. Despite the mice getting older, there does not seem to be a reduction in naïve CD4$^+$ T cells, including the YFP$^+$ naïve CD4 T cells. Furthermore, the surface markers expressed on these naïve CD4$^+$ T cells in aged mice do not differ much in comparison with the younger adult mice. Expression of CD28 was still present, and expression remains higher in the YFP$^+$ naïve CD4s. The 20-30% of YFP$^+$ naïve CD4 T cells that were CXCR3$^+$ in the older adult mice is similar to that observed in the younger adult mice.

4.4 Are the YFP$^+$ naïve CD4 T cells functionally different to YFP$^-$ naïve CD4 T cells?

The flow cytometry data demonstrates that YFP$^+$ naïve CD4 T cells are phenotypically different to YFP$^-$ naïve CD4 T cells and are possibly a novel and unknown cell type. There has been much research into naïve CD4 T cell immunology performed in the past by many different groups. Many of these groups have looked at naïve CD4 T cell differentiation, plasticity and their functional aspects during pathological responses in both *in vitro* and *in vivo* analysis.

4.4.1 *In vitro* analysis of the YFP$^+$ naïve CD4 T cells shows a dominant IFNγ production and possible predetermined T_H1 phenotype

In vitro T cell culture and T cell skewing of naïve CD4 T cells have been performed by many groups in the past, including within our lab (Brown et al., 2015, Canavan et al., 2016, Gökmen et al., 2013), to observe the differentiation and function of naïve CD4$^+$ T cells.

In vitro T cell cultures were first performed with only IL-2 and no skewing conditions. This initially involved sorting and purifying the YFP$^-$ and YFP$^+$ naïve and memory T cells from a BD Aria cell sorting machine using the gating strategy described in the methods section. The purified sorted naïve and memory CD4$^+$ T cells were then plated out at 1 x 10^6/ml onto anti-CD3 and anti-CD28 pre-incubated plates for 2 days and cultured with IL-2 for 7 days. Cells were then stimulated with PMA and ionomycin for 4 hours with monensin after 2 hours. The results of these experiments are shown in Figure 23.

28A **Representative flow plots showing cytokine production from naïve CD4$^+$ T cells**

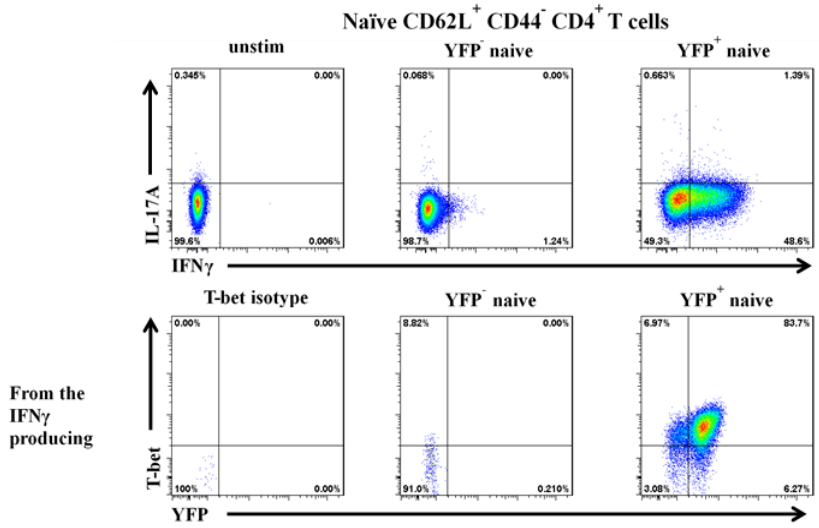

28B **Representative flow plots showing cytokine production from memory CD4$^+$ T cells cultured *in vitro***

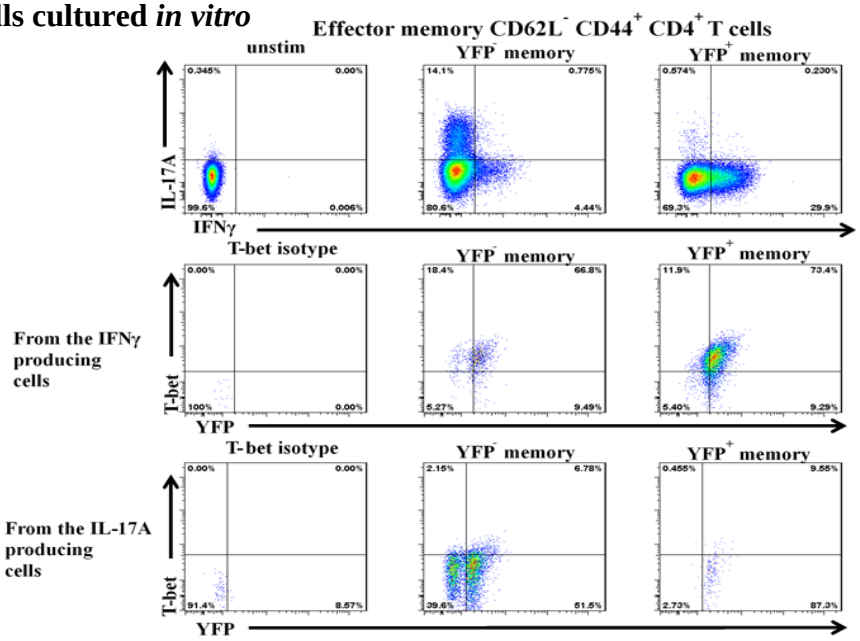

28C **ELISA showing cytokine production from the supernatant of naïve and memory CD4$^+$ T cells cultured *in vitro***

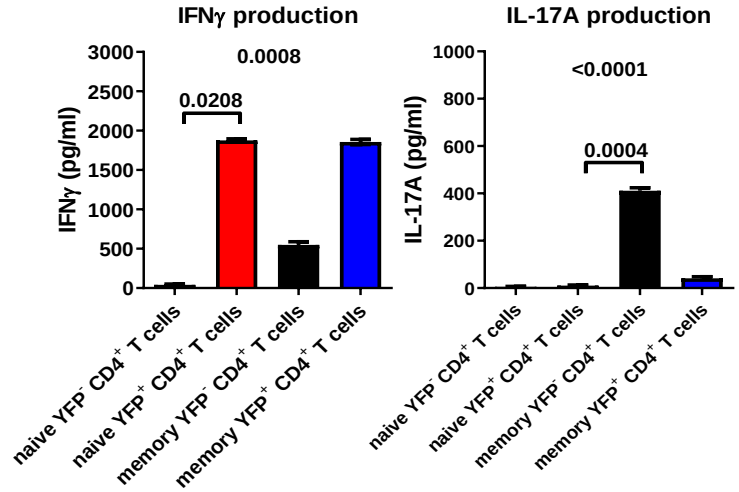

Figure 28: *In vitro* culture of YFP$^+$ CD4$^+$ T cells shows that even without skewing YFP$^+$ CD4$^+$ T cells can produce a large amount of IFNγ upon activation and stimulation.

A. Representative flow plots showing cytokine responses and T-bet expression from *in vitro* cultured cell with IL-2 and on pre-incubated anti-CD3/CD28 activation in sorted naïve (CD62L$^+$ CD44$^-$) CD4$^+$ T cells from T-bet^{cre} x ROSA26YFP$^{fl/fl}$ mice (Experiment was done in triplicate (except for naïve YFP$^+$ cells, which were pooled into one well) and replicated twice). B. Representative flow plots and overall dot plot showing cytokine responses and T-bet expression from *in vitro* cultured cell with IL-2 and on pre-incubated CD3/CD28 activation in sorted memory (CD62L$^-$CD44$^+$) CD4$^+$ T cells from T-bet^{cre} x ROSA26YFP$^{fl/fl}$ mice. (Experiment was done in triplicate and replicated twice) C. IFNγ and IL17A production from the supernatant of the cultured cells measured by ELISAs (n = 6 for YFP$^-$ naïve CD4 T cells, YFP$^-$ effector CD4 T cells and YFP$^+$ effector CD4 T cells and n = 2 for YFP$^+$ naïve CD4 T cells). Kruskal-Wallis test performed with Dunn's corrections showing overall statistical analysis for all groups and individual comparisons.

Remarkably, anti-CD3/CD28 stimulation and IL-2 led to high IFNγ production in comparison with the YFP$^-$ naïve CD4 T cells. The YFP$^+$ T cells also maintain their YFP$^+$ expression after activation. YFP$^-$ effector cells were able to produce both IL-17A and IFNγ, whereas the YFP$^+$ cells predominately produced IFNγ and barely any IL-17A. The ELISA data further confirmed the flow data showing that the YFP$^+$ CD4$^+$ T cells were more predisposed to producing IFNγ, probably due to their previous expression of T-bet. Also, it was useful to observe that the YFP$^-$ memory IFNγ producing cells became YFP$^+$ and T-bet$^+$. This helped to confirm that the mouse model was working correctly.

Next, differences in the differentiation of YFP$^-$ and YFP$^+$ naïve CD4$^+$ T cells when exposed to specific skewing conditions into T_H1, T_H2, T_H17 and T_{regs} lineages were tested. This was important to demonstrate if the T-bet fate mapped naïve CD4$^+$ T cells would still be able to skew towards these cell types and if they were still producing more IFNγ as seen previously with the cultured cells.

29A

Representative flow plots showing cytokine production from sorted skewed naïve CD4$^+$ T cells

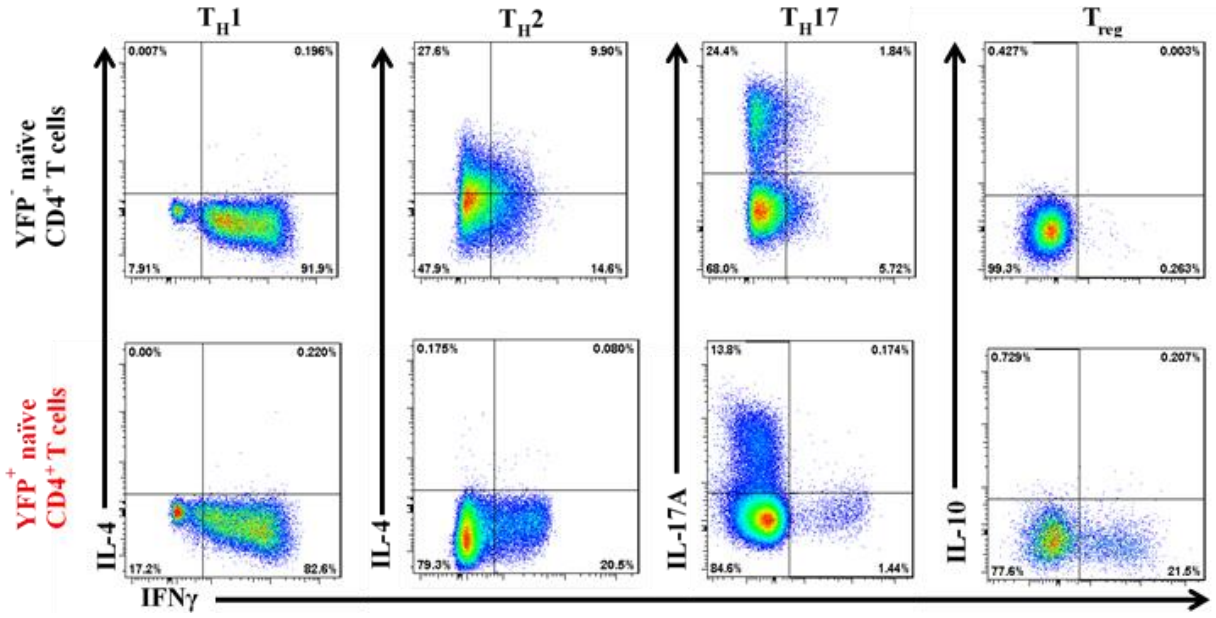

Figure 29: *In vitro* T cell skewing of YFP$^+$ CD4$^+$ T cells shows that even under T_H2, T_H17 and T_{reg} skewing conditions YFP$^+$ CD4$^+$ T cells can produce IFNγ upon activation and stimulation.

A. Representative flow plots showing cytokine responses from *in vitro* skewed cell on pre-incubated anti-CD3/CD28 activation in sorted naïve (CD62L$^+$ CD44$^-$) CD4$^+$ T cells from T-bet^{cre} x ROSA26YFP$^{fl/fl}$ mice. (experiment performed in triplicate and repeated twice)

Similarly, to the cells cultured only in IL-2, the YFP^+ naïve $CD4^+$ T cells under skewed conditions showed a likely trend to be able to produce high amounts of IFNγ and less of the other lineage specific cytokines; in comparison with their YFP^- naïve $CD4^+$ T cell counterpart. However, more replicates and repeats of this are necessary to conclude the skewing data.

In conclusion, both non-polarised and polarised *in vitro* cultures showed that YFP^+ naïve $CD4^+$ T cells have their own unique function compared to the YFP^- naïve $CD4^+$ T cells. They have a spontaneous and predetermined ability to readily produce high amounts of IFNγ. These YFP^+ naïve $CD4^+$ T cells could be early T_H1 immune responders to pathogens and provide an early source of IFNγ.

4.4.2 *In vivo* analysis of the YFP^+ naïve CD4 T cells

Figure 30 shows the typical T cell transfer from wildtype mice into *Rag2*$^{-/-}$ mice, demonstrating significantly high IFNγ production with little IL-17A production in this model (Figure 30B). Cells were sorted and purified using the same method as described before and $0.5x10^6$ $CD4^+$ T cells were transferred to each *Rag2*$^{-/-}$ mice by intraperitoneal injections. Typically, in the normal T cell transfer model, wasting can be observed after around 6 weeks of the initial injection and there is an increase in colon and spleen weight, as seen in Figure 30A.

30A

Clinical data showing percentage weight change and organ weights in a typical T cell transfer

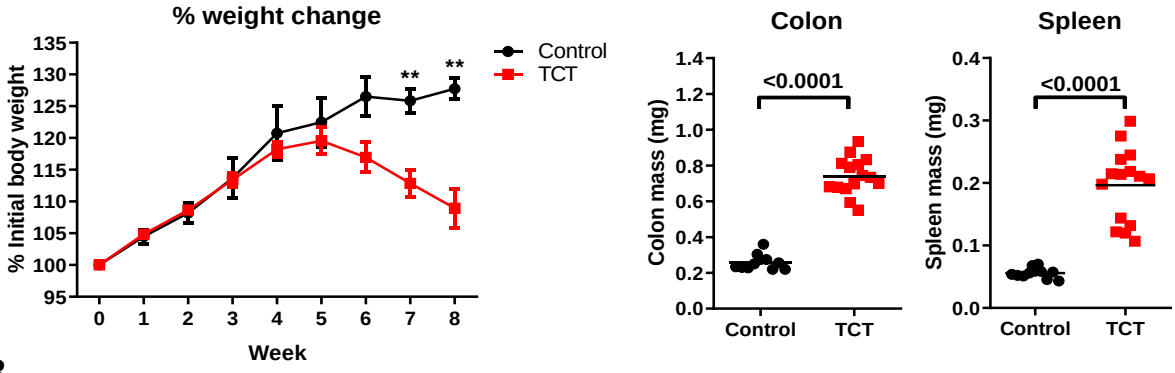

30B

Representative flow plot and dot plots showing cytokine production in a typical T cell transfer

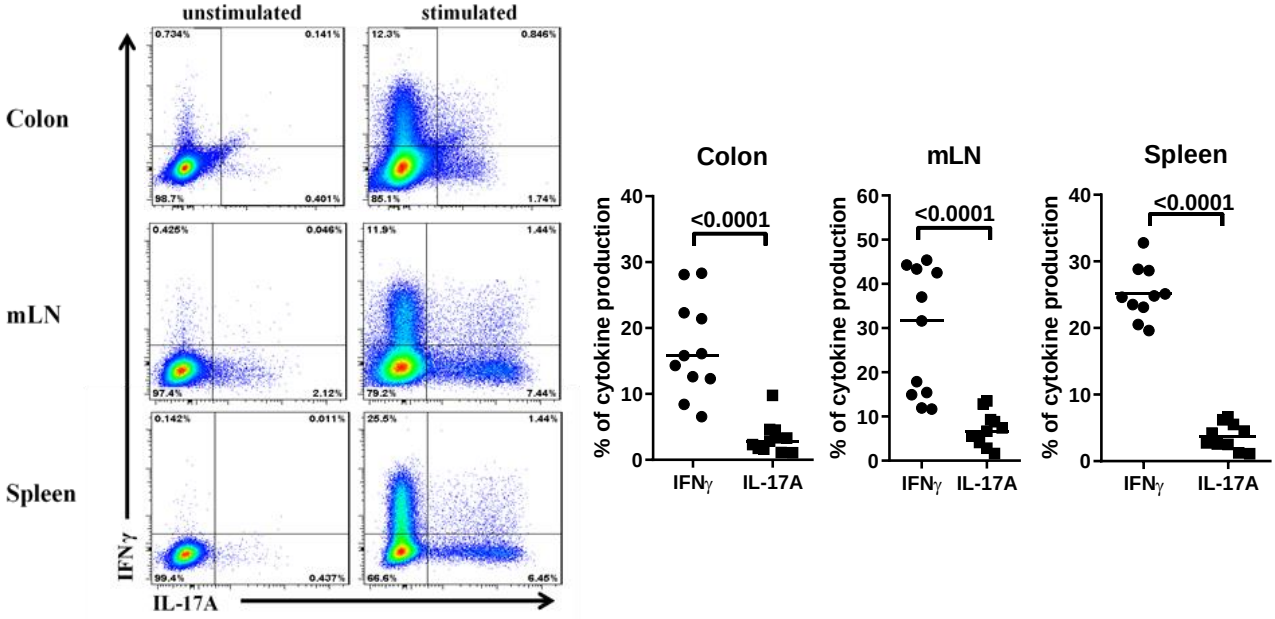

Figure 30: T cell transfer of 500,000 naïve CD4⁺ T cells generates a predominately IFNγ response and only a small IL-17A response.

A. Clinical data showing weight loss, spleen weight and colon weight in *Rag2*$^{-/-}$ mice given 500,000 naïve CD4^{+} T cells (n = 11 for colon, mLN and spleen). Multiple T test with Bonferonni-Dunn's correction performed on percentage weight change where ** = P<0.01, and Mann-Whitney Tests on colon and spleen. B. Representative flow plots and overall dot plot from spleen, mLN and colon showing IFNγ and IL-17A production after T cell transfer (n = 11 controls and n = 15 TCT for colon, mLN and spleen) with Mann-Whitney Tests performed. ** = P<0.01

The limiting factor for the transfers of YFP^{+} CD4^{+} naïve T cells was the small number of naïve T cells that could be found in these mice. In Figure 31, transferring 100,000 YFP^{+} naïve T cells alone was performed to test the model with reduced transfer of cells.

31A **Clinical data showing percentage weight change and organ weights after 100,000 naïve YFP$^+$ CD4$^+$ T cell transfer**

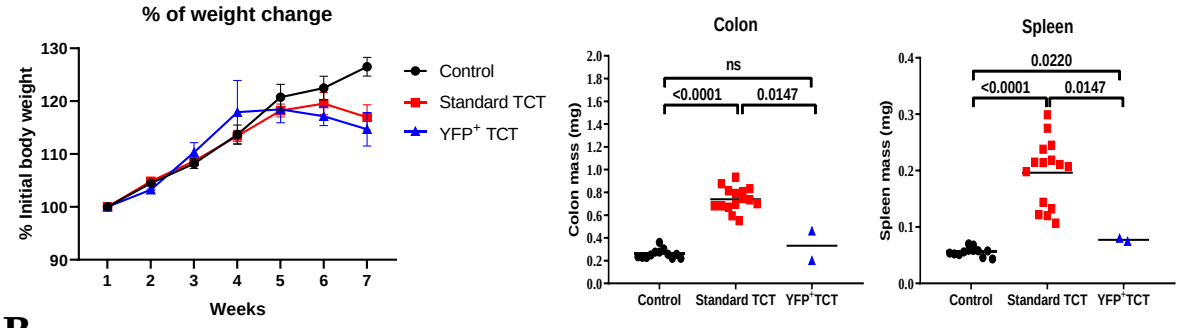

31B **Representative flow plot and dot plots showing cytokine production and transcription factor expression after 100,000 naïve YFP$^+$ CD4$^+$ T cell transfer**

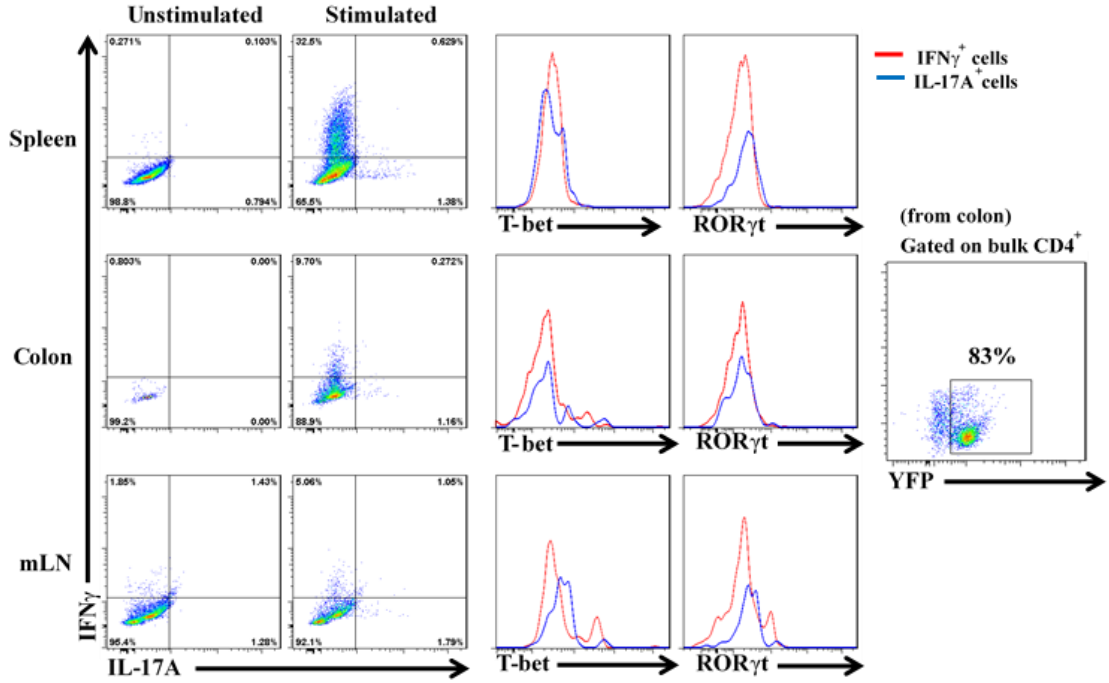

Figure 31: T cell transfer of 100,00 naïve YFP$^+$ CD4$^+$ T cells have a reduced disease phenotype despite still generating a predominately IFNγ response and lacks an IL-17A response.

A. Clinical data showing weight loss, spleen weight and colon weight in *Rag2*$^{-/-}$ mice given 100,000 naïve YFP$^+$ CD4$^+$ T cells and showing the same clinical features from the standard 500,000 naïve T cell transfer model (n=11 controls, n=15 for standard TCT and n=2 for YFP$^+$ TCT). Mann-Whitney Tests performed on colon and spleen. B. Representative flow plots showing cytokine response from live CD3$^+$ CD4$^+$ cells from spleen, mLN and colon showing IFNγ and IL-17A production after T cell transfer and histograms showing T-bet and RORγt expression from IFNγ and IL-17A producing cells. (n = 2)

Figure 26A shows that mice which received 100,000 naïve YFP$^+$ CD4$^+$ T cells started to have a similar trend to weight loss after 7 weeks; in comparison with the standard TCT mice,

whereas the untreated mice carried on gaining weight. However, with only a small sample size, more repeats of this will be needed to confirm this. From these two mice, there was still a possible comparison in weight loss with the standard 500,000 T cell transfer. Regarding, the organ weight loss, there was a significant increase seen in the spleen, but not in the colon weights in comparison to the control healthy organ weights. However, this macroscopic clinical feature is significantly decreased when compared to the standard 500,000 T cell transfer protocol. This could suggest that the mice needed to be kept for longer for a disease phenotype to become more established, or that 100,000 cells were not enough to generate a significant disease phenotype. However, Figure 31B did preliminary demonstrate that there was no IL-17A cytokine response found in the spleen, mLN or colon from these two samples. There was also a high amount of IFNγ production seen only in the spleen. Furthermore, as shown in the colon, the transferred YFP^+ $CD4^+$ T cells were still YFP^+ and still present within the mice and were able to migrate and survive to the colon. These data suggest that the YFP^+ naïve $CD4^+$ T cells are not able to cause a sufficient immune response without the bulk of the usual YFP^- $CD4^+$ T cells that are present. Further repeats of these 100,000 naïve YFP^+ T cell transfers will need to be performed in order to confirm this but due to the low percentage of YFP^+ naïve $CD4^+$ T cells found in the spleen and other organs of the T-bet^{cre} x $ROSA26YFP^{fl/fl}$ mice.

However, to get a better comparison of T cell transfer colitis disease read outs between the YFP^- vs YFP^+ naïve $CD4^+$ T cells, equal numbers of naïve YFP^- and YFP^+ $CD4^+$ T cells needed to be transferred into separate *Rag2*$^{-/-}$ mice. As reported already, since the percentage of YFP^+ naïve $CD4^+$ T cells was low in these mice, 25,000 cells were transferred in order to get some replicates. The results from this T cell transfer are shown in Figure 32. Supernatant was extracted from organ culture, in which a uniform 3mm biopsy punch sample from the colon was taken and placed in media and cultured for 48 hours at 37°C. Unfractionated cells from spleen, mLN and colon were also cultured for 48 hours at 37°C. Both supernatants were then analysed for their levels of IFNγ and IL-17A by ELISA.

32A **Clinical data showing percentage weight change and organ weights after 25,000 naïve YFP$^+$ and YFP$^-$ CD4$^+$ T cell transfer**

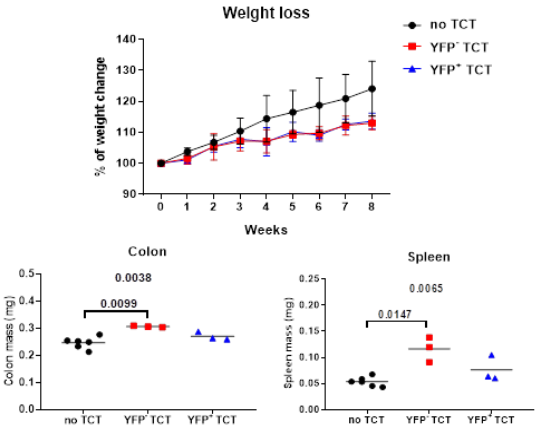

32B **Representative flow plot and dot plots showing cytokine production after 25,000 naïve YFP$^+$ and YFP$^-$ CD4$^+$ T cell transfer**

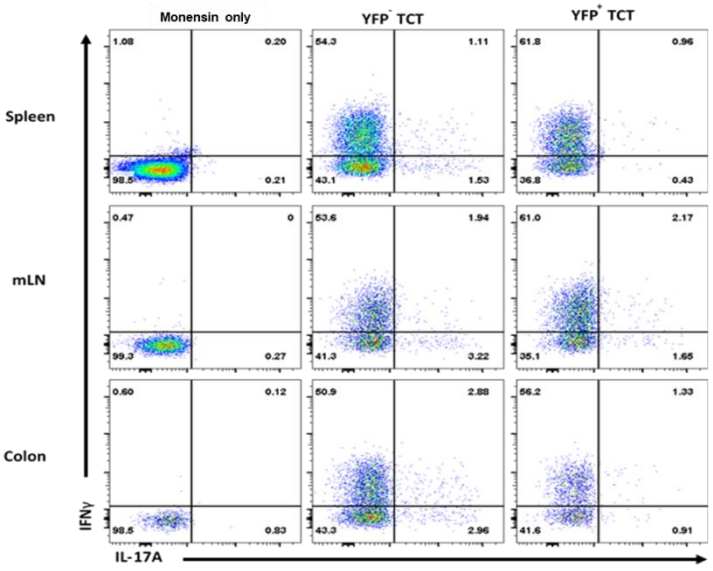

32C **Representative flow plots showing YFP expression from YFP$^-$ and YFP$^+$ naïve CD4$^+$ T cell transfers**

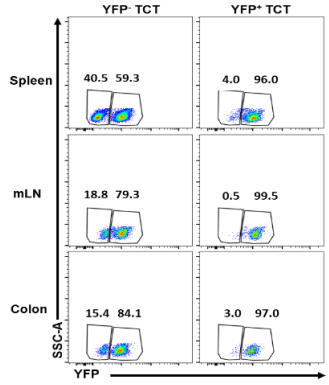

32D **IFNγ and IL-17A production from organ cultures of colon biopsies from YFP$^-$ and YFP$^+$ naïve CD4$^+$ T cell transfers**

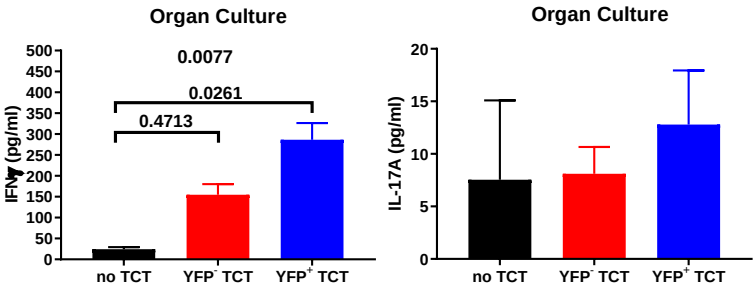

32E **IFNγ production from cell cultures of spleen, mLN and colon from YFP$^-$ and YFP$^+$ naïve CD4$^+$ T cell transfers**

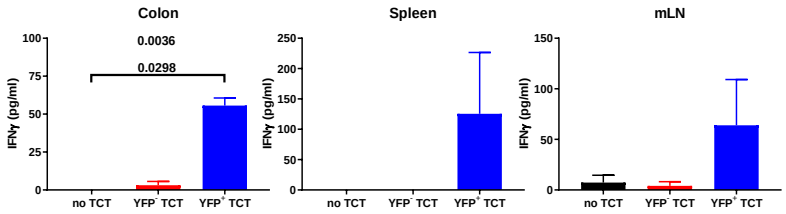

Figure 32: T cell transfer of 25,000 naïve YFP$^-$ and naïve YFP$^+$ CD4$^+$ T cells do not get a disease phenotype but YFP$^+$ CD4$^+$ T cell transferred still have an increased production of IFNγ and reduced IL-17A when compared to YFP$^-$ CD4$^+$ T cell transferred.

A. Clinical data showing weight loss, spleen weight and colon weight in *Rag2*$^{-/-}$ mice given either 25,000 naïve YFP$^+$ or naïve YFP$^-$ CD4$^+$ T cells. B. Representative flow plots showing cytokine response from live CD3$^+$ CD4$^+$ cells from spleen, mLN and colon showing IFNγ and IL-17A production after T cell transfer. C. Representative flow plots showing the expression of YFP in the CD3$^+$ CD4$^+$ naïve YFP$^-$ and naïve YFP$^+$ T cells in the spleen, mLN and colon in the Rag2$^{-/-}$ mice after T cell transfer. D. Cytokine production of IFNγ and IL-17A from supernatant of colon organ cultures measured by ELISA. E. Cytokine production of IFNγ from supernatant of unfractionated cell cultures from colon, spleen and mLN measured by ELISA. (n = 3 for each transfer and n = 6 for control). Kruskal-Wallis test performed with Dunn's corrections showing overall statistical analysis for all groups and individual comparisons.

Figure 32A showed that these mice did not develop any significant wasting disease, and this may be due to the much smaller number of naïve T cells that were transferred. Although both sets of recipient mice did not show signs of wasting, neither did they gain as much weight as the control mice. Furthermore, there was an overall significant difference when comparing the organ weights of untreated mice, YFP- naïve T cell transfer and YFP^+ naïve T cell transfer mice. However, there was only a significance increase in the spleens and colons between untreated and the YFP^- naïve T cell recipient mice. Despite the lack of wasting due to the low starting cell number transferred, the $CD4^+$ T cells were, not only still able to migrate to the colon, mLN and spleen after 9 weeks of transfer, but they were functionally able to produce cytokines. Figure 32B showed representative plots that the mice which received YFP^+ naïve T cells were predisposed to producing greater amounts of IFNγ and almost no IL-17A in comparison with the transferred YFP^- naïve T cells. Figure 32C further confirmed that a large proportion of YFP^- naïve $CD4^+$ T cells became YFP^+, consistent with IFNγ production and T-bet expression, and the injected YFP^+ $CD4^+$ T cells all remain YFP^+. Figure 32D and 32E show that even without PMA and ionomycin stimulation and simply culturing the full colon organ piece and unfractionated cells from spleen, mLN and colon, there was a significant increase in IFNγ production from the YFP^+ $CD4^+$ T cell transferred mice in the colonic cell cultures and from the organ cultures. Further repeats of these transfers would be necessary to confirm the findings in these data though.

4.5 Do YFP^+ naïve $CD4^+$ T cells require bystander activation for IFNγ production or provide bystander activation to YFP^- naïve $CD4^+$ T cells?

The data from both the 100,000 and 25,000 transfers of YFP^+ $CD4^+$ T cells into the *Rag2*$^{-/-}$ showed that they were unable to provoke a wasting disease phenotype or cause macroscopic inflammation of target organs; but still potentially to have the ability to produce IFNγ. As discussed before, $CD4^+$ T helper cells have been shown to exhibit bystander activation effects. Bystander activation is where unrelated T cells become stimulated and activated from cytokines, such as IL-15 and IFNγ, produced from other antigen-specific T cell stimulation (Boyman, 2010). It has also been shown that the $CD4^+$ T cell bystander activation might able to activate other T cells. Therefore, in order to test this hypothesis and ascertain if YFP^+ naïve

$CD4^+$ T cells had any potential bystander effect with their predisposed IFNγ production on YFP^- naïve $CD4^+$ T cells.

It was important to observe if naïve YFP^- $CD4^+$ T cells were able to become YFP^+ *in vivo* in a non-disease setting by transferring them into a congenic CD45.1 mice. Use of the congenic CD45.1 model is useful in order to identify the donor $CD4^+$ T cells from the CD45.2 T-bet^{cre} x $ROSA26^{fl/fl}$ mice. Next, using this congenic mouse model, if an immune response could be generated in both *in vitro* and *in vivo* at different proportions of CD45.2 YFP^+ CD4 T cells to CD45.1 $CD4^+$ T cells, to demonstrate IFNγ bystander activation of the CD45.2 YFP^+ CD4 T cells on the CD45.1 $CD4^+$ T cells in order to develop an inflammatory response and cause disease from the T cell transfer.

4.5.1 Transferred naïve YFP^- CD45.2 $CD4^+$ T cells do not become YFP^+ without the presence of a disease phenotype

10 x 10^6 $CD45.2^+$ naïve YFP^- $CD4^+$ T cells were transferred into CD45.1 mice and after 8 weeks of transfer the mice were analysed. In control experiments, transferring 10 x 10^6 CD45.2 naïve $CD4^+$ T cells into CD45.1 mice does not cause any wasting colitis disease.

33A **Representative flow plots showing the population of CD45.1 and CD45.2 cells in different organs of CD45.1 congenic mice post-CD45.2 YFP$^-$ naïve CD4$^+$ transfer**

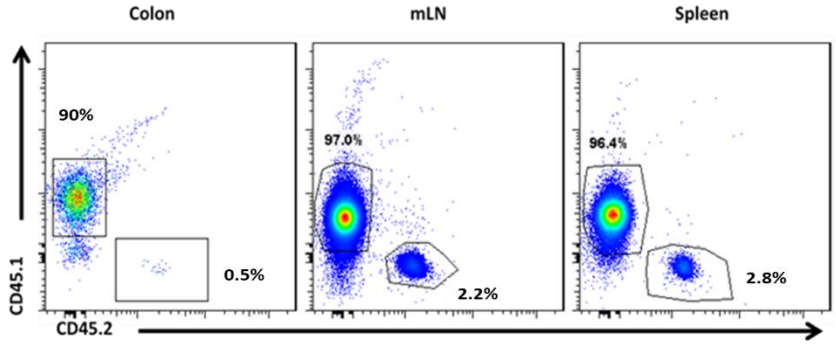

33B **Dot plot showing the percentage and exact cell number of CD4$^+$ CD45.2$^+$ found in the CD45.1 mice**

33C **Dot plot showing the percentage and exact cell number of YFP$^+$ CD4$^+$ CD45.2$^+$ found in the CD45.1 mice**

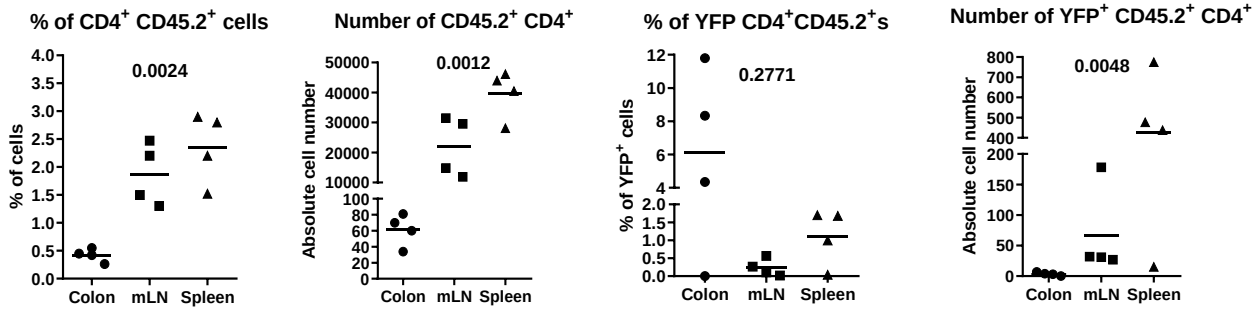

Figure 33: T cell transfer of 10,000,000 naïve CD45.2$^+$ CD4$^+$ YFP$^-$ T cells into CD45.1 mice do not develop a disease phenotype and remain YFP$^-$.

A. Representative flow plots showing rediscovery of CD45.2$^+$ CD4$^+$ T cells in the CD45.1 mice in the spleen, mLN and colon post-transfer. B. Dot plot showing the percentage and exact cell number of CD4$^+$ CD45.2$^+$ found in the CD45.1 mice. C. Dot plot showing the percentage and exact cell number of YFP$^+$ CD4$^+$ CD45.2$^+$ found in the CD45.1 mice. (n = 4). Kruskal-Wallis test performed showing overall statistical analysis for all groups.

The YFP$^-$ CD45.2 CD4$^+$ T cells that are transferred into the CD45.1 mice was shown to migrate to the organs in the mice and there was a significant difference in the amount and percentage of CD4$^+$ CD45.2 T cells found in the colon, spleen and mLN post-transfer. However, of these the CD45.1 mice were healthy and this could be the reason for why the CD45.2 CD4$^+$ T cells did not become YFP positive at all and did not produce any cytokines as they were not stimulated (data not shown). This also potentially showed that the YFP$^-$ naïve CD4$^+$ T cells from these mice do not spontaneously express T-bet and become YFP$^+$ without an inflammatory environment to stimulate them with an inflammatory T_H1 response, which was

shown in the *in vitro* culture experiments with YFP- naïve $CD4^+$ T cells. Furthermore, the possibility that the presence of other T cells (both CD4 and CD8), within the CD45.1 mice, does not have a bystander cytokine activation effects on the CD45.2 YFP^- $CD4^+$ T cells to stimulate them.

4.5.2 IFNγ production from CD45.2 YFP^+ cells was observed when there are limited cell numbers in co-culture with CD45.1 $CD4^+$ T cell

In vitro analysis of sorted naive YFP^- $CD4^+$ and naïve YFP^+ $CD4^+$ T cells (both CD45.2) and naïve CD45.1 $CD4^+$ T cells were cultured separately and co-cultured together to test for bystander activation from IFNγ production. These sorted cells were plated on pre-incubated CD3/CD28 and only given IL-2 and no skewing conditions. Cells were taken off and intracellular cytokine flow cytometry was performed after either 3 days, 5 days or 7 days of culture and the final supernatants were kept for ELISAs. As performed previously, 25,000 YFP^+ T cells were transferred *in vivo* with potentially some organ weight differences seen and also IFNγ production. Therefore, this number of co-cultured cells (resulting in 50,000 together) was also tested here *in vitro*, before an *in vivo* co-transfer of CD45.2 and CD45.1 cells into a *Rag2*$^{-/-}$ was performed.

34A **Representative flow plots showing IFNγ production from *in vitro* culture of sorted CD45.2 YFP$^-$, CD45.2 YFP$^+$, CD45.1 naïve CD4$^+$ T cells**

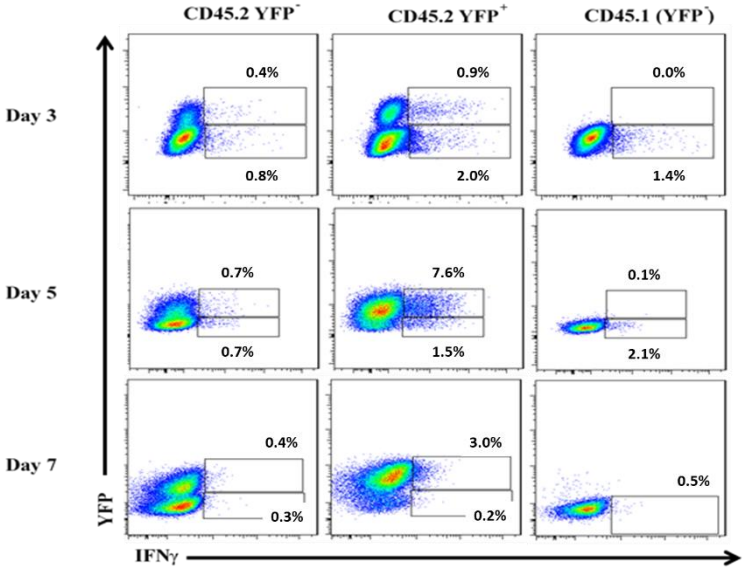

34B **Representative flow plots showing the proportion of CD45.1:CD45.2 YFP$^+$ *in vitro* co-culture**

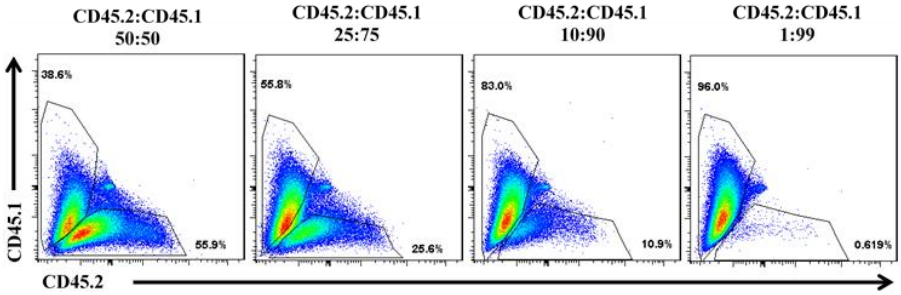

34C **Representative flow plots showing the proportion of CD45.1:CD45.2 YFP$^+$ *in vitro* co-culture**

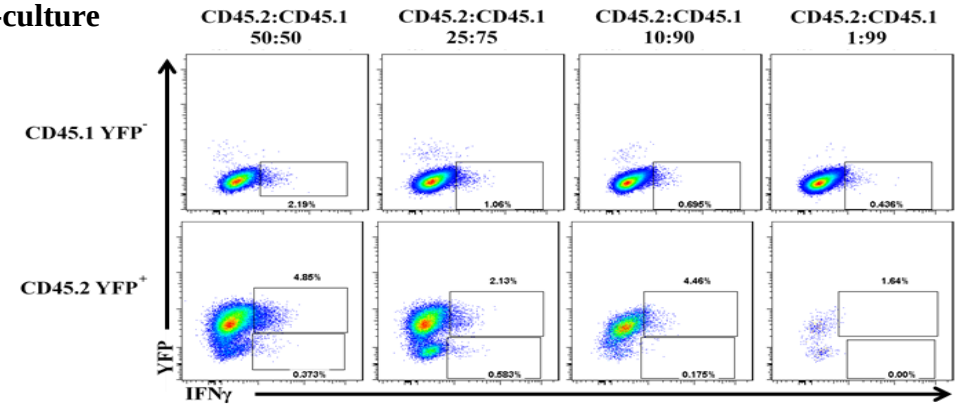

Figure 34: *In vitro* culture of CD45.1, CD45.2 YFP$^+$ and CD45.2 YFP$^-$ with IL-2 and anti-CD3/CD28 shows spontaneous production of IFNγ by CD45.2 YFP$^+$ to still occur.

A. Representative flow plots showing *in vitro* culture of sorted naïve (CD62L$^+$ CD44$^-$) CD4$^+$ T cells at 50,000 cells per well of CD45.1, CD45.2 YFP$^+$ and CD45.2 YFP$^-$ with IL-2 and anti-CD3/CD28 showing IFNγ production after 3, 5 and 7 days of culture. B. Representative flow plots showing the *in vitro* co-culture of sorted naïve (CD62L$^+$ CD44$^-$) CD4$^+$ T cells of CD45.1 and CD45.2 YFP$^+$ with IL-2 and anti-CD3/CD28 at different ratios shown of 50,000 cells per well after 7 days of culture. C. Representative flow plots showing the amount of IFNγ production from *in vitro* co-culture of sorted naïve (CD62L$^+$ CD44$^-$) CD4$^+$ T cells of CD45.1 and CD45.2 YFP$^+$ with IL-2 and anti-CD3/CD28 at different ratios shown of 50,000 cells per well after 7 days of culture. (n=3)

Although this experiment was only performed once and needs repeating to increase the sample representative size, there were some promising potential results in the *in vitro* cultures of the CD45.1, CD45.2 YFP^- and CD45.2 YFP^+, despite only starting with 50,000 cells. The CD45.2 YFP^+ $CD4^+$ T cells were still able to make large amounts of IFNγ after 5 days of culture with only IL-2 and CD3/CD28 stimulation, although oddly the day 7 cultures did not show high IFNγ production, like in Figure 28. Unexpectedly, the day 3 cultures of the CD45.2 YFP^+ showed a large proportion of YFP^- $CD4^+$. Interestingly, the CD45.2 YFP^- CD4 T cells and the CD45.1 $CD4^+$ T cells did not suggest to be producing a substantial level of IFNγ, as was seen previously with the CD45.2 YFP^- CD4 T cells in Figure 28. Interesting, the sorted YFP^+ naïve $CD4^+$ T cells appeared to lose YFP expression as seen in the flow plots for day 3, where so few cells are YFP^+ in comparison with day 5 and day 7 where they all are YFP^+. This doesn't make sense in the model and will need further replicates and also testing to see if this was the case in this experiment.

Following the results observed above showing that potentially the IFNγ production solely came from the YFP^+ naïve $CD4^+$ T cell population during *in vitro* culture, *in vitro* co-cultures of CD45 YFP^+ with CD45.1 $CD4^+$ T cells were cultured at ratios of 50:50, 25:75, 10:90 and 1:99 in a total of 50,000 cells in IL-2 and anti-CD3/CD28 for 5 days. Figure 34B shows that even at a ratio of 10:90 the CD45.2 YFP^+ T cells can still visibly be found in the cultures. As well as the cells proliferating and surviving at a ratio of 10:90, they were shown to still be functioning and together able to produce some IFNγ (Figure 34C). From Figure 34, there was plausibility that there might be a role for the YFP^+ $CD4^+$ T cells having bystander activation effect by spontaneously producing IFNγ and being able to act on the CD45.1 $CD4^+$ T cells and further stimulate them. However, these *in vitro* experiments were performed in triplicate and therefore these observations could further be concluded if more experiments were performed.

4.5.3 *In vivo* co-transfer of CD45.1 and CD45.2 YFP^+ naïve $CD4^+$ T cells shows bystander activation of CD45.2 YFP^+ naïve $CD4^+$ T cells to produce a sufficient disease phenotype

From the results of the *in vitro* co-culture, a co-transfer was next attempted of the naïve YFP^+ $CD4^+$ and naïve CD45.1 $CD4^+$ T cells in *Rag2*$^{-/-}$ mice, like previously performed. These were

injected at a ratio of 10:90 since *in vitro* they were still identifiable in culture and able to produce IFNγ. This was intended to cause a colitis disease within the mice, which is driven by the increased predominance of IFNγ producing $CD4^+$ T cells.

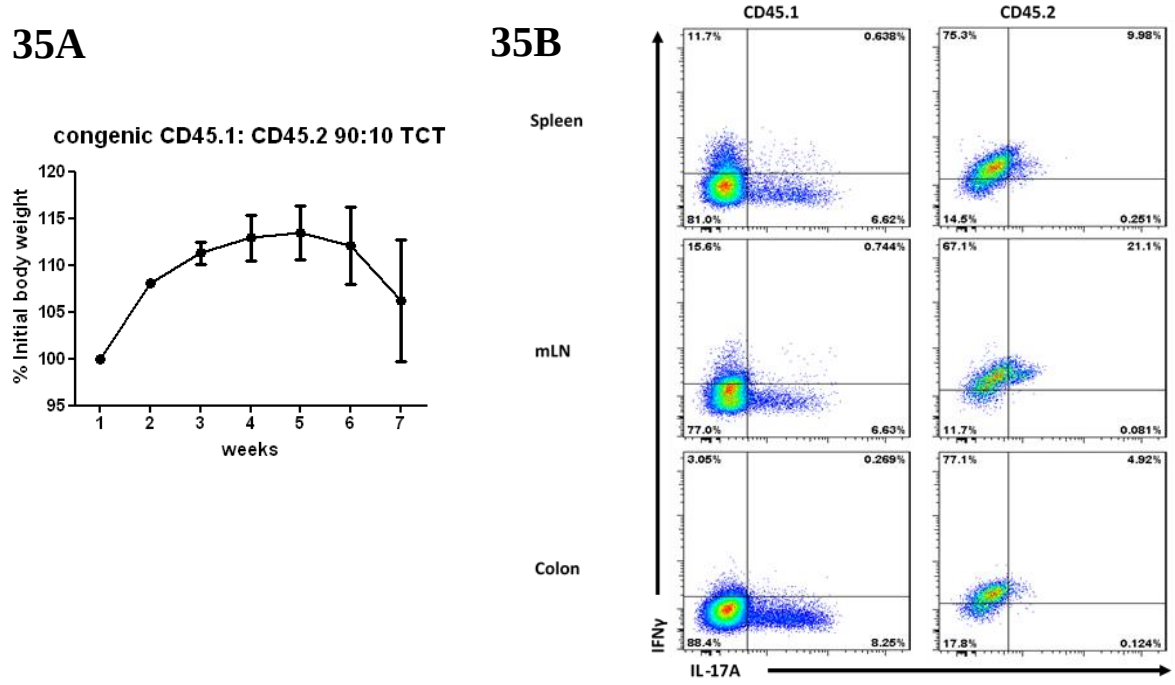

Figure 35: *Rag2*$^{-/-}$ mice co-transferred with 25,000 cells at a 90:10 ratio of CD45.1:CD45.2 YFP^+ naïve $CD4^+$ T cells

A. Clinical data showing weight loss after 7 weeks of co-transferred naïve $CD4^+$ T cells in *Rag2*$^{-/-}$ B. Representative flow plots showing IFNγ and IL-17A production from either the $CD45.1^+$ $CD4^+$ $CD25^-$ T cells or CD45.2 YFP^+ $CD4^+$ $CD25^-$ T cells. (n=5)

Co-transfer of both the naïve YFP^+ CD45.2 CD4 T cells and naïve CD45.1 $CD4^+$ T cells showed the possibility that they could produce a disease phenotype, with the weight loss after 7 weeks, similar to that of the normal T cell transfer, despite the lack of initial starting cell and in contrast to when the naïve YFP^+ $CD4^+$ T cells were transferred alone in Figure 32. From the flow plot, the YFP^+ $CD4^+$ T cells are producing only IFNγ and the CD45.1 $CD4^+$ T cells are producing a small amount of IFNγ and a lot more IL-17A. This experiment will need repeating in order to show this again and obtain further proof that the IFNγ from the YFP^+ $CD4^+$ T cells are able to activate and further enhance the activity of the YFP^- $CD4^+$ T cells

4.6 Discussion

The main aim of this chapter was to attempt to characterise this potentially newly identified small population of T-bet fate mapped naïve $CD4^+$ T cell. These cells have been shown not to be stem cell-like naïve or virtual memory cells, but they were $CD5^{high}$ and could be precursors to previously reported MP cells (Kawabe et al., 2017). Interestingly, 30% of the YFP^+ naïve CD4 T cells showed increased $CXCR3^+$ expression compared to the YFP^- naïve T cells. CXCR3 has been shown to be regulated by the expression of T-bet and T-bet is required for the migration of both $CD4^+$ and $CD8^+$ T cells (Groom and Luster, 2011, Oghumu et al., 2013, Tan et al., 2016b). These T-bet fate mapped YFP^+ $CXCR3^+$ $CD4^+$ T cells are interesting: they could be predetermined early immune responders that are able to migrate to areas of infection more readily due to their higher expression of CXCR3. Interestingly, CD28 remained highly expressed in the $CD44^+$ $CD62L^-$ effector $CD4^+$ T cells, although it has previously been reported to become downregulated when naïve T cells become activated.

The data gathered from these different aged T-bet^{cre} x $ROSA26^{fl/fl}$ mice shows that these YFP^+ naïve CD4 T cells appear to develop during the development of the mouse only after birth and are even visible from as early as 1 week after birth. It has been shown that T and B cells are not fully developed at birth and have also been shown to skew towards a T_H2-like response instead of a T_H1 response (Adkins et al., 2004, Basha et al., 2014, Papaioannou et al., 2019). The data shown here however suggests that there is a requirement for an environmental antigen to be present that the mice interact with after birth and only after birth does T-bet become expressed in a subset of naïve $CD4^+$ T cells. This further enhances the idea that T-bet fate mapped naïve $CD4^+$ T cells are predisposed and early inflammatory responders that react to environmental antigens. However, this experiment has only been performed once, and due to the lack of cell numbers the embryonic foetal livers had to be pooled; the conclusions would be stronger if this experiment were replicated. The older 25-week and 52-week mice also further demonstrate that the cells are still present in old age and not an artefact of the breeding as they are consistent in their expression as the mice age. Old mice are considered to be old at 18months, where thymic involution and the decline of naïve T cell output occurs (Aw and Palmer, 2011, Aw et al., 2007, Palmer, 2013). The phenotyping data gathered here therefore would need to be extended to around this age and beyond to confirm if there is a difference and

reduction seen in the population and percentages of naïve $CD4^+$ T cells in the mice and if the percentage of YFP^+ naïve $CD4^+$ T cells decline too.

In vitro and *in vivo* analyses of these YFP^+ T cells show that they have a different function to the YFP^- naïve T cells. They produce high amounts of IFNγ both *in vivo* and *in vitro* and from the T cell skewing experiments can cause a possible switch to T_H1 cell type with increased IFNγ production in the different skewed subtypes. This was more prominent in the YFP^+ T cell transfer experiments. Unfortunately, they were only performed once with a small sample size and would ideally need repeating to confirm reproducibility. However, preliminary data suggest YFP^+ naïve $CD4^+$ T cells have a function *in vivo* and possibly act as early IFNγ T_H1 responders when there is inflammation present. But this data also suggested that the YFP^+ naïve T cells are unable to initiate an inflammatory response on their own, and therefore might be able to induce bystander activation of the YFP^- naïve CD4 T cells to make them produce IFNγ.

Lastly, as shown by the co-transfer experiments, these YFP^+ $CD4^+$ naïve T cells have bystander activation effects, which polarise naïve YFP^- $CD4^+$ T cells in response pathogens and activate them to produce IFNγ. From the previous findings, the bystander activation shown here of the CD45.1 $CD4^+$ T cells by the CD45.2 YFP^+ $CD4^+$ T cells is able to drive the colitis and cause disease. This further demonstrated that these YFP^+ naïve $CD4^+$ T cells have a role within the naïve $CD4^+$ T cell compartment. As bystander activation has previously been reported in MP cells and this data shows that the YFP^+ naïve CD4 T cells also act with bystander activation (Boyman, 2010, Eberl et al., 2000), this data further supports the hypothesis that these cells could be precursors to the $CD5^+$ MP cells, as shown previously in the phenotyping data in this chapter, however further phenotyping and analysis of these cells would be needed to confirm this.

Chapter 5

Results: Identifying a role for T-bet in $CD4^+$ T cell plasticity

As explained in Chapter 1, the plasticity of $CD4^+$ T cells has been widely studied, including the role of cytokines, master regulator transcription factors and signal transducers and activators of transcription (STATs) in controlling and determining this plasticity (Caza and Landas, 2015, Zhou et al., 2009). Although the differentiation of naïve $CD4^+$ T cells has been previously studied and described extensively, research into plasticity of $CD4^+$ T helper subsets is still at an early stage. When naïve $CD4^+$ T helper cells are given a sufficient signal from cytokines and the transcription factors, they undergo activation and differentiate. However, these $CD4^+$ T helper cells have not become terminally differentiated. When a change in the inflammatory environment occurs, altering the cytokines that the subsets of $CD4^+$ T helper cell experiences, then these previously activated effector cells can switch helper subset. This provides a more efficient response to pathogens than having to constantly prime naïve $CD4^+$ T cells (Evans and Jenner, 2013, Hertweck et al., 2016, Kanhere et al., 2012, Lord et al., 2005, Nakayamada et al., 2012, O'Shea and Paul, 2010, Zhu and Paul, 2010).

The use of the T-bet^{cre} x $ROSA26^{fl/fl}$ mouse allows tracking previous T-bet expression in effector cytokine producing $CD4^+$ T cells at both healthy and disease models. As helper T cells have been shown to be so plastic, using this mouse model allows experiments on both YFP-IL-$17A^+$ cells and YFP^+ IL-$17A^+$ cells *in vitro* and *in vivo* to see if they can switch to a T_H1-like phenotype.

Furthermore, the role of T-bet in $CD4^+$ T helper can be characterised and the change after differentiation and plasticity can be monitored by deleting T-bet after the development of adult mice, by using a $CreER^{T2}$ x T-$bet^{fl/fl}$ tamoxifen inducible deletion model. This mouse model was established within the lab, whereby T-$bet^{fl/fl}$ mice were bred with $CreER^{T2}$. The $CreER^{T2}$ is a ligand-dependent chimeric Cre recombinase (Feil et al., 1996, Feil et al., 1997, Metzger et al., 1995, Sanchez-Fernandez et al., 2012, Zhang et al., 1996). The Cre enzyme is fused to the mutated hormone-binding domains of the oestrogen receptor. In normal circumstances, this Cre is inactive, however it is possible to be activated using the chemical compound 4-hydroxytamoxifen (OHT), which acts on the oestrogen receptor ligand. The ability to activate

the Cre with tamoxifen, which is converted to OHT, allows for exterior temporal control of the Cre enzyme. Since their first documentation in 1996 by Feil et al., the majority of these $CreER^{T2}$ models have now been used in conjunction with floxed mice models to allow temporally controlled deletion of tissue-specific or cell-specific models (Feil et al., 2009). In the $CreER^{T2}$ x $T\text{-}bet^{fl/fl}$ mouse line, upon delivery of the tamoxifen, the Cre enzyme is activated and T-bet is deleted in all cells. T_H2 cell function to expel helminths during a parasite infection. Upon infection by helminths, T_H2 cells produce IL-13, IL-4 and express GATA3 and STAT6 (Harvie et al., 2010, Pelly et al., 2016, Reynolds et al., 2012). Using models of IBD in the $CreER^{T2}$-$Tbet^{fl/fl}$ mice would provide a physiological readout of plasticity of $CD4^+$ T cells in the absence of T-bet.

5.1 Use of the T-bet fate mapping mouse line shows that previous T-bet expression allows for T_H17 cell plasticity

5.1.1 Previously naïve YFP^- $CD4^+$ T cells become effector YFP^+ IL-17A-producing $CD4^+$ T cells with the induction of colitis

As shown in chapter 4, the T cell transfer model of colitis is principally driven by IFNγ but is also associated with IL-17A production. Using this same model, the transfer of YFP^- naïve $CD4^+$ T cells was used to show the plasticity of the effector cells and allowed the plasticity of T-bet fate mapped cells to be tested. Figure 31 shows the YFP^- T cell transfer data using the same protocol as before, where 0.5×10^6 purified naïve YFP^- $CD4^+$ T cells were transferred, and the mice were observed for 7-8 weeks and then culled.

36A **Clinical data from control mice and T cell transfer mice**

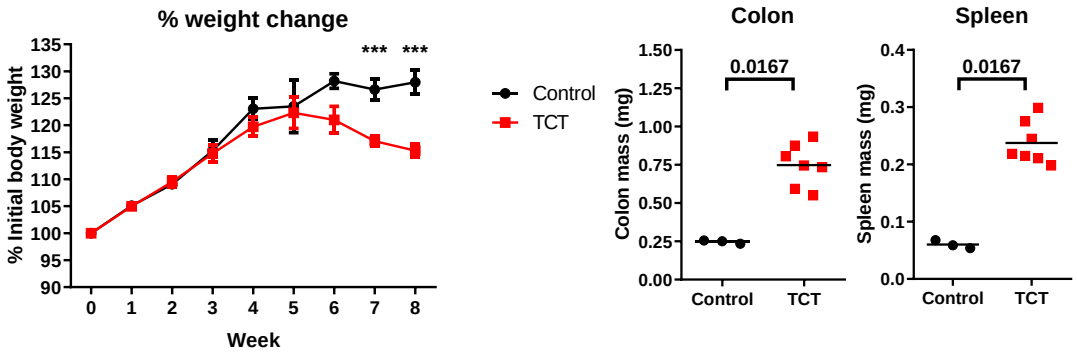

36B **IFNγ and IL-17A production from the colon and mLN**

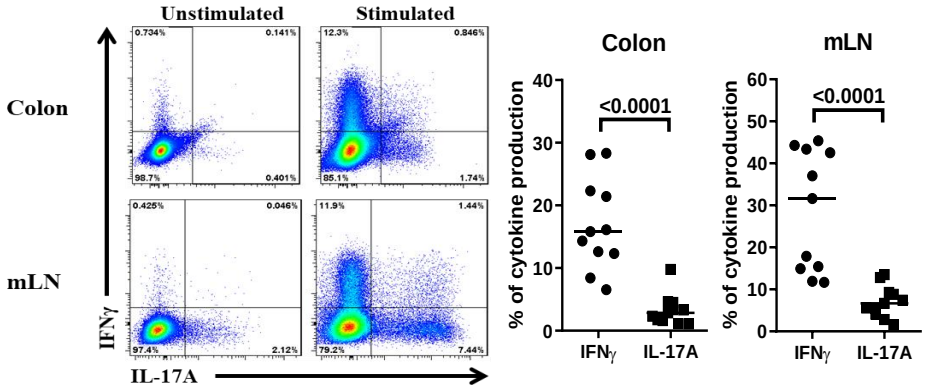

36C **YFP, T-bet and RORγt expression from the colon**

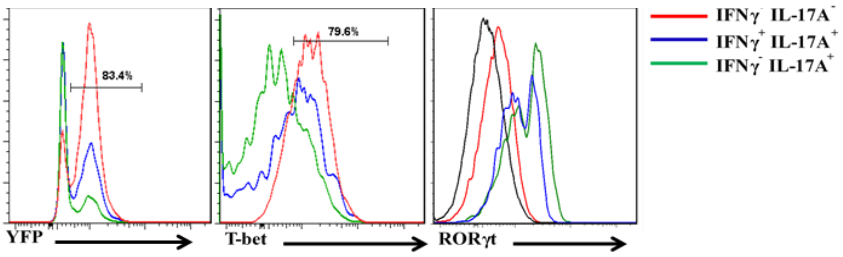

36D **YFP expression from the colon and mLN**

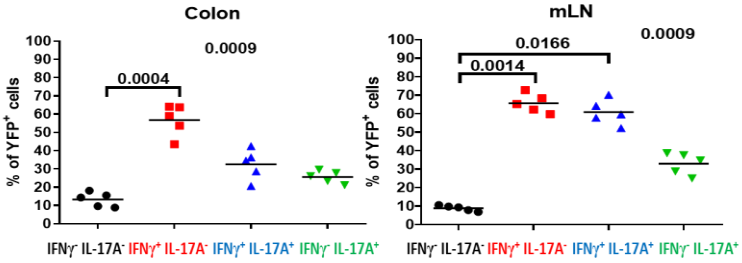

Figure 36: A subset of IL-17A$^+$ IFNγ$^-$ producing CD4$^+$ T cells express YFP during disease.

A. Clinical data showing weight loss, spleen weight and colon weight 8 weeks after transfer of naïve CD4$^+$ YFP$^-$ T cells into *Rag2*$^{-/-}$ mice (n=3 for control and n=7 from TCT mice showing Mann Whitney Test). B. Representative flow plot showing cytokine response from stimulated and unstimulated live CD3$^+$ CD4$^+$ CD25$^-$ cells from colon and mLN after 8 weeks after transfer of naïve CD4$^+$ YFP$^-$ T cells into *Rag2*$^{-/-}$ mice. (n=11) showing Mann Whitney Test C. Representative histograms showing YFP expression, T-bet expression and RORγt expression in IFNγ$^-$ IL-17A$^-$, IFNγ$^+$ IL-17A$^-$, IFNγ$^+$ IL-17A$^+$ and IFNγ$^-$ IL-17A$^+$ producing cells from the colon. D. Dot plots showing YFP expression in IFNγ$^-$ IL-17A$^-$, IFNγ$^+$ IL-17A$^-$, IFNγ$^+$ IL-17A$^+$ and IFNγ$^-$ IL-17A$^+$ producing cells in colon and mLN (n=5). Kruskal-Wallis test performed showing overall statistical analysis for all groups and with Dunn's corrections for individual comparisons. *** = P<0.001

Figure 36 shows a normal level of wasting colitis disease after 8 weeks and the mice suffered with increased colon and spleen sizes like Figure 30 from Chapter 4. The clinical data showed a significant difference from the YFP^- naïve $CD4^+$ transferred mice when compared with the control mice. Cytokine production was significantly found to be produced in the form of IFNγ with some IL-17A production too (Figure 36B). Figure 36C and 36D showing that there was YFP^+ IL-17A producing cells from the representative histograms of YFP expression and that there was a statistically significant difference between the percentage of YFP^+ cytokine producing subtypes. The histograms for T-bet and RORγt showed that these effector T_H1 and T_H17 cells were still positive for their representative transcription factors that control their differentiation. The $IFN\gamma^+$ $IL\text{-}17A^-$ single producing $CD4^+$ T cells were highly $T\text{-}bet^+$ and $ROR\gamma t^-$ and therefore YFP^+. The $IFN\gamma^+$ $IL\text{-}17A^+$ double producing $CD4^+$ T cells showed intermediate levels of both T-bet expression and RORγt and as expected there were some double producing $CD4^+$ T cells which were YFP^+. In comparison, the $IFN\gamma^-$ $IL\text{-}17A^+$ single producing $CD4^+$ T cells were $ROR\gamma t^+$ and $T\text{-}bet^-$. However, interestingly there were a small (approximately 20%) subset of $IL\text{-}17A^+$ $IFN\gamma^-$ cells that were YFP^+ in both the colon and the mLN, although these were not significantly different in comparison with the percentage of YFP^+ expressing $IFN\gamma^+$ $IL\text{-}17A^-$ single producing $CD4^+$ T cells. Since all the naïve $CD4^+$ T cells entered the mice as YFP^- when they were transferred, this however potentially suggests that during the differentiation of the T_H17 $CD4^+$ T cells to produce IL-17A, some of the T_H17 cells expressed T-bet; even if afterward they stopped expressing T-bet. Using this mouse model to trace the lineage of T-bet expressing T_H17 cells could provide further potential insight into the plasticity of T_H17.

5.1.2 *In vitro* culture of YFP^+ $IL17A^+$ $IFN\gamma^-$ $CD4^+$ T cells show a predominance to switching to IFNγ production

The data shown in Figure 36 showed the potential for certain YFP^+ $IL\text{-}17A^+$ effector $CD4^+$ T cells to possibly switch to an IFNγ producing phenotype. Therefore, in order to try and test this, a cytokine secretion assay was performed in order to sort and purify the different cytokine YFP expressing cells. $IL\text{-}17A^+$ YFP^-, $IL17A^+$ YFP^+, $IFN\gamma^+$ YFP^- and $IFN\gamma^+$ YFP^+ producing $CD4^+$ T cells from the mLN and colon of the *Rag2*$^{-/-}$ mice that had originally received naïve YFP^- $CD4^+$ T cells, as shown in the previous figure, were sorted and purified. The gating strategy used for these cytokine secretion sorts is shown in Figure 32A. These four different

populations were then plated onto pre-incubated anti-CD3/CD28 plates and given IL-2 for their survival, similar to the protocol shown in the *in vitro* culture of the naïve YFP^+ $CD4^+$ T cells. Flow cytometry and ELISAs of the supernatant were analysed from these *in vitro* cultured cells and are shown in Figure 37.

37A **Gating strategy used for cytokine secretion assay**

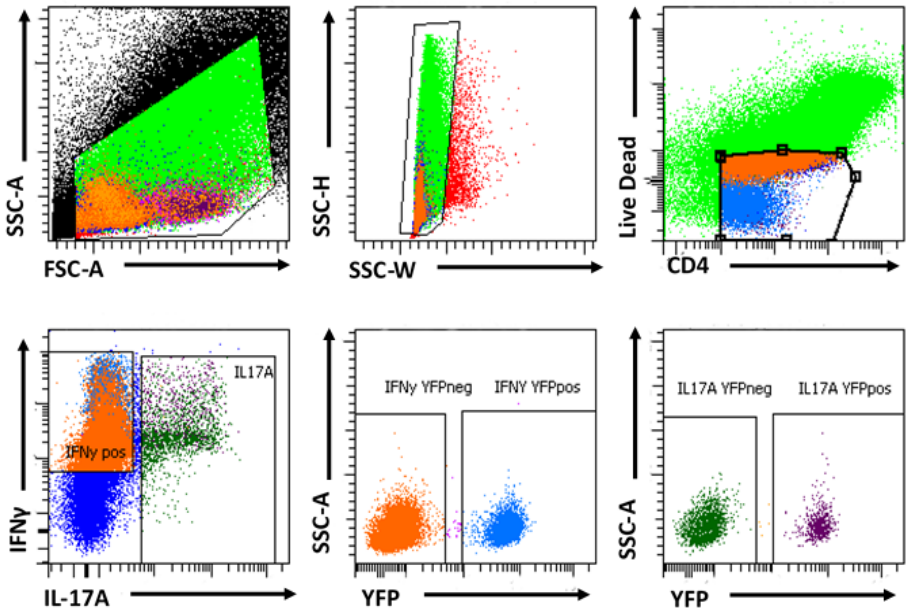

37B **Representative flow plots showing IFNγ and IL-17A production from *in vitro* cultured cytokine secretion sorted effector CD4$^+$ T cells**

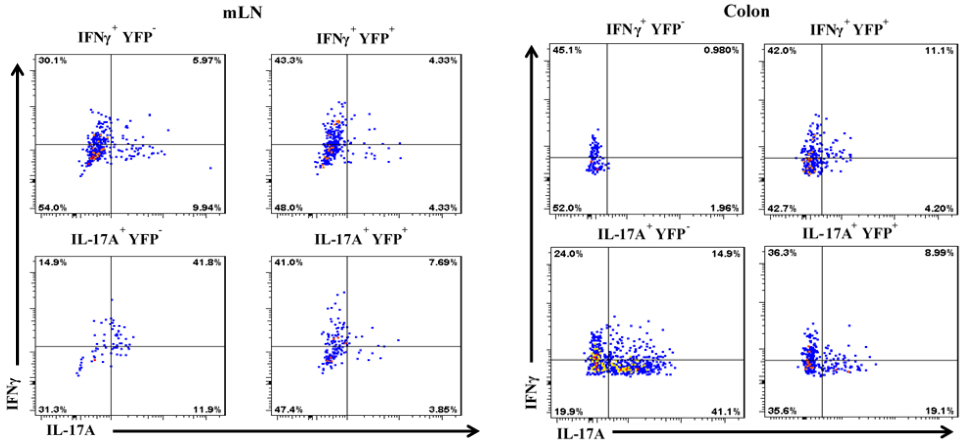

37C **ELISA data showing IFNγ and IL-17A production from *in vitro* cultured cytokine secretion sorted effector CD4$^+$ T cells**

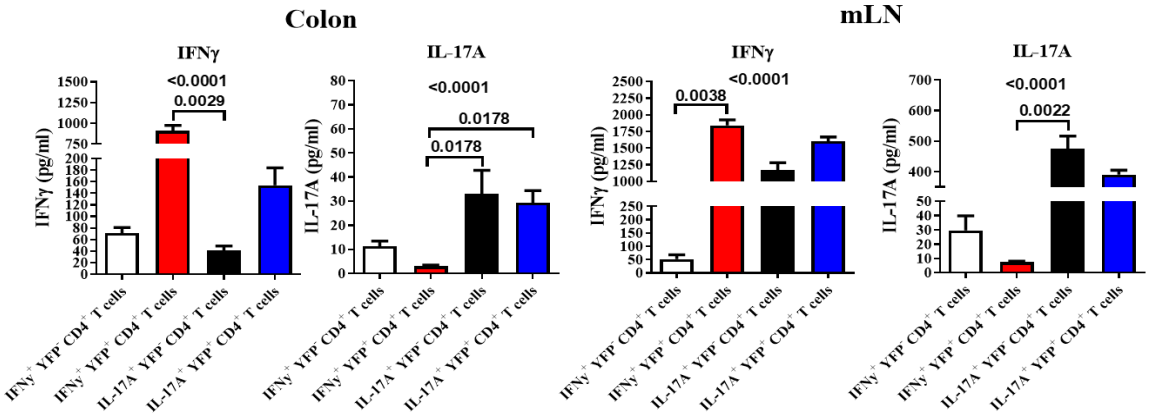

Figure 37: IL-17A$^+$ IFNγ$^-$ YFP$^+$ CD4$^+$ T cells produce more IFNγ and less IL-17A than IL-17A$^+$ IFNγ$^-$ YFP$^-$ CD4$^+$ T cells upon reactivation and re-stimulation *ex vivo* of T cell transfer colitis induced mice.

A. Gating strategy used to sort purified cytokine secreting CD4$^+$ T cells from the mLN and colon of *Rag2*$^{-/-}$ mice transferred with naïve YFP$^-$ CD4$^+$ T cells. B. Representative flow plot from the mLN and colon showing cytokine response from stimulated cytokine secretion YFP$^-$ or YFP$^+$ T cells after 7 days in culture *in vitro*. C. ELISA data showing cytokine production for IFNγ and IL-17A from the supernatant of the cultured cytokine secretion YFP$^-$ or YFP$^+$ CD4$^+$ T cells from both mLN and colon (n=4, with experiment performed twice). Kruskal-Wallis test performed showing overall statistical analysis for all groups and with Dunn's corrections for individual comparisons.

The flow plots and ELISA data in Figure 37 show the subsequent cytokine responses from the effector cells after 7 days of *in vitro* culture after TCR re-stimulation *ex vivo*. The ELISA data showed that there was a significant difference between all cell types sorted but there was only the IFNγ$^+$ YFP$^+$ significantly producing more IFNγ than the IL-17A$^+$ YFP$^-$ cells in the colon and mLN, and as expected the IFNγ$^+$ YFP$^+$ significantly producing more IFNγ than the IFNγ$^+$

YFP$^-$ cells in the mLN. Remarkably, this potentially showed a possibility that the IL-17A$^+$ YFP$^+$ CD4$^+$ T cells were, upon re-stimulation, able to produce a considerable amount of IFNγ and less IL-17A, especially in the colon, when compared with the IL-17A$^+$ YFP$^-$ CD4$^+$ T cells in both intracellular cytokine staining and by ELISAs; although these were not statistically significant, there was a trend towards this and with more sample repeats this would probably become significant. This helped to demonstrate that there could be the possibility that initial T-bet$^+$ fate mapped IL-17A$^+$ CD4$^+$ cells can switch to a more T_H1-like phenotype and produce IFNγ more readily, especially in a disease setting upon stimulation of TCR.

5.1.3 Transfers of YFP$^+$ IL17A$^+$ IFNγ$^-$ CD4$^+$ T cells into RAG2$^{-/-}$ mice reveals a possible predominance to switching to IFNγ production

From the data in Figure 37, the cytokine secretion assay allowed us to further adoptively transfer these sorted colitogenic effector cytokine producing cells from the colitis drive T cell transfer modelled cells into another *Rag2*$^{-/-}$. *In vivo* characterisation and differences between IL-17A$^+$ YFP$^-$, IL17A$^+$ YFP$^+$, IFNγ$^+$ YFP$^-$ and IFNγ$^+$ YFP$^+$ CD4$^+$ T cells could be established by transferring them into another *Rag2*$^{-/-}$ mouse. These populations were quite small and therefore after the sort only 1.5 x 10^4 of each population were able to be transferred to separate *Rag2*$^{-/-}$ mice. Figure 38 shows that the transferred CD4$^+$ T cells could be identified in all six recipient mice. Similarly, to the previous T cell transfer experiment, clinical data was recorded, and intracellular cytokine responses were measured using flow cytometry as before. Organ cultures using 3mm biopsy punches and unfractionated cell cultures for 24 hours were set up and ELISAs were performed, using the same concentration of cells (1 x 10^6/ml) for each condition, to measure the cytokine production in the supernatant of these cultures too.

38A

Clinical data showing weight loss and organ weights 9 weeks post transfer

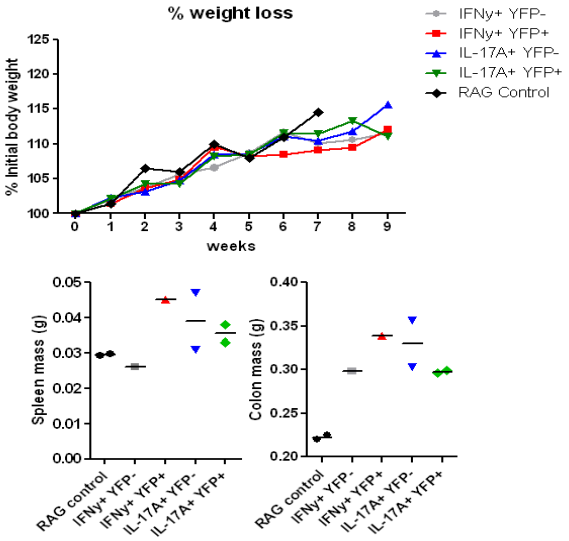

38B

Gating strategy used after stimulation of CD4$^+$ T cells

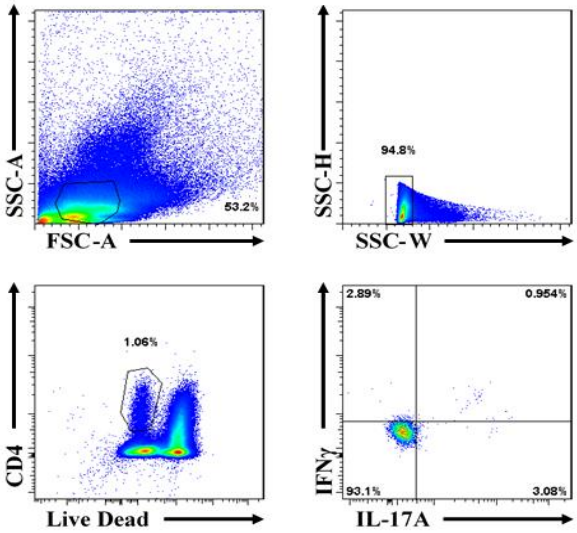

38C

Flow plots showing the percentage of live CD4$^+$ T cells in the spleen and colon

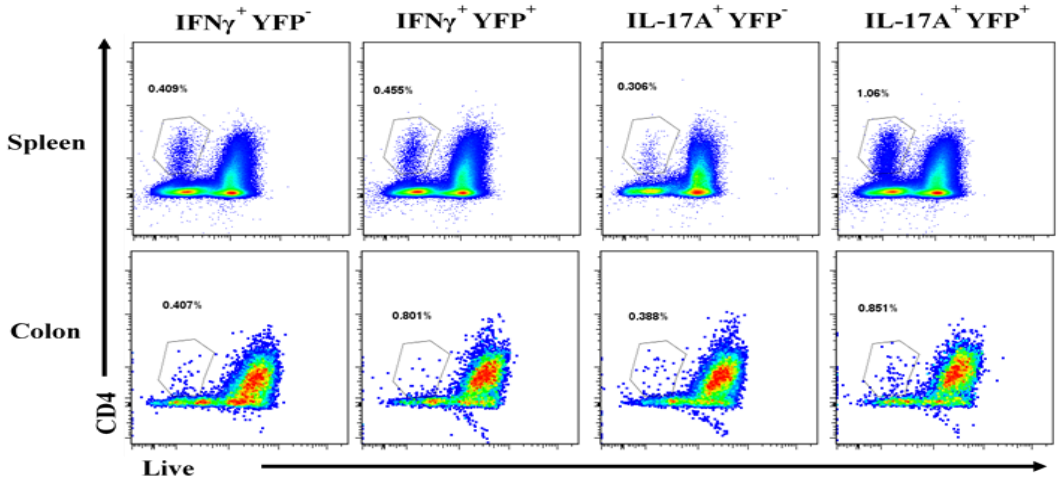

38D

Flow plots showing the percentage of IFNγ and IL-17A production from the spleen and colon

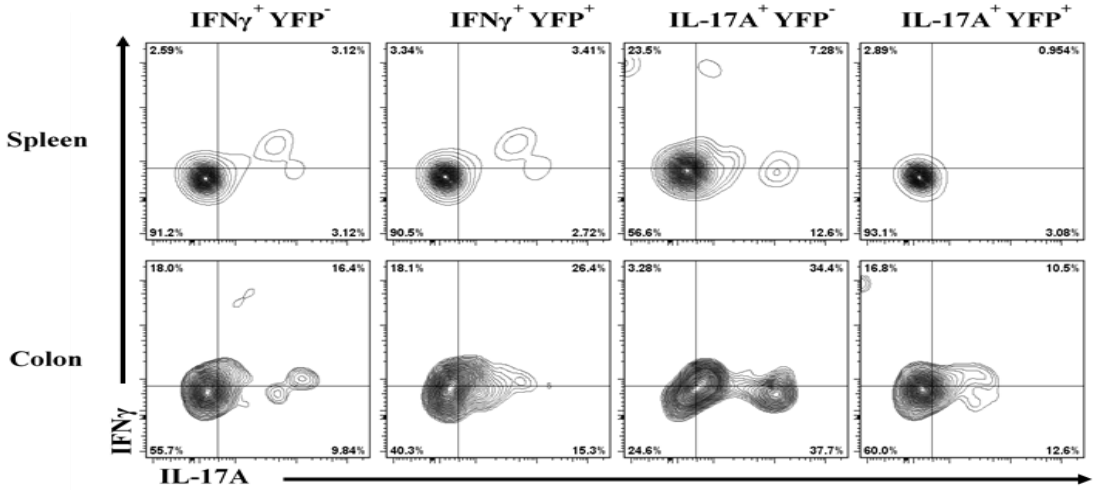

38E **ELISA data showing cytokine production from unfractionated cell cultures from the spleen, mLN and colon**

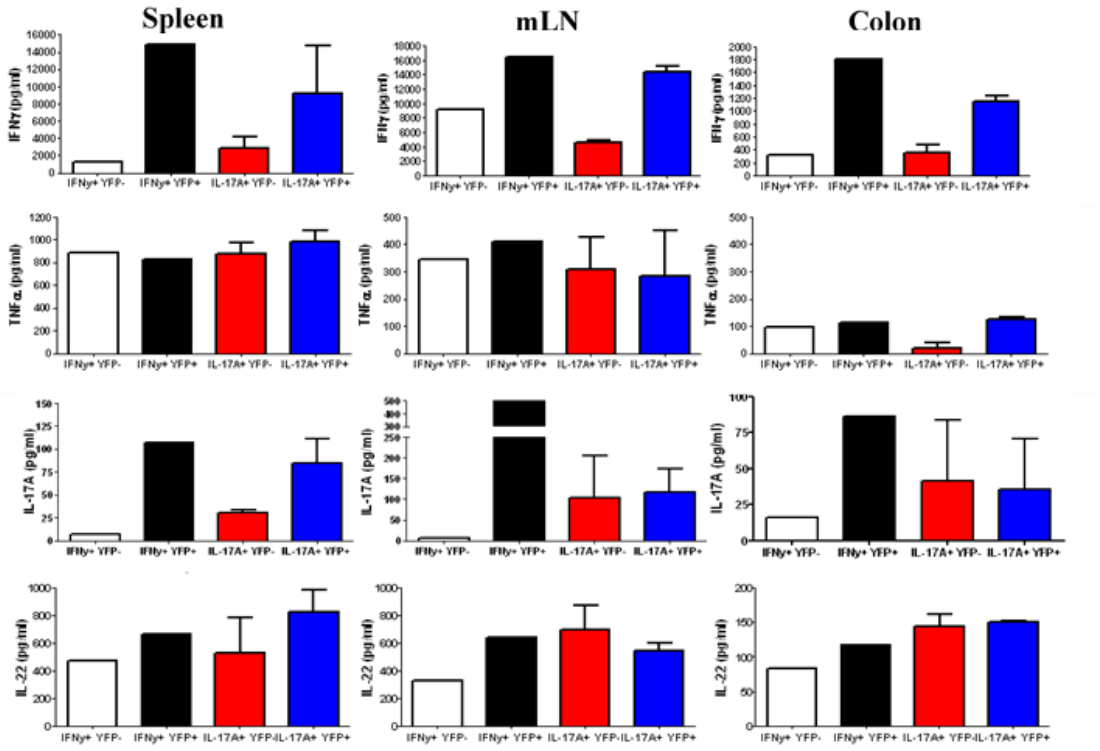

38F **ELISA data showing cytokine production from organ cultures**

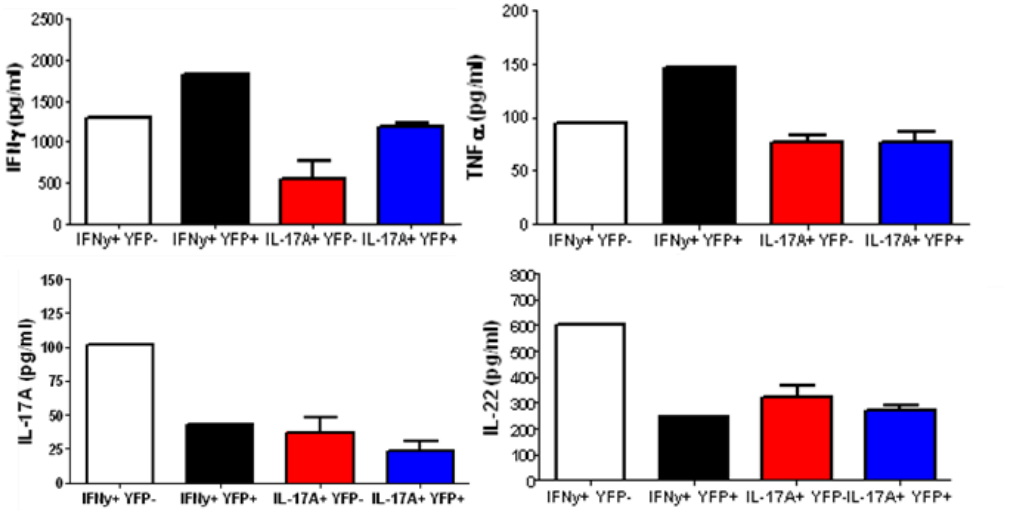

Figure 38: IL-17A$^+$ IFNγ$^-$ YFP$^+$ CD4$^+$ T cells produce more IFNγ and less IL-17A upon retransfer into *Rag2*$^{-/-}$ mice.

A. Weight changes over 9 weeks and spleen and colon weight at the end of the 9 weeks B. Gating strategy used to identify the CD4$^+$ T cells that had been transferred. C. Flow plots from the spleen and colon of post-transferred *Rag2*$^{-/-}$ mice identifying the CD4$^+$ T cell population in each organ D. Representative flow plots showing IL-17A and IFNγ production from the colon and spleen of recipient *Rag2*$^{-/-}$ mice. E. ELISA data for IL-17A, IFNγ, TNFα and IL-22 from the supernatant of unfractionated cell cultures from the spleen, mLN and colon. F. ELISA data for IL-17A, IFNγ, TNFα and IL-22 cytokine production from the supernatant of colonic organ culture. (n=1 for IFNγ$^+$ YFP$^-$ and IFN γ$^+$ YFP$^+$ and n = 2 for IL-17A$^+$ YFP$^-$, IL-17A$^+$ YFP$^+$ and *Rag2*$^{-/-}$ controls)

Firstly, to note that these results all need repeating due to the very low sample size, but they provided a tiny insight into the possible effects of the plasticity of T-bet YFP$^+$ IL-17A cells and their potential to switch to an IFNγ phenotype. Clinical data from the cytokine secretion sorted specific T cell transfer showed a possible trend for the IFNγ$^+$ YFP$^+$ recipient mice, which appeared to not gain as much weight, and the IL-17A$^+$ YFP$^+$ recipient mice had looked like they were starting to lose weight in comparison to the untreated *Rag2*$^{-/-}$ control mice. Surprisingly, given that such a small starting number of cells were transferred, the IFNγ$^+$ YFP$^+$, IL-17A$^+$ YFP$^-$ and IL-17A$^+$ YFP$^+$ recipient mice showed a potential trend to have larger spleens and colons compared to the *Rag2*$^{-/-}$ control mice; despite not showing wasting disease (Figure 38A). Figures 38B and 38C show the gating strategy and the CD4$^+$ live gate for the cells of the individual recipient mice. This was important to show because the starting number of CD4$^+$ T cells that were transferred was low, therefore it was vital to ensure that these CD4$^+$ T cells could be identified within the spleen and colon to illustrate that they not only survived but also were able to migrate to sites of inflammation. The intracellular cytokine response shows a trend that the IFNγ$^+$ YFP$^+$ recipient mouse produced more IFNγ in the colon compared to the IFNγ$^+$ YFP$^-$ transferred mouse (Figure 38D). The comparison in both spleen and colon between the IL-17A$^+$ YFP$^-$ and IL-17A$^+$ YFP$^+$ recipient mice showed that the IL-17A$^+$ YFP$^-$ cells had a trend to producing larger amounts of IL-17A and little IFNγ and the IL-17A$^+$ YFP$^+$ cells, in contrast, produced less IL-17A and switched to producing more IFNγ. The ELISA data, in Figure 38E and 38F, from both unfractionated cell cultures and colon organ culture further helped to confirm this trend in cytokine switch from IL-17A to IFNγ in both YFP$^+$ IFNγ and YFP$^+$ IL-17A$^+$ recipient mice and with further increased sample sizes could even become a statistically significant difference. The lack of wasting disease may have been due to the small number of cells transferred to the new *Rag2*$^{-/-}$ mice, similar to how little disease phenotype was observed in the 25,000 T cells transferred with the naïve YFP$^+$ CD4$^+$ T cells. More repeats of this transfer would be needed to test this and also transfers of more cell numbers would be ideal, since as seen in Figure 32 with the increased numbers of naïve YFP$^+$ CD4$^+$ transferred between 25,000 to 100,000 had clinical and phenotypic differences in inducing disease.

5.1.4 Summary of the plasticity of YFP$^+$ T$_H$17 cells

Previous studies within this group have shown that the suppression of T$_H$17 cell differentiation by T-bet occurred after the differentiation of naïve CD4$^+$ T cells (Gökmen et al., 2013).

However, now with the use of the T-bet lineage traceable mice and the T cell transfer model, an insight into the presence of differentiated effector IL-17A producing $CD4^+$ T cells that are YFP^+ and $ROR\gamma t^+$ but $T\text{-}bet^-$. The data shown in this thesis showed that there is a possibility of a pathogenic IL-17A-producing effector T_H17 cells that have previously expressed T-bet, demonstrating the plasticity of T_H17 cells. Cytokine secretion sorts of these cells further showed a potential trend that in both *in vivo* and *in vitro* experiments, the IL-17A YFP^+ $CD4^+$ T cells had the potential to switch into an IFNγ producing phenotype and downregulate IL-17A production in comparison to the IL-17A YFP^- $CD4^+$ T cells. This suggested that initial fate mapped expression of T-bet drives this plasticity in T_H17 cells to become T_H1-like. A possible observation was that the transferred IL-17A YFP^+ T cell did not cause more pathological disease than the other subtypes of cytokine producing $CD4^+$ T cells, although more repeats of this will be needed to prove this. However, the transfer of all sorted cytokine producing effector T cells by the cytokine secretion assay needs repeating to get more reliable and statistically significant results.

5.2 Using the inducible deletion model of T-bet in fully developed $CD4^+$ T cell populations to test for plasticity under healthy conditions

The $T\text{-}bet^{cre}$ x $ROSA26^{fl/fl}$ mouse line is a useful tool to investigate the plasticity of $CD4^+$ T cells in relation to their lineage of T-bet expression. However, the ability to conditionally delete T-bet in a mouse at any given time and space is potentially even more useful to show the plasticity of $CD4^+$ T cells. This has allowed experiments to test the plasticity of both $CD4^+$ T cells and innate lymphoid cells after the cells have developed within the mouse and control deletion of T-bet before inducing disease within these $CreER^{T2}$ x $T\text{-}bet^{fl/fl}$ tamoxifen inducible deletion mouse model. $T\text{-}bet^{fl/fl}$ mice were previously generated by our group and crossed with ER^{T2} mice to generate either $Cre\text{-}ER^{T2+/-}$ (Het) or $Cre\text{-}ER^{T2-/-}$ (WT) mice expressing $T\text{-}bet^{fl/fl}$ (Hom). *In vivo* depletion of T-bet was induced by consecutive intraperitoneal injections of tamoxifen on five consecutive days with one injection per day. Unless stated otherwise, tissues were harvested three weeks after the first injection of tamoxifen.

5.2.1 *In vitro* tamoxifen induced deletion of T-bet in cultures of CD4$^+$ cells from CreER^{T2}-Tbet$^{fl/fl}$ mice

For *in vitro* experiments, tamoxifen was given directly into cell culture media. Initial experiments were performed to test the length of time and dose response required to induce some T-bet deletion or reduction in CD4$^+$ T cells. Bulk CD4$^+$ T cells were sorted from the spleen of CreER^{T2}-Tbet$^{fl/fl}$ mice and cultured at 1 x 10^6/ml on CD3/CD28 with IL-2. The cells were also treated with *in vitro* tamoxifen for either 0, 4, 6, 12 or 24 hours and at concentrations of either 0, 0.25, 0.5, 1 or 2µM. Litter mate CreER^{T2}-Tbet$^{fl/fl}$ mice, which were WT for the CreER^{T2} line, were used as controls.

39A Flow plot and histograms showing T-bet expression between *in vitro* cultured cells from WT/Hom and Het/Hom CreER^{T2}-Tbet$^{fl/fl}$ mice treated with tamoxifen at different time points and concentrations

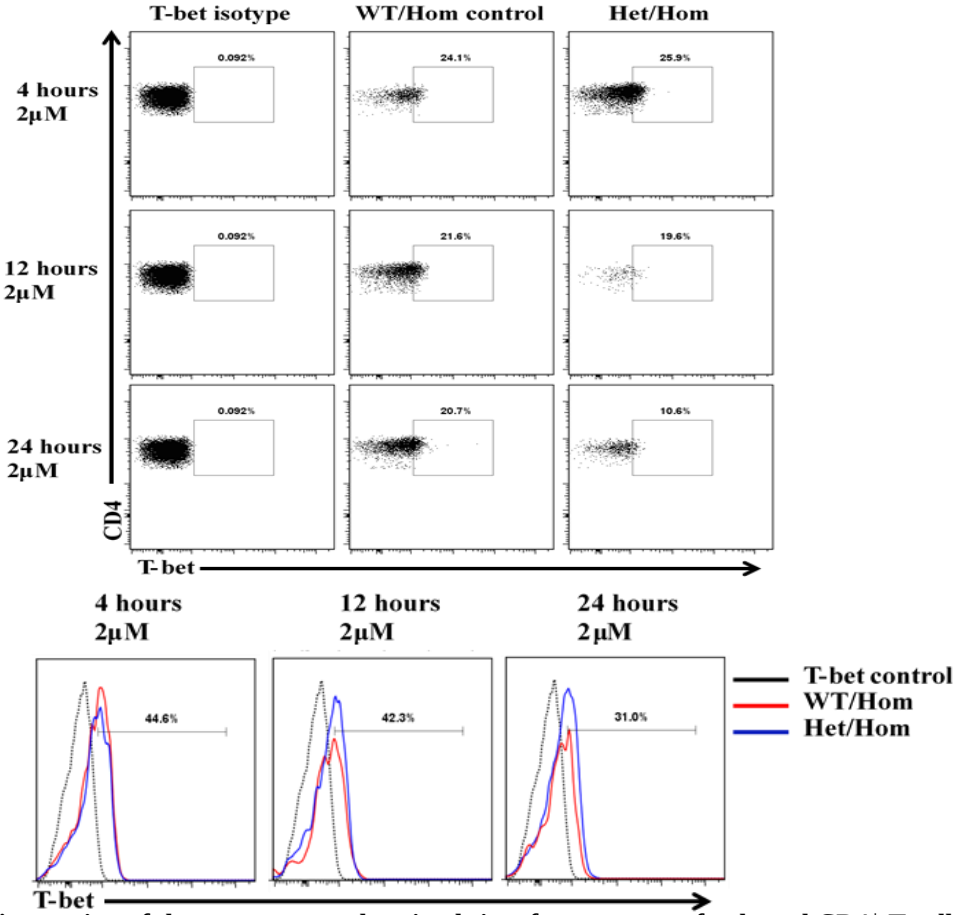

Figure 39: *In vitro* testing of dose response and optimal time for exposure of cultured CD4$^+$ T cells from CreER^{T2}-Tbet$^{fl/fl}$ with tamoxifen.

A. Representative flow plot and histograms showing the expression of T-bet in live CD3$^+$ CD4$^+$ T cells from WT/Hom and Het/Hom of CreER^{T2}-Tbet$^{fl/fl}$ after giving 2µM for either 4 hours, 12 hours or 24 hours. (n = 3)

Despite using different concentrations of tamoxifen, the only concentrations that showed any effect of T-bet expression in $CD4^+$ T cells was the 2µM dose. This experiment also established that the cells required at least 24 hours to achieve a considerable T-bet deletion/reduction in expression in $CD4^+$ T cells. At 24 hours exposure at 2µM, there is almost a 50% reduction in the percentage of cells expressing T-bet. The histogram showed the T-bet level was reduced by 10% (from around 40% to 30% comparing WT/Hom with Het/Hom). Interestingly, giving tamoxifen for the times and concentrations shown was not able to completely reduce T-bet expression in bulk cultured $CD4^+$ T cells *in vitro*. This observation potentially showed that in this $CreER^{T2}$-$Tbet^{fl/fl}$ model, tamoxifen Cre induced T-bet deletion does not completely reduce T-bet expression in fully developed $CD4^+$ T cells. From work within the lab investigating this same model in ILCs, the *in vitro* culture of sorted ILC1s from the colon of these mice showed marked reduction (over 50%) in T-bet. Consequently, this shows that the *in vitro* experiments with tamoxifen were able to reduce T-bet in these mice, but not in $CD4^+$ T cells.

5.2.2 *In vitro* skewing experiments in $CD4^+$ T cells after tamoxifen-induced T-bet deletion

In vitro experiments investigating specific T cell skewing protocols after treatment with tamoxifen were performed. The aim was to examine the effect of T-bet deletion $CD62L^+$ $CD44^-$ naïve $CD4^+$ T cell differentiation. Treatment with tamoxifen did not reduce the amount of T-bet expression in $CD4^+$ T cells in the presence of IL-2 only. For these skewing experiments, cells were treated with 1µM tamoxifen for the last five days, after the initial two days of activation on CD3/CD28. Standard skewing cytokine conditions were used as listed previously. Naïve $CD62L^+$ $CD44^-$ $CD4^+$ T cells were sorted from $CreER^{T2}$-$Tbet^{fl/fl}$ mice using the same sorting strategy as described previously.

40A **Flow plot and MFI showing cytokine production between *in vitro* skewed cells from WT/Hom and Het/Hom CreER^{T2}-Tbet$^{fl/fl}$ mice**

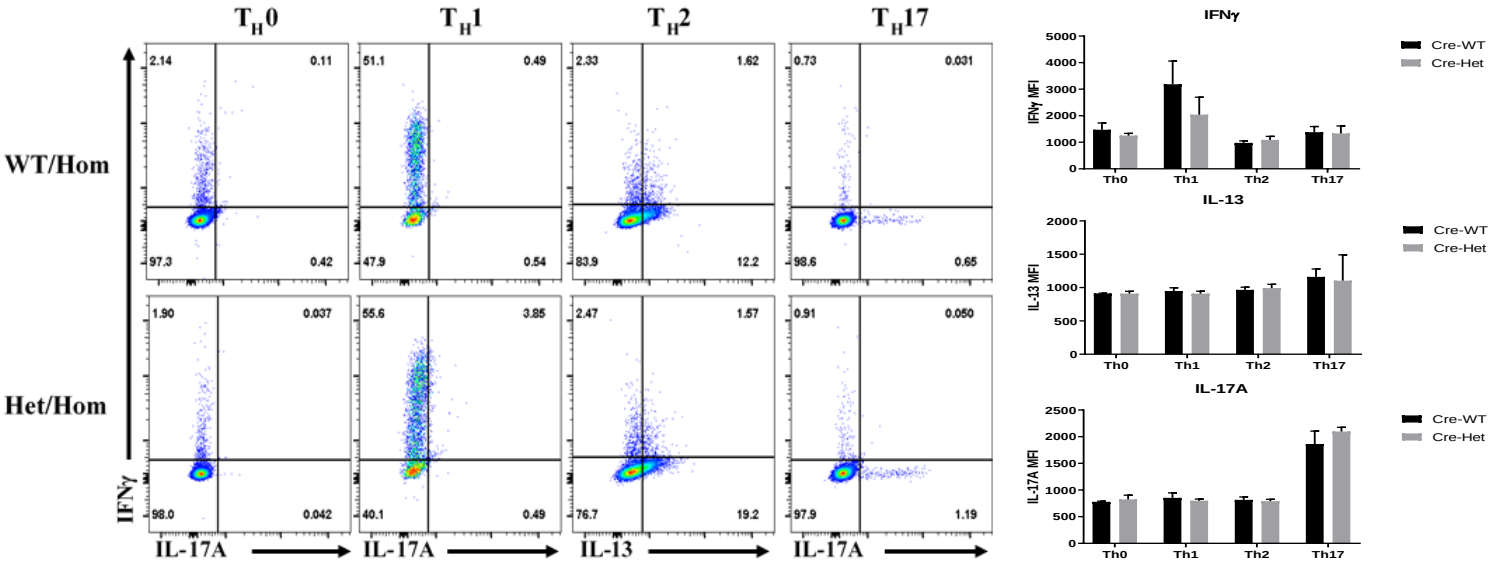

40B **Histograms and MFI showing transcription factor expression between *in vitro* skewed cells from WT/Hom and Het/Hom CreER^{T2}-Tbet$^{fl/fl}$ mice**

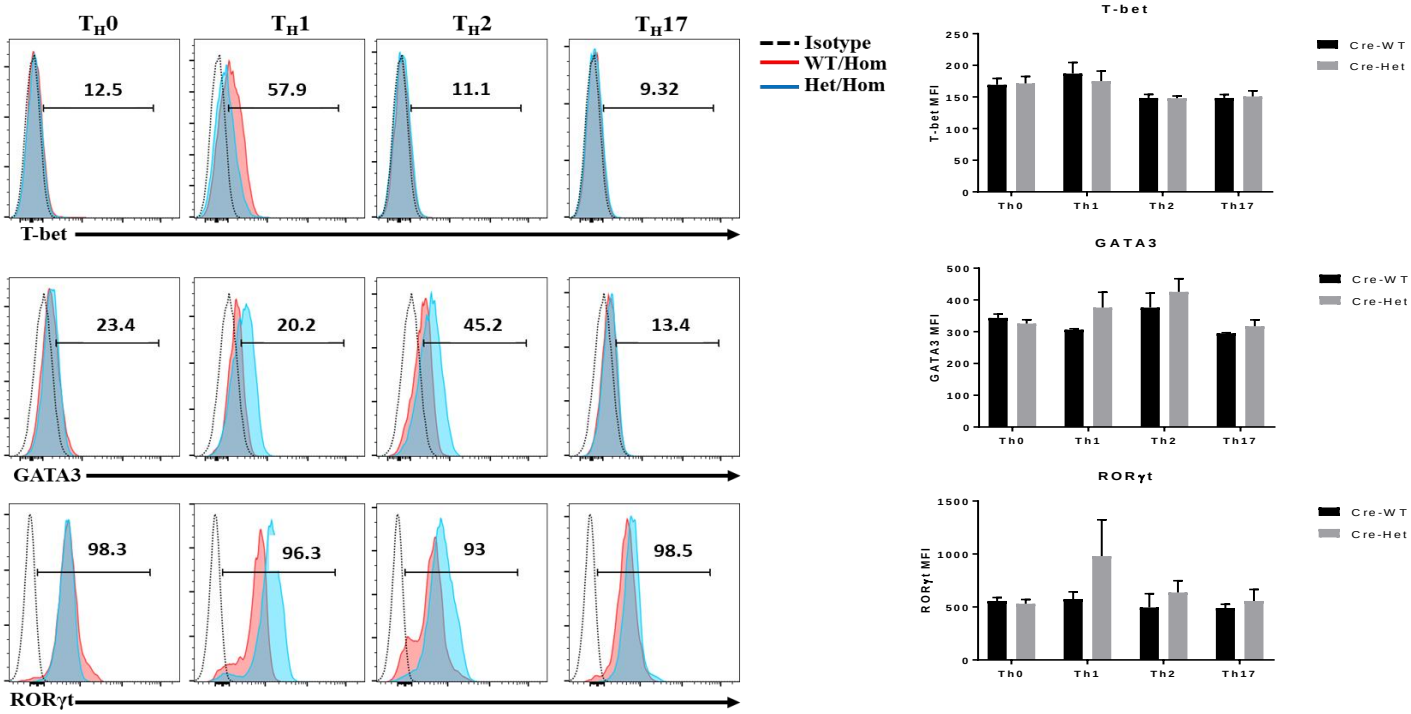

Figure 40: *In vitro* testing of naïve CD4$^+$ T cell skewing after tamoxifen induced deletion of T-bet in CD4$^+$ T cells from CreER^{T2}-Tbet$^{fl/fl}$ mice.

A. Representative flow plots and MFIs showing cytokine production (gated from unstimulated cells) from skewed CD4$^+$ T cells from WT/Hom and Het/Hom CreER^{T2}-Tbet$^{fl/fl}$ mice treated with tamoxifen. B. Representative histograms showing transcription factor expression from skewed CD4$^+$ T cells from WT/Hom and Het/Hom CreER^{T2}-Tbet$^{fl/fl}$ mice treated with tamoxifen. (cells plated in triplicate). Kruskal-Wallis test performed for all groups and with Dunn's corrections for individual comparisons.

In vitro tamoxifen treatment of $CD4^+$ T cells in different differentiation skewing conditions showed some possibly interesting results. The transcription factor expression histograms potentially showed a trend that giving tamoxifen for five days after activation with CD3/CD28 reduced T-bet expression in T_H1 cells (Figure 40B) from Het/Hom (blue) vs WT/Het control (red), although the MFI from these did not show a significant reduction in T-bet expression between the Het/Hom vs WT/Het control. Remarkably, GATA3 and RORγt expression showed a trend to being increased in T-bet-deleted cells in the Het/Hom T_H1, T_H2 and T_H17 skewed cells from the histogram plots, although again the increase in MFI for both GATA3 and RORγt expression was not statistically significant. The cytokine response data, in Figure 35A, showed that despite the reduction in T-bet in the T_H1 skewed cells there was no significant reduction in the percentage or MFI of IFNγ from Het/Hom treated with tamoxifen. Furthermore, there were only minor and, again, not significant increases in IL-13 and IL-17A production in T_H2 and T_H17 cells respectively, despite the relative increased expression of their respective transcription factors. Results from this skewing experiment showed a non-significant trend that despite the reduction in T-bet, the cytokine production was not vastly increased. However, it did demonstrate that the *in vitro* model of tamoxifen was able to slightly reduce T-bet expression in T_H1 cells.

5.2.3 *In vivo* tamoxifen induced deletion of T-bet in $CD4^+$ cell of $CreER^{T2}$-$Tbet^{fl/fl}$ mice

In vivo experiments were performed at healthy state to observe the effect that administering tamoxifen would have on $CD4^+$ T cell population in $CreER^{T2}$-$Tbet^{fl/fl}$ mice. As described before, intraperitoneal injections were administered to the mice daily for five days.

41A

Gating strategy used for *in vivo* tamoxifen treatment of CreER^{T2}-Tbet$^{fl/fl}$ mice

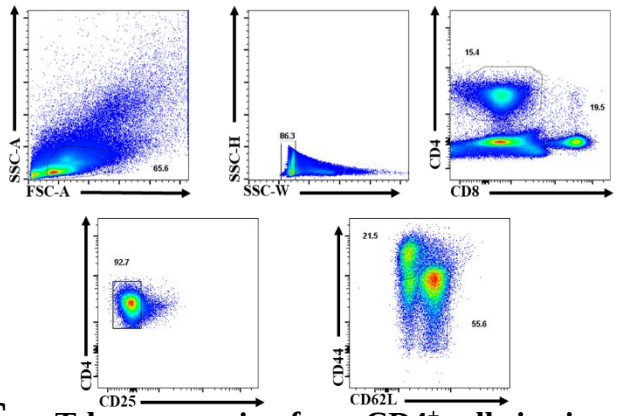

41B

Percentage of CD4$^+$ cells *in vivo* tamoxifen treatment of CreER^{T2}-Tbet$^{fl/fl}$ mice

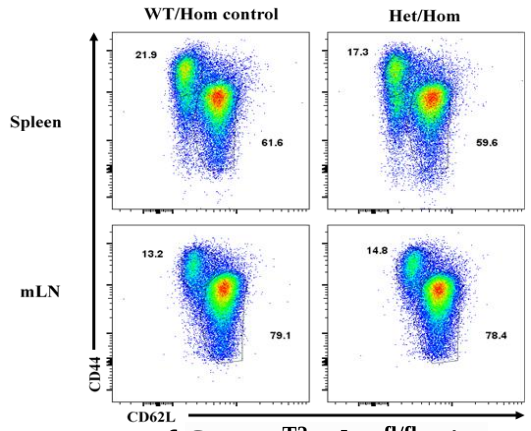

41C **T-bet expression from CD4$^+$ cells *in vivo* tamoxifen treatment of CreER^{T2}-Tbet$^{fl/fl}$ mice**

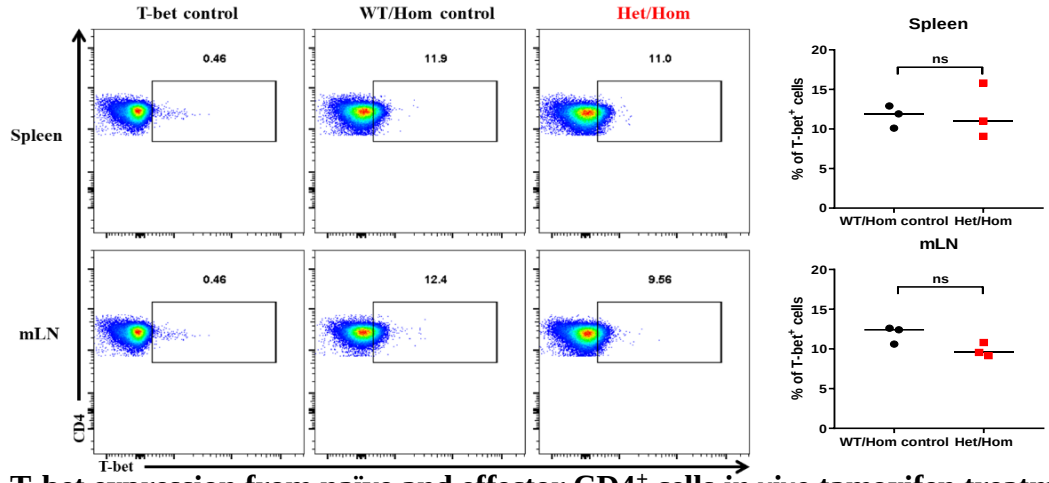

41D **T-bet expression from naïve and effector CD4$^+$ cells *in vivo* tamoxifen treatment of CreER^{T2}-Tbet$^{fl/fl}$ mice**

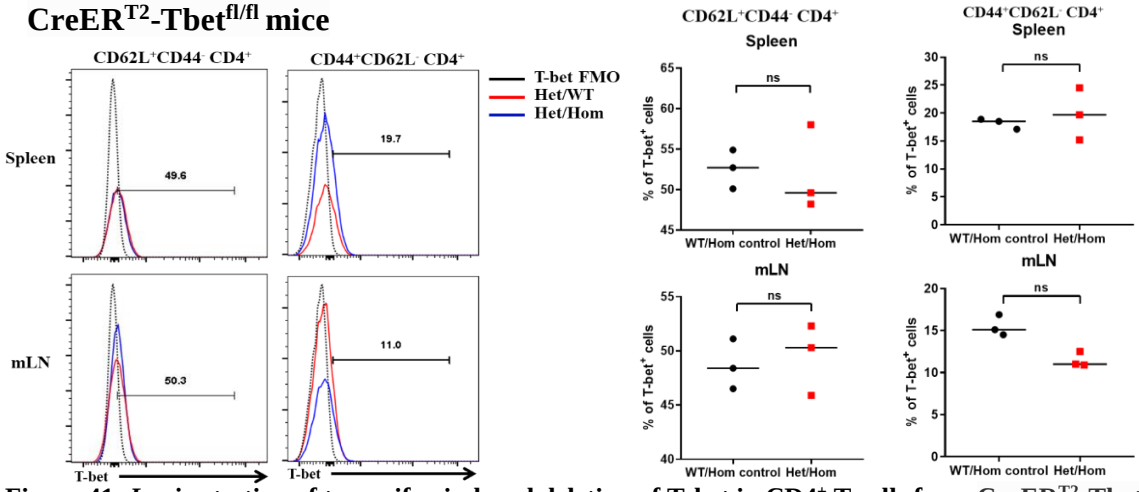

Figure 41: *In vivo* testing of tamoxifen induced deletion of T-bet in CD4$^+$ T cells from CreER^{T2}-Tbet$^{fl/fl}$.

A. Representative gating strategy used for gating of CD4$^+$ T cells in the spleens of CreER^{T2}-Tbet$^{fl/fl}$ mice. B. Representative flow plot showing the percentage of CD4$^+$ in the spleen and mLN from WT/Hom and Het/Hom CreER^{T2}-Tbet$^{fl/fl}$ mice treated with tamoxifen. C. Representative flow plots and dot plot showing T-bet expression in the spleen and mLN from live CD3$^+$ CD4$^+$ CD25$^-$ T cells from WT/Hom and Het/Hom CreER^{T2}-Tbet$^{fl/fl}$ mice treated with tamoxifen D. Representative histograms and dot plots showing T-bet expression in the spleen and mLN from both naïve (CD62L$^+$ CD44$^-$) and effector (CD44$^+$ CD62L$^-$) CD4$^+$ T cells from WT/Hom and Het/Hom CreER^{T2}-Tbet$^{fl/fl}$ mice treated with tamoxifen. (n = 3) Mann Whitney test performed for statistical analysis.

The *in vivo* experiments showing tamoxifen induced deletion of T-bet in healthy CreERT^{2}-Tbet$^{fl/fl}$ mice provided some interesting prospective findings with respect to the CD4^{+} T cell population. Firstly, the percentages and amount of both naïve (CD62L^{+} CD44^{-}) and effector (CD44^{+} CD62L^{-}) CD4^{+} T cells do not reduce at all when given tamoxifen and inducing Cre deletion (Figure 41B). T-bet was expressed within the CD4^{+} CD25^{-} T cell population in the Het/Hom mice and has not been deleted despite the use of tamoxifen (Figures 41C). Whilst there was also no significant change in the percentage of T-bet expressing specific effector and naïve CD4^{+} T cells (Figure 41D). This experiment was performed in collaboration with another project looking at the temporal deletion of T-bet in ILCs. In these same mice, during *in vivo* administered tamoxifen, the ILC1s were completely lost and T-bet reduction occurred in the NK cells. Evidence of the ILC cell loss and T-bet reduction again demonstrated that the results in the CD4^{+} T cells was not due to the tamoxifen administration failing.

Both these experiments were performed under healthy conditions where CD4^{+} T helper cell plasticity is not necessary. Hence, plasticity of CD4^{+} T helper cells would need to be investigated in both T_H2 and T_H17 driven disease models.

5.3 Using the inducible deletion model of T-bet to test for plasticity in pathological environments

5.3.1 Testing the plasticity of T_H2-driven parasite models after inducing T-bet deletion

The aim was to understand the plasticity of CD4^{+} T cells upon deletion of T-bet using models of helminth infection in the CreER^{T2}-Tbet$^{fl/fl}$ mice. As described previously, tamoxifen was administered for five consecutive days via intraperitoneal injections. After two weeks, mice were infected with either *Nippostrongylus brasiliensis* (Nippo) or *Heligmosomoides polygyrus* (H. poly) via oral gavage. Tissues were extracted after either seven days or nine days for Nippo experiments or fourteen days for the H. Poly infections. Results from these experiments are shown in Figures 42 and 43.

42A

Egg and worm count in CreER^{T2}-Tbet$^{fl/fl}$ mice treated with *Nippo*

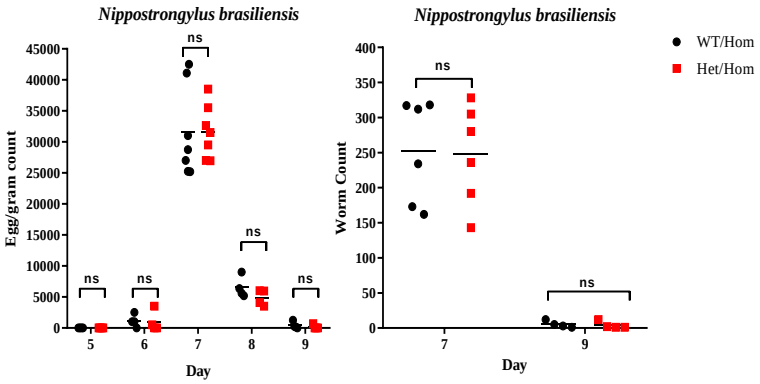

42B

Gating strategy used for CreER^{T2}-Tbet$^{fl/fl}$ mice treated with *Nippo*

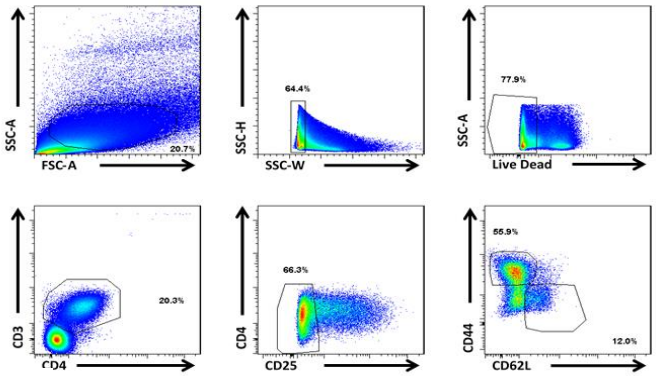

42C

Flow plots showing naïve and effector CD4^{+} in CreER^{T2}-Tbet$^{fl/fl}$ mice treated with *Nippo*

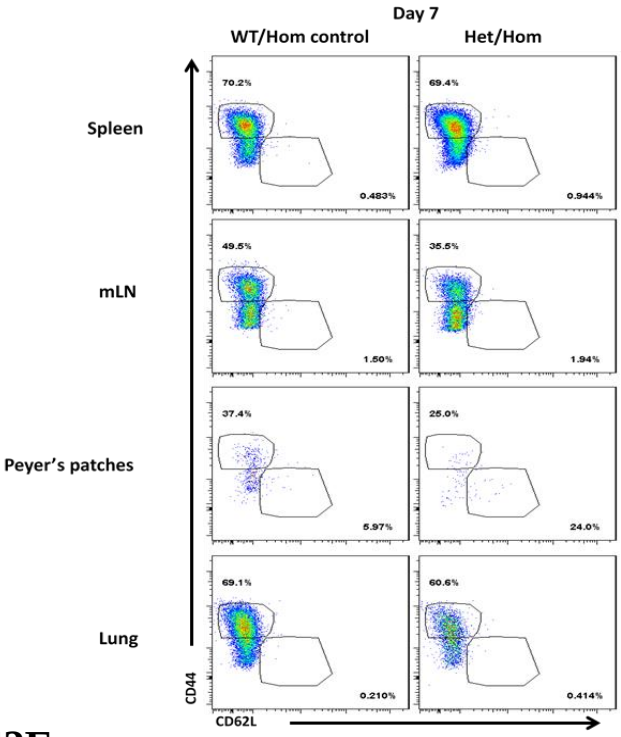

42D

Flow plots showing cytokine production from effector CD4^{+} in CreER^{T2}-Tbet$^{fl/fl}$ mice treated with *Nippo* for 7 days

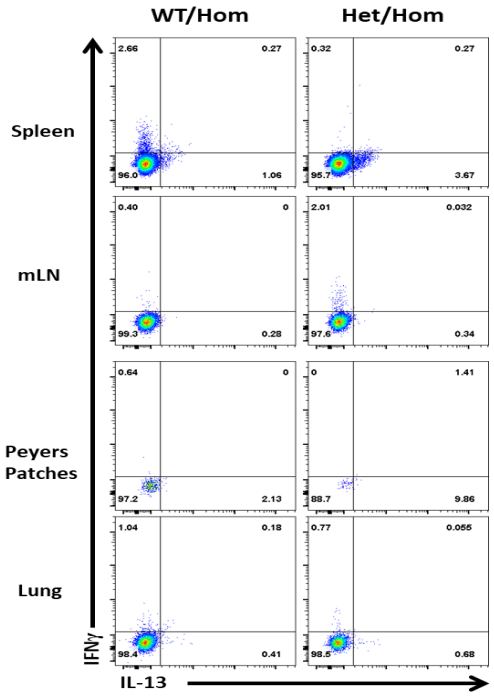

42E

Dot plots showing cytokine production from effector CD4^{+} in CreER^{T2}-Tbet$^{fl/fl}$ mice treated with *Nippo* for 7 days

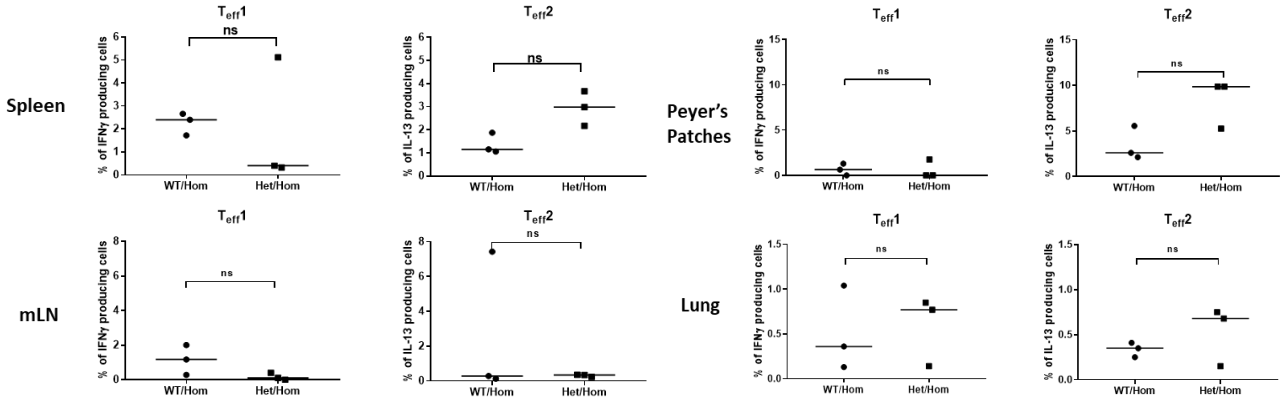

42F **Flow plots and dot plots showing cytokine production from effector CD4$^+$ in CreER^{T2}-Tbet$^{fl/fl}$ mice treated with *Nippo* for 9 days**

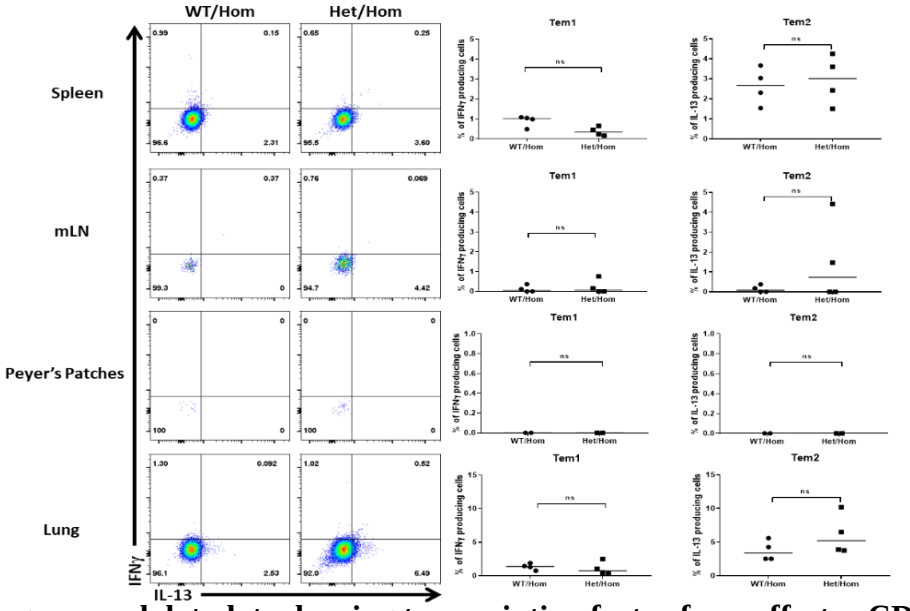

42G **Histogram and dot plots showing transcription factor from effector CD4$^+$ in CreER^{T2}-Tbet$^{fl/fl}$ mice treated with *Nippo* for 9 days**

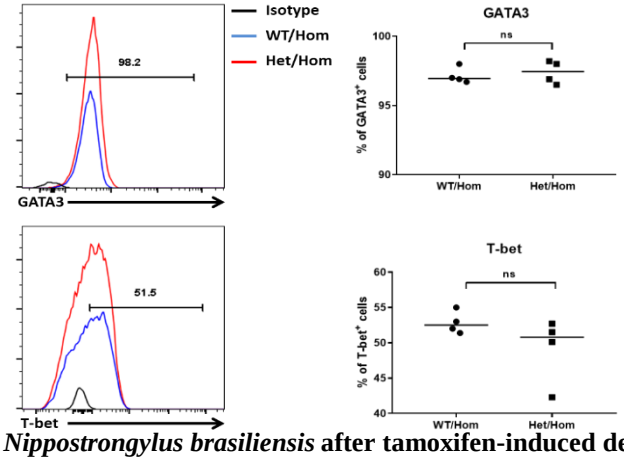

Figure 42: Infection with *Nippostrongylus brasiliensis* after tamoxifen-induced deletion of T-bet in CD4$^+$ T cells from CreER^{T2}-Tbet$^{fl/fl}$ mice.

A. Dot plot showing eggs per gram and worm count in the WT/Hom and Het/Hom CreER^{T2}-Tbet$^{fl/fl}$ mice post infection with Nippo and tamoxifen treatment. B. Representative gating strategy from the spleen of CreER^{T2}-Tbet$^{fl/fl}$ mice. C. Representative flow plots showing CD44 and CD62L expression on live CD3$^+$ CD4$^+$ CD25$^-$ from WT/Hom and Het/Hom CreER^{T2}-Tbet$^{fl/fl}$ mice after tamoxifen treatment and 7 days of Nippo infection. D. Representative flow plots showing IFNγ and IL-13 production (gated from unstimulated controls) from CD44$^+$ CD62L$^-$ effector CD4$^+$ T cells in WT/Hom and Het/Hom CreER^{T2}-Tbet$^{fl/fl}$ mice after tamoxifen treatment and 7 days of Nippo infection. E. Dot plots showing IFNγ and IL-13 production (gated from unstimulated controls) from CD44$^+$ CD62L$^-$ effector CD4$^+$ T cells in WT/Hom and Het/Hom CreER^{T2}-Tbet$^{fl/fl}$ mice after tamoxifen treatment and 7 days of Nippo infection. F. Representative flow plots and dot plot showing IFNγ and IL-13 production (gated from unstimulated controls) from CD44$^+$ CD62L$^-$ effector CD4$^+$ T cells in WT/Hom and Het/Hom CreER^{T2}-Tbet$^{fl/fl}$ mice after tamoxifen treatment and 9 days of Nippo infection. G. Representative histograms and dot plots showing T-bet and GATA3 expression (gated off isotype controls in black) from the lungs of CD44$^+$ CD62L$^-$ effector CD4$^+$ T cells in WT/Hom and Het/Hom CreER^{T2}-Tbet$^{fl/fl}$ mice after tamoxifen treatment and 9 days of Nippo infection. (n = 4 for day 9 and n = 7 for day 7 infections). Mann Whitney test performed for statistical analysis.

The Nippo egg and worm count showed no significant differences when tamoxifen was given in either of the groups of mice. Figure 42A did demonstrate, though, that eggs and worms were still present on day 7, but by day 9 were cleared from the mice. Surprisingly, use of the Nippo parasite model caused loss of all naïve ($CD62L^+$ $CD44^-$) $CD4^+$ T cells and only effector cells ($CD44^+$ $CD62L^-$) could be found (Figure 42C). This could possibly be due to tamoxifen usage in the $CreER^{T2}$ being cleaved or being downregulated. However, this has not been reported on. The loss of naïve ($CD62L^+$ $CD44^-$) $CD4^+$ T cells is odd since only one pathogen was given and should only have induced the response from certain naïve T cells that would respond that that. The cytokine response from mice infected on day 7, surprisingly showed no IL-13 production in the lung, mLN and Peyer's patches, despite day 7 showing the largest number of eggs and worms. There was only a slight increase in IL-13 production in the spleen in comparison with the WT/Hom control and Het/Hom, although this was not significant. This could potentially show that when deleting T-bet in this model there is a minimal switch to more of a T_H2-IL-13 response. The tissue from the infected mice at day 9 showed a marked, but not significant, increase in IL-13 production in the lung especially in the tamoxifen treated Het/Hom mice (Figure 42F). Figure 42G, further, shows that effector $CD4^+$ the Het/Hom tamoxifen treated mice, did not have significant reduced levels of T-bet or significantly increased levels of GATA3 expression.

ILC data acquired from these mice by others in the lab again were differentto the $CD4^+$ T cell data. Data from day 7 showed an IL-13 response from ILC2s, although there was no difference in the amount of IL-13 production between the WT/Hom and Het/Hom, whereas data from day 9 showed no IL-13 cytokine response from the ILC2 population in either genotype of mice. Since the innate immune response is quicker than the adaptive immune response, data from within the lab further helped to demonstrate this. Similar to the *in vivo* experiment performed on the healthy $Cre\text{-}ER^{T2}$ $Tbet^{fl/fl}$ mice, there was a reduction in the percentages of ILC1 seen in tissue in the Het/Hom mice, upon administering the tamoxifen.

43A

Egg and worm count in CreER^{T2}-Tbet$^{fl/fl}$ mice treated with *H. Poly*

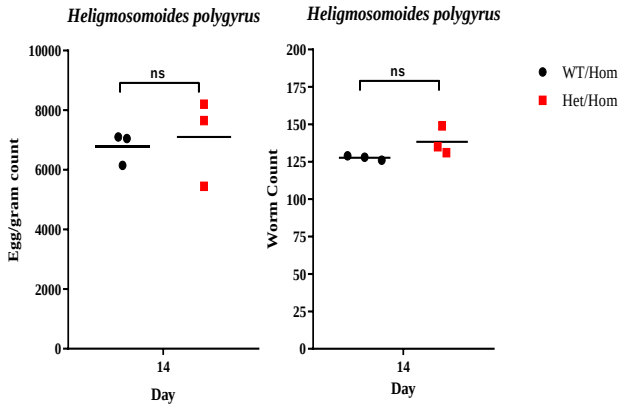

43B

Gating strategy used for CreER^{T2}-Tbet$^{fl/fl}$ mice treated with *H. Poly*

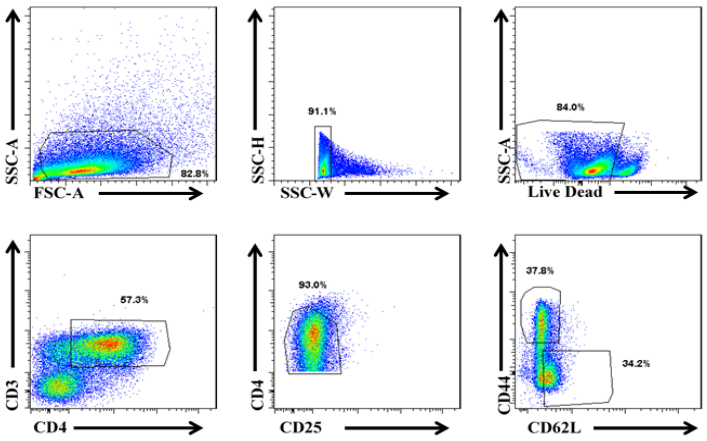

43C

low plots showing naïve and effector CD4^{+} in CreER^{T2}-Tbet$^{fl/fl}$ mice treated with *H. Poly* for 14 days

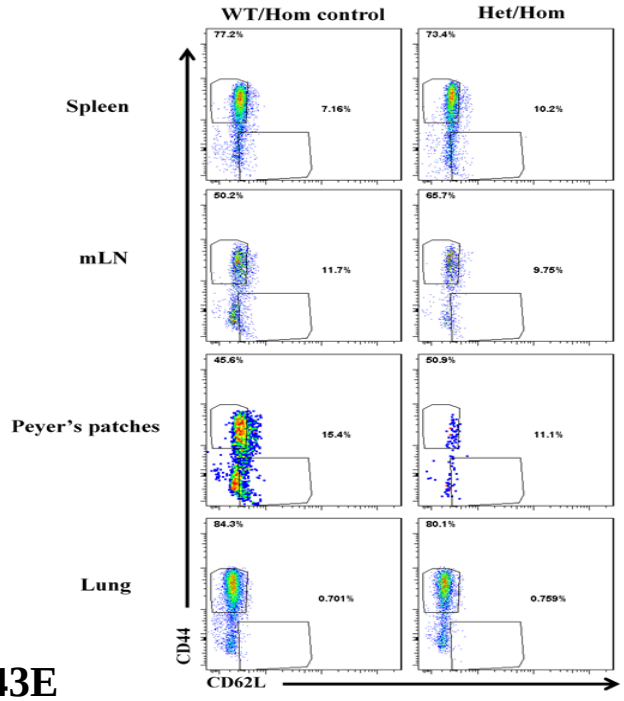

43D

Flow plots showing cytokine production from effector CD4^{+} in CreER^{T2}-Tbet$^{fl/fl}$ mice treated with *H. Poly* for 14 days

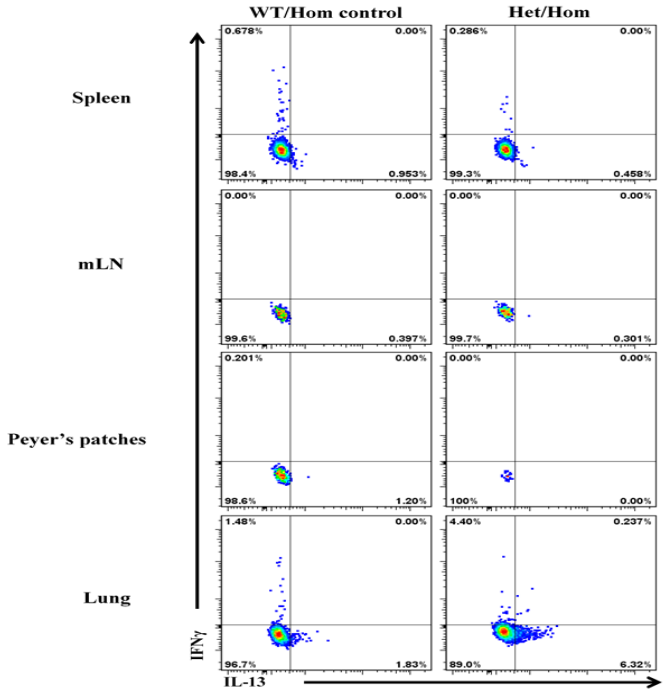

43E

Dot plots showing cytokine production from effector CD4^{+} in CreER^{T2}-Tbet$^{fl/fl}$ mice treated with *H. Poly* for 14 days

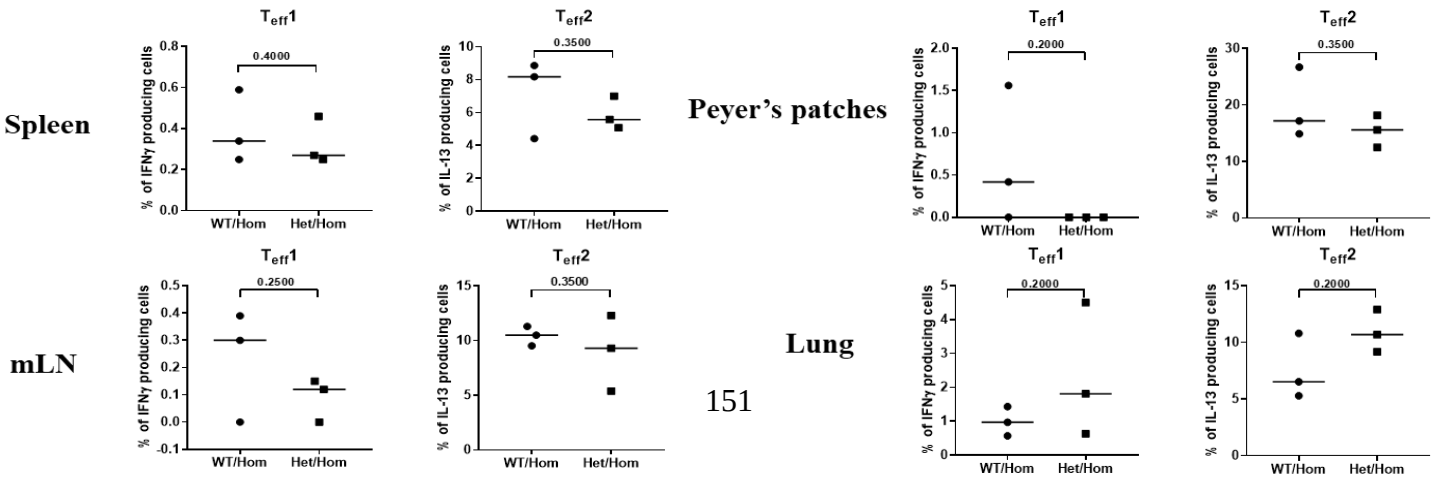

43F **Histogram and dot plots showing transcription factor from effector CD4$^+$ in CreER^{T2}-Tbet$^{fl/fl}$ mice treated with *H. Poly* for 14 days**

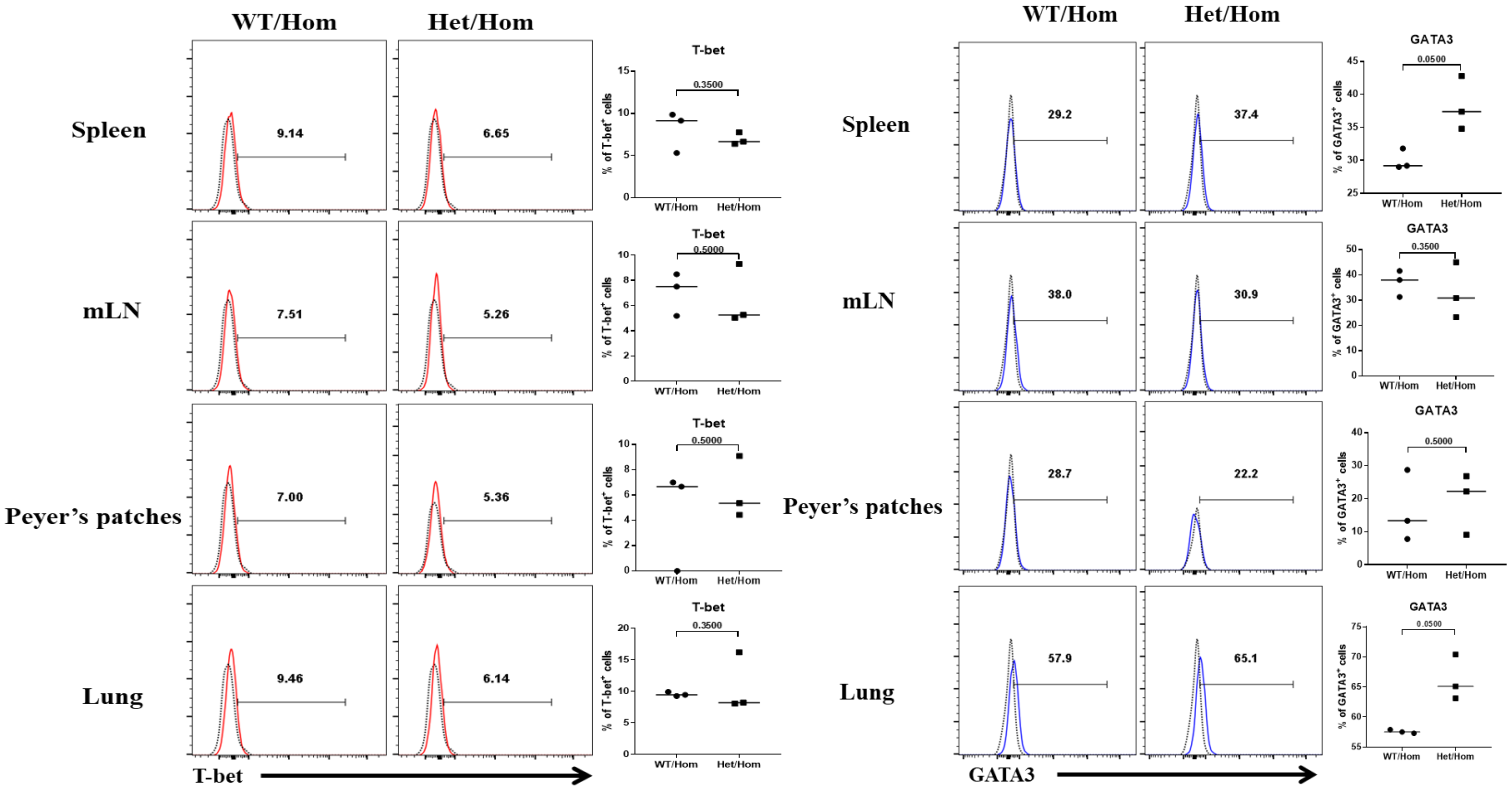

Figure 43: Parasite infection with *Heligmosomoides polygyrus* after tamoxifen induced deletion of T-bet in CD4$^+$ T cells from CreER^{T2}-Tbet$^{fl/fl}$.

A. Dot plot showing egg per gram and worm count in the WT/Hom and Het/Hom CreER^{T2}-Tbet$^{fl/fl}$ mice post infection with H.Poly and tamoxifen treatment. B. Representative gating strategy from the spleen of CreER^{T2}-Tbet$^{fl/fl}$ mice C. Representative flow plots showing CD44 and CD62L expression on live CD3$^+$ CD4$^+$ CD25$^-$ from WT/Hom and Het/Hom CreER^{T2}-Tbet$^{fl/fl}$ mice after tamoxifen treatment and 14 days of H.Poly infection. D. Representative flow plots showing IFNγ and IL-13 production (gated using unstimulated controls) from CD44$^+$ CD62L$^-$ effector CD4$^+$ T cells in WT/Hom and Het/Hom CreER^{T2}-Tbet$^{fl/fl}$ mice after tamoxifen treatment and 14 days of H.Poly infection. E. Dot plots showing IFNγ and IL-13 production from CD44$^+$ CD62L$^-$ effector CD4$^+$ T cells in WT/Hom and Het/Hom CreER^{T2}-Tbet$^{fl/fl}$ mice after tamoxifen treatment and 14 days of H.Poly infection. F. Representative histograms and dot plots showing T-bet and GATA3 expression (gated off isotype controls shown in black) from CD44$^+$ CD62L$^-$ effector CD4$^+$ T cells in WT/Hom and Het/Hom CreER^{T2}-Tbet$^{fl/fl}$ mice after tamoxifen treatment and 14 days of H.Poly infection. (n=3 in both groups). Mann Whitney test performed for statistical analysis.

H. Poly parasite infection experiments in these Cre-ER^{T2} x T-bet$^{fl/fl}$ mice showed very similar results to the Nippo infected mice. Firstly, egg and worm counts were visible, although not as high as in the Nippo infection, and again the results showed no significant difference between the WT/Hom compared with the Het/Hom when both were given tamoxifen prior to infection.

The egg and worm counts were not as high as the Nippo counts, possibly due to the reading being taken at 14 days; at which point H. Poly infections are known to be cleared by around day 10 (Filbey et al., 2014). Similarly to the Nippo infection, upon treatment with H. Poly there were no $CD62L^+$ $CD44^-$ naïve $CD4^+$ T cells to be found and only effector $CD44^+$ $CD62L^-$ $CD4^+$ T cells were found within the $CD4^+$ T cell compartment, which again didn't make sense, whereas in the DSS model in Figure 44, there are naïve $CD4^+$ T cells present still. Figure 43E showed similar results to the Nippo infection experiments, the level of IFNγ and IL-13 production from the tissue was not as great as expected for a pathogen response. However, interestingly there was an increase in the amount of IL-13 production in only the lungs in comparison between the Het/Hom and WT/Hom mice, although this was not significant. These data were consistent with the transcription factor expression data, shown in Figure 43F, when treated with tamoxifen. There was a slight trend in reduction in T-bet expression and only a significant (P=0.05) increase GATA3 expression in the lungs, and a trend in an increase in GATA3 expression in the other tissue, when comparing the Het/Hom mice with the WT/Hom control mice.

Again, comparing $CD4^+$ T cell population response with ILC data from others in the lab, there was a marked reduction in the percentages of ILC1s present in all tissue from the Het/Hom mice treated with tamoxifen, as seen with the other *in vivo* experiments. The ILC2 population in the lungs of the tamoxifen treated Het/Hom mice also produced a vast amount of IL-13.

5.3.2 Summary of plasticity of T_H2-driven parasite models after inducing T-bet deletion

Both the Nippo and H. Poly parasite infection models showed that there was no deletion or reduction of T-bet and only an increase in GATA3 expression in the Het/Hom mice in the H. Poly infection to drive expulsion of the worms and eggs compared with WT/Hom mice. There was a trend, even though not significant, showing an increase in IL-13. This showed that despite the slight reduction of T-bet, this was not enough to drive plasticity of T_H1 cells towards a T_H2 phenotype. This further demonstrates that the amount of plasticity between T_H1 and T_H2 is more fixed than between other types of $CD4^+$ T helper cells, as previously shown by others.

5.3.3 Testing the plasticity of T_H17-driven DSS-induced colitis after inducing T-bet deletion

The aim was to test plasticity of T_H17 cells after the induction of tamoxifen using the DSS colitis model in the Cre-ER^{T2} T-bet$^{fl/fl}$ mice. 3% DSS was given in the drinking water to mice over a period of five days and then given normal water for five days afterwards. Mice were monitored during this time for their weight and analysed after for clinical differences in spleen weight and colon weight and length.

44A **Clinical data showing weight loss and organ weights in for CreER^{T2}-Tbet$^{fl/fl}$ mice treated with 3% DSS**

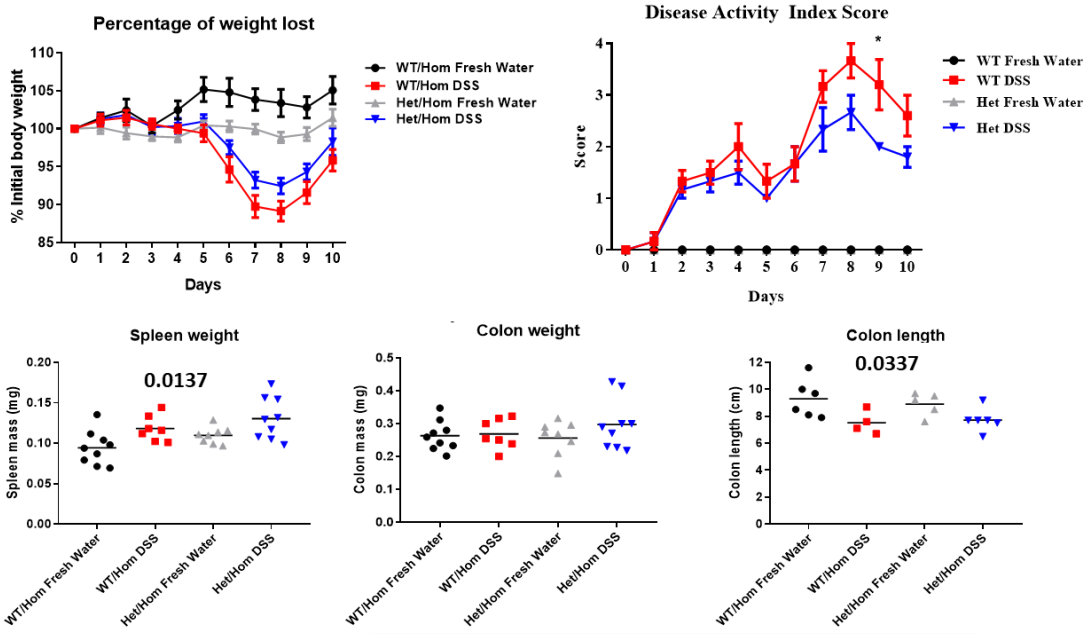

44B **Gating strategy used for CreER^{T2}-Tbet$^{fl/fl}$ mice treated with 3% DSS**

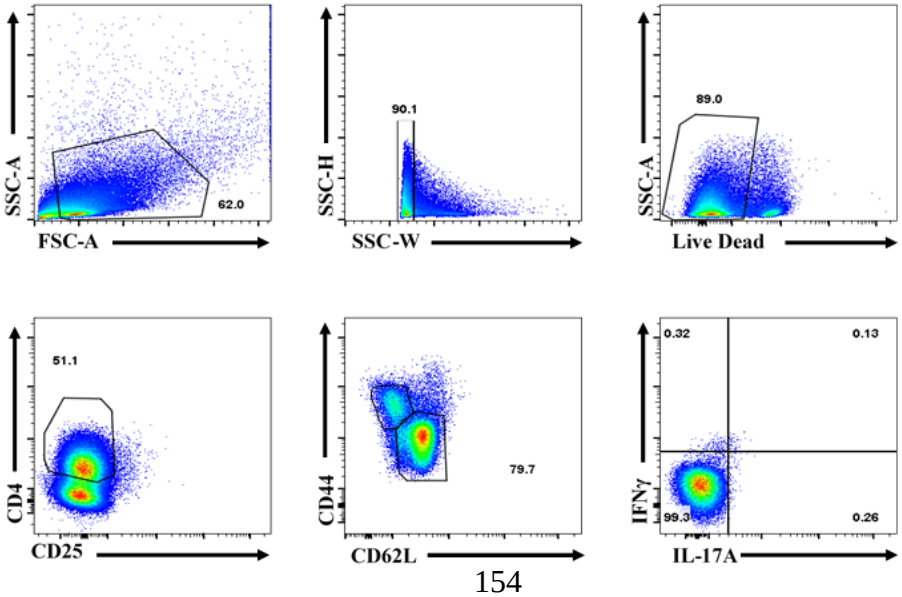

44C **Representative flow plots showing cytokine response in the spleen, colon, mLN and liver from WT/Hom and Het/Hom CreER^{T2} T-bet$^{fl/fl}$ mice given tamoxifen and 3% DSS**

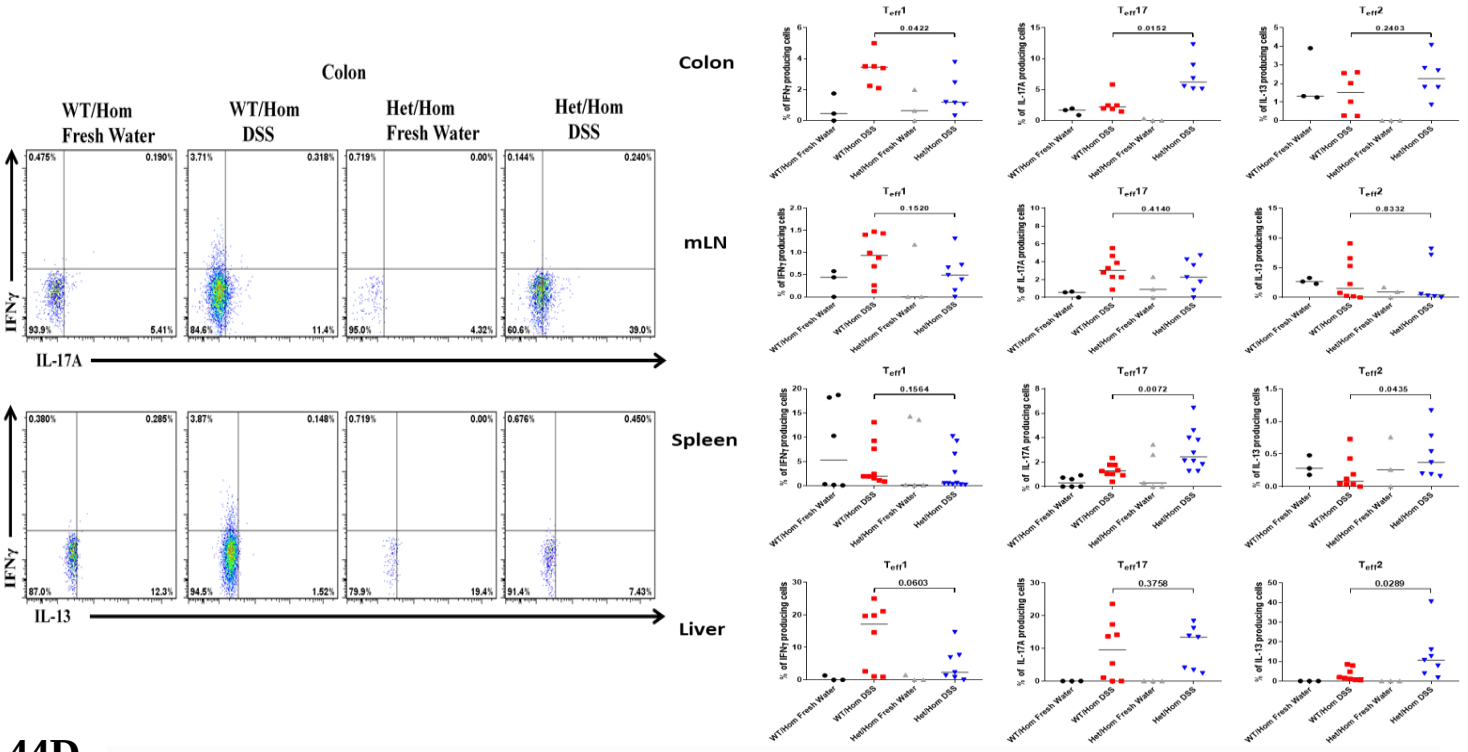

44D **Representative histograms showing transcription factor expression in the spleen and colon from WT/Hom and Het/Hom CreER^{T2} T-bet$^{fl/fl}$ mice given tamoxifen and 3% DSS**

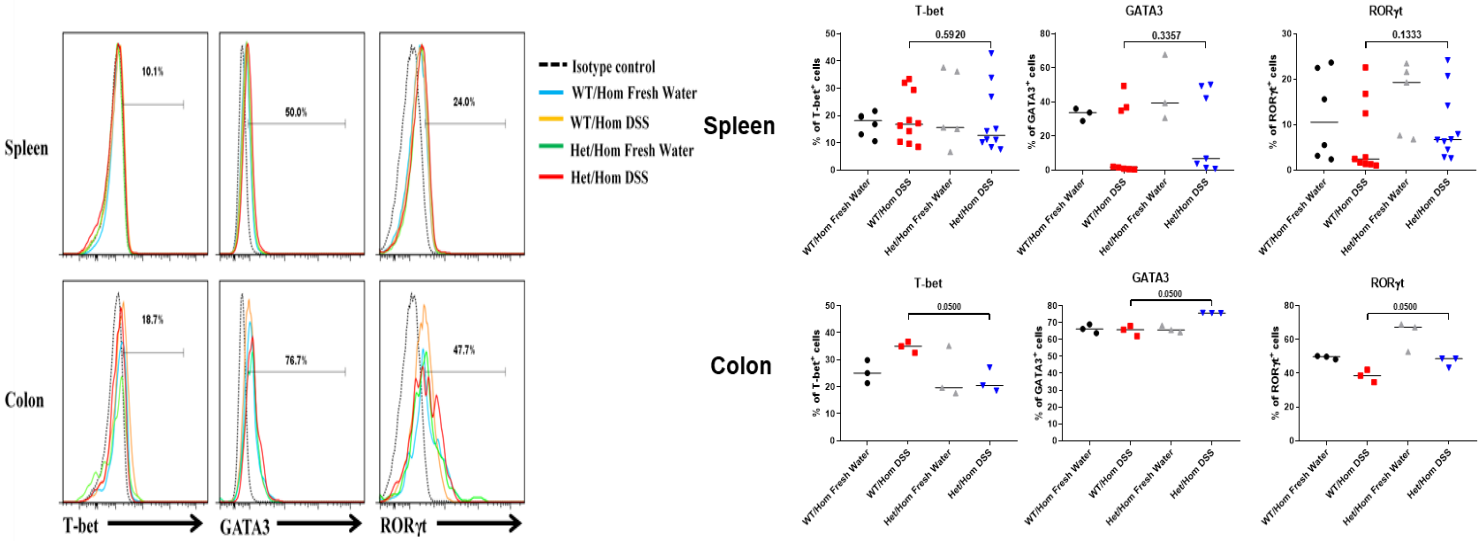

Figure 44: DSS-induced colitis in tamoxifen treated WT/Hom and Het/Hom CreER^{T2} Tbet$^{fl/fl}$ mice.

A. Clinical data showing weight loss, spleen weight, colon weight and colon length in WT/Hom and Het/Hom CreER^{T2} T-bet$^{fl/fl}$ mice given tamoxifen and then either fresh water (FW) or 3% DSS. B. from the spleen of CreER^{T2}-Tbet$^{fl/fl}$ mice. C. Cytokine response showing IFNγ, IL-17A and IL-13 production in the spleen, colon, mLN and liver of CD44^{+} CD62L^{-} effector CD4^{+} T cells from WT/Hom and Het/Hom CreER^{T2} T-bet$^{fl/fl}$ mice given tamoxifen and then either fresh water (FW) or 3% DSS. D. Transcription factor showing T-bet, GATA3 and RORγt production in the spleen and colon, of WT/Hom and Het/Hom CreER^{T2} T-bet$^{fl/fl}$ mice given tamoxifen and then either fresh water (FW) or 3% DSS. (n= 8 for fresh water treated mice and 14 for DSS treated mice). Kruskal-Wallis test performed for all groups and with Dunn's corrections for individual comparisons

DSS-induced colitis in tamoxifen treated WT/Hom and Het/Hom CreER^{T2} T-bet$^{fl/fl}$ mice provided some interesting data. Firstly, the clinical data demonstrated that the WT/Hom mice lost more weight than the Het/Hom mice, although this was not significant, possibly indicating that the reduction in T-bet results in less severe disease. This was also seen by the significantly higher disease activity index score at day 9 between the WT/Hom and Het/Hom mice treated with DSS. However, the spleen weight, colon weight and colon lengths were not significantly different between the WT/Hom and Het/Hom treated with DSS but were significantly different between all 4 groups. In the DSS treated mice, effector CD4$^+$ T cells producing IFNγ, IL-17A or IL-13 was not observed when compared with the fresh water treated healthy mice. However, as expected, there was a significant reduction in IFNγ and an increase in IL-17A in the spleen and colon of the T-bet-deleted Het/Hom mice. This was further confirmed by transcription factor expression data. RORγt exhibited increased expression in the colon, whilst T-bet expression was slightly reduced after treatment of Het/Hom mice with DSS and tamoxifen compared to the WT/Hom mice.

As with the parasite infection experiments, the ILCs were investigated in these mice in parallel with the CD4$^+$ T cells. As was seen in the previous models, the percentage of ILC1s was significantly diminished. The remaining ILC1s that were still present were found to have significantly reduced T-bet expression. Despite this, there was no difference in IFNγ, IL-13, IL-5 and IL-17A production in the ILC population.

5.3.4 Summary of the plasticity of T_H17 driven disease using DSS-induced colitis after inducing T-bet deletion

These experiments using the DSS-induced colitis model did not demonstrate as great a switch from the T_H1-IFNγ CD4$^+$ T cells to T_H17-like IL-17A producing CD4$^+$ T cells as expected. The clinical data showed that the WT/Hom mice lost more weight than the Het/Hom mice, but the other clinical readouts showed equivalent disease phenotypes. This provided further proof that T-bet is necessary to cause disease and the reduction in T-bet does not change the disease phenotype.

5.4 Discussion

Although a lot of the data in this chapter needs repeating due to the low sample size, especially the cytokine capture assay T cell transfers, there is a trend to potentially seeing a role that T-bet may have in controlling the plasticity of $CD4^+$ T helper cells when either historically expressed or temporally deleted. The T-bet fate mapping mouse and induced T-bet deletion model have been shown here to have potential as good models to investigate the role of T-bet in controlling plasticity of $CD4^+$ T cells.

Firstly, the observation of T-bet fate mapped T_H17 cells showed that T-bet plays a role in driving IFNγ production in T_H17 cells. The data shown here potentially showed that T-bet fate mapped cells were also more able to switch to a more T_H1-like phenotype if they had expressed T-bet in the past. However, this experiment needs repeating to confirm this due to the small sample size and difficulties experienced in replicating the experiment. However, when the opposite was not observed in the DSS-induced tamoxifen treated mice, which showed that the deletion of T-bet from these T_H17 RORγt$^+$ IL-17A producing cells did not drive increased IL-17A production. These experiments showed that it was the expression of T-bet that caused the T_H17 cells to become T_H1-like but the reduction in T-bet does not drive a more T_H17-like state. The cytokine secretion T cell transfer data has only been produced once and the findings are therefore still preliminary, and repetition would enhance reliability. However, the data has some implications despite the low sample size. Morrison et al. in 2013 showed that when either 3 x 10^4 IFNγ$^+$, IL-17A$^+$ or IFNγ$^+$ IL-17A$^+$ cells were transferred into *Rag2*$^{-/-}$ mice with *Helicobacter hepatic* induced colitis, after they were sorted using the cytokine secretion assay, the IFNγ$^+$ IL-17A$^+$ producing cells switched and produced predominately IFNγ, whereas the IL-17A$^+$ single positive cells remained IL-17A producing (Morrison et al., 2013). The T-bet$^+$ and RORγt$^+$ T cells preferentially switched into an IFNγ$^+$ T_H1-like phenotype. Sorting of IL-17A$^+$ and IFNγ$^+$ cells showed that IL-17A$^+$ T cells that have previously expressed T-bet were more likely to switch into a T_H1-like phenotype and produce IFNγ (Morrison et al., 2013). This plasticity is accompanied by a much-reduced disease colitis phenotype compared with the Morrison et al. results. The expression of T-bet, even if only the past, allows for T_H17 cells to become more T_H1-like.

Observations made from the *in vitro* and *in vivo* tamoxifen experiments were surprising. The administration of tamoxifen in both *in vitro* and *in vivo* models did not cause deletion or even reduction in the expression of T-bet in $CD4^+$ T cells. Furthermore, unlike in ILC1s where the reduction of T-bet in ILC1s causes them to be lost (data not shown), T-bet is clearly not an essential requirement for the survival of fully developed $CD4^+$ T cells. The parasite infection models showed that the deletion of T-bet also was unable to drive switching to a T_H2-like phenotype, although there were slight increases in expression of GATA3 and T_H2 cytokine production. These experiments further demonstrated T_H2 and T_H1 cells to be stable, as has previously been reported. The DSS-induced colitis models were also unable to show any plasticity between T_H1 and T_H17 cells despite the increase in IL-17A production and RORγt expression in the colon of these mice. These findings are interesting in context with past research with the loss of T-bet, in which full T-bet knockout ($T\text{-}bet^{-/-}$) mice were used. In these experiments, the mice were found to be deficient in T_H1 cells and also developed either T_H2 or T_H17 mediated diseases depending on what disease model the group were researching (Neurath et al., 2002, Bettelli et al., 2004, Finotto et al., 2002) . In these $T\text{-}bet^{-/-}$ mice, they found that they were also more resistant to the development of T_H1 mediated disease. Using the tamoxifen deletion model allowed for normal $CD4^+$ T cell development before then attempting to delete T-bet in these cells and as seen in my data, either the use of tamoxifen is not able to delete T-bet within developed naïve and effector $CD4^+$ T cell compartment or more time points and a higher dose of injections are required. However, since T-bet deletion occurred in the ILC compartment of these mice and when used by Wang et al showed T-bet deletion in T_{FH} cells occurred when used at the same dose and time points as used in my experiments (Wang et al. 2019). Wang et al. interestingly showed some reduction in the population of T_{FH} cells from fully mature $CD4^+$ T cells but the population of cells were not completely lost (Wang et al. 2019). From their results, they also showed the $CD4^+$ $CD44^+$ population still existed when tamoxifen was given, and this was supported by my data too (Wang et al. 2019). The complete loss of $CD4^+$ T cells expressing CD62L, still should not be the case in this mouse line, and yet it is seen in all organ types and in both the WT/Hom control line and Het/Hom, meaning the deletion of T-bet was not to blame. Whereas when using the DSS model, the naïve ($CD62L^+$ $CD44^-$) $CD4^+$ T cells are visible, shown in Figure 44B. Therefore, further analysis needs to be taken to explore this loss in CD62L in the parasite models used here.

Chapter 6

Results: Identifying a role for T-bet in other immune cells

As well as being the master transcription factor for $CD4^+$ T cell differentiation, T-bet is involved in the function of many other immune cells (Szabo et al., 2000). There are other mouse models within the lab which have been used to study the impact T-bet has in these other immune cells at both a steady healthy state and in response to pathogen induction.

T_{reg} cells also express T-bet to promote CXCR3 expression and aid in their migration to sites of inflammation (Tan et al., 2016a). $CXCR3^+$ T_{regs} increased the onset and severity of autoimmune diabetes in T-$bet^{-/-}$ mice. Use of a $Foxp3^{cre}$ $Tbet^{fl/fl}$ mouse line allowed specific deletion of T-bet in Foxp3 expressing cells only, i.e. the T_{reg} population. This makes this mouse line more suitable than a global T-bet knockout mice (Levine et al., 2017, Pandiyan and Zhu, 2015). Also, the role of T-bet in T_{regs} was investigated in relation to transplantation rejection in these mice, using a heart transplant model. Previous data have shown that T_{regs} require chemokines such as CCR6, CXCR3, CCR4 to be able to home to prevent graft rejection (Burrell et al., 2012). It has been shown though to be involved in the homing of T_{regs} to cardiac allografts. T-bet has been shown to control the expression of CXCR3 and in T-bet knockout mice it was found that T_{regs} lack CXCR3 but keep normal expression levels of CD103 and CCR6 (Lee et al., 2005). Xiong et al. also showed that activated T-$bet^{-/-}$ T_{regs} express increased CCR4 surface marker expression (Xiong et al., 2016).

Lastly, as previously discussed, innate lymphoid cells (ILCs) were a novel innate cell population, which was discovered only a few years ago (McKenzie et al., 2014, Spits and Cupedo, 2012). Since then, many similarities have been found between ILCs and $CD4^+$ T helper cells, both in terms of their immune function and cytokine production. Since the discovery of ILCs, conventional NK (cNK) cells have been coined “killer ILC1s”, due to their cytotoxic properties similar to cytotoxic T cells, and ILC1s have been named “helper-ILC1s” (Diefenbach et al., 2014). Further, cNK cells have been shown to have different surface marker properties dependent on which tissue they reside in. cNK also are not fully dependent on T-bet for their development. cNKs require both T-bet and Eomes to function. T-$bet^{-/-}$ mice still have cNK cells present, although their number are reduced (Diefenbach et al., 2014). NK cells

require T-bet when at the immature NK cell stage and help to stabilise the immature NK state during NK cell development (Gordon et al., 2012). Using the anti-CD40 colitis model to induce an IFNγ driven disease phenotype in the colon has allowed for study into the interaction of ILC1s in inflammation (Powell et al., 2012, Buonocore et al., 2010, Uhlig et al., 2006). This model also affects the liver and causes severe hepatitis, which is also driven by an IFNγ response from ILC1s. Liver ILCs and NK cells are defined as being TRAIL^{-} DX5^{+} NKp46^{+} cells, which are the liver resident NK cells and TRAIL^{+} DX5^{-} NKp46^{+} cells as liver ILC1s (Daussy et al., 2014, Marquardt et al., 2015, Peng et al., 2013, Takeda et al., 2005, Tang et al., 2016). T-bet is essential to the differentiation and effector function of ILC1s, and ILC1s have been found to be important in defence against many pathogens involved in diseases like IBD (Fuchs, 2016, Abt et al., 2015), liver disease (Liu and Zhang, 2017), ischemia injury in kidneys (Victorino et al., 2015) and also cytomegalovirus in the salivary glands (Schuster et al., 2014). Therefore, the role of T-bet in ILC1s and NK cells in relation to colitis and liver disease will be discussed and further investigated.

6.1 The role of T-bet in CD4^{+} T$_{reg}$

Using a Foxp3^{cre} Tbet$^{fl/fl}$ mouse model allowed for observations to be made in specific T-bet deletion in only Foxp3 expressing T$_{regs}$. Initial experiments performed were to analyse the difference in effector function these T-bet$^{-/-}$ T$_{regs}$ would have in comparison with normal T$_{regs}$. The Foxp3 expression in this mouse line was also identifiable due to a YFP insert in the Foxp3 gene (Rubtsov et al., 2008).

45A

Gating strategy shown from the Foxp3^{cre} x T-bet$^{fl/fl}$

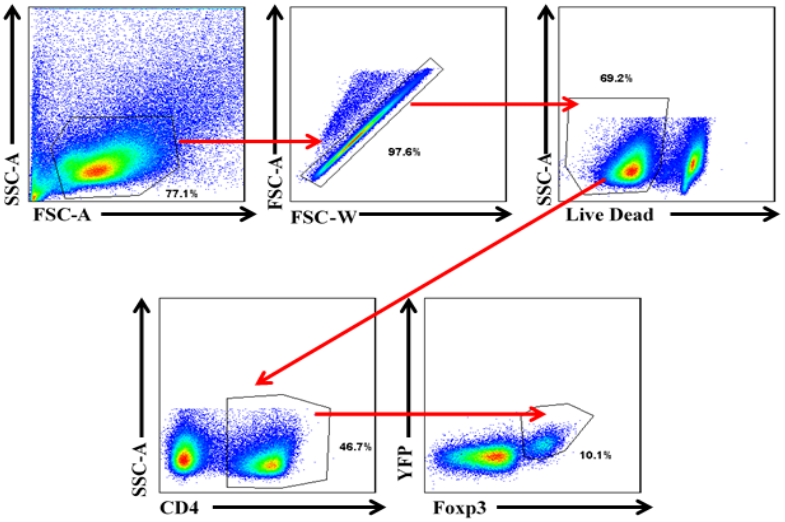

45B

Dot plot showing percentage of IL-10 producing Foxp3^{+} CD4^{+} in stimulated cells from mLN, pLN and spleen

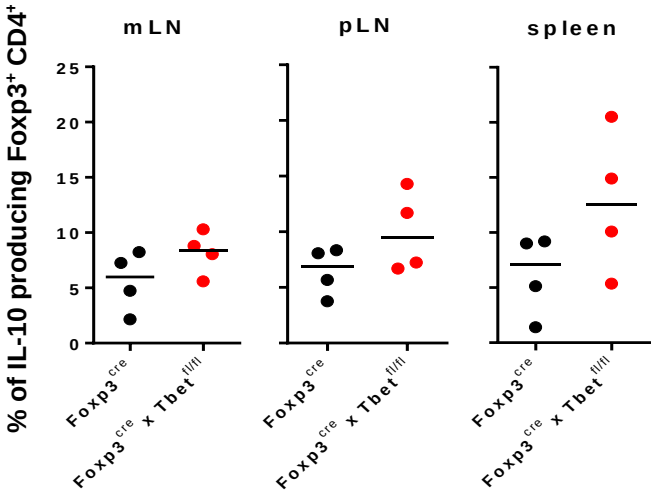

Figure 45: Phenotyping of the Foxp3^{cre} x T-bet$^{fl/fl}$ mouse line at steady state

A. Representative gating strategy shown from the spleen of the Foxp3cre x T-betfl/fl mouse line. B Dot plots showing the percentage of IL-10 producing Foxp3^{+} CD4^{+} in stimulated cells from mLN, pLN and spleen from Foxp3^{cre} x T-bet$^{fl/fl}$ and using Foxp3cre litter mates as controls. (n = 4 for both genotypes)

The Foxp3^{cre} Tbet$^{fl/fl}$ mice showed that when T-bet deletion occurred in Foxp3^{+} CD4^{+} T_{reg} cells there is a slight increase in IL-10 producing cells in the lymphoid organs, although this data was not significant. However, this trend of an increase in IL-10 produced by these T-bet deficient T_{regs} is contradictory from previously reported research. Koch et al., showed that in there was a slight reduction in TGFβ and IL-10 in T-bet$^{-/-}$ T_{regs} (Koch et al., 2009a).

As already described, T-bet has been involved in the chemokine expression on T_{regs} and therefore it would be of interest to investigate any effects after deleting T-bet in T_{regs}. The cardiac allograft rejection was determined by cessation of the graft cardiac pulse.

46A

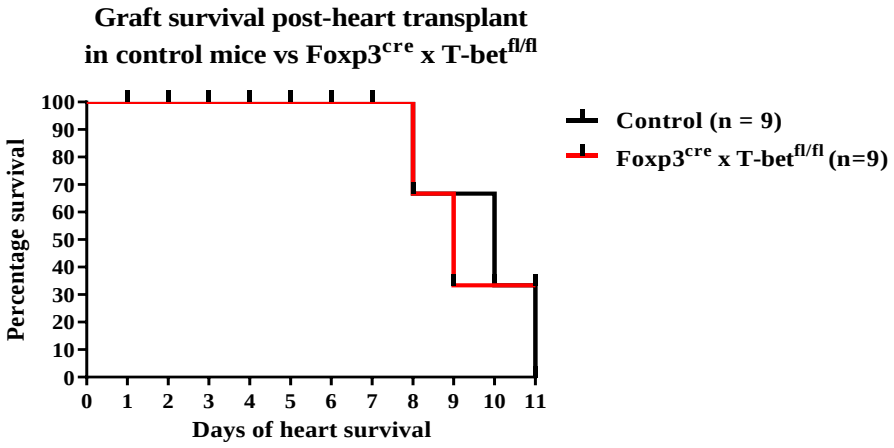

46B

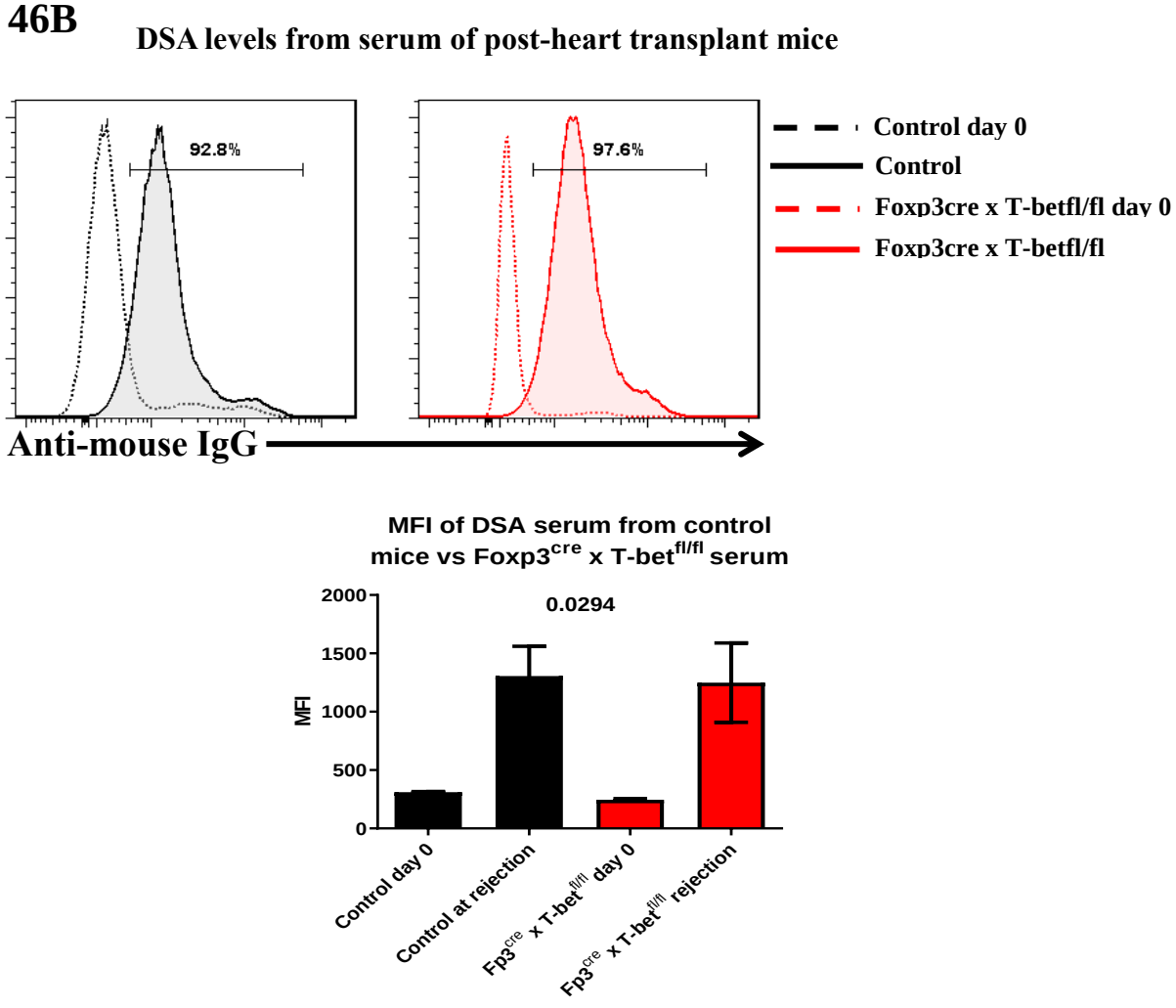

Figure 46: Cardiac allografts between Foxp3^{cre} mice and Foxp3^{cre} x T-bet$^{fl/fl}$

A. Survival graph showing transplanted cardiac allograft survival between Foxp3^{cre} control mice and Foxp3^{cre} x T-bet$^{fl/fl}$, mice were culled upon cessation of allograft. B. Representative histogram plots and bar graph of MFI showing the donor specific antibody response in serum of cardiac transplanted Foxp3^{cre} control mice vs Foxp3^{cre} x T-bet$^{fl/fl}$ at day 0 and rejection. (n = 10 for Foxp3^{cre} and 8 for Foxp3^{cre} x T-bet$^{fl/fl}$ mice). Kruskal-Wallis test performed showing overall statistical analysis for all.

There was no significant change in graft survival for the transplanted heart between the litter mate control Foxp3^{cre} mice and T-bet-deficient T_{regs} of Foxp3^{cre} T-bet$^{fl/fl}$ mice(Figure 46A). Figure 46B shows the flow cytometry data for donor specific antibody (DSA) response in serum taken from both test groups. Both the histogram and MFI of DSA response shows that there was no statistical difference in level of rejection between the Foxp3^{cre} mice and Foxp3^{cre} x T-bet$^{fl/fl}$ test mice, even though between all 4 groups the Kruskal-Wallis test showed significant difference between all groups.

6.2 The role of T-bet in NK cells and ILC1s in liver disease

6.2.1 Activation of CD40 causes severe inflammation of the colon, but also causes severe inflammatory hepatocellular injury in the liver

As previously stated, ILC1s are involved in IBD. One of the models of colitis involves the activation of myeloid cells, by anti-CD40 in *Rag2*$^{-/-}$ mice, to produce IL-12 and IL-23 and cause an increase in IFNγ production from ILC1s in the intestine, which drives the wasting disease and systemic inflammation (Uhlig et al., 2006, Buonocore et al., 2010, Powell et al., 2012). Figure 47 shows the typical disease phenotypes within this model of colitis.

47A

Clinical data showing weight loss, colon and spleen mass and macroscopic images of the spleen after treatment of anti-CD40

47B

Representative flow plot and histogram showing the increase in lymphocyte infiltration and increased Gr-1 neutrophil

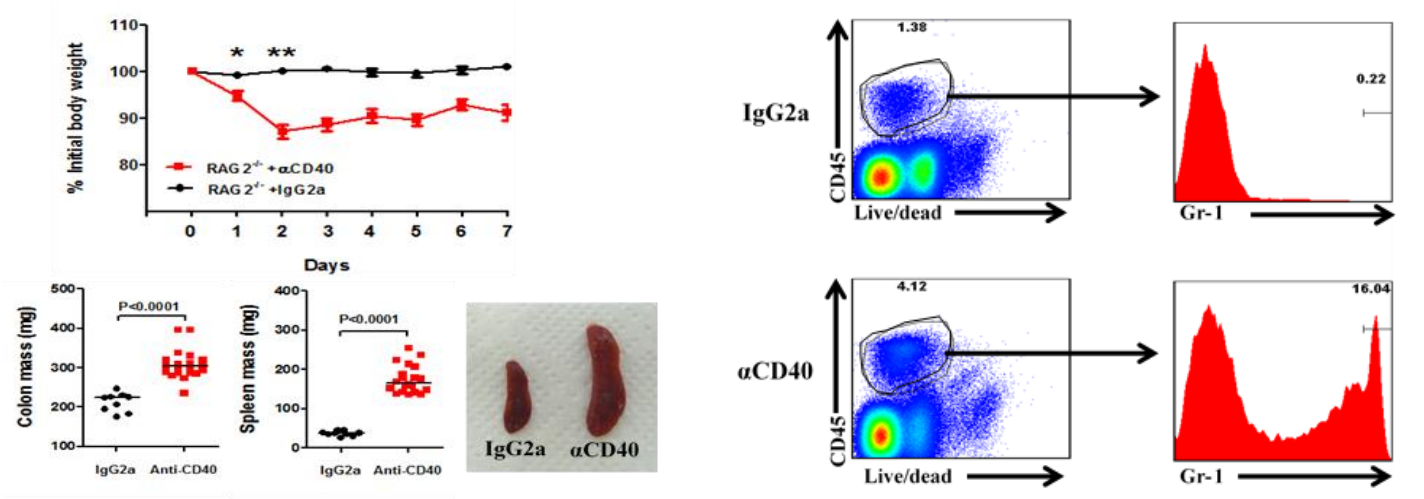

Figure 47: Typical colitis clinical aspects of the anti-CD40 colitis model in *Rag2*$^{-/-}$ mice

A. Clinical data showing overall weight loss over seven days, colon and spleen mass at the end point and representative macroscopic photo of spleens from *Rag2*$^{-/-}$ given isotype control or anti-CD40 via intraperitoneal injections. B. Representative flow plot and histogram showing the increase in lymphocyte infiltration and increased Gr-1 neutrophil population within the colonic lamina propria of *Rag2*$^{-/-}$ (n = 9 for isotype control treated and n=20 for anti-CD40 treated mice). Mann-Whitney test performed showing statistical analysis and * showing P<0.05 and ** showing P<0.01

In this standard model of colitis, systemic inflammation of the colon and spleen were observed. From previous published data and Figure 47, there is a big infiltration of Gr-1^{+} neutrophils. This is most likely driven by the activation of myeloid cells producing IL-12 and IL-23 and recruiting both neutrophils and pro-inflammatory ILC1s to the mucosal site. However, even though the anti-CD40 model affects the mice systemically, the liver of these mice has not been reported on, especially as the hepatic portal vein flows directs from the colon to the liver. Therefore, analysis of the liver and possible inflammatory hepatic disease phenotypes was measured.

48A

Clinical data showing liver mass and macroscopic images of the liver after treatment of anti-CD40

48B

Histology with H&E staining showing inflammation after treatment of anti-CD40

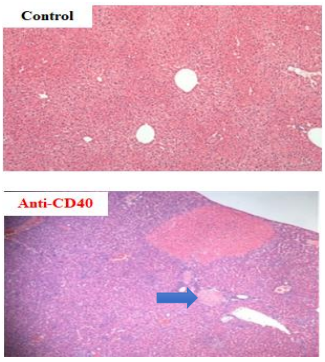

48C

ALT and ALP readings after treatment of anti-CD40 in Balb/C *Rag2*$^{-/-}$ and C57BL/6 *Rag1*$^{-/-}$

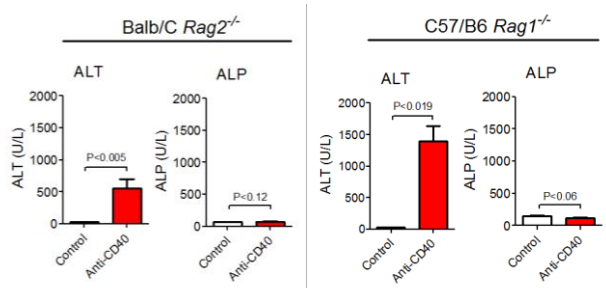

48D

Representative flow plots showing cytokine production from CD45^{+} cells from the liver

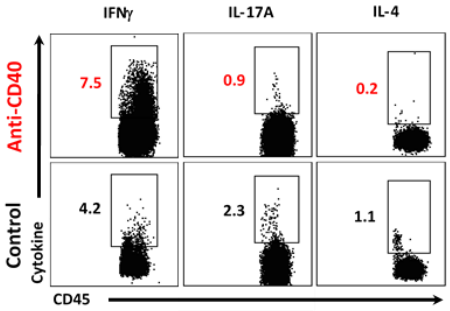

48E

ALT and ALP readings after treatment of anti-CD40 in Balb/C *Rag2*$^{-/-}$ and C57BL/6 *Rag1*$^{-/-}$

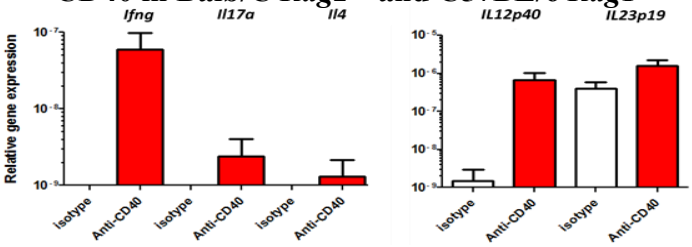

48G

F4/80 staining after treatment of anti-CD40 in the liver

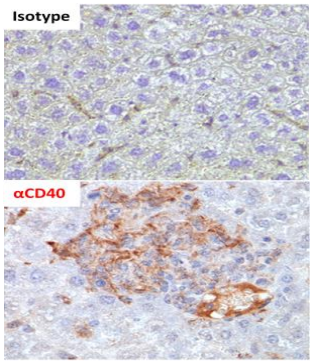

48F

Representative flow plots showing macrophage staining from CD45^{+} cells from the liver

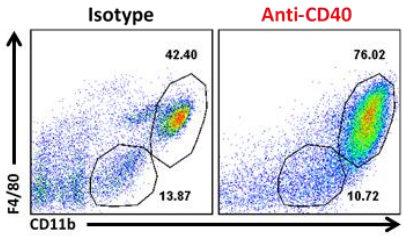

Figure 48: Clinical aspects in the liver of the anti-CD40 colitis model in *Rag2*$^{-/-}$ mice

A. Clinical data showingmacroscopic photographs of livers and liver mass from *Rag2*$^{-/-}$ given either isotype control or anti-CD40. B. Representative haemotoxylin and eosin histology staining showing the histological differences in *Rag2*$^{-/-}$ given either isotype control or anti-CD40. C. Alanine transaminase and alkaline phosphatase readings from the serum of either Balb/C *Rag2*$^{-/-}$ or C57/B6 *Rag1*$^{-/-}$ with either control or anti-CD40 treatment. D. Representative flow plots showing the IFNγ, IL-17A and IL-4 production from live CD45^{+} cells from the liver of *Rag2*$^{-/-}$ mice either treated with isotype control or anti-CD40. E. qPCR data showing the IFNγ, IL-17A, IL-4, IL-12p40 and IL-23p19 production from whole pieces of liver of *Rag2*$^{-/-}$ mice either treated with isotype control or anti-CD40. F. Representative flow plots showing increased macrophage infiltration in the liver (gated on live CD45^{+} cells) of *Rag2*$^{-/-}$ mice either treated with isotype control or anti-CD40. G. Representative F4/80 (shown in brown) histology staining showing F4/80^{+} cells in *Rag2*$^{-/-}$given either isotype control or anti-CD40 via intraperitoneal injections. (n = 9 for isotype control treated and n=20 for anti-CD40 treated mice). Mann-Whitney test performed showing statistical analysis.

Figure 48 significantly demonstrates that *Rag2*$^{-/-}$ mice suffer from severe acute liver inflammation in the anti-CD40 colitis model. When anti-CD40 was administered, there was marked increase in liver masses in the mice and macroscopically the livers of these mice were paler and white spots were visible on the surface of the liver (Figure 48A). Histologically, the anti-CD40 treated livers showed increased infiltration of lymphocytes and the white spots that were seen macroscopically were identified as zones of necrosis. Furthermore, there was also hepatic portal vein thrombosis observed in some mice (marked in blue in Figure 48B). Serum from the mice was analysed for the enzymes: alanine transaminase (ALT) and alkaline phosphatase (ALP), to determine where the main source of liver injury was occurring. Consequently, the ALT and ALP readings from the mice treated with anti-CD40 showed them to have highly elevated ALTs and no changes to their ALP levels. This was further proved using flow cytometry and qPCR, where a large production of IFNγ was found in the CD45^{+} cells in the liver, and they also showed much greater relative gene expression from the qPCR results. As was reported by Uhlig et al. in 2006, there was a vast production of IL-12 and this was shown by the qPCR mRNA result in Figure 48E where there was highly elevated gene expression for IL-12. This was further highlighted by the increased infiltration of CD11b^{+} F4/80^{+} macrophages shown both by flow (Figure 48F) and histologically (Figure 48G).

6.2.2 Hepatic CD90^{+} NKp46^{+} cells are more prolific activated producers of IFNγ

As described, ILC1s are the main group of cells producing IFNγ in the anti-CD40 colitis model in the intestine. Therefore, analysis of the cells involved in causing the severe hepatitis and IFNγ production within the liver of this model was also performed.

49A

Representative flow plots showing CD90$^+$ NKp46$^+$ from the liver of aCD40 treated mice

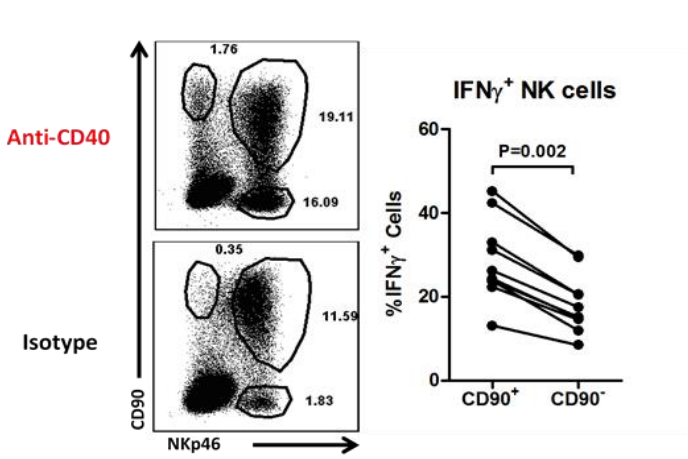

49B

Representative flow plots showing IFNγ production from CD90$^+$ NKp46$^+$ from the liver of aCD40 treated mice

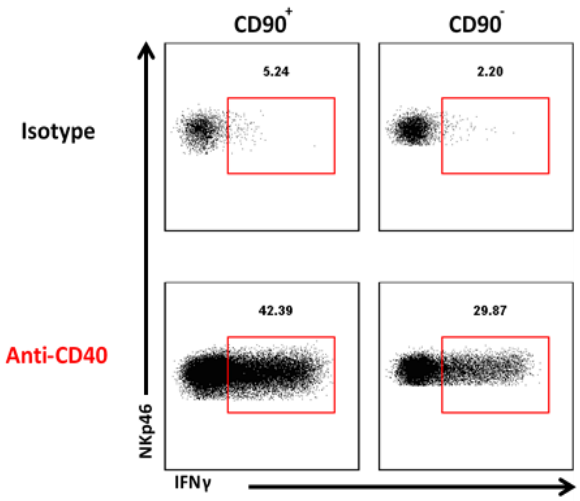

49C

NKp46 staining after treatment of anti-CD40 in the liver

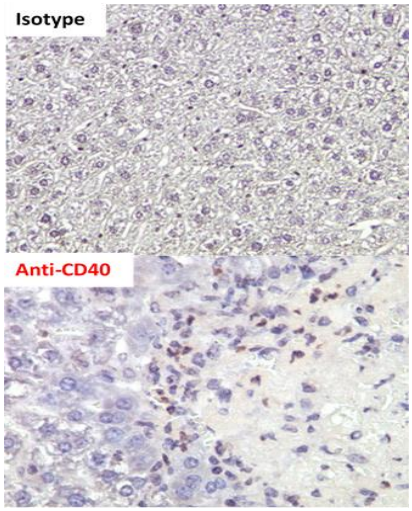

49D

Representative histograms for typical NK activation markers from NKp46$^+$ CD90$^+$ cells in the liver

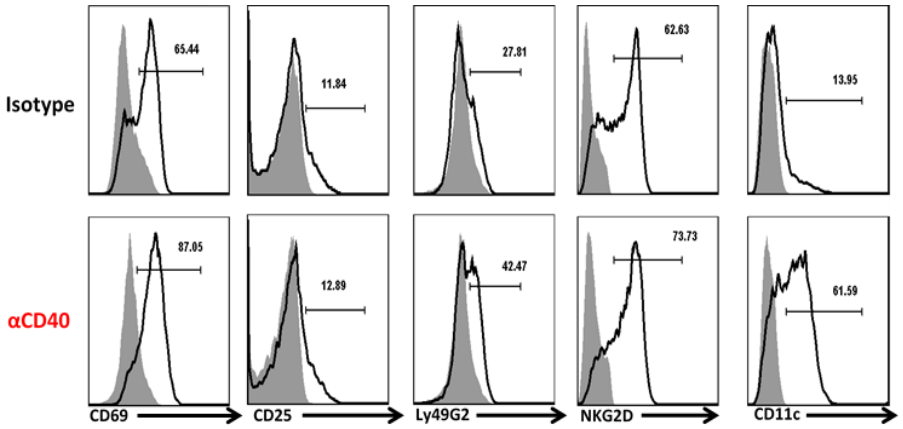

Figure 49: IFNγ production in the liver is produced predominately from CD90$^+$ NKp46$^+$ cells

A. Representative flow plot gated on live CD45$^+$ cells in the liver and dot plot showing the percentage of IFNγ producing cells in the same samples with CD90$^+$ and CD90$^-$ gated cells in *Rag2*$^{-/-}$ given either isotype control or anti-CD40. B. Representative flow plots showing IFNγ production from either CD90$^-$ NKp46$^+$ or CD90$^+$ NKp46$^+$ cells from the liver in *Rag2*$^{-/-}$ given either isotype control or anti-CD40. C. Representative Nkp46 (shown in brown) histology staining showing the increase and cluster of Nkp46$^+$ cells in *Rag2*$^{-/-}$ given either isotype control or anti-CD40. D. Representative histograms showing typical NK cell markers gated off Nkp46$^+$ CD90$^+$ cells in the liver in *Rag2*$^{-/-}$ given either isotype control or anti-CD40. (n = 9 for isotype control treated and n=10 for anti-CD40 treated mice). Wilcoxon matched pairs signed rank test performed showing statistical analysis.

Analysis of the $CD45^+$ cells in the liver showed that CD90 was significantly upregulated in $NKp46^+$ cells when comparing the treated and untreated samples. Additionally, the $Nkp46^+$ $CD90^+$ produced significantly higher levels of IFN-γ production compared with the $NKp46^+$ $CD90^-$ in the treated and non-treated mice. The histology samples stained for NKp46 in the anti-CD40 treated mice were found in abundance mainly around the zone of necrosis. Figure 44D shows higher levels of activation of typical NK cell markers like CD69, Ly49G2, NKG2D and CD11c in the live $Nkp46^+$ hepatocytes from the anti-CD40 treated mice. These results indicate that the large IFNγ production were from highly activated $NKp46^+$ $CD90^+$ cells. Further analysis to determine if they were ILC1s or cNK cells was needed.

6.2.3 Conventional NK cells and not ILC1s are the main population of IFNγ producing cell in anti-CD40 mediated hepatitis

The previous data only indicated that the cells responsible were $NKp46^+$ $CD90^+$ cells. However, as $NKp46^+$ $CD90^+$ cells encompass conventional NK cells, ILC1s and $NKp46^+$ ILC3s, more thorough phenotyping of these cells was required. Liver ILC1s and cNK cells express different surface markers to those found in the intestine.

50A **Gating strategy used to identify NK cells and ILCs from the liver**

50B

Percentage of NK cells and ILCs from the liver in mice treated with anti-CD40

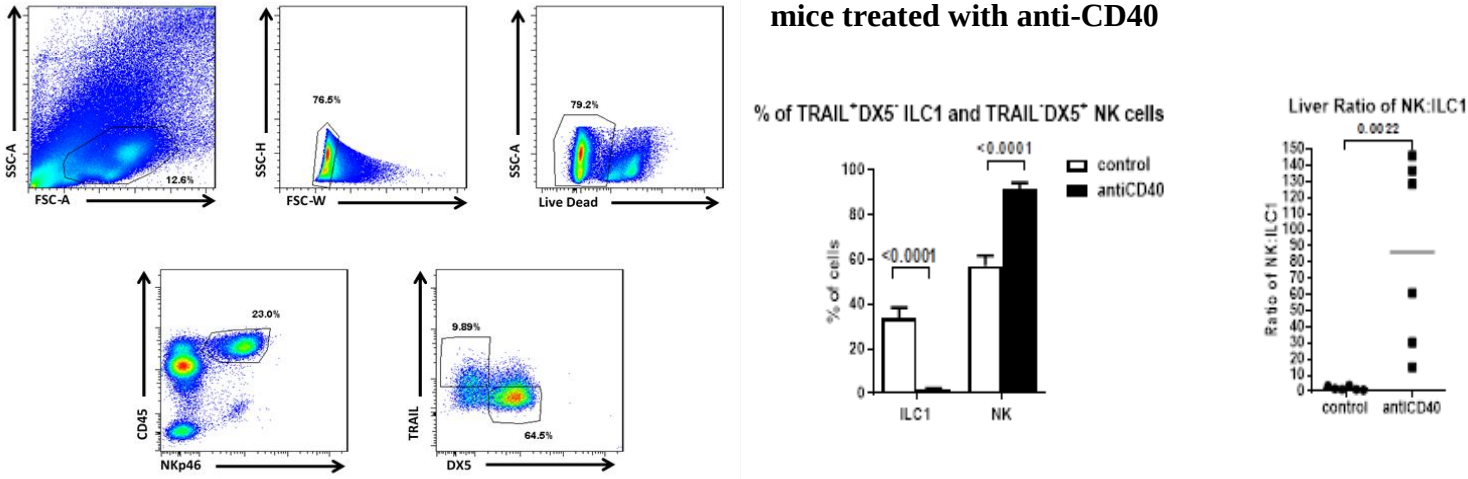

50C **Representative histograms NK cells and ILCs from the liver**

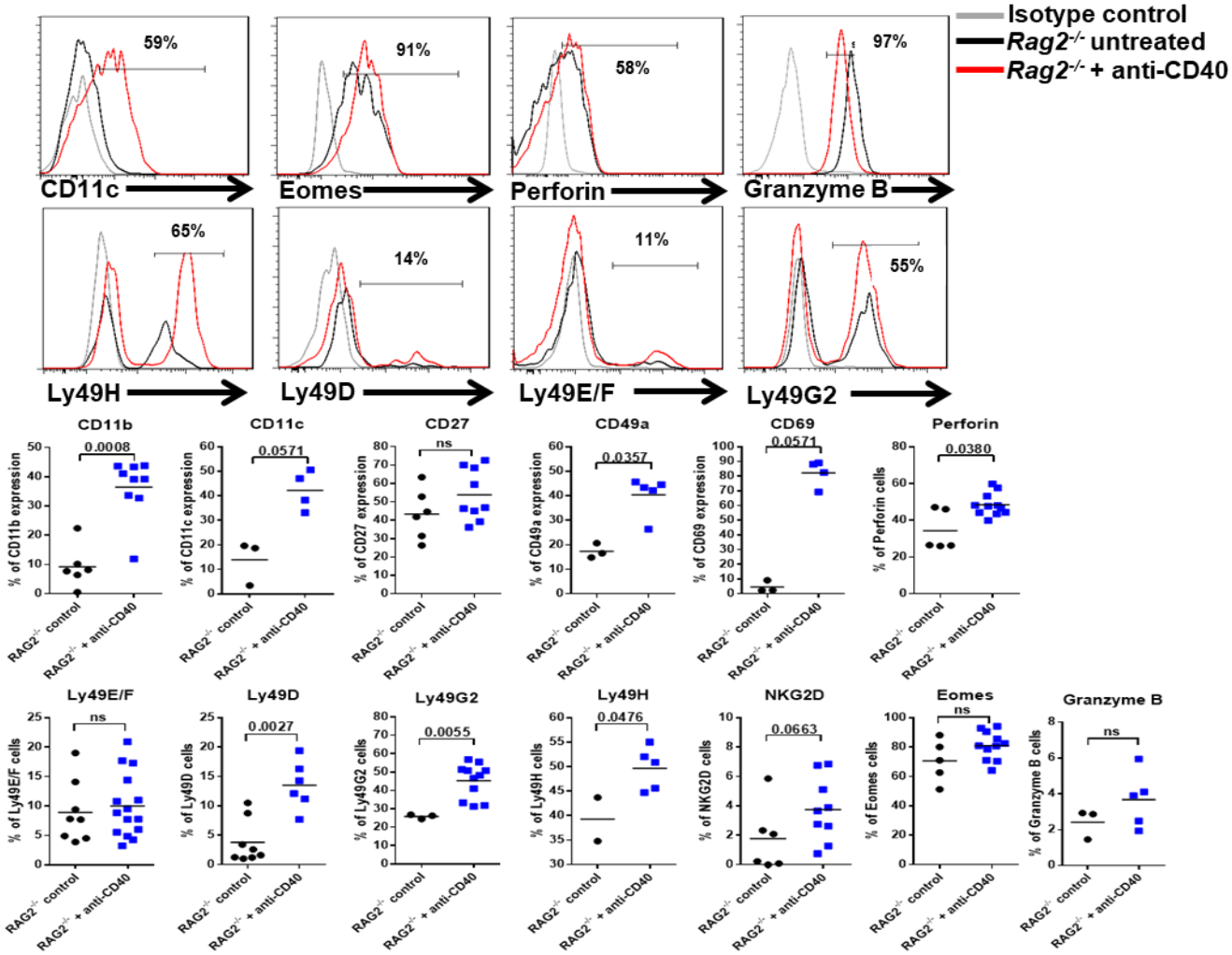

Figure 50: Phenotyping the CD90$^+$ NKp46$^+$ NK and ILC1 population in the liver

A. Representative gating strategy from the liver of *Rag2*$^{-/-}$mice given isotype control. B. Graph showing the percentage of either TRAIL$^-$ DX5$^+$ NKp46$^+$ NK cells or TRAIL$^+$ DX5$^-$ NKp46$^+$ ILC1s from the liver in *Rag2*$^{-/-}$ given either isotype control or anti-CD40. C. Representative histograms and dot plots showing NK markers from the TRAIL$^-$ DX5$^+$ NKp46$^+$ NK cells in the liver of *Rag2*$^{-/-}$given either isotype control (n = 6) or anti-CD40 (n = 6 or 9). Two-way ANOVA with Sidak multiple corrections performed and Mann-Whitney Test performed for statistical analysis

The main type of cell present in the liver during the induction of anti-CD40 was the TRAIL^{-} DX5^{+} NK cell. More surprisingly, the TRAIL^{+} DX5^{-} ILC1s reduce and almost disappear in number when given anti-CD40. Phenotyping of typical NK cell markers showed that these TRAIL^{-} DX5^{+} cells were NK cells and furthermore, upon administering anti-CD40, they highly expressed both the activating receptors, Ly49D and Ly49H, and the inhibitory receptors, Ly49E/F and Ly49G, although the expression of Ly49E/F was not significantly different between the control and anti-CD40 treated cells. Both untreated and anti-CD40 treated NK cells were also high producers of both perforin and granzyme B, as well as being Eomes^{high}.

6.2.4 Anti-CD40 mediated hepatitis is not dependent on T-bet to drive the disease phenotype

Since NK cells are not completely dependent on T-bet for their survival, it was interesting to investigate if T-bet has an essential role in IFNγ producing anti-CD40 mediated hepatitis. To determine this, experiments were carried out using the *T-bet*$^{-/-}$ *Rag2*$^{-/-}$ (TRnUC) mice.

51A

Clinical data showing weight loss of the liver after treatment of anti-CD40

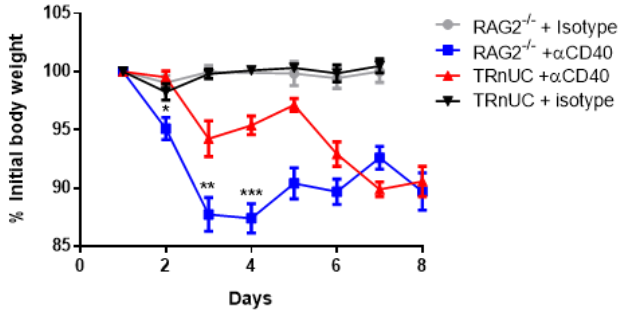

ALT readings from serum after treatment of anti-CD40

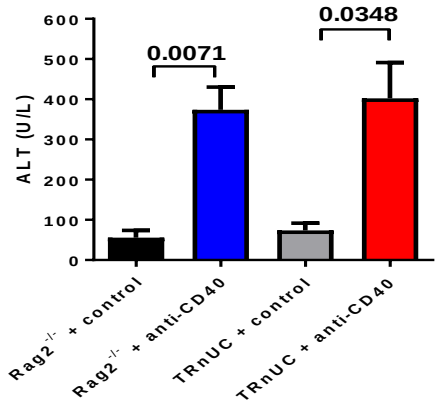

Liver weights after treatment of anti-CD40

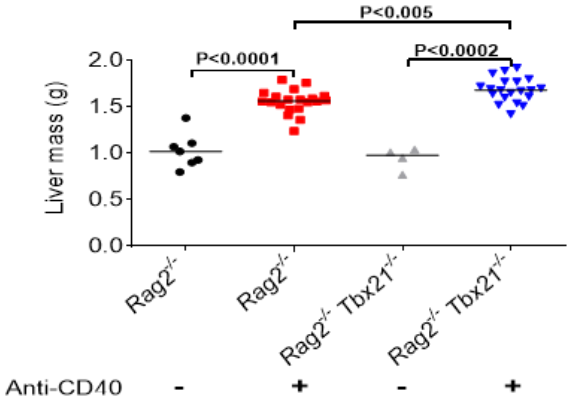

51B

Representative flow plots showing DX5 vs TRAIL staining from the liver

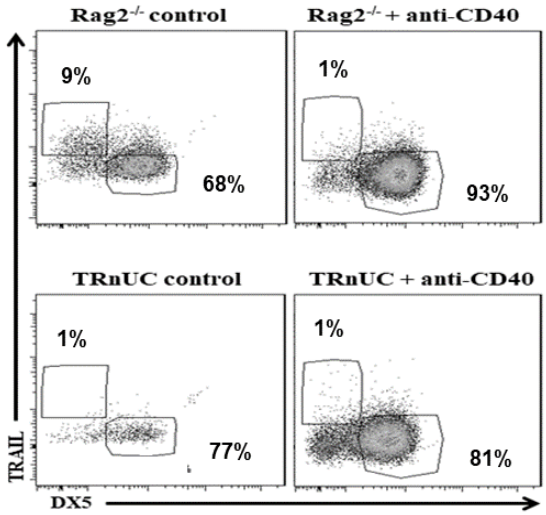

51C

Percentage of NK cells and ILCs from the liver in mice treated with anti-CD40

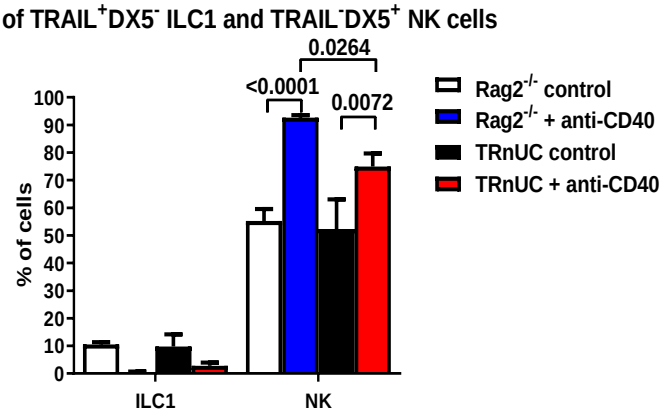

51D **Representative flow plots showing cytokine production and T-bet expression from DX5⁺ TRAIL⁻ NK cells**

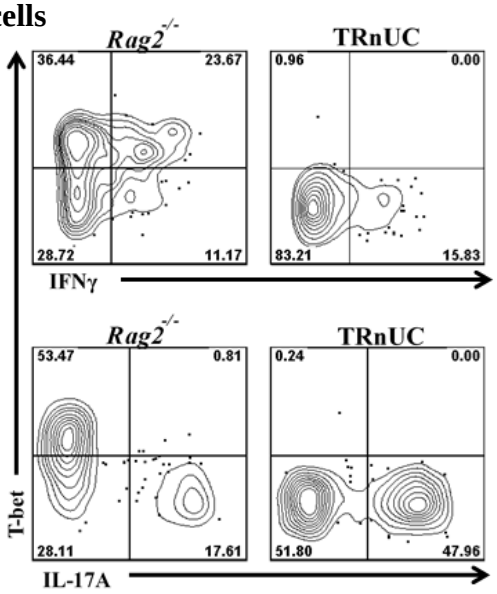

Figure 51: Comparing liver disease in *Rag2*$^{-/-}$ vs TRnUC mice with anti-CD40

A. Clinical data showing weight loss, liver and ALT levels from the serum in the liver of *Rag2*$^{-/-}$ and TRnUC mice given either isotype control or anti-CD40 B. Representative flow plots showing the NK (CD45^{+} NKp46^{+} TRAIL^{-} DX5^{+}) and ILC1 (CD45^{+} NKp46^{+} TRAIL^{+} DX5^{-}) percentages, using the gating strategy as before, in the liver of *Rag2*$^{-/-}$ and TRnUC mice given either isotype control or anti-CD40. C. Bar graph showing the NK (CD45^{+} NKp46^{+} TRAIL^{-} DX5^{+}) and ILC1 (CD45^{+} NKp46^{+} TRAIL^{+} DX5^{-}) percentages, using the gating strategy as before, in the liver of *Rag2*$^{-/-}$ and TRnUC mice given either isotype control or anti-CD40. D. IFNγ and IL-17A production from T-bet^{+} TRAIL^{-} DX5^{+} NK cells of *Rag2*$^{-/-}$ and TRnUC mice given anti-CD40 (n = 2 for *Rag2*$^{-/-}$ isotype control, 5 for *Rag2*$^{-/-}$ with anti-CD40, 4 for TRnUC control and 9 for TRnUC with anti-CD40). Two-way ANOVA with Sidak multiple corrections performed and Kruskal-Wallis test performed showing overall statistical analysis.

The TRnUC mice developed a similar disease phenotype compared to the clinical aspects of the *Rag2*$^{-/-}$ mice, in terms of enlarged liver mass and heightened ALT levels. They suffered less drastic weight loss. Whereas, in the anti-CD40 driven hepatitis, the NK cells drive the disease, and this is shown by the continued presence of TRAIL^{-} DX5^{+} NK cells in the TRnUC mice (Figures 51B and 51C).

6.3 Discussion

As explained above, T-bet is involved in the expression of chemokine surface receptors, such as CXCR3, CCR4 and CCR6, in CD4^{+} T_{reg} cells. Furthermore, T_{regs} are highly involved in tolerance and preventing graft transplantation rejection. Using the whole MHC mismatched Balb/C (H2^{d} donors) and C57BL/6 (H2^{b} recipients) mice model of transplantation (Corry et al., 1973), investigations could be made into the role of T-bet in T_{regs} in cardiac allografts by transplanting Balb/C hearts into the Foxp3^{cre} T-bet$^{fl/fl}$ mice. From the data shown in the heart transplant in T-bet-deficient T_{regs}, there was no significant change in graft survival when compared with the control T_{regs}. In fact, in this model, there was slightly worse survival rate in the T_{regs} lacking T-bet. Since T-bet$^{-/-}$ T_{regs} showed increased expression in CCR4, but are also required for the expression of CXCR3, T-bet$^{-/-}$ T_{regs} may not been able to migrate effectively to the cardiac graft. DSA responses are readouts of hyperacute and acute rejection from transplanted grafts (Haarberg and Tambur, 2014). No difference is seen in T-bet-deficient T_{regs} mice in these experiments: this shows that T-bet is not capable in preventing graft rejection and nor is it able to prolong the survival of grafts. The *in vivo* studies showed that deleting T-bet in T_{regs}, however, increased the amount of IL-10 produced. This means that functionally they have potential to reduce the inflammation from T_H1 driven phenotypes.

The anti-CD40 model of colitis has been well documented in the colon by both groups within this lab and by other groups (Buonocore et al., 2010, Powell et al., 2012, Uhlig et al., 2006). In this study the impact of innate immune activation following systemic delivery of agonistic anti-CD40 monoclonal antibodies (mAbs) to *Rag2*$^{-/-}$ mice was evaluated in the gut. However, no reports have been made in this model with regards to the liver. Therefore, we administered agonistic anti-CD40 mAbs to *Rag2*$^{-/-}$ mice in order to study innate immunity in the liver. The anti-CD40 model of colitis also affected the liver causing severe acute hepatitis, which was driven by IFNγ produced by NKp46^{+} CD90^{+} TRAIL^{-} DX5^{+} NK cells. This contrasts with the

colon, where the main disease inducing cell are ILCs, and furthermore when T-bet was deficient the ILC1s in the colon disappeared and the IFNγ production switched to an IL-17A phenotype (Powell et al., 2012). The liver disease was observed with the typical weight loss wasting model but also enlarged livers and increased ALT levels. ALT measures direct hepatocellular damage via damage to cell membrane functions of the liver cells (Lenaerts et al., 2005), whereas ALP is an enzyme found within the cells of the biliary duct in the liver. This highlighted that the inflammation experienced by these mice was due to injury directly to the hepatocytes and not being produced from the biliary ducts. Moreover, the ALT readings in C57/B6 *Rag1*$^{-/-}$ mice were more than double the reading in Balb/C *Rag2*$^{-/-}$ showing that this was predominantly an IFNγ driven disease as C57/B6 background mice have previously been shown to be more T_H1-like in their phenotype and Balb/C background mice to be T_H2 driven (Watanabe et al., 2004). The main liver cell type found to induce the disease was NKp46^{+} CD90^{+} TRAIL^{-} DX5^{+} NK cells, which also had increased NK cell activation markers when anti-CD40 was administered. Unlike in the colon, in the liver disease model, T-bet is not a determining factor in causing this disease. This is expected as NK cells are not reliant on the expression of T-bet to function. Despite the disease phenotype not being dependent on T-bet, there was a 6-fold increase in *Tbx21* gene expression in the *Rag2*$^{-/-}$ mice, when given anti-CD40, and is upregulated leading to the IFNγ production (Data not shown). Despite the disease phenotype not being dependent on T-bet, it is expressed in the *Rag2*$^{-/-}$ mice, when given anti-CD40, and is upregulated leading to the IFNγ production. However, there was still a small amount of IFNγ production from the NKp46^{+} CD90^{+} TRAIL^{-} DX5^{+} NK cells in the TRnUC mice.

Further experiments will be and are required to obtain better understanding of the hepatitis model in this setting. However, current data suggests that activation of anti-CD40 in the liver causes severe acute inflammation. Using known reposited RNA sequencing data sets and obtaining human samples from the different types of human hepatitis would be valuable information in order to try and identify this pathway within patients suffering from the same version of anti-CD40 activated hepatitis. This would allow for any potential treatments that patients could be directed towards in order to help treat their liver inflammation.

Furthermore, IL-22 was first discovered in 2000 (Xie et al., 2000a). IL-22 has shown differing roles depending on the circumstance and depending on the organ of interest. In the gut, IL-22

has been shown to be both protective and inflammatory depending on the impacting situation (Hainzl et al., 2015, Li et al., 2014, Mizoguchi et al., 2018, Sugimoto et al., 2008, Xie et al., 2000b). However, IL-22 has not been reported on yet in this model of hepatitis and so a clearer understanding of the role of IL-22 would be useful in this model and in context to T-bet.

Chapter 7

Conclusion

7.1 The use of the lineage T-bet expressing mouse model provided insights into immune cells that have previously expressed T-bet

The data in this thesis was useful to identify populations of cells that were expected to express T-bet. The use of a novel T-bet^{cre} x ROSA26YFP$^{fl/fl}$ mouse line has been revolutionary in being able to trace the lineage of cells that have expressed T-bet in their past, despite not expressing T-bet at the time. As described already, T-bet expression is important for the function of many immune cells, including CD4^{+} T cells (Szabo et al., 2000, Koch et al., 2012, Lazarevic et al., 2010), CD8^{+} T cells (Intlekofer et al., 2005), B cells (Peng et al., 2002), DCs (Lugo-Villarino et al., 2003), ILCs (Bernink et al., 2017, Klose et al., 2013), NK cells (Townsend et al., 2004), NKT cells (Matsuda et al., 2006), γδ T cells (Yin et al., 2002). From the phenotyping data of the spleen of the T-bet^{cre} x ROSA26YFP$^{fl/fl}$ mice, the percentage of cells expressing YFP were representative of the cells that have been reported to require T-bet expression for either their development, maturation and/or function. This was a good indication that the mouse model itself was a viable and usable mouse model to trace the lineage of T-bet expressing cells. Furthermore, this novel mouse line has been pioneering in being able to trace the lineage of cells that have expressed T-bet in the past, despite not necessarily being T-bet^{+} anymore.

The most interesting finding from the phenotyping data in this thesis was the observation of the YFP^{+} identified naïve CD4^{+} T cells. The percentage of these cells that were discovered within each of the organs in the mouse were very small (around 0.5-5% depending on the organ and age), and therefore, even from previous research by other groups, these cells may have gone undetected in not only mice but also humans. This is because naïve CD4^{+} T cells are naïve and therefore have been shown to not express the relevant and appropriate master transcription factors required for their different subtype of helper CD4^{+} T cells until they have differentiated. Therefore, previous studies typically show negative T-bet expression in naïve CD4^{+} T cells (Ariga et al., 2007, Placek et al., 2009). However, with the use of the T-bet^{cre} x ROSA26YFP$^{fl/fl}$

mouse line, the novel discovery of previous T-bet$^+$ naïve CD4$^+$ T cells has been found. These cells were found to be functionally active and different to their YFP$^-$ naïve CD4$^+$ subset. From the *in vitro* anti-CD3/CD28 culture data, it was found that the YFP$^+$ naïve T cells were able to produce a large amount of IFNγ both with only IL-2 and with the differentiation skewing conditions. In fact, even when given the skewing conditions, the YFP$^+$ CD4$^+$ T cells were found to be able to possibly switch to a more T_H1 cell type and increase the production of IFNγ in that differentiated subtype of CD4 T cell. This was even more evident in the YFP$^+$ naïve T cell transfer experiments, which showed increased production of IFNγ. Furthermore, the co-transfer experiments of CD45.1:CD45.2 YFP$^+$ naïve CD4$^+$ T cells at a low cell ratio of 90:10 showed possible bystander activation of the naïve CD45.1 CD4$^+$ T cells to produce increased IFNγ (Boyman, 2010, van Aalst et al., 2017), suggesting that these naïve YFP$^+$ CD4$^+$ T cells could be early responders to produce IFNγ during inflammation. As these cells have been previously unidentified without the use of this T-bet lineage tracking mouse, they might have been involved in previous studies of CD4$^+$ T cell biology, especially in response to diseases and therefore further studies into their role in disease and CD4$^+$ T cell biology is essential.

However, as shown by the phenotyping data in Chapter 4, these YFP$^+$ CD4$^+$ naïve T cells themselves still have also yet to be fully identified. They were identified to express the typical surface markers that CD4$^+$ naïve T cells expressed (CD25$^-$ CD44$^-$ CD62L$^+$ CCR7$^+$ CD27$^+$ CD28$^+$). However, the YFP$^+$ CD4$^+$ T cells did not fit any of the other known surface markers that had been used to identify the previously published naïve-like cell types, like stem-cell like naïve T cells (Gattinoni et al., 2011, Gattinoni et al., 2009), memory T cells with a naïve phenotype (Pulko et al., 2016) or virtual memory T cells (Haluszczak et al., 2009). But, they were CD5^{high} and could be precursors to previously reported MP cells (Kawabe et al., 2017). Remarkably, there was an increase in CXCR3$^+$ expression in 30% of YFP$^+$ naïve CD4 T cells showed increased CXCR3$^+$ expression compared to the YFP$^-$ naïve T cells. CXCR3 has been shown to have an importance during the differentiation of naïve CD4$^+$ T cells into effector T_H1 cells (Groom and Luster, 2011) and is driven by T-bet expression (Lord et al., 2005). These T-bet fate mapped YFP$^+$ CXCR3$^+$ CD4$^+$ T cells could be predetermined T_H1 early immune responders.

Ongoing and future experiments are planned to further analyse and phenotype these YFP^+ naïve $CD4^+$ T cells. Firstly, the expression of CD31 on these cells was not studied and this would be important to identify whether these cells are recent thymic emigrants (RTEs) (Hue et al., 2006). Although these were discounted due to the percentage of YFP^+ naïve $CD4^+$ T cells remaining consistent as the mice got older. In humans, $CD31^+$ expressing RTEs have been shown to decrease rapidly with age, around 85% in children and declining to 40% in adults older than sixty (Song et al., 2015). Furthermore, it has been shown that CD31 expression on naïve $CD4^+$ T cells ceases once the TCR becomes activated (Demeure C et al., 1996). The data from groups have shown that CD31 acts as a negative regulator of TCR and BCR signalling in both T and B cells (Henshall et al., 2001, Kohler and Thiel, 2009, Newton-Nash and Newman, 1999, Ignacio et al., 2017). With this in mind, if possible, further data on the older aged phenotyping of the mice would also be beneficial as in this thesis the oldest mice phenotyped were 50-week-old mice and mice have a lifespan of at least two years. Therefore, if even older mice could be phenotyped that would be ideal in order to get a full spectrum of how these YFP^+ naïve $CD4^+$ T cells behave as the mice become really old.

The YFP^+ naïve $CD4^+$ T cell data presented in this thesis so far has only shown functional proteomic data. The main problem with obtaining the genomic data for this was being able to acquire enough cells from each of the naïve $CD4^+$ YFP^+ T cell sorts and getting a sufficient amount of RNA extracted even with using the small cell number RNA extraction kits by Qiagen, like the RNeasy Micro Kit. However, currently, RNA-seq data is being sourced with assistance due to the low yield of good quality RNA. The RNA-seq data will look at the comparison between YFP^- naïve $CD4^+$ T cells, YFP^+ naïve $CD4^+$ T cells, YFP^- effector memory $CD4^+$ T cells and lastly YFP^+ effector memory $CD4^+$ T cells, in order to look at the difference in gene expressions between the different subsets on $CD4^+$ T cell and more importantly between the YFP^- and YFP^+. The hypothesis would be that the YFP^+ naïve $CD4^+$ T cells would have increased gene expression in T-bet mediated genes like IFNγ, compared with the YFP^- $CD4^+$ T cells. This would be expected if the cells have already previously expressed T-bet in order to become YFP^+. Further genomic plans would be to use ChIP-seq data to investigate the change in protein and DNA modifications along the genome in these different subsets of $CD4^+$ T cells, especially in relation to the T-bet region of the genome. The hypothesis being that the YFP+ cell subsets would have more open chromatin regions around the T-bet region and have higher levels of H3K4me3 and H3K4me1 for promoter and enhancer regions respectively and lower

levels of H3K27me3 showing repression of a gene. Lastly, single cell sequencing and TCR repertoire sequencing would be important in order to investigate the difference in TCR signalling in these different YFP^+ and YFP^- subset of cells. The hypothesis being that there would be a difference in the YFP^+ naïve $CD4^+$ T cells with respect TCR activation and their antigen repertoire. Furthermore, using this genomic data could also help us to potentially identify if these YFP^+ naïve $CD4^+$ T cells are present in humans, as the genomic data could be compared with the genomic data already available from the human equivalent data sets. Since it is impossible to obviously trace the lineage of the cells in a human, this would be the most ideal method to see the functional relevance and be able to identify these cells in humans.

Further functional experiments would also be important to further investigate the role and expression of T-bet in these cells. Establishing if these YFP^+ fate mapped cells still express T-bet is difficult to the nature of when and where transcription factors are regulated and expressed. Plus, using external stimuli like PMA and ionomycin or cytokines in order to induce T-bet expression can masks which YFP^+ cells are T-bet^+. However, from the *in vitro* skewed T_H1 cells, all YFP^+ cells were also T-bet^+. It has been shown that naïve $CD4^+$ T cells are T-bet^- (Ariga et al., 2007), but this was never checked in the naïve YFP^+ $CD4^+$ T cell panels used and ought to be just to confirm that this is still the case.

Within the group, a T-bet amcyan reporter mouse has been bred and this mouse line is able to trace cells currently expressing T-bet and marks them in an amcyan colour. However, whenever the cells stop express T-bet they lose their amcyan colour, therefore this mousseline is unable to trace the cells expressing T-bet but able to report on the ones presently expressing T-bet. Initial experiments performed have shown issues with the breeding of the T-bet^{Amcyan} mouse with the T-bet^{cre} x $ROSA26^{fl/fl}$ and results from T cell skewing have not shown results that would have been expected. Initial phenotyping of the T-bet^{Amcyan} mouse line revealed that there was 0.5-1% $amcyan^+$ naïve $CD4^+$ T cells, which correlated with the phenotyping data of the T-bet^{cre} x $ROSA26YFP^{fl/fl}$ mouse data. However, when naive $CD4^+$ T cells were taken from the T-bet^{cre} x $ROSA26YFP^{fl/fl}$ x T-bet^{Amcyan} mouse and skewed to T_H1 using the T_H1 skewing conditions, the cells were not shown to be $Amcyan^+$ as well as being YFP^+, which they would have been expected to be as differentiated T_H1 cells should presently express T-bet, as well as having expressed it in the past.

7.2 The expression of T-bet is not necessary to maintain $CD4^+$ T cell survival or plasticity

T-bet has been shown to be important in the plasticity of T_H2 cells (Hegazy et al., 2010, Kanhere et al., 2012, Murphy et al., 1996, Sundrud et al., 2003), T_H17 cells (Bending et al., 2009, Garrido-Mesa et al., 2013, Hirota et al., 2011) and T_{reg} cells (McPherson et al., 2015, Koch et al., 2012, Koch et al., 2009a, Koch et al., 2009b) to become more T_H1-like, especially in response to inflammation and pathogens. The majority of the studies performed in the past have been on global T-bet knockout or conditional T-bet knockout and the results from this thesis have shown new data using the temporal deletion of T-bet with the $ERTH2^{cre}$ x $T\text{-}bet^{fl/fl}$ mouse line. Interestingly, when using tamoxifen to delete T-bet in adult mice to show a difference in $CD4^+$ T cells, in both *in vitro* and *in vivo* experiments, there did not seem to be deletion or even reduction in the expression of T-bet in $CD4^+$ T cells. Unlike in ILC1s where the reduction of T-bet in ILC1s causes them to be lost (data not shown), T-bet is clearly not an essential requirement for the survival of fully developed $CD4^+$ T cells or possibly the temporal deletion of T-bet is not enough to delete T-bet from the fully mature $CD4^+$ T cells and the cells are able to express T-bet themselves and compensate for any attempted loss of T-bet. T-bet has been shown to promote the expression of FasL (Eshima et al., 2012, Eshima et al., 2018) and FasL has been shown to be important in the deletion of mature T cells (Nicholas Crisps, 1994). This therefore contradicts the findings shown when tamoxifen treatment was used as the mature $CD4^+$ T cells were not deleted.

The parasite infection models showed that the deletion of T-bet also was unable to drive switching to a T_H2-like phenotype, although there were slight increases in expression of GATA3 and T_H2 cytokine production. These experiments further demonstrated T_H2 and T_H1 cells to be stable, as has previously been reported (Zhou et al., 2009). The DSS-induced colitis models were also unable to show any plasticity between T_H1 and T_H17 cells despite the increase in IL-17A production and RORγt expression and therefore the CD4+ T cells must require external cytokine stimuli, such as TGFβ and IL-6, as well as the transcriptional change or deletion in this case, as it has been previously reported (Garrido-Mesa et al., 2013, Geginat et al., 2016).

The plasticity experiments using the T-bet^{cre} x ROSA26$^{fl/fl}$ showed interesting results. From the cytokine secretion sorted T cell transfer experiments shown in Chapter 5, it was observed, although from a n of 1, that the YFP^{+} IL-17A^{+} cells were able to switch to a more T_H1-like phenotype and produce a higher amount of IFNγ as they had previously expressed T-bet. However, again due to the small cell numbers acquired, it was difficult to perform these experiments and repeating them would be required in order to make this assumption into a real observation. Further experimental plans for these cells again would involve investigating how they differ from each other on a genomic level by using RNA-seq, ChIP-seq and single cell sequencing.

7.3 A novel model of hepatitis involving the activation of CD40L on NK cells

Using the anti-CD40 model of colitis (Uhlig et al., 2006), a novel model of hepatitis has been developed and shown in this thesis. Interestingly, the liver disease was mediated by NKp46^{+} CD90^{+} TRAIL^{-} DX5^{+} NK cells and not by ILC1s or NKp46^{+} ILC3s, like in the colon (Fuchs, 2016, Fuchs et al., 2013). Similar to the colitis model, the NK cells in the liver cause severe inflammation with the production of IFNγ and actually cause visible macroscopic zones of necrosis of the liver. This model of anti-CD40 mediated hepatitis was also not dependent on T-bet, which makes sense as NK cells do not fully depend on T-bet to develop and as shown in T-bet$^{-/-}$ mice where there are still NK cells develop (Simonetta et al., 2016, Townsend et al., 2004).

Future experiments regarding this model will involve investigating the role of IL-22. In the colitis model it has been shown that IL-22 to have both a protective and pathogenic role in T_H17 cell mediated disease, but IL-22 has been reported to have only a protective purpose in the innate ILC3 cell mediate colitis (Eken et al., 2014, Hue et al., 2006, Ignacio et al., 2017, Song et al., 2015, Powell et al., 2012). Therefore, it would be important to investigate whether IL-22 is able to protect the mice from suffering hepatitis. This can be achieved by using a RAG2$^{-/-}$ x IL-22$^{-/-}$ mouse and to determine if the clinical data is worse and if there is an increase in ALT levels when anti-CD40 is administered. Further experiments to test the role of IL-22 in this model of hepatitis would be to induce the disease in the RAG2-/- mice and give either an IL-22 blocking antibody to block either the cytokine production itself or the IL-22 receptor or

give the RAG2-/- mice recombinant IL-22. In these experiments, if IL-22 is indeed still protective and able to stop the disease inflammation like in the colitis model, then the hypothesis would be that either knocking out or blocking IL-22 would cause more severe disease in the mice and giving recombinant IL-22 during the disease model would ameliorate the inflammation.

BIBLIOGRAPHY

ABT, MICHAEL C., LEWIS, BRITTANY B., CABALLERO, S., XIONG, H., CARTER, REBECCA A., SUŠAC, B., LING, L., LEINER, I. & PAMER, ERIC G. 2015. Innate Immune Defenses Mediated by Two ILC Subsets Are Critical for Protection against Acute Clostridium difficile Infection. *Cell Host & Microbe,* 18**,** 27-37.

ADKINS, B., LECLERC, C. & MARSHALL-CLARKE, S. 2004. Neonatal adaptive immunity comes of age. *Nature Reviews Immunology,* 4**,** 553-564.

AHMED, R., ROGER, L., COSTA DEL AMO, P., MINERS, K. L., JONES, R. E., BOELEN, L., FALI, T., ELEMANS, M., ZHANG, Y., APPAY, V., BAIRD, D. M., ASQUITH, B., PRICE, D. A., MACALLAN, D. C. & LADELL, K. 2016. Human Stem Cell-like Memory T Cells Are Maintained in a State of Dynamic Flux. *Cell Reports,* 17**,** 2811-2818.

AKIRA, S., UEMATSU, S. & TAKEUCHI, O. 2006. Pathogen Recognition and Innate Immunity. *Cell,* 124**,** 783-801.

ALLMAN, D., SAMBANDAM, A., KIM, S., MILLER, J. P., PAGAN, A., WELL, D., MERAZ, A. & BHANDOOLA, A. 2003. Thymopoiesis independent of common lymphoid progenitors. *Nature Immunology,* 4**,** 168.

ARANDA, R., SYDORA, B. C., MCALLISTER, P. L., BINDER, S. W., YANG, H. Y., TARGAN, S. R. & KRONENBERG, M. 1997. Analysis of intestinal lymphocytes in mouse colitis mediated by transfer of CD4+, CD45RBhigh T cells to SCID recipients. *The Journal of Immunology,* 158**,** 3464.

ARIGA, H., SHIMOHAKAMADA, Y., NAKADA, M., TOKUNAGA, T., KIKUCHI, T., KARIYONE, A., TAMURA, T. & TAKATSU, K. 2007. Instruction of naive CD4+ T-cell fate to T-bet expression and T helper 1 development: roles of T-cell receptor-mediated signals. *Immunology,* 122**,** 210-221.

ARTIS, D. & SPITS, H. 2015. The biology of innate lymphoid cells. *Nature,* 517**,** 293.

AVNI, O., LEE, D., MACIAN, F., SZABO, S. J., GLIMCHER, L. H. & RAO, A. 2002. TH cell differentiation is accompanied by dynamic changes in histone acetylation of cytokine genes. *Nature Immunology,* 3**,** 643.

AW, D. & PALMER, D. B. 2011. The origin and implication of thymic involution. *Aging and disease,* 2**,** 437-443.

AW, D., SILVA, A. B. & PALMER, D. B. 2007. Immunosenescence: emerging challenges for an ageing population. *Immunology,* 120**,** 435-446.

BAGGIOLINI, M. 2001. Chemokines in pathology and medicine. *Journal of Internal Medicine,* 250**,** 91-104.

BAL, S. M., BERNINK, J. H., NAGASAWA, M., GROOT, J., SHIKHAGAIE, M. M., GOLEBSKI, K., VAN DRUNEN, C. M., LUTTER, R., JONKERS, R. E., HOMBRINK, P., BRUCHARD, M., VILLAUDY, J., MUNNEKE, J. M., FOKKENS, W., ERJEFÄLT, J. S., SPITS, H. & ROS, X. R. 2016. IL-1β, IL-4 and IL-12 control the fate of group 2 innate lymphoid cells in human airway inflammation in the lungs. *Nature Immunology,* 17**,** 636.

BARNETT, B. E., STAUPE, R. P., ODORIZZI, P. M., PALKO, O., TOMOV, V. T., MAHAN, A. E., GUNN, B., CHEN, D., PALEY, M. A., ALTER, G., REINER, S. L., LAUER, G. M., TEIJARO, J. R. & WHERRY, E. J. 2016. Cutting Edge: B Cell–Intrinsic T-bet Expression Is Required To Control Chronic Viral Infection. *The Journal of Immunology*.

BARROS-MARTINS, J., SCHMOLKA, N., FONTINHA, D., PIRES DE MIRANDA, M., SIMAS, J. P., BROK, I., FERREIRA, C., VELDHOEN, M., SILVA-SANTOS, B. & SERRE, K. 2016. Effector γδ T Cell Differentiation Relies on Master but Not Auxiliary Th Cell Transcription Factors. *The Journal of Immunology,* 196**,** 3642.

BASHA, S., SURENDRAN, N. & PICHICHERO, M. 2014. Immune responses in neonates. *Expert review of clinical immunology,* 10**,** 1171-1184.

BAUMGART, D. C. & SANDBORN, W. J. 2007. Inflammatory bowel disease: clinical aspects and established and evolving therapies. *The Lancet,* 369**,** 1641-1657.

BELZ, G. T. 2016. ILC2s masquerade as ILC1s to drive chronic disease. *Nature Immunology,* 17**,** 611.

BENDING, D., DE LA PEÑA, H., VELDHOEN, M., PHILLIPS, J. M., UYTTENHOVE, C., STOCKINGER, B. & COOKE, A. 2009. Highly purified Th17 cells from BDC2.5NOD mice convert into Th1-like cells in NOD/SCID recipient mice. *The Journal of Clinical Investigation,* 119**,** 565-572.

BERARD, M. & TOUGH, D. F. 2002. Qualitative differences between naïve and memory T cells. *Immunology,* 106**,** 127-138.

BERNINK, J. H., MJÖSBERG, J. & SPITS, H. 2017. Human ILC1: To Be or Not to Be. *Immunity,* 46**,** 756-757.

BERNINK, J. H., PETERS, C. P., MUNNEKE, M., TE VELDE, A. A., MEIJER, S. L., WEIJER, K., HREGGVIDSDOTTIR, H. S., HEINSBROEK, S. E., LEGRAND, N., BUSKENS, C. J., BEMELMAN, W. A., MJÖSBERG, J. M. & SPITS, H. 2013. Human type 1 innate lymphoid cells accumulate in inflamed mucosal tissues. *Nature Immunology,* 14**,** 221.

BETTELLI, E., CARRIER, Y., GAO, W., KORN, T., STROM, T. B., OUKKA, M., WEINER, H. L. & KUCHROO, V. K. 2006. Reciprocal developmental pathways for the generation of pathogenic effector TH17 and regulatory T cells. *Nature,* 441**,** 235.

BETTELLI, E., SULLIVAN, B., SZABO, S. J., SOBEL, R. A., GLIMCHER, L. H. & KUCHROO, V. K. 2004. Loss of T-bet, But Not STAT1, Prevents the Development of Experimental Autoimmune Encephalomyelitis. *The Journal of Experimental Medicine,* 200**,** 79.

BEUTLER, B. & CERAMI, A. 1989. The Biology of Cachectin/TNF -- A Primary Mediator of the Host Response. *Annual Review of Immunology,* 7**,** 625-655.

BISSET, L. R. & SCHMID-GRENDELMEIER, P. 2005. Chemokines and their receptors in the pathogenesis of allergic asthma: Progress and perspective. *Current Opinion in Pulmonary Medicine,* 11**,** 35-42.

BLAIR, P. A., CHAVEZ-RUEDA, K. A., EVANS, J. G., SHLOMCHIK, M. J., EDDAOUDI, A., ISENBERG, D. A., EHRENSTEIN, M. R. & MAURI, C. 2009. Selective targeting of B cells with agonistic anti-CD40 is an efficacious strategy for the generation of induced regulatory T2-like B cells and for the suppression of lupus in MRL/lpr mice(). *Journal of immunology (Baltimore, Md. : 1950),* 182**,** 3492-3502.

BORN, W., MILES, C., WHITE, J., O'BRIEN, R., FREED, J. H., MARRACK, P., KAPPLER, J. & KUBO, R. T. 1987. Peptide sequences of T-cell receptor δ and γ chains are identical to predicted X and γ proteins. *Nature,* 330**,** 572-574.

BOYMAN, O. 2010. Bystander activation of CD4+ T cells. *European Journal of Immunology,* 40**,** 936-939.

BRIGHT, J. J. & SRIRAM, S. 1998. TGF-beta inhibits IL-12-induced activation of Jak-STAT pathway in T lymphocytes. *J Immunol,* 161**,** 1772-7.

BROWN, CHRYSOTHEMIS C., ESTERHAZY, D., SARDE, A., LONDON, M., PULLABHATLA, V., OSMA-GARCIA, I., AL-BADER, R., ORTIZ, C., ELGUETA, R., ARNO, M., DE RINALDIS, E., MUCIDA, D., LORD, GRAHAM M. & NOELLE, RANDOLPH J. 2015. Retinoic Acid Is Essential for Th1 Cell Lineage Stability and Prevents Transition to a Th17 Cell Program. *Immunity,* 42**,** 499-511.

BUONOCORE, S., AHERN, P. P., UHLIG, H. H., IVANOV, I. I., LITTMAN, D. R., MALOY, K. J. & POWRIE, F. 2010. Innate lymphoid cells drive interleukin-23-dependent innate intestinal pathology. *Nature,* 464**,** 1371.

BURCHILL, M. A., YANG, J., VOGTENHUBER, C., BLAZAR, B. R. & FARRAR, M. A. 2007. IL-2 Receptor β-Dependent STAT5 Activation Is Required for the Development of Foxp3⁺ Regulatory T Cells. *The Journal of Immunology,* 178**,** 280.

BURRELL, B. E., NAKAYAMA, Y., XU, J., BRINKMAN, C. C. & BROMBERG, J. S. 2012. Treg induction, migration, and function in transplantation. *Journal of immunology (Baltimore, Md. : 1950),* 189**,** 4705-4711.

C A JANEWAY, J. 1992. The T Cell Receptor as a Multicomponent Signalling Machine: CD4/CD8 Coreceptors and CD45 in T Cell Activation. *Annual Review of Immunology,* 10**,** 645-674.

CANAVAN, J. B., SCOTTÀ, C., VOSSENKÄMPER, A., GOLDBERG, R., ELDER, M. J., SHOVAL, I., MARKS, E., STOLARCZYK, E., LO, J. W., POWELL, N., FAZEKASOVA, H., IRVING, P. M., SANDERSON, J. D., HOWARD, J. K., YAGEL, S., AFZALI, B., MACDONALD, T. T., HERNANDEZ-FUENTES, M. P., SHPIGEL, N. Y., LOMBARDI, G. & LORD, G. M. 2016. Developing in vitro expanded CD45RA(+) regulatory T cells as an adoptive cell therapy for Crohn's disease. *Gut,* 65**,** 584-594.

CAZA, T. & LANDAS, S. 2015. Functional and Phenotypic Plasticity of CD4(+) T Cell Subsets. *BioMed Research International,* 2015**,** 521957.

CELLA, M., FUCHS, A., VERMI, W., FACCHETTI, F., OTERO, K., LENNERZ, J. K. M., DOHERTY, J. M., MILLS, J. C. & COLONNA, M. 2008. A human natural killer cell subset provides an innate source of IL-22 for mucosal immunity. *Nature,* 457**,** 722.

CEREDIG, R. & ROLINK, T. 2002. A positive look at double-negative thymocytes. *Nature Reviews Immunology,* 2**,** 888.

CHAPLIN, D. D. 2010. Overview of the immune response. *The Journal of allergy and clinical immunology,* 125**,** S3-S23.

CHASSAING, B., AITKEN, J. D., MALLESHAPPA, M. & VIJAY-KUMAR, M. 2014a. Dextran sulfate sodium (DSS)-induced colitis in mice. *Current protocols in immunology,* 104**,** Unit-15.25.

CHASSAING, B., AITKEN JESSE, D., MALLESHAPPA, M. & VIJAY-KUMAR, M. 2014b. Dextran Sulfate Sodium (DSS)-Induced Colitis in Mice. *Current Protocols in Immunology,* 104**,** 15.25.1-15.25.14.

CHEN, L., HE, W., KIM, S. T., TAO, J., GAO, Y., CHI, H., INTLEKOFER, A. M., HARVEY, B., REINER, S. L., YIN, Z., FLAVELL, R. A. & CRAFT, J. 2007a. Epigenetic and Transcriptional Programs Lead to Default IFN-γ Production by γδ T Cells. *The Journal of Immunology,* 178**,** 2730.

CHEN, W., JIN, W., HARDEGEN, N., LEI, K.-J., LI, L., MARINOS, N., MCGRADY, G. & WAHL, S. M. 2003. Conversion of Peripheral CD4⁺CD25[−] Naive T Cells to CD4⁺CD25⁺ Regulatory T Cells by TGF-β Induction of Transcription Factor <em>Foxp3</em&gt. *J Exp Med,* 198**,** 1875.

CHEN, Z., LAURENCE, A. & O'SHEA, J. J. 2007b. Signal transduction pathways and transcriptional regulation in the control of Th17 differentiation. *Seminars in immunology,* 19**,** 400-408.

CHO, B.-A., SIM, J. H., PARK, J. A., KIM, H. W., YOO, W.-H., LEE, S.-H., LEE, D.-S., KANG, J. S., HWANG, Y.-I., LEE, W. J., KANG, I., LEE, E. B. & KIM, H.-R. 2012. Characterization of Effector Memory CD8+ T Cells in the Synovial Fluid of Rheumatoid Arthritis. *Journal of Clinical Immunology,* 32**,** 709-720.

COHEN, J. 2002. The immunopathogenesis of sepsis. *Nature,* 420**,** 885-891.

COOMBES JANINE, L., ROBINSON NICHOLAS, J., MALOY KEVIN, J., UHLIG HOLM, H. & POWRIE, F. 2005. Regulatory T cells and intestinal homeostasis. *Immunological Reviews,* 204**,** 184-194.

COOPER, H. S., MURTHY, S. N., SHAH, R. S. & SEDERGRAN, D. J. 1993. Clinicopathologic study of dextran sulfate sodium experimental murine colitis. *Lab Invest,* 69**,** 238-49.

CORRY, R. J., WINN, H. J. & RUSSELL, P. S. 1973. Primarily vascularized allografts of hearts in mice. The role of H-2D, H-2K, and non-H-2 antigens in rejection. *Transplantation,* 16**,** 343-50.

DAUSSY, C., FAURE, F., MAYOL, K., VIEL, S., GASTEIGER, G., CHARRIER, E., BIENVENU, J., HENRY, T., DEBIEN, E., HASAN, U. A., MARVEL, J., YOH, K., TAKAHASHI, S., PRINZ, I., DE BERNARD, S., BUFFAT, L. & WALZER, T. 2014. T-bet and Eomes instruct the development of two distinct natural killer cell lineages in the liver and in the bone marrow. *J Exp Med,* 211**,** 563-577.

DEMEURE C, E., BYUN D, G., YANG L, P., VEZZIO, N. & DELESPESSE, G. 1996. CD31 (PECAM-1) is a differentiation antigen lost during human CD4 T-cell maturation into Th1 or Th2 effector cells. *Immunology,* 88**,** 110-115.

DI GENOVA, G., SAVELYEVA, N., SUCHACKI, A., THIRDBOROUGH STEPHEN, M. & STEVENSON FREDA, K. 2010. Bystander stimulation of activated CD4+ T cells of unrelated specificity following a booster vaccination with tetanus toxoid. *European Journal of Immunology,* 40**,** 976-985.

DIEFENBACH, A., COLONNA, M. & KOYASU, S. 2014. Development, Differentiation, and Diversity of Innate Lymphoid Cells. *Immunity,* 41**,** 354-365.

DJURETIC, I. M., LEVANON, D., NEGREANU, V., GRONER, Y., RAO, A. & ANSEL, K. M. 2006. Transcription factors T-bet and Runx3 cooperate to activate Ifng and silence Il4 in T helper type 1 cells. *Nature Immunology,* 8**,** 145.

DONSKOW-ŁYSONIEWSKA, K., BIEN, J., BRODACZEWSKA, K., KRAWCZAK, K. & DOLIGALSKA, M. 2013. Colitis Promotes Adaptation of an Intestinal Nematode: A Heligmosomoides Polygyrus Mouse Model System. *PLOS ONE,* 8**,** e78034.

DUTTON, E., CAMELO, A., SLEEMAN, M., HERBST, R., CARLESSO, G., BELZ, G. & WITHERS, D. 2018. Characterisation of innate lymphoid cell populations at different sites in mice with defective T cell immunity [version 3; peer review: 2 approved]. *Wellcome Open Research,* 2.

E ROBEY, A. & FOWLKES, B. J. 1994. Selective Events in T Cell Development. *Annual Review of Immunology,* 12**,** 675-705.

EBERL, G., BRAWAND, P. & MACDONALD, H. R. 2000. Selective Bystander Proliferation of Memory CD4⁺ and CD8⁺ T Cells Upon NK T or T Cell Activation. *The Journal of Immunology,* 165**,** 4305.

EICHELE, D. D. & KHARBANDA, K. K. 2017. Dextran sodium sulfate colitis murine model: An indispensable tool for advancing our understanding of inflammatory bowel diseases pathogenesis. *World Journal of Gastroenterology,* 23**,** 6016-6029.

EKEN, A., SINGH, A. K., TREUTING, P. M. & OUKKA, M. 2014. IL-23R(+) innate lymphoid cells induce colitis via interleukin-22-dependent mechanism. *Mucosal Immunology,* 7**,** 10.1038/mi.2013.33.

ELLIOTT, D. E., SUMMERS, R. W. & WEINSTOCK, J. V. 2007. Helminths as governors of immune-mediated inflammation. *International Journal for Parasitology,* 37**,** 457-464.

ERI, R., MCGUCKIN, M. A. & WADLEY, R. 2012. T Cell Transfer Model of Colitis: A Great Tool to Assess the Contribution of T Cells in Chronic Intestinal Inflammation. *In:* ASHMAN, R. B. (ed.) *Leucocytes: Methods and Protocols.* Totowa, NJ: Humana Press.

ESHIMA, K., CHIBA, S., SUZUKI, H., KOKUBO, K., KOBAYASHI, H., IIZUKA, M., IWABUCHI, K. & SHINOHARA, N. 2012. Ectopic expression of a T-box transcription factor, eomesodermin, renders CD4+ Th cells cytotoxic by activating both perforin- and FasL-pathways. *Immunology Letters,* 144**,** 7-15.

ESHIMA, K., MISAWA, K., OHASHI, C. & IWABUCHI, K. 2018. Role of T-bet, the master regulator of Th1 cells, in the cytotoxicity of murine CD4+ T cells. *Microbiology and Immunology,* 62**,** 348-356.

EVANS, C. M. & JENNER, R. G. 2013. Transcription factor interplay in T helper cell differentiation. *Briefings in Functional Genomics,* 12**,** 499-511.

FEIL, R., BROCARD, J., MASCREZ, B., LEMEUR, M., METZGER, D. & CHAMBON, P. 1996. Ligand-activated site-specific recombination in mice. *Proceedings of the National Academy of Sciences,* 93**,** 10887.

FEIL, R., WAGNER, J., METZGER, D. & CHAMBON, P. 1997. Regulation of Cre Recombinase Activity by Mutated Estrogen Receptor Ligand-Binding Domains. *Biochemical and Biophysical Research Communications,* 237**,** 752-757.

FEIL, S., VALTCHEVA, N. & FEIL, R. 2009. Inducible Cre Mice. *In:* WURST, W. & KÜHN, R. (eds.) *Gene Knockout Protocols: Second Edition.* Totowa, NJ: Humana Press.

FILBEY, K. J., GRAINGER, J. R., SMITH, K. A., BOON, L., VAN ROOIJEN, N., HARCUS, Y., JENKINS, S., HEWITSON, J. P. & MAIZELS, R. M. 2014. Innate and adaptive type 2 immune cell responses in genetically controlled resistance to intestinal helminth infection. *Immunology and Cell Biology,* 92**,** 436-448.

FINOTTO, S., NEURATH, M. F., GLICKMAN, J. N., QIN, S., LEHR, H. A., GREEN, F. H. Y., ACKERMAN, K., HALEY, K., GALLE, P. R., SZABO, S. J., DRAZEN, J. M., DE SANCTIS, G. T. & GLIMCHER, L. H. 2002. Development of Spontaneous Airway Changes Consistent with Human Asthma in Mice Lacking T-bet. *Science,* 295**,** 336-338.

FIORENTINO, D. F., BOND, M. W. & MOSMANN, T. R. 1989. Two types of mouse T helper cell. IV. Th2 clones secrete a factor that inhibits cytokine production by Th1 clones. *The Journal of Experimental Medicine,* 170**,** 2081.

FLAJNIK, M. F. & KASAHARA, M. 2009. Origin and evolution of the adaptive immune system: genetic events and selective pressures. *Nature Reviews Genetics,* 11**,** 47.

FONTENOT, J. D., GAVIN, M. A. & RUDENSKY, A. Y. 2003. Foxp3 programs the development and function of CD4+CD25+ regulatory T cells. *Nature Immunology,* 4**,** 330.

FUCHS, A. 2016. ILC1s in Tissue Inflammation and Infection. *Frontiers in Immunology,* 7**,** 104.

FUCHS, A., VERMI, W., LEE, JACOB S., LONARDI, S., GILFILLAN, S., NEWBERRY, RODNEY D., CELLA, M. & COLONNA, M. 2013. Intraepithelial Type 1 Innate Lymphoid Cells Are a Unique Subset of IL-12- and IL-15-Responsive IFN-γ-Producing Cells. *Immunity,* 38**,** 769-781.

GANDHI, R., LARONI, A. & WEINER, H. L. 2010. Role of the innate immune system in the pathogenesis of multiple sclerosis. *Journal of neuroimmunology,* 221**,** 7-14.

GARRETT, W. S., LORD, G. M., PUNIT, S., LUGO-VILLARINO, G., MAZMANIAN, S., ITO, S., GLICKMAN, J. N. & GLIMCHER, L. H. 2007. Communicable ulcerative colitis induced by T-bet deficiency in the innate immune system. *Cell,* 131**,** 33-45.

GARRIDO-MESA, N., ALGIERI, F., RODRÍGUEZ NOGALES, A. & GÁLVEZ, J. 2013. Functional Plasticity of Th17 Cells: Implications in Gastrointestinal Tract Function. *International Reviews of Immunology,* 32**,** 493-510.

GARRIDO-MESA, N., SCHROEDER, J. H., STOLARCZYK, E., GALLAGHER, A. L., LO, J. W., BAILEY, C., CAMPBELL, L., SEXL, V., MACDONALD, T. T., HOWARD, J. K., GRENCIS, R. K., POWELL, N. & LORD, G. M. 2019. T-bet controls intestinal mucosa immune responses via repression of type 2 innate lymphoid cell function. *Mucosal Immunology,* 12**,** 51-63.

GATTINONI, L., LUGLI, E., JI, Y., POS, Z., PAULOS, C. M., QUIGLEY, M. F., ALMEIDA, J. R., GOSTICK, E., YU, Z., CARPENITO, C., WANG, E., DOUEK, D. C., PRICE, D. A., JUNE, C. H., MARINCOLA, F. M., ROEDERER, M. & RESTIFO, N. P. 2011. A human memory T-cell subset with stem cell-like properties. *Nature medicine,* 17**,** 1290-1297.

GATTINONI, L., ZHONG, X.-S., PALMER, D. C., JI, Y., HINRICHS, C. S., YU, Z., WRZESINSKI, C., BONI, A., CASSARD, L., GARVIN, L. M., PAULOS, C. M., MURANSKI, P. & RESTIFO, N. P. 2009. Wnt signaling arrests effector T cell differentiation and generates CD8+ memory stem cells. *Nature Medicine,* 15**,** 808.

GEGINAT, J., PARONI, M., KASTIRR, I., LARGHI, P., PAGANI, M. & ABRIGNANI, S. 2016. Reverse plasticity: TGF-β and IL-6 induce Th1-to-Th17-cell transdifferentiation in the gut. *European Journal of Immunology,* 46**,** 2306-2310.

GEISER, J., VENKEN, K. J., DE LISLE, R. C. & ANDREWS, G. K. 2012. A mouse model of acrodermatitis enteropathica: loss of intestine zinc transporter ZIP4 (Slc39a4) disrupts the stem cell niche and intestine integrity. *PLoS Genet,* 8**,** e1002766.

GERMAIN, R. N. 2002. T-cell development and the CD4–CD8 lineage decision. *Nature Reviews Immunology,* 2**,** 309.

GLASS, W. G., ROSENBERG, H. F. & MURPHY, P. M. 2003. Chemokine regulation of inflammation during acute viral infection. *Current Opinion in Allergy and Clinical Immunology,* 3**,** 467-473.

GLOBIG, A.-M., HENNECKE, N., MARTIN, B., SEIDL, M., RUF, G., HASSELBLATT, P., THIMME, R. & BENGSCH, B. 2014. Comprehensive Intestinal T Helper Cell Profiling Reveals Specific Accumulation of IFN-γ+IL-17+Coproducing CD4+ T Cells in Active Inflammatory Bowel Disease. *Inflammatory Bowel Diseases,* 20**,** 2321-2329.

GODFREY, D. I. & BERZINS, S. P. 2007. Control points in NKT-cell development. *Nature Reviews Immunology,* 7**,** 505.

GODFREY, D. I., KENNEDY, J., SUDA, T. & ZLOTNIK, A. 1993. A developmental pathway involving four phenotypically and functionally distinct subsets of CD3-CD4-CD8- triple-negative adult mouse thymocytes defined by CD44 and CD25 expression. *The Journal of Immunology,* 150**,** 4244.

GODFREY, D. I., MACDONALD, H. R., KRONENBERG, M., SMYTH, M. J. & KAER, L. V. 2004. NKT cells: what's in a name? *Nature Reviews Immunology,* 4**,** 231-237.

GODFREY, D. I., MCCLUSKEY, J. & ROSSJOHN, J. 2005. CD1d antigen presentation: treats for NKT cells. *Nature Immunology,* 6**,** 754.

GODFREY, D. I., STANKOVIC, S. & BAXTER, A. G. 2010. Raising the NKT cell family. *Nature Immunology,* 11**,** 197.

GÖKMEN, M. R., DONG, R., KANHERE, A., POWELL, N., PERUCHA, E., JACKSON, I., HOWARD, J. K., HERNANDEZ-FUENTES, M., JENNER, R. G. & LORD, G. M. 2013. Genome-wide regulatory analysis reveals T-bet controls Th17 lineage differentiation through direct suppression of IRF4. *Journal of immunology (Baltimore, Md. : 1950),* 191**,** 10.4049/jimmunol.1202254.

GORDON, J. & MANLEY, N. R. 2011. Mechanisms of thymus organogenesis and morphogenesis. *Development,* 138**,** 3865.

GORDON, SCOTT M., CHAIX, J., RUPP, LEVI J., WU, J., MADERA, S., SUN, JOSEPH C., LINDSTEN, T. & REINER, STEVEN L. 2012. The Transcription Factors T-bet and Eomes Control Key Checkpoints of Natural Killer Cell Maturation. *Immunity,* 36**,** 55-67.

GROOM, J. R. & LUSTER, A. D. 2011. CXCR3 in T cell function. *Experimental cell research,* 317**,** 620-631.

HAARBERG, K. M. K. & TAMBUR, A. R. 2014. Detection of donor-specific antibodies in kidney transplantation. *British Medical Bulletin,* 110**,** 23-34.

HAINZL, E., STOCKINGER, S., RAUCH, I., HEIDER, S., BERRY, D., LASSNIG, C., SCHWAB, C., ROSEBROCK, F., MILINOVICH, G., SCHLEDERER, M., WAGNER, M., SCHLEPER, C., LOY, A., URICH, T., KENNER, L., HAN, X., DECKER, T., STROBL, B. & MULLER, M. 2015. Intestinal Epithelial Cell Tyrosine Kinase 2 Transduces IL-22 Signals To Protect from Acute Colitis. *J Immunol,* 195**,** 5011-24.

HALUSZCZAK, C., AKUE, A. D., HAMILTON, S. E., JOHNSON, L. D. S., PUJANAUSKI, L., TEODOROVIC, L., JAMESON, S. C. & KEDL, R. M. 2009. The antigen-specific CD8(+) T cell repertoire in unimmunized mice includes memory phenotype cells bearing markers of homeostatic expansion. *The Journal of Experimental Medicine,* 206**,** 435-448.

HAMADA, H., GARCIA-HERNANDEZ, M. D. L. L., REOME, J. B., MISRA, S. K., STRUTT, T. M., MCKINSTRY, K. K., COOPER, A. M., SWAIN, S. L. & DUTTON, R. W. 2009. Tc17, a Unique Subset of CD8 T Cells That Can Protect against Lethal Influenza Challenge. *The Journal of Immunology,* 182**,** 3469.

HARBOUR, S. N., MAYNARD, C. L., ZINDL, C. L., SCHOEB, T. R. & WEAVER, C. T. 2015. Th17 cells give rise to Th1 cells that are required for the pathogenesis of colitis. *Proceedings of the National Academy of Sciences,* 112**,** 7061.

HARRINGTON, L. E., HATTON, R. D., MANGAN, P. R., TURNER, H., MURPHY, T. L., MURPHY, K. M. & WEAVER, C. T. 2005. Interleukin 17–producing CD4+ effector T cells develop via a lineage distinct from the T helper type 1 and 2 lineages. *Nature Immunology,* 6**,** 1123.

HARVIE, M., CAMBERIS, M., TANG, S.-C., DELAHUNT, B., PAUL, W. & LE GROS, G. 2010. The Lung Is an Important Site for Priming CD4 T-Cell-Mediated Protective Immunity against Gastrointestinal Helminth Parasites. *Infection and Immunity,* 78**,** 3753-3762.

HATTON, R. D., HARRINGTON, L. E., LUTHER, R. J., WAKEFIELD, T., JANOWSKI, K. M., OLIVER, J. R., LALLONE, R. L., MURPHY, K. M. & WEAVER, C. T. 2006. A Distal Conserved Sequence Element Controls Ifng Gene Expression by T Cells and NK Cells. *Immunity,* 25**,** 717-729.

HAYDAY, A. & PAO, W. 1998. T Cell Receptor, γδ A2 - Delves, Peter J. *Encyclopedia of Immunology (Second Edition).* Oxford: Elsevier.

HAYDAY, A. C. 2000. γδ Cells: A Right Time and a Right Place for a Conserved Third Way of Protection. *Annual Review of Immunology,* 18**,** 975-1026.

HAYDAY, A. C., SAITO, H., GILLIES, S. D., KRANZ, D. M., TANIGAWA, G., EISEN, H. N. & TONEGAWA, S. 1985. Structure, organization, and somatic rearrangement of T cell gamma genes. *Cell,* 40**,** 259-269.

HEGAZY, A. N., PEINE, M., HELMSTETTER, C., PANSE, I., FRÖHLICH, A., BERGTHALER, A., FLATZ, L., PINSCHEWER, D. D., RADBRUCH, A. & LÖHNING, M. 2010. Interferons Direct Th2 Cell

Reprogramming to Generate a Stable GATA-3+T-bet+ Cell Subset with Combined Th2 and Th1 Cell Functions. *Immunity,* 32**,** 116-128.

HENSHALL, T. L., JONES, K. L., WILKINSON, R. & JACKSON, D. E. 2001. Src Homology 2 Domain-Containing Protein-Tyrosine Phosphatases, SHP-1 and SHP-2, Are Required for Platelet Endothelial Cell Adhesion Molecule-1/CD31-Mediated Inhibitory Signaling. *The Journal of Immunology,* 166**,** 3098.

HERTWECK, A., EVANS, CATHERINE M., ESKANDARPOUR, M., LAU, JONATHAN C., OLEINIKA, K., JACKSON, I., KELLY, A., AMBROSE, J., ADAMSON, P., COUSINS, DAVID J., LAVENDER, P., CALDER, VIRGINIA L., LORD, GRAHAM M. & JENNER, RICHARD G. 2016. T-bet Activates Th1 Genes through Mediator and the Super Elongation Complex. *Cell Reports,* 15**,** 2756-2770.

HINRICHS, C. S., KAISER, A., PAULOS, C. M., CASSARD, L., SANCHEZ-PEREZ, L., HEEMSKERK, B., WRZESINSKI, C., BORMAN, Z. A., MURANSKI, P. & RESTIFO, N. P. 2009. Type 17 CD8⁺ T cells display enhanced antitumor immunity. *Blood,* 114**,** 596.

HIROTA, K., DUARTE, J. H., VELDHOEN, M., HORNSBY, E., LI, Y., CUA, D. J., AHLFORS, H., WILHELM, C., TOLAINI, M., MENZEL, U., GAREFALAKI, A., POTOCNIK, A. J. & STOCKINGER, B. 2011. Fate mapping of IL-17-producing T cells in inflammatory responses. *Nature Immunology,* 12**,** 255.

HORI, S., NOMURA, T. & SAKAGUCHI, S. 2003. Control of Regulatory T Cell Development by the Transcription Factor <em>Foxp3</em&gt. *Science,* 299**,** 1057.

HORTON AMY, C. & GIBSON-BROWN JEREMY, J. 2002. Evolution of developmental functions by the Eomesodermin, T-brain-1, Tbx21 subfamily of T-box genes: insights from amphioxus. *Journal of Experimental Zoology,* 294**,** 112-121.

HSIEH, C. S., MACATONIA, S. E., TRIPP, C. S., WOLF, S. F., GARRA, A. & MURPHY, K. M. 1993. Development of TH1 CD4+ T cells through IL-12 produced by Listeria-induced macrophages. *Science,* 260**,** 547.

HU, J. & AUGUST, A. 2008. Naïve and Innate Memory phenotype CD4(+) T-cells have different requirements for active Itk for their development. *Journal of immunology (Baltimore, Md. : 1950),* 180**,** 6544-6552.

HUBER, M., HEINK, S., PAGENSTECHER, A., REINHARD, K., RITTER, J., VISEKRUNA, A., GURALNIK, A., BOLLIG, N., JELTSCH, K., HEINEMANN, C., WITTMANN, E., BUCH, T., DA COSTA, O. P., BRÜSTLE, A., BRENNER, D., MAK, T. W., MITTRÜCKER, H.-W., TACKENBERG, B., KAMRADT, T. & LOHOFF, M. 2013. IL-17A secretion by CD8+ T cells supports Th17-mediated autoimmune encephalomyelitis. *The Journal of Clinical Investigation,* 123**,** 247-260.

HUE, S., AHERN, P., BUONOCORE, S., KULLBERG, M. C., CUA, D. J., MCKENZIE, B. S., POWRIE, F. & MALOY, K. J. 2006. Interleukin-23 drives innate and T cell–mediated intestinal inflammation. *J Exp Med,* 203**,** 2473-2483.

HWANG, E. S., SZABO, S. J., SCHWARTZBERG, P. L. & GLIMCHER, L. H. 2005. T Helper Cell Fate Specified by Kinase-Mediated Interaction of T-bet with GATA-3. *Science,* 307**,** 430.

IGNACIO, A., BREDA, C. N. S. & CAMARA, N. O. S. 2017. Innate lymphoid cells in tissue homeostasis and diseases. *World J Hepatol,* 9**,** 979-989.

INTLEKOFER, A. M., TAKEMOTO, N., KAO, C., BANERJEE, A., SCHAMBACH, F., NORTHROP, J. K., SHEN, H., WHERRY, E. J. & REINER, S. L. 2007. Requirement for T-bet in the aberrant differentiation of unhelped memory CD8⁺ T cells. *J Exp Med,* 204**,** 2015.

INTLEKOFER, A. M., TAKEMOTO, N., WHERRY, E. J., LONGWORTH, S. A., NORTHRUP, J. T., PALANIVEL, V. R., MULLEN, A. C., GASINK, C. R., KAECH, S. M., MILLER, J. D., GAPIN, L., RYAN, K., RUSS, A. P., LINDSTEN, T., ORANGE, J. S., GOLDRATH, A. W., AHMED, R. & REINER, S. L. 2005. Effector and memory CD8+ T cell fate coupled by T-bet and eomesodermin. *Nature Immunology,* 6**,** 1236.

ITO, K., YANAGIDA, A., OKADA, K., YAMAZAKI, Y., NAKAUCHI, H. & KAMIYA, A. 2013. Mesenchymal progenitor cells in mouse foetal liver regulate differentiation and proliferation of hepatoblasts. *Liver International,* 34**,** 1378-1390.

ITO, R., KITA, M., SHIN-YA, M., KISHIDA, T., URANO, A., TAKADA, R., SAKAGAMI, J., IMANISHI, J., IWAKURA, Y., OKANOUE, T., YOSHIKAWA, T., KATAOKA, K. & MAZDA, O. 2008. Involvement of IL-17A in the pathogenesis of DSS-induced colitis in mice. *Biochemical and Biophysical Research Communications,* 377**,** 12-16.

ITO, R., SHIN-YA, M., KISHIDA, T., URANO, A., TAKADA, R., SAKAGAMI, J., IMANISHI, J., KITA, M., UEDA, Y., IWAKURA, Y., KATAOKA, K., OKANOUE, T. & MAZDA, O. 2006. Interferon-gamma is causatively involved in experimental inflammatory bowel disease in mice. *Clinical and Experimental Immunology,* 146**,** 330-338.

IVANOV, I. I., MCKENZIE, B. S., ZHOU, L., TADOKORO, C. E., LEPELLEY, A., LAFAILLE, J. J., CUA, D. J. & LITTMAN, D. R. 2006. The Orphan Nuclear Receptor RORγt Directs the Differentiation Program of Proinflammatory IL-17⁺ T Helper Cells. *Cell,* 126**,** 1121-1133.

IWASAKI, A. & MEDZHITOV, R. 2015. Control of adaptive immunity by the innate immune system. *Nature Immunology,* 16**,** 343.

IZCUE, A., COOMBES JANINE, L. & POWRIE, F. 2006. Regulatory T cells suppress systemic and mucosal immune activation to control intestinal inflammation. *Immunological Reviews,* 212**,** 256-271.

IZCUE, A. & POWRIE, F. 2008. Special regulatory T-cell review: regulatory T cells and the intestinal tract – patrolling the frontier. *Immunology,* 123**,** 6-10.

JANKOVIC, M., CASELLAS, R., YANNOUTSOS, N., WARDEMANN, H. & NUSSENZWEIG, M. C. 2004. RAGs and Regulation of Autoantibodies. *Annual Review of Immunology,* 22**,** 485-501.

JENNER, R. G., TOWNSEND, M. J., JACKSON, I., SUN, K., BOUWMAN, R. D., YOUNG, R. A., GLIMCHER, L. H. & LORD, G. M. 2009. The transcription factors T-bet and GATA-3 control alternative pathways of T-cell differentiation through a shared set of target genes. *Proceedings of the National Academy of Sciences,* 106**,** 17876.

JENSEN, K. D. C., SU, X., SHIN, S., LI, L., YOUSSEF, S., YAMASAKI, S., STEINMAN, L., SAITO, T., LOCKSLEY, R. M., DAVIS, M. M., BAUMGARTH, N. & CHIEN, Y.-H. 2008. Thymic Selection Determines γδ T Cell Effector Fate: Antigen-Naive Cells Make Interleukin-17 and Antigen-Experienced Cells Make Interferon γ. *Immunity,* 29**,** 90-100.

JOSEFOWICZ, S. Z. & RUDENSKY, A. 2009. Control of regulatory T cell lineage commitment and maintenance. *Immunity,* 30**,** 616-625.

JOSHI, N. S., CUI, W., DOMINGUEZ, C. X., CHEN, J. H., HAND, T. W. & KAECH, S. M. 2011. Increased Numbers of Preexisting Memory CD8 T Cells and Decreased T-bet Expression Can Restrain Terminal Differentiation of Secondary Effector and Memory CD8 T Cells. *The Journal of Immunology,* 187**,** 4068.

KAECH, S. M. & CUI, W. 2012a. Transcriptional control of effector and memory CD8(+) T cell differentiation. *Nature reviews. Immunology,* 12**,** 749-761.

KAECH, S. M. & CUI, W. 2012b. Transcriptional control of effector and memory CD8+ T cell differentiation. *Nature Reviews Immunology,* 12**,** 749.

KANHERE, A., HERTWECK, A., BHATIA, U., GÖKMEN, M. R., PERUCHA, E., JACKSON, I., LORD, G. M. & JENNER, R. G. 2012. T-bet and GATA3 orchestrate Th1 and Th2 differentiation through lineage-specific targeting of distal regulatory elements. *Nature Communications,* 3**,** 1268.

KAWABE, T., JANKOVIC, D., KAWABE, S., HUANG, Y., LEE, P.-H., YAMANE, H., ZHU, J., SHER, A., GERMAIN, R. N. & PAUL, W. E. 2017. Memory-phenotype CD4(+) T cells spontaneously generated under steady state conditions exert innate Th1-like effector function. *Science immunology,* 2**,** eaam9304.

KIESLER, P., FUSS, I. J. & STROBER, W. 2015. Experimental Models of Inflammatory Bowel Diseases. *Cellular and Molecular Gastroenterology and Hepatology,* 1**,** 154-170.

KILLAR, L., MACDONALD, G., WEST, J., WOODS, A. & BOTTOMLY, K. 1987. Cloned, Ia-restricted T cells that do not produce interleukin 4(IL 4)/B cell stimulatory factor 1(BSF-1) fail to help antigen-specific B cells. *The Journal of Immunology,* 138**,** 1674.

KIM, C. H. 2004. Chemokine-chemokine receptor network in immune cell trafficking. *Current Drug Targets: Immune, Endocrine and Metabolic Disorders,* 4**,** 343-361.

KIM, H.-J., WANG, X., RADFAR, S., SPROULE, T. J., ROOPENIAN, D. C. & CANTOR, H. 2011. CD8⁺ T regulatory cells express the Ly49 Class I MHC receptor and are defective in autoimmune prone B6-Yaa mice. *Proceedings of the National Academy of Sciences,* 108**,** 2010.

KIM, K. S., HONG, S.-W., HAN, D., YI, J., JUNG, J., YANG, B.-G., LEE, J. Y., LEE, M. & SURH, C. D. 2016. Dietary antigens limit mucosal immunity by inducing regulatory T cells in the small intestine. *Science,* 351**,** 858-863.

KLOSE, C. S. N., FLACH, M., MOHLE, L., ROGELL, L., HOYLER, T., EBERT, K., FABIUNKE, C., PFEIFER, D., SEXL, V., FONSECA-PEREIRA, D., DOMINGUES, R. G., VEIGA-FERNANDES, H., ARNOLD, S. J., BUSSLINGER, M., DUNAY, I. R., TANRIVER, Y. & DIEFENBACH, A. 2014. Differentiation of type 1 ILCs from a common progenitor to all helper-like innate lymphoid cell lineages. *Cell,* 157**,** 340-356.

KLOSE, C. S. N., KISS, E. A., SCHWIERZECK, V., EBERT, K., HOYLER, T., D'HARGUES, Y., GÖPPERT, N., CROXFORD, A. L., WAISMAN, A., TANRIVER, Y. & DIEFENBACH, A. 2013. A T-bet gradient controls the fate and function of CCR6−RORγt+ innate lymphoid cells. *Nature,* 494**,** 261.

KNIGHT, S. C. & STAGG, A. J. 1993. Antigen-presenting cell types. *Current Opinion in Immunology,* 5**,** 374-382.

KOBAYASHI, H. & TANAKA, Y. 2015. γδ T Cell Immunotherapy—A Review. *Pharmaceuticals,* 8**,** 40-61.

KOCH, MEGHAN A., THOMAS, KERRI R., PERDUE, NIKOLE R., SMIGIEL, KATE S., SRIVASTAVA, S. & CAMPBELL, DANIEL J. 2012. T-bet⁺ Treg Cells Undergo Abortive Th1 Cell Differentiation due to Impaired Expression of IL-12 Receptor β2. *Immunity,* 37**,** 501-510.

KOCH, M. A., TUCKER-HEARD, G. S., PERDUE, N. R., KILLEBREW, J. R., URDAHL, K. B. & CAMPBELL, D. J. 2009a. T-bet controls regulatory T cell homeostasis and function during type-1 inflammation. *Nature Immunology,* 10**,** 595-602.

KOCH, M. A., TUCKER-HEARD, G. S., PERDUE, N. R., KILLEBREW, J. R., URDAHL, K. B. & CAMPBELL, D. J. 2009b. The transcription factor T-bet controls regulatory T cell homeostasis and function during type 1 inflammation. *Nature Immunology,* 10**,** 595.

KOHLER, S. & THIEL, A. 2009. Life after the thymus: CD31⁺ and CD31[−] human naive CD4⁺ T-cell subsets. *Blood,* 113**,** 769-774.

KONDO, M., WEISSMAN, I. L. & AKASHI, K. 1997. Identification of Clonogenic Common Lymphoid Progenitors in Mouse Bone Marrow. *Cell,* 91**,** 661-672.

KORTEKAAS KROHN, I., SHIKHAGAIE, M. M., GOLEBSKI, K., BERNINK, J. H., BREYNAERT, C., CREYNS, B., DIAMANT, Z., FOKKENS, W. J., GEVAERT, P., HELLINGS, P., HENDRIKS, R. W., KLIMEK, L., MJÖSBERG, J., MORITA, H., OGG, G. S., O'MAHONY, L., SCHWARZE, J., SEYS, S. F., SHAMJI, M. H. & BAL, S. M. 2017. Emerging roles of innate lymphoid cells in inflammatory diseases: Clinical implications. *Allergy,* 73**,** 837-850.

LANTZ, O. & BENDELAC, A. 1994. An invariant T cell receptor alpha chain is used by a unique subset of major histocompatibility complex class I-specific CD4+ and CD4-8- T cells in mice and humans. *J Exp Med,* 180**,** 1097.

LAZAREVIC, V., CHEN, X., SHIM, J.-H., HWANG, E.-S., JANG, E., BOLM, A. N., OUKKA, M., KUCHROO, V. K. & GLIMCHER, L. H. 2010. T-bet represses TH17 differentiation by preventing Runx1-mediated activation of the gene encoding RORγt. *Nature Immunology,* 12**,** 96.

LAZAREVIC, V. & GLIMCHER, L. H. 2011. T-bet in disease. *Nature Immunology,* 12**,** 597.

LAZAREVIC, V., GLIMCHER, L. H. & LORD, G. M. 2013. T-bet: a bridge between innate and adaptive immunity. *Nature Reviews Immunology,* 13**,** 777.

LE GROS, G., BEN-SASSON, S. Z., SEDER, R., FINKELMAN, F. D. & PAUL, W. E. 1990. Generation of interleukin 4 (IL-4)-producing cells in vivo and in vitro: IL-2 and IL-4 are required for in vitro generation of IL-4-producing cells. *J Exp Med,* 172**,** 921.

LEBIEN, T. W. & TEDDER, T. F. 2008. B lymphocytes: how they develop and function. *Blood,* 112**,** 1570.

LEE, I., WANG, L., WELLS, A. D., DORF, M. E., OZKAYNAK, E. & HANCOCK, W. W. 2005. Recruitment of Foxp3⁺ T regulatory cells mediating allograft tolerance depends on the CCR4 chemokine receptor. *J Exp Med,* 201**,** 1037.

LEE, J.-Y., HAMILTON, S. E., AKUE, A. D., HOGQUIST, K. A. & JAMESON, S. C. 2013. Virtual memory CD8 T cells display unique functional properties. *Proceedings of the National Academy of Sciences of the United States of America,* 110**,** 13498-13503.

LEE, Y. K., MUKASA, R., HATTON, R. D. & WEAVER, C. T. 2009. Developmental plasticity of Th17 and Treg cells. *Current Opinion in Immunology,* 21**,** 274-280.

LEFEBVRE, J. S. & HAYNES, L. 2012. Aging of the CD4 T Cell Compartment. *Open Longevity Science,* 6**,** 83-91.

LENAERTS, A. J., JOHNSON, C. M., MARRIETA, K. S., GRUPPO, V. & ORME, I. M. 2005. Significant increases in the levels of liver enzymes in mice treated with anti-tuberculosis drugs. *International Journal of Antimicrobial Agents,* 26**,** 152-158.

LEVINE, A. G., MENDOZA, A., HEMMERS, S., MOLTEDO, B., NIEC, R. E., SCHIZAS, M., HOYOS, B. E., PUTINTSEVA, E. V., CHAUDHRY, A., DIKIY, S., FUJISAWA, S., CHUDAKOV, D. M., TREUTING, P. M. & RUDENSKY, A. Y. 2017. Stability and function of regulatory T cells expressing the transcription factor T-bet. *Nature,* 546**,** 421.

LEVY, D. E. & DARNELL, J. E. 2002. STATs: transcriptional control and biological impact. *Nature Reviews Molecular Cell Biology,* 3**,** 651-662.

LI, L. J., GONG, C., ZHAO, M. H. & FENG, B. S. 2014. Role of interleukin-22 in inflammatory bowel disease. *World J Gastroenterol,* 20**,** 18177-88.

LI, W. X. 2008. Canonical and non-canonical JAK-STAT signaling. *Trends in cell biology,* 18**,** 545-551.

LICONA-LIMÓN, P., KIM, L. K., PALM, N. W. & FLAVELL, R. A. 2013. TH2, allergy and group 2 innate lymphoid cells. *Nature Immunology,* 14**,** 536.

LIGHVANI, A. A., FRUCHT, D. M., JANKOVIC, D., YAMANE, H., ALIBERTI, J., HISSONG, B. D., NGUYEN, B. V., GADINA, M., SHER, A., PAUL, W. E. & SHEA, J. J. 2001. T-bet is rapidly induced by interferon-γ in lymphoid and myeloid cells. *Proceedings of the National Academy of Sciences,* 98**,** 15137.

LIU, M. & ZHANG, C. 2017. The Role of Innate Lymphoid Cells in Immune-Mediated Liver Diseases. *Frontiers in Immunology,* 8**,** 695.

LIU, N., OHNISHI, N., NI, L., AKIRA, S. & BACON, K. B. 2003. CpG directly induces T-bet expression and inhibits IgG1 and IgE switching in B cells. *Nature Immunology,* 4**,** 687.

LIU, Z., COLPAERT, S., D'HAENS, G. R., KASRAN, A., DE BOER, M., RUTGEERTS, P., GEBOES, K. & CEUPPENS, J. L. 1999. Hyperexpression of CD40 ligand (CD154) in inflammatory bowel disease and its contribution to pathogenic cytokine production. *Journal of Immunology,* 163**,** 4049-4057.

LIU, Z., GEBOES, K., COLPAERT, S., OVERBERGH, L., MATHIEU, C., HEREMANS, H., DE BOER, M., BOON, L., D'HAENS, G., RUTGEERTS, P. & CEUPPENS, J. L. 2000. Prevention of Experimental Colitis in SCID Mice Reconstituted with CD45RB^{high} CD4⁺ T Cells by Blocking the CD40-CD154 Interactions. *The Journal of Immunology,* 164**,** 6005.

LORD, G. M., RAO, R. M., CHOE, H., SULLIVAN, B. M., LICHTMAN, A. H., LUSCINSKAS, F. W. & GLIMCHER, L. H. 2005. T-bet is required for optimal proinflammatory CD4⁺ T-cell trafficking. *Blood,* 106**,** 3432.

LU, Y.-C., YEH, W.-C. & OHASHI, P. S. 2008. LPS/TLR4 signal transduction pathway. *Cytokine,* 42**,** 145-151.

LUCI, C., REYNDERS, A., IVANOV, I. I., COGNET, C., CHICHE, L., CHASSON, L., HARDWIGSEN, J., ANGUIANO, E., BANCHEREAU, J., CHAUSSABEL, D., DALOD, M., LITTMAN, D. R., VIVIER, E. & TOMASELLO, E. 2008. Influence of the transcription factor RORγt on the development of NKp46+ cell populations in gut and skin. *Nature Immunology,* 10**,** 75.

LUCKETT-CHASTAIN, L., CALHOUN, K., KEMP, J. & GALLUCCI, R. 2015. Immunological difference in Th1 and Th2 dominant mouse strains in an ICD model. (IRM15P.601). *The Journal of Immunology,* 194**,** 199.13.

LUGO-VILLARINO, G., ITO, S.-I., KLINMAN, D. M. & GLIMCHER, L. H. 2005. The adjuvant activity of CpG DNA requires T-bet expression in dendritic cells. *Proceedings of the National Academy of Sciences of the United States of America,* 102**,** 13248.

LUGO-VILLARINO, G., MALDONADO-LÓPEZ, R., POSSEMATO, R., PEÑARANDA, C. & GLIMCHER, L. H. 2003. T-bet is required for optimal production of IFN-γ and antigen-specific T cell activation by dendritic cells. *Proceedings of the National Academy of Sciences,* 100**,** 7749.

MALISAN, F., BRIÈRE, F., BRIDON, J. M., HARINDRANATH, N., MILLS, F. C., MAX, E. E., BANCHEREAU, J. & MARTINEZ-VALDEZ, H. 1996. Interleukin-10 induces immunoglobulin G isotype switch recombination in human CD40-activated naive B lymphocytes. *The Journal of Experimental Medicine,* 183**,** 937.

MAN, K., MIASARI, M., SHI, W., XIN, A., HENSTRIDGE, D. C., PRESTON, S., PELLEGRINI, M., BELZ, G. T., SMYTH, G. K., FEBBRAIO, M. A., NUTT, S. L. & KALLIES, A. 2013. The transcription factor IRF4 is essential for TCR affinity–mediated metabolic programming and clonal expansion of T cells. *Nature Immunology,* 14**,** 1155.

MANGAN, P. R., HARRINGTON, L. E., O'QUINN, D. B., HELMS, W. S., BULLARD, D. C., ELSON, C. O., HATTON, R. D., WAHL, S. M., SCHOEB, T. R. & WEAVER, C. T. 2006. Transforming growth factor-β induces development of the TH17 lineage. *Nature,* 441**,** 231.

MARQUARDT, N., BÉZIAT, V., NYSTRÖM, S., HENGST, J., IVARSSON, M. A., KEKÄLÄINEN, E., JOHANSSON, H., MJÖSBERG, J., WESTGREN, M., LANKISCH, T. O., WEDEMEYER, H., ELLIS, E. C., LJUNGGREN, H.-G., MICHAËLSSON, J. & BJÖRKSTRÖM, N. K. 2015. Cutting Edge: Identification and Characterization of Human Intrahepatic CD49a⁺ NK Cells. *The Journal of Immunology,* 194**,** 2467.

MARSHALL, HEATHER D., CHANDELE, A., JUNG, YONG W., MENG, H., POHOLEK, AMANDA C., PARISH, IAN A., RUTISHAUSER, R., CUI, W., KLEINSTEIN, STEVEN H., CRAFT, J. & KAECH, SUSAN M. 2011. Differential Expression of Ly6C and T-bet Distinguish Effector and Memory Th1 CD4+ Cell Properties during Viral Infection. *Immunity,* 35**,** 633-646.

MARTIN, B., HIROTA, K., CUA, D. J., STOCKINGER, B. & VELDHOEN, M. 2009. Interleukin-17-Producing γδ T Cells Selectively Expand in Response to Pathogen Products and Environmental Signals. *Immunity,* 31**,** 321-330.

MATSUDA, J. L., ZHANG, Q., NDONYE, R., RICHARDSON, S. K., HOWELL, A. R. & GAPIN, L. 2006. T-bet concomitantly controls migration, survival, and effector functions during the development of Vα14i NKT cells. *Blood,* 107**,** 2797-2805.

MCKENZIE, ANDREW N. J., SPITS, H. & EBERL, G. 2014. Innate Lymphoid Cells in Inflammation and Immunity. *Immunity,* 41**,** 366-374.

MCPHERSON, R. C., TURNER, D. G., MAIR, I., O'CONNOR, R. A. & ANDERTON, S. M. 2015. T-bet Expression by Foxp3(+) T Regulatory Cells is Not Essential for Their Suppressive Function in CNS Autoimmune Disease or Colitis. *Frontiers in Immunology,* 6**,** 69.

MEDINA, K. L. 2016. Chapter 4 - Overview of the immune system. *In:* PITTOCK, S. J. & VINCENT, A. (eds.) *Handbook of Clinical Neurology.* Elsevier.

MEDZHITOV, R. & JANEWAY, C. 2000. Innate Immunity. *New England Journal of Medicine,* 343**,** 338-344.

MELO-GONZALEZ, F. & HEPWORTH, M. R. 2017. Functional and phenotypic heterogeneity of group 3 innate lymphoid cells. *Immunology,* 150**,** 265-275.

METZGER, D., CLIFFORD, J., CHIBA, H. & CHAMBON, P. 1995. Conditional site-specific recombination in mammalian cells using a ligand-dependent chimeric Cre recombinase. *Proceedings of the National Academy of Sciences,* 92**,** 6991.

MILLER SARA, A. & WEINMANN AMY, S. 2010. Molecular mechanisms by which T-bet regulates T-helper cell commitment. *Immunological Reviews,* 238**,** 233-246.

MITTRÜCKER, H.-W., VISEKRUNA, A. & HUBER, M. 2014. Heterogeneity in the Differentiation and Function of CD8+ T Cells. *Archivum Immunologiae et Therapiae Experimentalis,* 62**,** 449-458.

MIZOGUCHI, A. 2012. Animal Models of Inflammatory Bowel Disease. *In:* CONN, P. M. (ed.) *Progress in Molecular Biology and Translational Science.* Academic Press.

MIZOGUCHI, A., YANO, A., HIMURO, H., EZAKI, Y., SADANAGA, T. & MIZOGUCHI, E. 2018. Clinical importance of IL-22 cascade in IBD. *J Gastroenterol,* 53**,** 465-474.

MJÖSBERG, J. M., TRIFARI, S., CRELLIN, N. K., PETERS, C. P., VAN DRUNEN, C. M., PIET, B., FOKKENS, W. J., CUPEDO, T. & SPITS, H. 2011. Human IL-25- and IL-33-responsive type 2 innate lymphoid cells are defined by expression of CRTH2 and CD161. *Nature Immunology,* 12**,** 1055.

MOGENSEN, T. H. 2009. Pathogen recognition and inflammatory signaling in innate immune defenses. *Clinical microbiology reviews,* 22**,** 240-273.

MOHAMED, R. & LORD GRAHAM, M. 2016. T-bet as a key regulator of mucosal immunity. *Immunology,* 147**,** 367-376.

MOHAMMADI, R., HOSSEINI-SAFA, A., EHSANI ARDAKANI, M. J. & ROSTAMI-NEJAD, M. 2015. The relationship between intestinal parasites and some immune-mediated intestinal conditions. *Gastroenterology and hepatology from bed to bench,* 8**,** 123-131.

MOMBAERTS, P., IACOMINI, J., JOHNSON, R. S., HERRUP, K., TONEGAWA, S. & PAPAIOANNOU, V. E. 1992. RAG-1-deficient mice have no mature B and T lymphocytes. *Cell,* 68**,** 869-77.

MONTICELLI, L. A., SONNENBERG, G. F., ABT, M. C., ALENGHAT, T., ZIEGLER, C. G. K., DOERING, T. A., ANGELOSANTO, J. M., LAIDLAW, B. J., YANG, C. Y., SATHALIYAWALA, T., KUBOTA, M., TURNER, D., DIAMOND, J. M., GOLDRATH, A. W., FARBER, D. L., COLLMAN, R. G., WHERRY, E. J. & ARTIS, D. 2011. Innate lymphoid cells promote lung-tissue homeostasis after infection with influenza virus. *Nature Immunology,* 12**,** 1045.

MORO-GARCÍA, M. A., ALONSO-ARIAS, R. & LÓPEZ-LARREA, C. 2013. When Aging Reaches CD4+ T-Cells: Phenotypic and Functional Changes. *Frontiers in Immunology,* 4**,** 107.

MORO, K., YAMADA, T., TANABE, M., TAKEUCHI, T., IKAWA, T., KAWAMOTO, H., FURUSAWA, J.-I., OHTANI, M., FUJII, H. & KOYASU, S. 2009. Innate production of TH2 cytokines by adipose tissue-associated c-Kit+Sca-1+ lymphoid cells. *Nature,* 463**,** 540.

MORRIS, D. H. & BULLOCK, F. D. 1919. THE IMPORTANCE OF THE SPLEEN IN RESISTANCE TO INFECTION. *Annals of Surgery,* 70**,** 513-521.

MORRISON, P. J., BENDING, D., FOUSER, L. A., WRIGHT, J. F., STOCKINGER, B., COOKE, A. & KULLBERG, M. C. 2013. Th17-cell plasticity in Helicobacter hepaticus–induced intestinal inflammation. *Mucosal Immunology,* 6**,** 1143.

MOSMANN, T. R., CHERWINSKI, H., BOND, M. W., GIEDLIN, M. A. & COFFMAN, R. L. 1986. Two types of murine helper T cell clone. I. Definition according to profiles of lymphokine activities and secreted proteins. *The Journal of Immunology,* 136**,** 2348.

MOTTET, C., UHLIG, H. H. & POWRIE, F. 2003. Cutting Edge: Cure of Colitis by CD4<sup>+</sup&gtCD25⁺ Regulatory T Cells. *The Journal of Immunology,* 170**,** 3939.

MUELLER, S. N. & MACKAY, L. K. 2015. Tissue-resident memory T cells: local specialists in immune defence. *Nature Reviews Immunology,* 16**,** 79.

MULLEN, A. C., HIGH, F. A., HUTCHINS, A. S., LEE, H. W., VILLARINO, A. V., LIVINGSTON, D. M., KUNG, A. L., CEREB, N., YAO, T.-P., YANG, S. Y. & REINER, S. L. 2001. Role of T-bet in Commitment of T_H1 Cells Before IL-12-Dependent Selection. *Science,* 292**,** 1907.

MURPHY, E., SHIBUYA, K., HOSKEN, N., OPENSHAW, P., MAINO, V., DAVIS, K., MURPHY, K. & GARRA, A. 1996. Reversibility of T helper 1 and 2 populations is lost after long-term stimulation. *The Journal of Experimental Medicine,* 183**,** 901.

MYLES, A., GEARHART, P. J. & CANCRO, M. P. 2017. Signals that drive T-bet expression in B cells. *Cellular Immunology,* 321**,** 3-7.

NAKAYAMADA, S., TAKAHASHI, H., KANNO, Y. & O'SHEA, J. J. 2012. Helper T cell diversity and plasticity. *Current Opinion in Immunology,* 24**,** 297-302.

NEILL, D. R., WONG, S. H., BELLOSI, A., FLYNN, R. J., DALY, M., LANGFORD, T. K. A., BUCKS, C., KANE, C. M., FALLON, P. G., PANNELL, R., JOLIN, H. E. & MCKENZIE, A. N. J. 2010. Nuocytes represent a new innate effector leukocyte that mediates type-2 immunity. *Nature,* 464**,** 1367.

NEURATH, M. F., WEIGMANN, B., FINOTTO, S., GLICKMAN, J., NIEUWENHUIS, E., IIJIMA, H., MIZOGUCHI, A., MIZOGUCHI, E., MUDTER, J., GALLE, P. R., BHAN, A., AUTSCHBACH, F., SULLIVAN, B. M., SZABO, S. J., GLIMCHER, L. H. & BLUMBERG, R. S. 2002. The Transcription Factor T-bet Regulates Mucosal T Cell Activation in Experimental Colitis and Crohn's Disease. *The Journal of Experimental Medicine,* 195**,** 1129.

NEWTON-NASH, D. K. & NEWMAN, P. J. 1999. A New Role for Platelet-Endothelial Cell Adhesion Molecule-1 (CD31): Inhibition of TCR-Mediated Signal Transduction. *The Journal of Immunology,* 163**,** 682.

NICHOLAS CRISPS, I. 1994. Fatal interactions: fas-induced apoptosis of mature T cells. *Immunity,* 1**,** 347-349.

NIKOLICH-ŽUGICH, J. 2005. T cell aging: naive but not young. *The Journal of Experimental Medicine,* 201**,** 837-840.

NISTALA, K., ADAMS, S., CAMBROOK, H., URSU, S., OLIVITO, B., DE JAGER, W., EVANS, J. G., CIMAZ, R., BAJAJ-ELLIOTT, M. & WEDDERBURN, L. R. 2010. Th17 plasticity in human autoimmune arthritis is driven by the inflammatory environment. *Proceedings of the National Academy of Sciences of the United States of America,* 107**,** 14751-14756.

O'SHEA, J. J., LAHESMAA, R., VAHEDI, G., LAURENCE, A. & KANNO, Y. 2011. Genomic views of STAT function in CD4+ T helper cell differentiation. *Nature Reviews Immunology,* 11**,** 239.

O'SHEA, J. J. & MURRAY, P. J. 2008. Cytokine Signaling Modules in Inflammatory Responses. *Immunity,* 28**,** 477-487.

O'SHEA, J. J. & PAUL, W. E. 2010. Mechanisms Underlying Lineage Commitment and Plasticity of Helper CD4⁺ T Cells. *Science,* 327**,** 1098.

OGHUMU, S., DONG, R., VARIKUTI, S., SHAWLER, T., KAMPFRATH, T., TERRAZAS, C. A., LEZAMA-DAVILA, C., AHMER, B. M. M., WHITACRE, C. C., RAJAGOPALAN, S., LOCKSLEY, R., SHARPE, A. H. & SATOSKAR, A. R. 2013. Distinct Populations of Innate CD8⁺ T Cells Revealed in a CXCR3 Reporter Mouse. *The Journal of Immunology,* 190**,** 2229.

OHKUSA, T. 1985. Production of experimental ulcerative colitis in hamsters by dextran sulfate sodium and changes in intestinal microflora. Nihon Shokakibyo Gakkai zasshi: Japan J Gastroenterol. 1985; 82 (5): 1327–36. Epub 1985/05/01. Google Scholar.

OHNE, Y., SILVER, J. S., THOMPSON-SNIPES, L., COLLET, M. A., BLANCK, J. P., CANTAREL, B. L., COPENHAVER, A. M., HUMBLES, A. A. & LIU, Y.-J. 2016. IL-1 is a critical regulator of group 2 innate lymphoid cell function and plasticity. *Nature Immunology,* 17**,** 646.

OKAYASU, I., HATAKEYAMA, S., YAMADA, M., OHKUSA, T., INAGAKI, Y. & NAKAYA, R. 1990. A novel method in the induction of reliable experimental acute and chronic ulcerative colitis in mice. *Gastroenterology,* 98**,** 694-702.

OMORI, M., YAMASHITA, M., INAMI, M., UKAI-TADENUMA, M., KIMURA, M., NIGO, Y., HOSOKAWA, H., HASEGAWA, A., TANIGUCHI, M. & NAKAYAMA, T. 2003. CD8 T Cell-Specific Downregulation of Histone Hyperacetylation and Gene Activation of the IL-4 Gene Locus by ROG, Repressor of GATA. *Immunity,* 19**,** 281-294.

OPPENHEIM, J. J. 2001. Cytokines: past, present, and future. *Int J Hematol,* 74**,** 3-8.

OSTANIN, D. V., BAO, J., KOBOZIEV, I., GRAY, L., ROBINSON-JACKSON, S. A., KOSLOSKI-DAVIDSON, M., PRICE, V. H. & GRISHAM, M. B. 2009. T cell transfer model of chronic colitis: concepts, considerations, and tricks of the trade. *American Journal of Physiology - Gastrointestinal and Liver Physiology,* 296**,** G135-G146.

PALMER, D. 2013. The Effect of Age on Thymic Function. *Frontiers in Immunology,* 4.

PANDIYAN, P. & ZHU, J. 2015. Origin and functions of pro-inflammatory cytokine producing Foxp3(+) regulatory T cells. *Cytokine,* 76**,** 13-24.

PANG, D. J., NEVES, J. F., SUMARIA, N. & PENNINGTON, D. J. 2012. Understanding the complexity of γδ T-cell subsets in mouse and human. *Immunology,* 136**,** 283-290.

PAPAIOANNOU, N. E., PASZTOI, M. & SCHRAML, B. U. 2019. Understanding the Functional Properties of Neonatal Dendritic Cells: A Doorway to Enhance Vaccine Effectiveness? *Frontiers in Immunology,* 9.

PARIGI, S. M., CZARNEWSKI, P., DAS, S., STEEG, C., BROCKMANN, L., FERNANDEZ-GAITERO, S., YMAN, V., FORKEL, M., HÖÖG, C., MJÖSBERG, J., WESTERBERG, L., FÄRNERT, A., HUBER, S., JACOBS, T. & VILLABLANCA, E. J. 2018. Flt3 ligand expands bona fide innate lymphoid cell precursors in vivo. *Scientific Reports,* 8**,** 154.

PARK, H., LI, Z., YANG, X. O., CHANG, S. H., NURIEVA, R., WANG, Y.-H., WANG, Y., HOOD, L., ZHU, Z., TIAN, Q. & DONG, C. 2005. A distinct lineage of CD4 T cells regulates tissue inflammation by producing interleukin 17. *Nature Immunology,* 6**,** 1133.

PARKIN, J. & COHEN, B. 2001. An overview of the immune system. *The Lancet,* 357**,** 1777-1789.

PAUL, S., SINGH, A. K., SHILPI & LAL, G. 2014. Phenotypic and Functional Plasticity of Gamma–Delta (γδ) T Cells in Inflammation and Tolerance. *International Reviews of Immunology,* 33**,** 537-558.

PELLY, V. S., KANNAN, Y., COOMES, S. M., ENTWISTLE, L. J., RÜCKERL, D., SEDDON, B., MACDONALD, A. S., MCKENZIE, A. & WILSON, M. S. 2016. IL-4-producing ILC2s are required for the differentiation of T(H)2 cells following Heligmosomoides polygyrus infection. *Mucosal Immunology,* 9**,** 1407-1417.

PENG, H., JIANG, X., CHEN, Y., SOJKA, D. K., WEI, H., GAO, X., SUN, R., YOKOYAMA, W. M. & TIAN, Z. 2013. Liver-resident NK cells confer adaptive immunity in skin-contact inflammation. *The Journal of Clinical Investigation,* 123**,** 1444-1456.

PENG, S. L., SZABO, S. J. & GLIMCHER, L. H. 2002. T-bet regulates IgG class switching and pathogenic autoantibody production. *Proceedings of the National Academy of Sciences,* 99**,** 5545.

PERŠE, M. & CERAR, A. 2012. Dextran Sodium Sulphate Colitis Mouse Model: Traps and Tricks. *Journal of Biomedicine and Biotechnology,* 2012**,** 13.

PHILLIPS, J. E. & CORCES, V. G. 2009. CTCF: Master Weaver of the Genome. *Cell,* 137**,** 1194-1211.

PLACEK, K., GASPARIAN, S., COFFRE, M., MAIELLA, S., SECHET, E., BIANCHI, E. & ROGGE, L. 2009. Integration of Distinct Intracellular Signaling Pathways at Distal Regulatory Elements Directs T-bet Expression in Human CD4⁺ T Cells. *The Journal of Immunology,* 183**,** 7743.

PORRITT, H. E., RUMFELT, L. L., TABRIZIFARD, S., SCHMITT, T. M., ZÚÑIGA-PFLÜCKER, J. C. & PETRIE, H. T. 2004. Heterogeneity among DN1 Prothymocytes Reveals Multiple Progenitors with Different Capacities to Generate T Cell and Non-T Cell Lineages. *Immunity,* 20**,** 735-745.

POWELL, N., LO, J. W., BIANCHERI, P., VOSSENKÄMPER, A., PANTAZI, E., WALKER, A. W., STOLARCZYK, E., AMMOSCATO, F., GOLDBERG, R., SCOTT, P., CANAVAN, J. B., PERUCHA, E., GARRIDO-MESA, N., IRVING, P. M., SANDERSON, J. D., HAYEE, B., HOWARD, J. K., PARKHILL, J., MACDONALD, T. T. & LORD, G. M. 2015. Interleukin 6 Increases Production of Cytokines by Colonic Innate Lymphoid Cells in Mice and Patients With Chronic Intestinal Inflammation. *Gastroenterology,* 149**,** 456-467.e15.

POWELL, N., WALKER, ALAN W., STOLARCZYK, E., CANAVAN, JAMES B., GÖKMEN, M. R., MARKS, E., JACKSON, I., HASHIM, A., CURTIS, MICHAEL A., JENNER, R. G., HOWARD, JANE K., PARKHILL, J., MACDONALD, THOMAS T. & LORD, GRAHAM M. 2012. The Transcription Factor T-bet Regulates Intestinal Inflammation Mediated by Interleukin-7 Receptor+ Innate Lymphoid Cells. *Immunity,* 37**,** 674-684.

POWRIE, F., LEACH, M. W., MAUZE, S., CADDIE, L. B. & COFFMAN, R. L. 1993. Phenotypically distinct subsets of CD4+ T cells induce or protect from chronic intestinal inflammation in C. B-17 scid mice. *International Immunology,* 5**,** 1461-1471.

POWRIE, F., LEACH, M. W., MAUZE, S., MENON, S., BARCOMB CADDLE, L. & COFFMAN, R. L. 1994. Inhibition of Thl responses prevents inflammatory bowel disease in scid mice reconstituted with CD45RBhi CD4+ T cells. *Immunity,* 1**,** 553-562.

POWRIE, F., MAUZE, S. & COFFMAN, R. L. 1997. CD4+ T-cells in the regulation of inflammatory responses in the intestine. *Research in Immunology,* 148**,** 576-581.

PRICE, A. E., LIANG, H.-E., SULLIVAN, B. M., REINHARDT, R. L., EISLEY, C. J., ERLE, D. J. & LOCKSLEY, R. M. 2010. Systemically dispersed innate IL-13–expressing cells in type 2 immunity. *Proceedings of the National Academy of Sciences,* 107**,** 11489.

PULKO, V., DAVIES, J. S., MARTINEZ, C., LANTERI, M. C., BUSCH, M. P., DIAMOND, M. S., KNOX, K., BUSH, E. C., SIMS, P. A., SINARI, S., BILLHEIMER, D., HADDAD, E. K., MURRAY, K. O., WERTHEIMER, A. M. & NIKOLICH-ŽUGICH, J. 2016. Human memory T cells with a naive phenotype accumulate with aging and respond to persistent viruses. *Nature Immunology,* 17**,** 966.

RADTKE, F., WILSON, A., STARK, G., BAUER, M., VAN MEERWIJK, J., MACDONALD, H. R. & AGUET, M. Deficient T Cell Fate Specification in Mice with an Induced Inactivation of Notch1. *Immunity,* 10**,** 547-558.

RADTKE, F., WILSON, A., STARK, G., BAUER, M., VAN MEERWIJK, J., MACDONALD, H. R. & AGUET, M. 1999. Deficient T Cell Fate Specification in Mice with an Induced Inactivation of Notch1. *Immunity,* 10**,** 547-558.

RANKIN, L. C., GROOM, J. R., CHOPIN, M., HEROLD, M. J., WALKER, J. A., MIELKE, L. A., MCKENZIE, A. N. J., CAROTTA, S., NUTT, S. L. & BELZ, G. T. 2013. The transcription factor T-bet is essential for the development of NKp46+ innate lymphocytes via the Notch pathway. *Nature Immunology,* 14**,** 389.

RAO, R. R., LI, Q., ODUNSI, K. & SHRIKANT, P. A. 2010. The mTOR Kinase Determines Effector versus Memory CD8⁺ T Cell Fate by Regulating the Expression of Transcription Factors T-bet and Eomesodermin. *Immunity,* 32**,** 67-78.

REINERT-HARTWALL, L., HONKANEN, J., SALO, H. M., NIEMINEN, J. K., LUOPAJÄRVI, K., HÄRKÖNEN, T., VEIJOLA, R., SIMELL, O., ILONEN, J., PEET, A., TILLMANN, V., KNIP, M., VAARALA, O., THE, D. S. G., KNIP, M., KOSKI, K., KOSKI, M., HÄRKÖNEN, T., RYHÄNEN, S., HÄMÄLÄINEN, A.-M., ORMISSON, A., PEET, A., TILLMANN, V., ULICH, V., KUZMICHEVA, E., MOKUROV, S., MARKOVA, S., PYLOVA, S., ISAKOVA, M., SHAKUROVA, E., PETROV, V., DORSHAKOVA, N. V., KARAPETYAN, T., VARLAMOVA, T., ILONEN, J., KIVINIEMI, M., ALNEK, K., JANSON, H., UIBO, R., SALUM, T., VON MUTIUS, E., WEBER, J., AHLFORS, H., KALLIONPÄÄ, H., LAAJALA, E., LAHESMAA, R., LÄHDESMÄKI, H., MOULDER, R., NIEMINEN, J., RUOHTULA, T., VAARALA, O., HONKANEN, H., HYÖTY, H., KONDRASHOVA, A., OIKARINEN, S., HARMSEN, H. J. M., DE GOFFAU, M. C., WELLING, G., ALAHUHTA, K. & VIRTANEN, S. M. 2015. Th1/Th17 Plasticity Is a Marker of Advanced β Cell Autoimmunity and Impaired Glucose Tolerance in Humans. *The Journal of Immunology Author Choice,* 194**,** 68-75.

REYNOLDS, L. A., FILBEY, K. J. & MAIZELS, R. M. 2012. Immunity to the model intestinal helminth parasite Heligmosomoides polygyrus. *Seminars in Immunopathology,* 34**,** 829-846.

RIBOT, J. C., DEBARROS, A., PANG, D. J., NEVES, J. F., PEPERZAK, V., ROBERTS, S. J., GIRARDI, M., BORST, J., HAYDAY, A. C., PENNINGTON, D. J. & SILVA-SANTOS, B. 2009. CD27 is a thymic determinant of the balance between interferon-γ- and interleukin 17–producing γδ T cell subsets. *Nature Immunology,* 10**,** 427.

ROSSI, D. & ZLOTNIK, A. 2000. The Biology of Chemokines and their Receptors. *Annual Review of Immunology,* 18**,** 217-242.

RUBTSOV, Y. P., RASMUSSEN, J. P., CHI, E. Y., FONTENOT, J., CASTELLI, L., YE, X., TREUTING, P., SIEWE, L., ROERS, A., HENDERSON, W. R., MULLER, W. & RUDENSKY, A. Y. 2008. Regulatory T Cell-Derived Interleukin-10 Limits Inflammation at Environmental Interfaces. *Immunity,* 28**,** 546-558.

SAENZ, S. A., SIRACUSA, M. C., PERRIGOUE, J. G., SPENCER, S. P., URBAN JR, J. F., TOCKER, J. E., BUDELSKY, A. L., KLEINSCHEK, M. A., KASTELEIN, R. A., KAMBAYASHI, T., BHANDOOLA, A. & ARTIS, D. 2010. IL25 elicits a multipotent progenitor cell population that promotes TH2 cytokine responses. *Nature,* 464**,** 1362.

SAKAGUCHI, S., SAKAGUCHI, N., ASANO, M., ITOH, M. & TODA, M. 1995. Immunologic self-tolerance maintained by activated T cells expressing IL-2 receptor alpha-chains (CD25). Breakdown of a single mechanism of self-tolerance causes various autoimmune diseases. *The Journal of Immunology,* 155**,** 1151.

SALLUSTO, F., LENIG, D., FÖRSTER, R., LIPP, M. & LANZAVECCHIA, A. 1999. Two subsets of memory T lymphocytes with distinct homing potentials and effector functions. *Nature,* 401**,** 708.

SANCHEZ-FERNANDEZ, M. A., SBACCHI, S., CORREA-TAPIA, M., NAUMANN, R., KLEMM, J., CHAMBON, P., AL-ROBAIY, S., BLESSING, M. & HOFLACK, B. 2012. Transgenic Mice for a Tamoxifen-Induced, Conditional Expression of the Cre Recombinase in Osteoclasts. *PLOS ONE,* 7**,** e37592.

SANOS, S. L., BUI, V. L., MORTHA, A., OBERLE, K., HENERS, C., JOHNER, C. & DIEFENBACH, A. 2008. RORγt and commensal microflora are required for the differentiation of mucosal interleukin 22–producing NKp46+ cells. *Nature Immunology,* 10**,** 83.

SANOS, S. L. & DIEFENBACH, A. 2010. Isolation of NK Cells and NK-Like Cells from the Intestinal Lamina Propria. *In:* CAMPBELL, K. S. (ed.) *Natural Killer Cell Protocols: Cellular and Molecular Methods.* Totowa, NJ: Humana Press.

SCHMIDLIN, H., DIEHL, S. A. & BLOM, B. 2009. New insights into the regulation of human B-cell differentiation. *Trends in Immunology,* 30**,** 277-285.

SCHMITTGEN, T. D. & LIVAK, K. J. 2008. Analyzing real-time PCR data by the comparative CT method. *Nature Protocols,* 3**,** 1101.

SCHROEDER, H. W., JR. & CAVACINI, L. 2010. Structure and function of immunoglobulins. *The Journal of allergy and clinical immunology,* 125**,** S41-S52.

SCHULZ, E. G., MARIANI, L., RADBRUCH, A. & HÖFER, T. 2009. Sequential Polarization and Imprinting of Type 1 T Helper Lymphocytes by Interferon-γ and Interleukin-12. *Immunity,* 30**,** 673-683.

SCHUSTER, IONA S., WIKSTROM, MATTHEW E., BRIZARD, G., COUDERT, JEROME D., ESTCOURT, MARIE J., MANZUR, M., O'REILLY, LORRAINE A., SMYTH, MARK J., TRAPANI, JOSEPH A., HILL, GEOFFREY R., ANDONIOU, CHRISTOPHER E. & DEGLI-ESPOSTI, MARIAPIA A. 2014. TRAIL+ NK Cells Control CD4+ T Cell Responses during Chronic Viral Infection to Limit Autoimmunity. *Immunity,* 41**,** 646-656.

SEIF, F., KHOSHMIRSAFA, M., AAZAMI, H., MOHSENZADEGAN, M., SEDIGHI, G. & BAHAR, M. 2017. The role of JAK-STAT signaling pathway and its regulators in the fate of T helper cells. *Cell communication and signaling : CCS,* 15**,** 23-23.

SEILLET, C., BELZ, G. T. & HUNTINGTON, N. D. 2016. Development, Homeostasis, and Heterogeneity of NK Cells and ILC1. *In:* VIVIER, E., DI SANTO, J. & MORETTA, A. (eds.) *Natural Killer Cells.* Cham: Springer International Publishing.

SEKIMATA, M., PÉREZ-MELGOSA, M., MILLER, S. A., WEINMANN, A. S., SABO, P. J., SANDSTROM, R., DORSCHNER, M. O., STAMATOYANNOPOULOS, J. A. & WILSON, C. B. 2009. CCCTC-Binding Factor and the Transcription Factor T-bet Orchestrate T Helper 1 Cell-Specific Structure and Function at the Interferon-γ Locus. *Immunity,* 31**,** 551-564.

SHERIDAN, B. S., ROMAGNOLI, P. A., PHAM, Q. M., FU, H. H., ALONZO, F., 3RD, SCHUBERT, W. D., FREITAG, N. E. & LEFRANCOIS, L. 2013. gammadelta T cells exhibit multifunctional and protective memory in intestinal tissues. *Immunity,* 39**,** 184-95.

SILVER, J. S., KEARLEY, J., COPENHAVER, A. M., SANDEN, C., MORI, M., YU, L., PRITCHARD, G. H., BERLIN, A. A., HUNTER, C. A., BOWLER, R., ERJEFALT, J. S., KOLBECK, R. & HUMBLES, A. A. 2016. Inflammatory triggers associated with exacerbations of COPD orchestrate plasticity of group 2 innate lymphoid cells in the lungs. *Nature Immunology,* 17**,** 626.

SIMONETTA, F., PRADIER, A. & ROOSNEK, E. 2016. T-bet and Eomesodermin in NK Cell Development, Maturation, and Function. *Frontiers in Immunology,* 7**,** 241.

SODERQUEST, K., POWELL, N., LUCI, C., VAN ROOIJEN, N., HIDALGO, A., GEISSMANN, F., WALZER, T., LORD, G. M. & MARTÍN-FONTECHA, A. 2011. Monocytes control natural killer cell differentiation to effector phenotypes. *Blood,* 117**,** 4511.

SONG, A. J. & PALMITER, R. D. 2018. Detecting and Avoiding Problems When Using the Cre–lox System. *Trends in Genetics,* 34**,** 333-340.

SONG, C., LEE, J. S., GILFILLAN, S., ROBINETTE, M. L., NEWBERRY, R. D., STAPPENBECK, T. S., MACK, M., CELLA, M. & COLONNA, M. 2015. Unique and redundant functions of NKp46⁺ ILC3s in models of intestinal inflammation. *J Exp Med,* 212**,** 1869.

SPITS, H., ARTIS, D., COLONNA, M., DIEFENBACH, A., DI SANTO, J. P., EBERL, G., KOYASU, S., LOCKSLEY, R. M., MCKENZIE, A. N. J., MEBIUS, R. E., POWRIE, F. & VIVIER, E. 2013. Innate lymphoid cells — a proposal for uniform nomenclature. *Nature Reviews Immunology,* 13**,** 145.

SPITS, H. & CUPEDO, T. 2012. Innate Lymphoid Cells: Emerging Insights in Development, Lineage Relationships, and Function. *Annual Review of Immunology,* 30**,** 647-675.

SPRENT, J. 1995. Antigen-Presenting Cells: Professionals and amateurs. *Current Biology,* 5**,** 1095-1097.

SPRENT, J. & SURH, C. D. 2011. Normal T cell homeostasis: the conversion of naïve cells into memory-phenotype cells. *Nature immunology,* 12**,** 478-484.

STARR, T. K., JAMESON, S. C. & HOGQUIST, K. A. 2003. Positive and negative selection of T cells. *Annu Rev Immunol,* 21**,** 139-76.

STOCK, P., AKBARI, O., BERRY, G., FREEMAN, G. J., DEKRUYFF, R. H. & UMETSU, D. T. 2004. Induction of T helper type 1–like regulatory cells that express Foxp3 and protect against airway hyper-reactivity. *Nature Immunology,* 5**,** 1149.

SUGIMOTO, K., OGAWA, A., MIZOGUCHI, E., SHIMOMURA, Y., ANDOH, A., BHAN, A. K., BLUMBERG, R. S., XAVIER, R. J. & MIZOGUCHI, A. 2008. IL-22 ameliorates intestinal inflammation in a mouse model of ulcerative colitis. *J Clin Invest,* 118**,** 534-44.

SUMARIA, N., GRANDJEAN, C. L., SILVA-SANTOS, B. & PENNINGTON, D. J. 2017. Strong TCRγδ Signaling Prohibits Thymic Development of IL-17A-Secreting γδ T Cells. *Cell reports,* 19**,** 2469-2476.

SUNDRUD, M. S., GRILL, S. M., NI, D., NAGATA, K., ALKAN, S. S., SUBRAMANIAM, A. & UNUTMAZ, D. 2003. Genetic Reprogramming of Primary Human T Cells Reveals Functional Plasticity in Th Cell Differentiation. *The Journal of Immunology,* 171**,** 3542.

SUTTON, C. E., LALOR, S. J., SWEENEY, C. M., BRERETON, C. F., LAVELLE, E. C. & MILLS, K. H. G. 2009. Interleukin-1 and IL-23 Induce Innate IL-17 Production from γδ T Cells, Amplifying Th17 Responses and Autoimmunity. *Immunity,* 31**,** 331-341.

SWAIN, S. L., WEINBERG, A. D., ENGLISH, M. & HUSTON, G. 1990. IL-4 directs the development of Th2-like helper effectors. *The Journal of Immunology,* 145**,** 3796.

SZABO, S. J., KIM, S. T., COSTA, G. L., ZHANG, X., FATHMAN, C. G. & GLIMCHER, L. H. 2000. A novel transcription factor, T-bet, directs Th1 lineage commitment. *Cell,* 100**,** 655-69.

TAKEDA, K., CRETNEY, E., HAYAKAWA, Y., OTA, T., AKIBA, H., OGASAWARA, K., YAGITA, H., KINOSHITA, K., OKUMURA, K. & SMYTH, M. J. 2005. TRAIL identifies immature natural killer cells in newborn mice and adult mouse liver. *Blood,* 105**,** 2082.

TAKEDA, K., TANAKA, T., SHI, W., MATSUMOTO, M., MINAMI, M., KASHIWAMURA, S.-I., NAKANISHI, K., YOSHIDA, N., KISHIMOTO, T. & AKIRA, S. 1996. Essential role of Stat6 in IL-4 signalling. *Nature,* 380**,** 627.

TAKEMOTO, N., INTLEKOFER, A. M., NORTHRUP, J. T., WHERRY, E. J. & REINER, S. L. 2006. Cutting Edge: IL-12 Inversely Regulates T-bet and Eomesodermin Expression during Pathogen-Induced CD8⁺ T Cell Differentiation. *The Journal of Immunology,* 177**,** 7515.

TAN, T. G., MATHIS, D. & BENOIST, C. 2016a. Singular role for T-BET(+)CXCR3(+) regulatory T cells in protection from autoimmune diabetes. *Proceedings of the National Academy of Sciences of the United States of America,* 113**,** 14103-14108.

TAN, T. G., MATHIS, D. & BENOIST, C. 2016b. Singular role for T-BET⁺CXCR3⁺ regulatory T cells in protection from autoimmune diabetes. *Proceedings of the National Academy of Sciences,* 113**,** 14103-14108.

TANG, L., PENG, H., ZHOU, J., CHEN, Y., WEI, H., SUN, R., YOKOYAMA, W. M. & TIAN, Z. 2016. Differential phenotypic and functional properties of liver-resident NK cells and mucosal ILC1s. *Journal of Autoimmunity,* 67**,** 29-35.

TANG, Y., GUAN, S. P., CHUA, B. Y. L., ZHOU, Q., HO, A. W. S., WONG, K. H. S., WONG, K. L., WONG, W. S. F. & KEMENY, D. M. 2012. Antigen-specific effector CD8 T cells regulate allergic responses via IFN-γ and dendritic cell function. *Journal of Allergy and Clinical Immunology,* 129**,** 1611-1620.e4.

THIEU, V. T., YU, Q., CHANG, H.-C., YEH, N., NGUYEN, E. T., SEHRA, S. & KAPLAN, M. H. 2008. Signal Transducer and Activator of Transcription 4 Is Required for the Transcription Factor T-bet to Promote T Helper 1 Cell-Fate Determination. *Immunity,* 29**,** 679-690.

THOMAS, L. R., COBB, R. M. & OLTZ, E. M. 2009. Dynamic Regulation of Antigen Receptor Gene Assembly. *In:* FERRIER, P. (ed.) *V(D)J Recombination.* New York, NY: Springer New York.

THOMAS, M. J., MACARY, P. A., NOBLE, A., ASKENASE, P. W. & KEMENY, D. M. 2001. T Cytotoxic 1 and T Cytotoxic 2 CD8 T Cells Both Inhibit IgE Responses. *International Archives of Allergy and Immunology,* 124**,** 187-189.

THOMSON, A. W. & KNOLLE, P. A. 2010. Antigen-presenting cell function in the tolerogenic liver environment. *Nature Reviews Immunology,* 10**,** 753.

TONEGAWA, S. 1976. Reiteration frequency of immunoglobulin light chain genes: further evidence for somatic generation of antibody diversity. *Proceedings of the National Academy of Sciences,* 73**,** 203.

TOSI, M. F. 2005. Innate immune responses to infection. *Journal of Allergy and Clinical Immunology,* 116**,** 241-249.

TOUGH, D. F., BORROW, P. & SPRENT, J. 1996. Induction of Bystander T Cell Proliferation by Viruses and Type I Interferon in Vivo. *Science,* 272**,** 1947.

TOUGH, D. F., ZHANG, X. & SPRENT, J. 2001. An IFN-γ-Dependent Pathway Controls Stimulation of Memory Phenotype CD8⁺ T Cell Turnover In Vivo by IL-12, IL-18, and IFN-γ. *The Journal of Immunology,* 166**,** 6007.

TOWNSEND, M. J., WEINMANN, A. S., MATSUDA, J. L., SALOMON, R., FARNHAM, P. J., BIRON, C. A., GAPIN, L. & GLIMCHER, L. H. 2004. T-bet Regulates the Terminal Maturation and Homeostasis of NK and Vα14i NKT Cells. *Immunity,* 20**,** 477-494.

TURCHINOVICH, G. & PENNINGTON, D. J. 2011. T cell receptor signalling in gammadelta cell development: strength isn't everything. *Trends Immunol,* 32**,** 567-73.

TURVEY, S. E. & BROIDE, D. H. 2010. Innate immunity. *The Journal of allergy and clinical immunology,* 125**,** S24-S32.

UHLIG, H. H., MCKENZIE, B. S., HUE, S., THOMPSON, C., JOYCE-SHAIKH, B., STEPANKOVA, R., ROBINSON, N., BUONOCORE, S., TLASKALOVA-HOGENOVA, H., CUA, D. J. & POWRIE, F. 2006. Differential Activity of IL-12 and IL-23 in Mucosal and Systemic Innate Immune Pathology. *Immunity,* 25**,** 309-318.

UHLIG HOLM, H. & POWRIE, F. 2009. Mouse models of intestinal inflammation as tools to understand the pathogenesis of inflammatory bowel disease. *European Journal of Immunology,* 39**,** 2021-2026.

UNUTMAZ, D. 2009. RORC2: The master of human Th17 cell programming. *European Journal of Immunology,* 39**,** 1452-1455.

URBAN, J. F., NOBEN-TRAUTH, N., DONALDSON, D. D., MADDEN, K. B., MORRIS, S. C., COLLINS, M. & FINKELMAN, F. D. 1998. IL-13, IL-4Rα, and Stat6 Are Required for the Expulsion of the Gastrointestinal Nematode Parasite Nippostrongylus brasiliensis. *Immunity,* 8**,** 255-264.

VAN AALST, S., LUDWIG, I. S., VAN DER ZEE, R., VAN EDEN, W. & BROERE, F. 2017. Bystander activation of irrelevant CD4+ T cells following antigen-specific vaccination occurs in the presence and absence of adjuvant. *PLOS ONE,* 12**,** e0177365.

VAN OERS, N. S., VON BOEHMER, H. & WEISS, A. 1995. The pre-T cell receptor (TCR) complex is functionally coupled to the TCR-zeta subunit. *J Exp Med,* 182**,** 1585-90.

VARGAS, C. L., POURSINE-LAURENT, J., YANG, L. & YOKOYAMA, W. M. 2011. Development of thymic NK cells from double negative 1 thymocyte precursors. *Blood,* 118**,** 3570.

VELDHOEN, M., HOCKING, R. J., ATKINS, C. J., LOCKSLEY, R. M. & STOCKINGER, B. 2006. TGFβ in the Context of an Inflammatory Cytokine Milieu Supports De Novo Differentiation of IL-17-Producing T Cells. *Immunity,* 24**,** 179-189.

VICTORINO, F., SOJKA, D. K., BRODSKY, K. S., MCNAMEE, E. N., MASTERSON, J. C., HOMANN, D., YOKOYAMA, W. M., ELTZSCHIG, H. K. & CLAMBEY, E. T. 2015. Tissue-Resident NK Cells Mediate Ischemic Kidney Injury and Are Not Depleted by Anti–Asialo-GM1 Antibody. *The Journal of Immunology,* 195**,** 4973.

VILLARINO, A. V., KANNO, Y., FERDINAND, J. R. & O'SHEA, J. J. 2015. Mechanisms of Jak/STAT signaling in immunity and disease. *Journal of immunology (Baltimore, Md. : 1950),* 194**,** 21-27.

VON BOEHMER, H., TEH, H. S. & KISIELOW, P. 1989. The thymus selects the useful, neglects the useless and destroys the harmful. *Immunology Today,* 10**,** 57-61.

VOSSHENRICH, C. A. J., GARCÍA-OJEDA, M. E., SAMSON-VILLÉGER, S. I., PASQUALETTO, V., ENAULT, L., GOFF, O. R.-L., CORCUFF, E., GUY-GRAND, D., ROCHA, B., CUMANO, A., ROGGE, L., EZINE, S. & DI SANTO, J. P. 2006. A thymic pathway of mouse natural killer cell development characterized by expression of GATA-3 and CD127. *Nature Immunology,* 7**,** 1217.

WAHID, F. N. & BEHNKE, J. M. 1992. Stimuli for acquired resistance to Heligmosomoides polygyrus from intestinal tissue resident L3 and L4 larvae. *International Journal for Parasitology,* 22**,** 699-710.

WANG, N. S., MCHEYZER-WILLIAMS, L. J., OKITSU, S. L., BURRIS, T. P., REINER, S. L. & MCHEYZER-WILLIAMS, M. G. 2012. Divergent transcriptional programming of class-specific B cell memory by T-bet and RORα. *Nature Immunology,* 13**,** 604.

WANG, Y., GODEC, J., BEN-AISSA, K., CUI, K., ZHAO, K., PUCSEK, ALEXANDRA B., LEE, YUN K., WEAVER, CASEY T., YAGI, R. & LAZAREVIC, V. 2014. The Transcription Factors T-bet and Runx Are Required for the Ontogeny of Pathogenic Interferon-γ-Producing T Helper 17 Cells. *Immunity,* 40**,** 355-366.

WATANABE, H., NUMATA, K., ITO, T., TAKAGI, K. & MATSUKAWA, A. 2004. INNATE IMMUNE RESPONSE IN TH1- AND TH2-DOMINANT MOUSE STRAINS. *Shock,* 22**,** 460-466.

WEAVER, C. T., HARRINGTON, L. E., MANGAN, P. R., GAVRIELI, M. & MURPHY, K. M. 2006. Th17: An Effector CD4 T Cell Lineage with Regulatory T Cell Ties. *Immunity,* 24**,** 677-688.

WEIGERT, M. G., CESARI, I. M., YONKOVICH, S. J. & COHN, M. 1970. Variability in the lambda light chain sequences of mouse antibody. *Nature,* 228**,** 1045-7.

WHITE, J. T., CROSS, E. W., BURCHILL, M. A., DANHORN, T., MCCARTER, M. D., ROSEN, H. R., O'CONNOR, B. & KEDL, R. M. 2016. Virtual memory T cells develop and mediate bystander protective immunity in an IL-15-dependent manner. *Nature Communications,* 7**,** 11291.

WILLIAMS, K. M., DOTSON, A. L., OTTO, A. R., KOHLMEIER, J. E. & BENEDICT, S. H. 2011. Choice of resident costimulatory molecule can influence cell fate in human naïve CD4+ T cell differentiation. *Cellular immunology,* 271**,** 418-427.

WILSON, C. B., ROWELL, E. & SEKIMATA, M. 2009. Epigenetic control of T-helper-cell differentiation. *Nature Reviews Immunology,* 9**,** 91.

XIE, M.-H., AGGARWAL, S., HO, W.-H., FOSTER, J., ZHANG, Z., STINSON, J., WOOD, W. I., GODDARD, A. D. & GURNEY, A. L. 2000a. Interleukin (IL)-22, a Novel Human Cytokine That Signals through the Interferon Receptor-related Proteins CRF2–4 and IL-22R. *Journal of Biological Chemistry,* 275**,** 31335-31339.

XIE, M. H., AGGARWAL, S., HO, W. H., FOSTER, J., ZHANG, Z., STINSON, J., WOOD, W. I., GODDARD, A. D. & GURNEY, A. L. 2000b. Interleukin (IL)-22, a novel human cytokine that signals through the interferon receptor-related proteins CRF2-4 and IL-22R. *J Biol Chem,* 275**,** 31335-9.

XIONG, Y., AHMAD, S., IWAMI, D., BRINKMAN, C. C. & BROMBERG, J. S. 2016. T-bet regulates natural Treg afferent lymphatic migration and suppressive function. *Journal of immunology (Baltimore, Md. : 1950),* 196**,** 2526-2540.

XU, W., DOMINGUES, R. G., FONSECA-PEREIRA, D., FERREIRA, M., RIBEIRO, H., LOPEZ-LASTRA, S., MOTOMURA, Y., MOREIRA-SANTOS, L., BIHL, F., BRAUD, V., KEE, B., BRADY, H., COLES, M. C., VOSSHENRICH, C., KUBO, M., DI SANTO, J. P. & VEIGA-FERNANDES, H. 2015. NFIL3 orchestrates the emergence of common helper innate lymphoid cell precursors. *Cell Rep,* 10**,** 2043-54.

YAO, Z., KANNO, Y., KERENYI, M., STEPHENS, G., DURANT, L., WATFORD, W. T., LAURENCE, A., ROBINSON, G. W., SHEVACH, E. M., MORIGGL, R., HENNIGHAUSEN, L., WU, C. & SHEA, J. J. 2007. Nonredundant roles for Stat5a/b in directly regulating <em>Foxp3</em&gt. *Blood,* 109**,** 4368.

YIN, Z., CHEN, C., SZABO, S. J., GLIMCHER, L. H., RAY, A. & CRAFT, J. 2002. T-Bet Expression and Failure of GATA-3 Cross-Regulation Lead to Default Production of IFN-γ by γδ T Cells. *The Journal of Immunology,* 168**,** 1566.

ZHANG, D.-H., COHN, L., RAY, P., BOTTOMLY, K. & RAY, A. 1997. Transcription Factor GATA-3 Is Differentially Expressed in Murine Th1 and Th2 Cells and Controls Th2-specific Expression of the Interleukin-5 Gene. *Journal of Biological Chemistry,* 272**,** 21597-21603.

ZHANG, Y., RIESTERER, C., AYRALL, A. M., SABLITZKY, F., LITTLEWOOD, T. D. & RETH, M. 1996. Inducible site-directed recombination in mouse embryonic stem cells. *Nucleic Acids Research,* 24**,** 543-548.

ZHAO, Y., NIU, C. & CUI, J. 2018. Gamma-delta (γδ) T cells: friend or foe in cancer development? *Journal of Translational Medicine,* 16**,** 3.

ZHENG, W.-P. & FLAVELL, R. A. 1997. The Transcription Factor GATA-3 Is Necessary and Sufficient for Th2 Cytokine Gene Expression in CD4 T Cells. *Cell,* 89**,** 587-596.

ZHOU, L., CHONG, M. M. W. & LITTMAN, D. R. 2009. Plasticity of CD4+ T Cell Lineage Differentiation. *Immunity,* 30**,** 646-655.

ZHU, J., GUO, L., WATSON, C. J., HU-LI, J. & PAUL, W. E. 2001. Stat6 Is Necessary and Sufficient for IL-4's Role in Th2 Differentiation and Cell Expansion. *The Journal of Immunology,* 166**,** 7276.

ZHU, J., JANKOVIC, D., OLER, ANDREW J., WEI, G., SHARMA, S., HU, G., GUO, L., YAGI, R., YAMANE, H., PUNKOSDY, G., FEIGENBAUM, L., ZHAO, K. & PAUL, WILLIAM E. 2012. The Transcription Factor T-bet Is Induced by Multiple Pathways and Prevents an Endogenous Th2 Cell Program during Th1 Cell Responses. *Immunity,* 37**,** 660-673.

ZHU, J. & PAUL, W. E. 2008. CD4 T cells: fates, functions, and faults. *Blood,* 112**,** 1557.

ZHU, J. & PAUL, W. E. 2010. CD4+ T Cell Plasticity—Th2 Cells Join the Crowd. *Immunity,* 32**,** 11-13.

ZHU, J., YAMANE, H. & PAUL, W. E. 2010. Differentiation of Effector CD4 T Cell Populations. *Annual review of immunology,* 28**,** 445-489.

ZORN, A. M. 2008. Liver development. *StemBook.* Cambridge (MA).